MARITIME UNIVERSITY CONSTANTA

CONSTANTA MARITIME UNIVERSITY

ANNALS

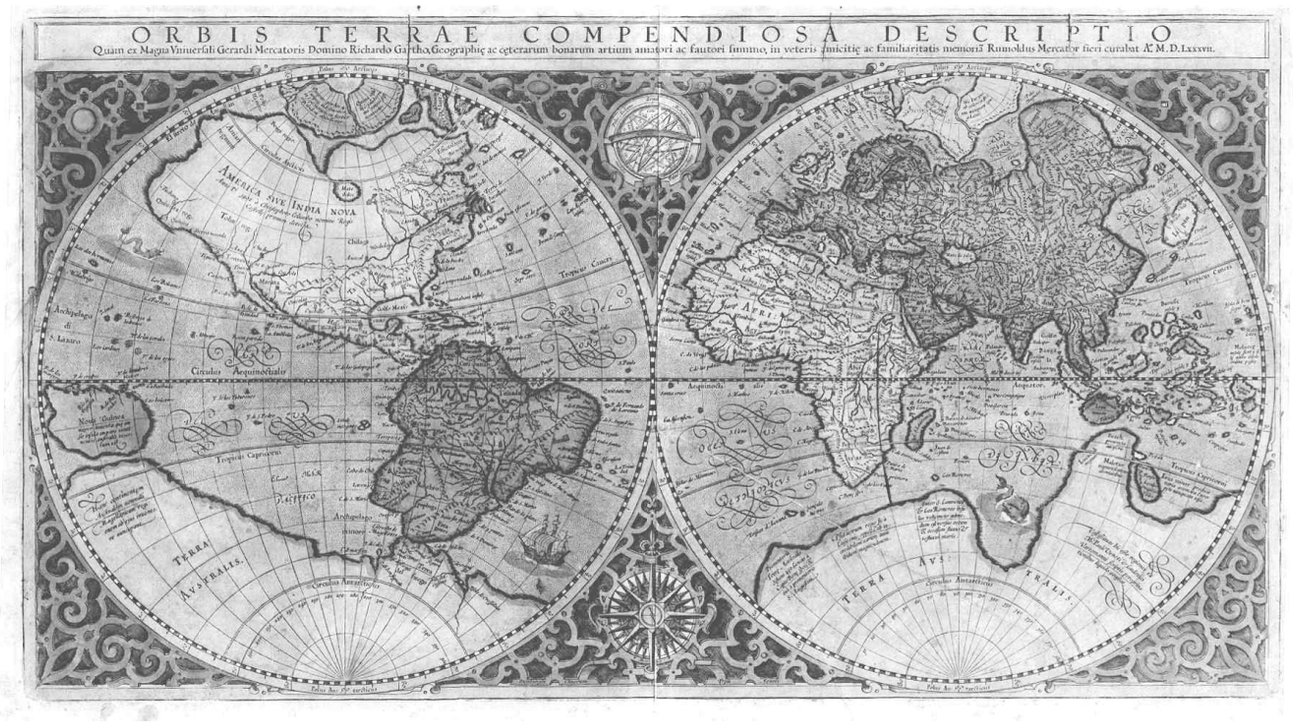

YEAR XV, 22nd issue

Editura NAUTICA

CONSTANŢA 2014

Editor-in-Chief
Assoc.prof. Emil Oanță Ph.D

Secretary-in-Chief
Ionela Dănilă

Computerized Tehnoredactation
Anişoara Toma
Minodora Badea

Web Administrator
George Popescu

SCIENTIFIC COMMITTEE

President:

Cornel Panait	**Vice-rector, Constanta Maritime University, Romania**

Members:

Violeta-Vali Ciucur	**Rector, Constanta Maritime University, Romania**
Eliodor Constantinescu	**Vice-rector, Constanta Maritime University, Romania**
Mihail Alexandrescu	**Professor, Transport Faculty, Politehnica University of Bucharest, Romania**
Toader Munteanu	**Professor, "Dunarea de Jos" University, Galati, Romania**
Mariana Jurian	**Professor, Faculty of Electronics, Communications and Computers, University of Pitesti, Romania**
Alexandru Jipa	**Physics Faculty, University of Bucharest, Romania**
Corneliu Burileanu	**Vice-rector, Politehnica University of Bucharest, Romania**
Silviu Ciochină	**Chair of Telecommunications, Faculty of Electronics, Telecommunications and Information Technology, Politehnica University of Bucharest, Romania**
Dan Stoichescu	**Professor, Faculty of Electronics, Telecommunications and Information Technology, Politehnica University of Bucharest, Romania**
Teodor Petrescu	**Professor, Faculty of Electronics, Telecommunications and Information Technology, Politehnica University of Bucharest, Romania**
Marin Drăgulinescu	**Professor, Faculty of Electronics, Telecommunications and Information Technology, Politehnica University of Bucharest, Romania**
Cornel Ioana	**Associate Professor - Researcher, Grenoble INP/ENSE3, GIPSA-lab, Department Images-Signal, France**
Ovidiu Dragomirescu	**Professor, Faculty of Electronics, Telecommunications and Information Technology, Politehnica University of Bucharest, Romania**
Ricardo Rodríguez-Martos	**Director, Department of Nautical Sciences and Engineering, Polytechnical University of Catalonia, Spain**
Donna J. Nincic	**Professor and Chair, Department of Maritime Policy and Management, California Maritime Academy, California State University**
Anto Raukas	**Professor, Estonia Maritime Academy**
Wang Zuwen	**President of Dalian Maritime University**
De Melo German	**Professor, Faculty of Nautical Studies - Polytechnical University of Catalonia, Spain**
Mykhaylo V. Miyusov	**Rector, Odessa National Maritime Academy, Ukraine**
Güler Nil	**Dean, Maritime Faculty, Istanbul Technical University, Turkey**
Cwilewicz Romuald	**President, Gdynia Maritime University, Poland**
Sag Osman Kamil	**Rector, Piri Reis Maritime University, Turkey**
Gruenwald Norbert	**Rector, Hochschule Wismar, University of Technology, Business and Design, Germany**
Boyan Mednikarov	**Professor, N.Y. Vaptsarov Naval Academy, Bulgaria**
Dimitar Angelov	**Professor, N.Y. Vaptsarov Naval Academy, Bulgaria**
Oh Keo-Don	**President of Korea Maritime University, Korea**
Eisenhardt William	**President, California Maritime Academy, USA**
Laczynski Bogumil	**Professor, Faculty of Navigation - Gdynia Maritime University, Poland**

CONTENTS

SECTION I – NAVIGATION AND MARITIME TRANSPORT

SECTION II – MECHANICAL ENGINEERING AND ENVIRONMENT

SECTION V – TRANSPORT ECONOMICS

SECTION I
NAVIGATION AND MARITIME TRANSPORT

THE STOWAGE AND SEGREGATION OF DANGEROUS GOODS ON A CONTAINER SHIP THROUGH USE OF ARTIFICIAL NEURAL NETWORK APROACH

[1]BAL ELIF, [2]BAYRAKTAR DEMET, [3]KILIC ALPER, [4]OZTURK EMIN

[1]Istanbul Technical University, [2,3,4]Balikesir University Bandirma Maritime Faculty, Turkey

ABSTRACT

Container ships carry most seagoing non-bulk cargo through major seaports today. Due to the increased demand in a variety of industrial fields, the movement of dangerous goods has increased through seaborne trade. One of the greatest challenges of container shipping is the transportation of dangerous cargo onboard. The preservation methods for dangerous goods during transport can have serious consequences onboard a ship. The loading or stowage for a container ship is one of the serious problems that has to be solved by each company that manage a container terminal. The stowage of dangerous goods requires more attention due to the hazardous consequences, which are monitored using strict regulations by IMDG Code. This study aims to create a Decision Support System (DSS) by using Multi-Layer Perceptron (MLP) as an Artificial Neural Network Model which may help in determination of the proper locations for these dangerous goods on a ship. In this way, the operator (maritime terminal or agency) will have more awareness of the situation and it would be possible to prevent maritime accidents due to improper stowage and segregation of dangerous goods.

Keywords: *Container Ship, Dangerous Goods, Ship Accidents, Artificial Neural Network, Multi Layer Perception.*

1. INTRODUCTION

Container transportation is one of the most important elements of the global shipping industry. Container transportation has had a significant role in world trade since the 1950s. It is stated the containerization of cargoes has gained importance for maritime transportation worldwide since the 1970s [1]. The biggest reason for the fast growth of container transportation is that it provides a reduction in transportation costs by bringing standardization to the maritime industry. Transportation of cargoes or products in containers is the beginning of a more efficient and economical period both for cargo owners and ship owners.

Maritime transportation and consequently transport of dangerous goods have increased with globalization [2]. 'Dangerous goods' are designated as the substances, materials and articles covered by the International Maritime Dangerous Goods (IMDG) Code.

Approximately 10% of dangerous goods are carried by containers on many shipping routes [3]. It was reported that hazardous cargo constitutes approximately 10 - 40% of total cargo for container ships [4]. One of the biggest challenges of container shipping is the transportation of dangerous cargo on board [5].

In recent years, there have been serious accidents during transportation of dangerous goods by sea. A fire on the Sea Elegance container ship ended in loss of life and the loss of the ship in 2003. An explosion and fire on the Hyundai Fortune, and the fire on the Zim Haifa in 2007 are similar examples [6]. According to the research, the majority of contributing factors to dangerous goods releases identified by the UK's Marine Accident Investigation Branch (MAIB) for the cases between 1998 and 2008. An estimated 91% of the contributing faults occurred prior to the loading of the dangerous goods onto the ship. Problems with the loading of cargo transport units represents the significant category of contributing factors for dangerous good releases because of reactions between different cargoes. Only 2% of releases were attributed to excessive ship motions and storms [6].

The loading or stowage of a container ship is one of the most serious problems that have to be solved in every day operations by any company which manages a container terminal [7]. Previously, stowage plans for containers were performed by the captain of ship, however nowadays, the maritime terminal or agency has to establish the master bay plan in accordance with the stowage instructions of the ship co-ordinator representing the company holding the ship [8].

The stowage and segregation of dangerous goods on a ship possess great risks therefore international regulations are mandatory for loading and stowage of these goods. The maritime terminal or agency has to plan the stowage of containerized dangerous goods according to international requirements. The proper loading and stowage of dangerous goods requires great attention. However, it is known that generally faults and mistakes occur in cases that have grave results due to the shortage of time and insufficient care during operations.

Decision Support Systems (DSSs) with quick and accurate response are needed to reduce mistakes and so disasters caused by the maritime terminal or agency. DSSs are a group of procedures based on models with data processing and judgement to help managers (maritime terminal and agency) decide on the most appropriate course of action [9]. Over time, large amount of data have been processed through the computer and database technology, thus, DSS became an important tool for managers that makes it easier to make a decision. The use of Artificial Intelligence Systems as a DSSs is increasing day by day due to advances in computer technology. Artificial Neural Network (ANN) models are one of Artificial Intelligence techniques that

can be used by researchers which has shown promising results. An Artificial Neural Network approach, pioneered by McCulloch and Pitts (1943), can be used to classify large amounts of items in terms of a multi criteria classification in order to reach proper stowage management objectives.

This study aims to establish a DSS model using the Artificial Neural Network for maritime terminal or agency operators. The Database used for the model is composed of various containerized dangerous goods that have different characteristics. Multi-layer perceptron (MLP) as an Artificial Neural Network Model has been used to support the users for determining suitable locations for containerized dangerous goods in the stowage plan. The stowage and segregation of packaged dangerous goods on a ship has been addressed with consideration of danger classes, international regulations for stowage and segregation of dangerous goods regulations indicated in the United Nation Number (stowage on deck - in hold and clear living of quarters). Priority unloading ports have also been considered to eliminate the accidents or incidents due to the incorrect stowage of these goods on the ship and to save time at ports. In conclude, the fast and safe stowage and segregation of dangerous goods has been assured by designating the location of dangerous goods stowage on container ships through using this DSS.

2. ARTIFICIAL NEURAL NETWORK

Due to the limitation of human brain capacity for the storage and procession of data, Decision Support Systems have been developed for solving complex problems. Decision Support Systems are computer-based systems which aims to help the decision-maker achieve the optimal solution in very complex problems. The use of Artificial Intelligence Systems as DSS is increasing day by day due to the advances in computer technology. Artificial Neural Network as a form of artificial intelligence techniques have been used by researchers as a promising method in forecasting studies.

Artificial Neural Networks (ANNs) are computer systems developed to imitate activities of the human brain by mathematically modelling its neuro-physiological structure. Artificial Neural Networks have been shown to be effective at approximating complex nonlinear functions [11]. ANNs are used to model complex relationships between inputs and outputs or to find correlations in the data. Unlike traditional computational models, ANN models have a brain like structure and functionality similar to brain cells [12].

ANNs generally have 3 layers which are listed as input layer, hidden layer and output layer. The input layers function is getting information from the external environment and transmitting it to the hidden layer. The hidden layer processes and transmits information to the output layer. The output layer is responsible for transmitting the processed information received from the hidden layer to the external environment. The model is characterized by a network of three layers of simple processing units connected by acyclic links (Figure 1). A single hidden layer feed forward network is the most widely used form for modelling, forecasting, and classification [13].

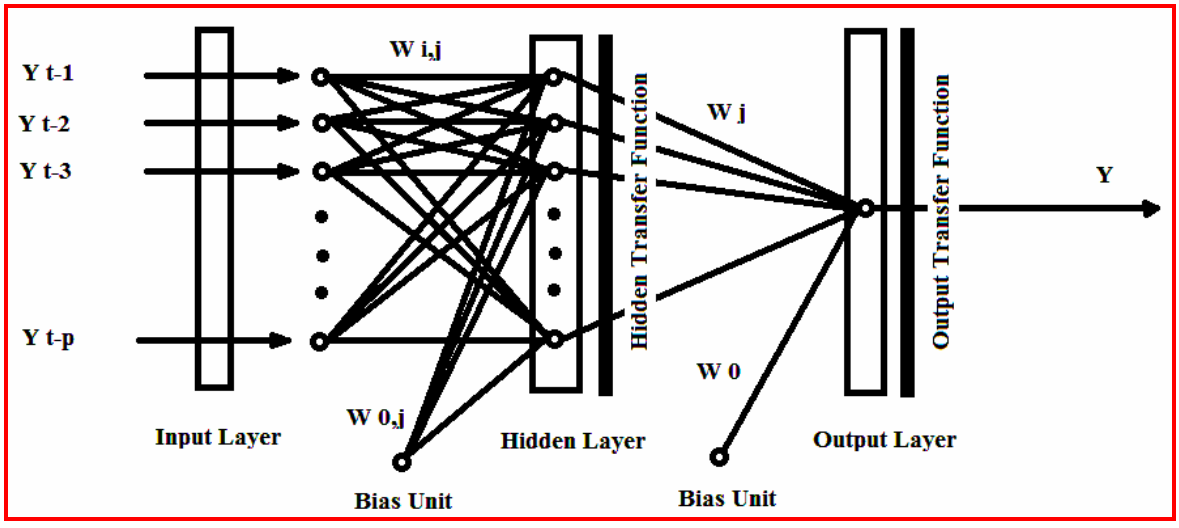

Figure 1 Neural network structure

The Artificial Neural Network structure may have to change according to nodes and their connections. Most research models use a three layer network that consists of one input, one hidden and one output layer. Hidden nodes with their activation function are required to introduce nonlinearity in the neural network. The most popular network model used for classification problems is the Multi-Layer Perceptron (MLP) network [13, 14, 15]. Networks that consist of a set of neurons that are logically arranged into two or more layers are known as multi-layer feed-forward neural networks [16].

3. METHODOLOGY

3.1 Evaluation criteria

In maritime transportation, the International Maritime Organization (IMO) has been developing regulations regarding the dangerous goods. Regulations

introduced by the IMO for dangerous goods carried by container ships have been included in the IMDG Code (International Maritime Dangerous Goods Code). In addition, the International Convention for the Safety of Life at Sea (SOLAS) entails IMDG Code in Part A for packaged dangerous goods as well as including regulations about dangerous goods in SOLAS section 7.

According to the IMDG Code, hazardous cargo is divided into 9 danger classes and their sub classes. Annex 1 shows the danger classes of goods according to the IMDG Code.

Ships are classified into two distinct groups except for class 1: cargo ships and passenger ships, and there are five different “stowage” categories from A to D. Substances, materials or articles must be stowed in accordance with these categories. Class 1-Explosives are divided into six subclasses from Class 1.1 to 1.6, but due to extreme risk of hazard, most ports only accept Class 1.4 which has no significant explosion hazard, therefore only this type of explosives (Class 1.4) are considered in the study.

Dangerous goods that have different United Nation numbers (UN numbers) are subject to different stowage and segregation rules even if they are in the same danger class. Thus, members of the same dangerous goods class can be stowed in different cargo spaces on a ship, and this detail is taken into account when building the model.

Dangerous goods are represented by UN numbers in the IMDG Code. There are approximately 2500 different UN numbers, and each of these numbers has information about proper shipping name, danger class, packing groups, whether the goods contain a marine pollutant or not, and flash points, the limited amount of records, packaging details that can be used in transport, stacking and separation rules (UN Recommendations). Each UN number has 18 columns that give information about dangerous goods. Column 16 provides information about the rules regarding stowage and separation.

"Clear of living quarters" refers to the rule that the substance should be kept away from the accommodation area of the ship. "Category A, B and E" implies that the goods should be kept on deck or under deck. "Category C and D" implies that the goods must be transported on open decks only for container ships.

The term “segregation” means stowing apart various dangerous goods which can interact to cause hazardous reactions between them. The segregation is achieved applying IMDG rules, establishing a certain distance between the goods or putting them in different cargo holds. These rules have different applications depending on the type of cargo transportation unit or position of the cargo on board the ship. Ship types, cargo stowage on longitudinal or cross sections, on deck, or in hold stowage cover other important criteria.

Table 1 indicates the segregation levels between different hazard classes modelled in the study. The fourth level of segregation requires separation of goods longitudinally by an intervening compartment or hold, thus if there is the fourth level of segregation between classes, they are not stowed in the same defined longitudinal cargo areas. For example, there is fourth degree segregation between class 6.2 and class 1.4 or class 2.1.

Table 1 Danger Classes and Segregation Levels

Class	**1.4**	**2.1**	**2.2**	**2.3**	**3**	**4.1**	**4.2**	**4.3**	**5.1**	**5.2**	**6.1**	**6.2**	**7**	**8**	**9**
1.4	*	2	1	1	2	2	2	2	2	2	x	4	2	2	x
2.1	2	x	x	x	2	1	2	x	2	2	x	4	2	1	x
2.2	1	x	x	x	1	x	1	x	x	1	x	2	1	x	x
2.3	1	x	x	x	2	x	2	x	x	2	x	2	1	x	x
3	2	2	1	2	x	x	2	1	2	2	x	3	2	x	x
4.1	2	1	x	x	x	x	1	x	1	2	x	3	2	1	x
4.2	2	2	1	2	2	1	x	1	2	2	1	3	2	1	x
4.3	2	x	x	x	1	x	1	x	2	2	x	2	2	1	x
5.1	2	2	x	x	2	1	2	2	x	2	1	3	1	2	x
5.2	2	2	2	2	2	2	2	2	2	x	1	3	2	2	x
6.1	x	x	x	x	x	x	1	x	1	1	x	1	x	x	x
6.2	4	4	2	2	3	3	3	2	3	3	1	x	3	3	x
7	2	2	1	1	2	2	2	2	1	2	x	3	x	2	x
8	2	1	x	x	x	1	1	1	2	2	x	3	2	x	x
9	x	x	x	x	x	x	x	x	x	x	x	x	x	x	x

Container ships usually visit more than one port in their total voyage so the priority port is taken into consideration for the cargo stowage plan to save time in unloading processes at ports.

To summarize, a total of five criteria (input parameters) are chosen to decide how to plan the stowage of dangerous goods on a ship which are; danger classes of goods, obligations about whether the cargo should be stowed on deck or under deck, placement clear of living quarters and unloading priority of the cargo. Table 2 summarizes the dimensions of criteria used in this study [14].

Table 2. Dimensions of Evaluation Criteria for Classification of Containerized Dangerous Goods in Stowage Plan

Criteria	Dimension
Danger Class	IMDG Code Classes
On Deck Only	Yes =1 No = 0
In Hold Only	Yes =1 No = 0
Clear of Living Quarters	Yes = 1 No = 0
Unloading Priority	1 = First Port 2 = Second Port (there are 2 ports in this study)

While creating a decision support system for stowing the dangerous cargo, regulations about keeping the cargo clear of living quarters should be taken into account, as well as different stowage categories which provide the information on whether the cargo should be carried in an open space or indoors. For example, cargo space 1-d is for the cargo which is carried in open cargo space at the fore side of the ship, while cargo space 2-h is for the closed cargo hold in amidships.

Table 3 illustrates a schematic diagram of a cargo ship. Cargo stowage areas are roughly split according to IMDG stowage rules.

Table 3. Ship Stowage Parts

		3	2	1	
Poop deck	Accommodation	3- deck (3-d)	2- deck (2-d)	1- deck (1-d)	D
Steering room	Engine room	3- hold (3-h)	2- hold (2-h)	1- hold (1-h)	H

Cargo ships usually have accommodation near the poop deck. Cargo holds between bow and accommodation area are divided into three parts. Vertically, cargo can be stowed either on deck or in a hold. The poop deck is used for stowage as well. The seven different parts are determined for modelling of the stowage of cargo depending on the danger.

3.2 Network building

Several parameters and variables which define the network and which have an impact on the performance of the network have to be decided on; while designing a neural network. The number of layers, the number of processing elements in every layer and the number of synapses that are connected to each node are the main factors which are necessary in the determination of the architecture. In addition, it is important to choose the appropriate activation function of the hidden nodes and output nodes, as well as the training algorithm, data transformation and normalization methods, training and testing sets, and the performance criteria [17].

3.2.1 Network structure

A Multi-Layer Perceptron (MLP) model was chosen for the classification of containerized dangerous goods in a stowage plan due to its simple architecture and algorithm [15]. The Learning method of the Artificial Neural Network model is contextualized as supervised learning, specifically with a back-propagation algorithm for the classification in their network building method suggested by Partovi and Anandarajan [13]. The activation function is generally taken as a hyperbolic tangent or logistic sigmoid in the hidden layer [13, 14, 15]. The activation function is important and it depends on the nature of the output of the network. Both the hyperbolic tangent and logistic sigmoid were considered to compare the results.

3.2.2 Determination of hidden layer number and nodes in hidden layer

Two hidden layer networks may slow the learning rate and affect the overall performance of the network [16]. Therefore, only one hidden layer is used for the network. After determination of the hidden layer number, the number of nodes in the hidden layer has to be identified by trial and error. The number of neurons in the hidden layer is calculated based on the five-fold cross validation method.

In five-fold cross validation method, the number of nodes in the hidden layer is calculated by a step by step training of five subsets from training data, in order to select the model which minimizes the generalization error. Training data is divided into five disjointed subsets. One of these subsets is held as validation data and the other four subsets are utilized as the training data

set. The network is run five times by a thousand iterations which can be selected by the user intuitively and by changing the number of nodes from two to twenty in the hidden layer. The minimum of the mean square error (MSE) of training and cross validation data, which is obtained from the experiments, is noted. Then, the first subset of the input is fed back into the training set and second subset is chosen as the validation set and training is repeated again while noting the minimum MSE for the second subset.

This procedure is performed until all five subsets are used as validation sets and we receive the result containing the data from a minimum MSE for five subsets for different numbers of nodes in the hidden layer [14]. The MSE or mean squared error function calculates the accuracy rate of the configuration model by determining the difference between the output of the model and the desired output as can be seen in equation 1.

$$MSE = \frac{1}{n} x \sum_{i=1}^{n} (d_i - y_i) \quad (1)$$

The average of the minimum MSE for five subsets is calculated and the network model with hidden nodes which has the lowest average of minimum MSE for cross validation data is chosen as the best configuration.

The learning process should be stopped when the network reaches a pre-defined criterion. The training is stopped either when training performance reaches the target performance or when a specific epoch number is achieved. In our Multi-Layer Perceptron network model, the stopping criterion for the training process was marked as the minimum of mean square error (MSE) or the point when the network reaches a certain number of epochs. Çelebi and Bayraktar have stopped training of the neural network as the epoch number reached 1000 iterations or the MSE for the cross validation set drops below the threshold value of 0.01 [14].

The learning rate of the network is dependent on the step size and the momentum in each layer. Ghate and Dudul (2010) have evaluated optimal parameters for the multi-layer perceptron model with three layers and have found that optimal step sizes should to be 1.0 and 0.1 for hidden and output layers respectively and moreover, for the momentum of hidden and output layers the optimal value was determined to be 0.7.

The network parameters for the neural network are given in Table 4 as a summary. Neurosolutions 5.0 software was used to run the neural network model for the classification of containerized dangerous goods in a stowage plan. The study was conducted on 102 dangerous packaged goods or containers.

Table 4. Network Parameters for the proposed ANN Model

Learning Method	Supervised
Learning Model and Type	Multi-Layer Perceptron with back propagation algorithm
Performance Function	Mean Square Error (MSE)< 0.01
Number of Hidden Layers	1
Number of Neurons in Hidden Layer	To be determined by Five Fold Cross Validation Method
Transfer Function	Sigmoid functions
Number of Input Neurons	5 (Danger Class, On Deck Only, In Hold Only, Clear of Living Quarters and Unloading Priority)
Number of Output Neurons	7 (1-d, 1-h, 2-d, 2-h, 3-d, 3-h and poop deck)
Hidden Layer Step Size	1.0
Output Layer Step Size	0.1
Momentum for Hidden and Output Layer	0.7
Number of Maximum Epoch	1000 iterations
Learning mode	Batch

From the total data, approximately 85% (70% training and 15% cross validation) of data was selected as training and about 15% of data was used as testing data as suggested by Ghate and Dudul (2010) [18]. For determination of hidden nodes in the hidden layer for classification of containerized dangerous goods, accuracy was assessed via 5-fold cross-validation, with model tuning by a cross-validation nestled within the training samples. Evaluation data for the 5-fold cross validation method consists of 85 data, of which 68 taken as training data and 17 are in the validation set.

The structure of the neural network which will have the minimum Mean Squared Error (MSE) at the end of the training process was chosen for the evaluation of the testing data.

Data for 17 dangerous packaged goods or containers are left out for the testing process to check the validity of the trained network.

The training data set is divided into 5 disjointed subsets; one of these subsets is retained as cross validation data and others are selected as training data subsets. For a different number of hidden neurons, the network is run 5 times by 1000 iterations by choosing one subset as cross validation data from the divided 5 subsets until all subsets has been used as validation data once. The minimum MSE for training and cross validation data is recorded for each subset.

The average minimum MSE for five subsets is calculated for each number of hidden neurons in the hidden layer. The neural network was run for sigmoid activation function. The neural network with 12 nodes in the hidden layer, gives the lowest MSE data as 0.00993, in the five-fold cross-validation method for sigmoid function.

After the number of hidden neurons in the hidden layer has been determined to be 12 for sigmoid function model, networks have been trained with 85 data (68 training and 17 cross validation data) 2 times each by 10 runs and 1000 iterations with randomized initial weights in order to avoid networks becoming stuck at local minima. As can be seen from the results of training the network with a sigmoid function network, the minimum mean squared error is 0.00737 which is shown in Table 5. Training for the network with sigmoid function was stopped at the 5th run and 711th iteration.

Table 5. Results of Training for Sigmoid Transfer Function

Best Networks	Sigmoid Function
Run #	5
Epoch #	711
Min. MSE	0.00737

Finally, the network chosen consists of 5 nodes in input layer, 12 nodes in hidden layer and 7 nodes in output layer as shown in. (Figure 2).

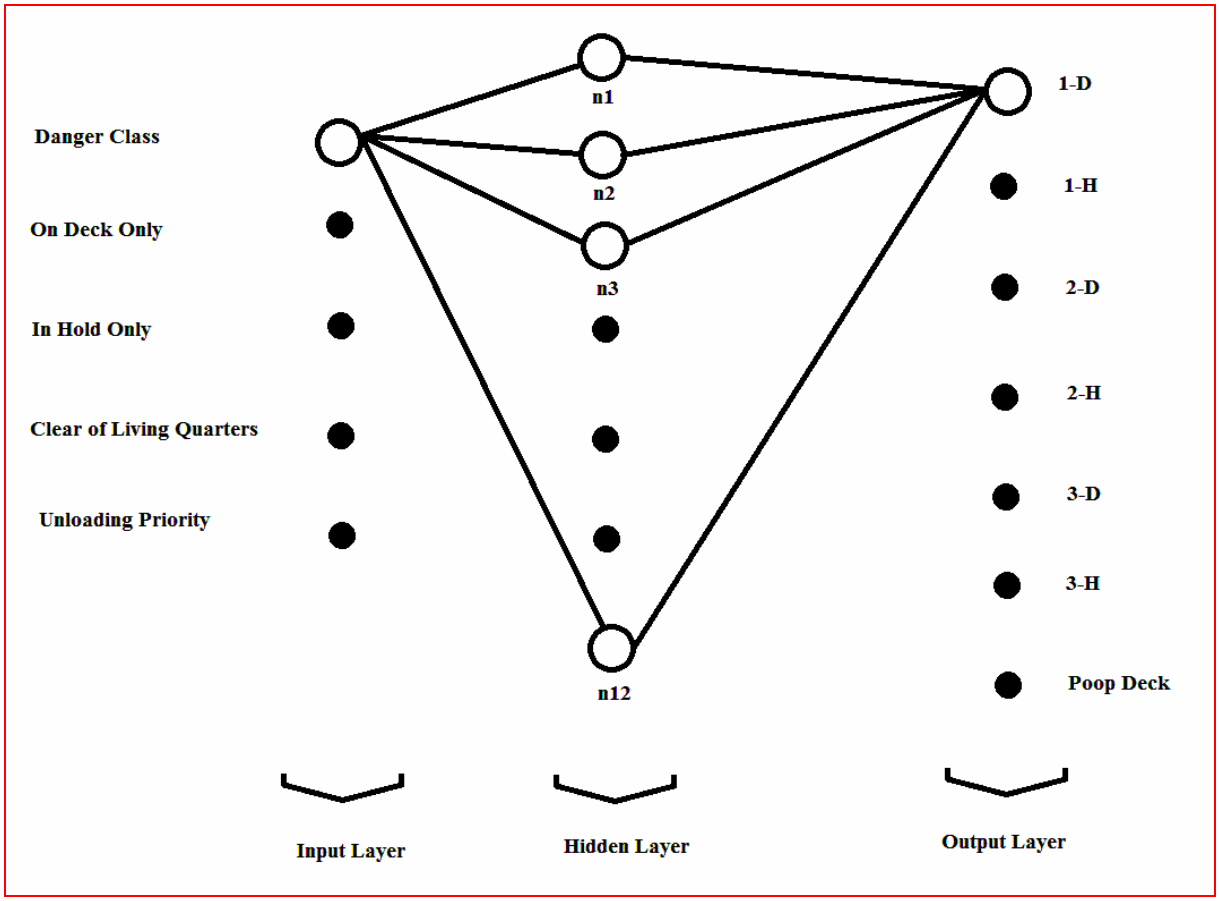

Figure 2 The ANN model used for this study.

3.3 Testing the neural network

In order to validate the training results, 17 dangerous containers data which were not introduced to the network previously, were used for testing process. The results of overall testing of the network are given in Table 6.

Table 6: Results of Testing Process for the Proposed Neural Network.

							Poop Deck	Overall
MSE	0.0438	0.0170	0.0586	0.0171	0.0184	0.0233	0.0203	0.0297
NMSE	0.2111	0.1634	0.2822	0.1649	0.0887	0.1294	0.0978	0.1684
MAE	0.1447	0.1066	0.1647	0.1101	0.1043	0.1126	0.1159	0.1238
Min Abs Error	0.0202	0.0227	0.0348	0.0315	0.0008	0.0128	0.0130	0.0008
Max Abs Error	0.6821	0.2828	0.8065	0.2305	0.3048	0.3749	0.2932	0.8065
R	0.8932	0.9371	0.8502	0.9325	0.9660	0.9498	0.9691	0.9278
Percent Correct	100	0	100	-	100	100	-	88.24

As can be seen from the performance measurements, the overall correlation (r) of the testing is 0.9278 for the testing data. The mean absolute error for the overall testing network is determined to be 0.1238 which shows that the developed neural network gives results that are acceptable solutions.

5. CONCLUSIONS

The stowage of dangerous goods on a ship has great importance due to the high risk of the cargo. Inappropriate stowage of goods during loading the ship is the main factor that contributes to the release of the dangerous goods on board. Although there have been several grievous disasters in the previous years due to the deficiencies in application, the stowage of dangerous goods or containers is still typically carried out in the traditional way which takes more time and pays less attention to safety during planning.

The traditional stowage method of dangerous goods or containers on a ship uses the UN number and needs expert staff for planning. Yet, in some cases, it is known that there are errors due to the time constraints and insufficient care in application. The comparison of neural network output and desired data are given in Table 7.

Table 7. Desired Data and NN Output

1-d Output	1-h Output	2-d Output	2-h Output	3-d Output	3-h Output	poop deck Output	Output (Symbolic)
-0.0488	0.02268	-0.0452	0.03147	0.30483	0.77744	0.29317	3-h
0.86475	0.11486	0.84633	0.11428	0.05658	-0.0447	0.06183	1-d
0.12443	-0.0477	0.1306	-0.0473	0.89647	0.02321	0.83881	3-d
0.86419	0.11687	0.8504	0.12561	0.06071	-0.0463	0.0604	1-d
-0.0494	0.03996	-0.0466	0.03746	0.16978	0.81546	0.17644	3-h
0.16016	0.71723	0.19104	0.76954	-0.0471	0.10309	-0.0466	2-h
0.03761	-0.0406	0.0524	-0.0426	0.7641	0.15084	0.74568	3-d
0.82163	0.09964	0.80652	0.11411	0.06769	-0.0441	0.06416	1-d
-0.0426	0.02956	-0.0376	0.04204	0.27609	0.62513	0.23005	3-h
0.04867	0.79468	0.07947	0.82606	-0.0517	0.30377	-0.05	2-h
0.02017	-0.0455	0.03482	-0.0455	0.89156	0.15434	0.85912	3-d
0.10224	-0.0482	0.117	-0.0475	0.91393	0.02907	0.85735	3-d
-0.0526	0.16763	-0.0502	0.18442	-0.0008	0.9027	0.01305	3-h
0.13792	-0.048	0.14551	-0.0464	0.91695	0.01284	0.85172	3-d
0.68208	0.13208	0.74467	0.1885	0.01099	-0.0404	0.02952	2-d
0.73453	0.21044	0.73393	0.22619	0.04485	-0.0402	0.03967	1-d
0.76216	0.16106	0.76154	0.17418	0.06499	-0.0425	0.0578	1-d

This study aims to propose a Decision Support System for proper stowage of dangerous goods on a ship. Multi-Layer Perceptron (MLP) as an ANN has been used for determining the proper locations of dangerous goods in a stowage plan. The proposed solution method has shown very good performances in terms of suitable and fast planning of stowage and segregation.

The model gives ample possibilities for future research on a number of themes. First of all, this study can be considered as combining an overall ship loading problem with consideration to different types of containers, ship sizes, and ports as well. Secondly, the other steps associated with management of dangerous containers such as packaging or placement in containers can be classified by using an ANN model. Thirdly, different criteria may be considered as evaluation criteria depending on the nature of loading operations. Finally, the problem can be solved with other methodologies and the study can be extended to be used in comparisons with the results acquired through the application of a genetic algorithm.

7. REFERENCES

[1] CHEUNG RK, CHEN CY., *A Two-Stage Stochastic Network Model and Solution Methods for the Dynamic Empty Container Allocation Problem.* Transportation Science. 1998; 32 (2): 142-62.

[2] ZORBA Y., KIŞI H., *Uluslararası Deniz Ticaretinde Tehlikeli Yüklere ilişkin Emniyet Yönetimi Ve Türk Limanları Üzerine Uygulama.* Dokuz Eylül Üniversitesi Denizcilik Dergisi. 2009; 1 (1): 27-45. Turkish.

[3] BURGESS K., *Of critical concern.* Seatrade May/June. 2006; 31-33.

[4] MUNICH RE GROUP., *Containers Transport Technology Insurance.* 2002.

[5] MAWSON JP., *Issues arising from the development in design and operation of Container Ships. The impact on the safe carriage of goods and crew.* MA Dissertation. University of Greenwich, Greenwich Maritime Institute, Greenwich, UK. 2003.

[6] ELLIS J., *Analysis of accidents and incidents occurring during transport of packaged dangerous goods by sea.* Safety Science. 2011; 49: 1231-37.

[7] THOMAS BJ., *Management of port maintenance: A review of current problems and practices.* 1989.

[8] SCIOMACHEN A, TANFANI E., *A 3D-BPP approach for optimising stowage plans and terminal productivity.* European Journal of Operational Research. 2007; 183: 1433-46.

[9] OZGUR M., *Hava Trafik Yol Kontrol Sektöründeki Çatışmaların Bilgi Tabanlı Karar Destek Aracıyla Çözümü.* Yüksek Lisans Tezi, Anadolu Üniversitesi, Sivil Havacılık Anabilim Dalı. 2007. Turkish.

[10] MCCULLOCH W., PITTS W., *A logical calculus of ideas immanent in neural activity.* Bulletin of Mathematical Biophysics. 1943; 5: 115-33.

[11] ZHANG GP., *An investigation of neural networks for linear time-series forecasting.* Computers and Operations Research. 2001; 28: 1112-83.

[12] HAYKIN S., *Neural Networks: A Comprehensive Foundation.* New Jersey: Prentice Hall; 1999.

[13] SILVA L, MARQUES J., Alexandre LA. *Data classification with multilayer perceptrons using a generalized error function.* Neural Networks. 2008; 21: 1302-10.

[13] PARTOVI FY, ANANDARAJAN M., *Classifying inventory using an artificial neural network appoach.* Computer and Industrial Engineering. 2002; 41: 389-404.

[14] CELEBI D, BAYRAKTAR D., *An integrated neural network and data envelopment analysis for supplier evaluation under incomplete information.* Expert Systems with Applications. 2008; 35: 1698-710.

[15] TURER S, AYVAZ B, BAYRAKTAR D, BOLAT B., *Tedarikçi Değerlendirme Süreci için bir Yapay Sinir Ağı Yaklasımı: Gıda Sektöründe bir uygulama.* Endütsri Mühendisliği Dergisi. 2009; 20 (2): 31-40. Turkish.

[16] MASTERS T., *Practical Neural Network recipes in C++.* Academic Press Inc; 1993.

[17] ZHANG G, PATUWO BE, HU MY., *Forecasting with artificial neural networks: The state of the art.* International Journal of Forecasting. 1998; 14: 35-62.

[18] GHATE VN, DUDUL SV., *Optimal MLP neural network classifier for faultdetection of three phase induction motor.* Expert Systems with Applications. 2010; 37: 3468-81.

DYNAMIC ANALYSIS FOR CALCULATING THE MARINE STRUCTURAL DESIGN BY USING THE FINITE ELEMENT METHOD

[1]ION ALINA, [2]TICU IONELA–RODICA

[1,2]*Constanta Maritime University, Romania*

ABSTRACT

The design of ship structures is a technical process that includes a series of structural analysis and the synthesis itself – when from a range of sheets and profiles, the project of the ship's resistance structure is done. In this process, a number of requirements of reliability and efficiency are taken into account and they must be satisfied so that after the materialization of the project to achieve an optimal construction

Keywords: *material, resistance, finite elements, design.*

1. INTRODUCTION

Throughout history, shipping has played a key role in transport and trade. Today, about 95 % of traded goods are transported by sea. The remarkable expansion of trade and industry markets in the last 50 years would have been impossible without a stable, secure and diversified network of naval, maritime and river transport.

The Finite element method (FEM) allows to numerically solve the most diverse problems of solid Mechanics (which also includes the Structural Mechanics of ships), but also from many other areas (Fluids, Thermodynamics, Electromagnetism, etc.). The MEF idea consists in modeling the field studied through a number of elements with finite dimensions, connected to each other in a number of nodal points in which the solution is sought. The operation is called finite element mesh. In structures, the values of linear and, sometimes, angular shifts are determined in nodal points. The Finite element model must simulate as correct as possible the behavior of the real structure which is and remains continue even after deformation and each infinitesimal element inside of it or on its boundary should be in equilibrium under the action of internal and external forces.

2. CURRENT STATUS IN THE FIELD OF MARINE STRUCTURAL DESIGN

The design of ship structures is a technical process that includes a series of structural analysis and the synthesis itself – when from a range of sheets and profiles, the project of the ship's resistance structure is done. In this process, a number of requirements of reliability and efficiency are taken into account and they must be satisfied so that after the materialization of the project to achieve an optimal construction.

Among these requirements, the following facts are stated: safety with a coefficient of risk as small as possible to a minimum weight; maintaining the original quality throughout the operation period; competitive workload and manufacturing cost, minimum envelope structures for achieving maximum interior spaces; easy accessibility for maintenance, inspection and possible repair; wider use of standardized components; comfort and pleasant overall appearance.

Until very recently, the structural ship design was done with predilection (sometimes even exclusively) by Rules of Classification and Shipbuilding Societies (Books), set mostly based on experience in design, construction and operation.

The Book's rules are largely empirical and based on experience and feedback from ships in service. They are formulas and sometimes simplified algorithms applicable to all structural elements of a type of ship. These rules were obtained by tracking a multitude of ships at all stages and by transforming findings observed in established rules that apply not only in the design stage, but also in the construction and approval stages. In the construction stage, a careful control in all key stages is run and from the moment of entry into service, regular checks of class recertification are run. Structural integrity is pursued until the ship is out of service, by estimations on its lifetime. If damages are found or accidents caused by failure of structural elements happen, the classification society can update the rules. Achieving the maximum efficiency of an optimal algorithm to design a certain type of ship can last decades.

Although it is widely recognized the relative ease of designing structures by Registration Rules - which provides simple scaling relations for certification, the extension of water transport (the cheapest means of transport), functional/constructive diversification of vessels and the increase of their size , the change of ratios between the main dimensions required by new forms of transport and the categories of goods transported, as well as the increasing requirements regarding the handling of dangerous goods and environmental protection require increasingly a joint design based both on Rules and calculation, Rules serving to an initial operative assessment. For the types of ships that do not fall into Rules, the design by direct calculation is indispensable.

The very development of rules for such vessels requires research teams to seek new methods of design, by direct calculation. Designing only based on algorithms of the classification societies have a number of disadvantages and risks.

Firstly, structural failure modes are numerous, complex and interdependent and the simplification brought by the rules can not estimate the exact extent to which the vessel is considered safe. In other words, the difference between necessity and oversize cannot be made. Therefore, sometimes these formulas are not completely effective. In some cases, it appears that excessive oversizing of some ships produces waste throughout its service. Moreover, oversizing does not always necessarily mean also safety. For example, in the case of vibration and fatigue, the oversizing of a structure might be a negative factor for its behavior in operation.

Secondly, formulas and algorithms of rules are aiming at avoiding structural failure. Although there are several ways to reach the same result, the particular method required by the rules is not always best suited to the specific features and tasks of the ship, given the economic criteria. Sizing relations under the Registration Rules is often aprons; they refer to a specific range of situations in which the structure can be found. It is possible that these relations, although possibly having a fairly wide applicability, may not match their intended purpose, efficiency criteria of the designed ship and other requirements of the beneficiary. The design process must be developed based on the functionality of the ship, trying to optimize structures in order to achieve the desired purpose.

Thirdly, and perhaps most importantly, these rules imply the introduction of a number of simplifying assumptions. Therefore, they can be used only within certain limits (application conditions of the simplifying assumptions). Beyond these limits, formulas lose their accuracy. The history of structural design is rich in examples of defective design (ships, bridges, and aircraft) in which methods proven by experience were used, but the accuracy and application limits of which were not sufficiently known from scientific point of view.

The computer-aided rational design has as starting point, the goal that must meet the ship and takes into account all aspects of performance and structure, achieving precise estimations about the hull's behavior. Designed ships must fulfill their mission in the safest way possible and under economic conditions. Compared to traditional design methods, the design on rational grounds requires a greater computational effort that would be impossible without the help of computers. Nowadays, the naval design is computerized and semi-automatic (not fully automated because during a project, a number of specific decisions on objectives, priorities and criteria of verification, constraints etc. must be made).

Due to the development of information technology, in the last half century, numerical and analytical methods have also strongly developed. Introducing the finite element method has allowed new approaches to the complex issues of structural analysis. By using the finite element method, more accurate calculations on resistance and assessment criteria for fatigue of structures can be achieved.

The finite element method also allows the iterative optimization of size structures until the fulfillment of all requirements. Without the advanced calculation procedures based on finite element analysis, many of the vessels placed in service in the last 40-50 years could not have been built: modern vessels to transport containers, vessels for the transport of oil, liquefied gas, large passenger ships, catamaran and trimaran ferryboats etc. Figure 1.1 shows the nodes network of the finite element model analysis of a medium sized container ship). The evolution of the first container ships built in the 60s (with maximum capacity of 1000 TEU) to huge container ships that can carry more than 13,500 TEU was only possible due to the development of computational techniques.

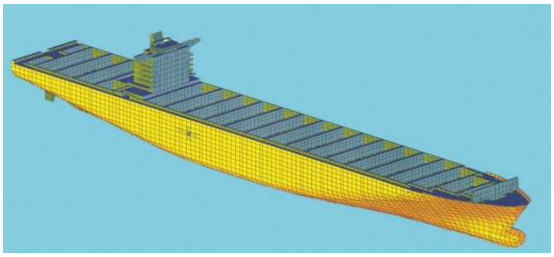

Figure 1 Nodes network of finite elements of a medium sized container ship

2.1 Forces acting on the hull

Forces (or loads) acting on the hull come either from interacting with the gravitational field (force of gravity) and the environment (forces created by water and wind pressure) or are generated by the vessel in its movement. These loads determine the emergence of stresses in the hull and structures within it. Most often stresses caused by the load are influenced by the size of the vessel, the shape of the hull, the type and distribution of the load. After the way they vary in time, loads can be static, quasi-static or dynamic. Loads of all three categories are commonly acting on the hull. To decrease the computation time, tests are usually performed separately, the overall response of the structure being determined by summing the partial results.

2.2 Static loads

It is believed that this type of loads is constant throughout the time they are acting on the vessel. This includes: all hydrostatic loads: external pressures generated on the wetted surface of the vessel and internal pressures generated by liquid cargo; all the forces of gravity: weight of the empty ship, cargo, equipment, crew etc., reactions of supports when docking; thermal stresses.

2.3 Quasi-static loads

Quasi-static loads are those loads with maximum frequency lower than the minimum natural frequency of the structure. The quasi-static analysis is a static analysis in which, after motion estimation and its characteristics, the effect on the structure is considered by introducing inertial forces. Examples of stresses that are submitted to quasi-static analysis are:

- the distribution of the dynamic pressure on the hull, caused by a combination of wave action and movement of the ship; the pressure, thus defined, will have two components: one, mainly determined by wave action in the absence of the vessel and an additional component conditioned by the presence of the ship in the wave;

- tasks given by the dynamic pressure distribution on the hull during oscillation on calm water ; in this case, there are two components: a resistance component (wave) and a component of inertia of the driven masses of water in motion at the same time as the ship; stresses that develop during berthing and departure maneuvers at dockside .

2.4 Dynamic loads

Dynamic loads are considered those loads that have a frequency sufficient to induce a response to the hull structure. In these cases, stresses with low amplitudes can create at resonance, high amplitude variations of stresses and strains.

Examples of loads dynamically approached : dynamic loads induced by the propeller on the hull ; loads generated by alternating movements of the main engine components ; hydro-elastic loads resulting from the interaction of the hull projections with the stream lines; loads induced by waves, the frequency beam of which overlaps the natural frequency of vibration of the hull, a phenomenon called *springing*; loads resulting from the wave hitting the stem, or the flared board, or other parts of the hull structure, including the effects of depositions from the deck; this phenomenon is called *slamming*; impact loads can induce temporary hull vibrations, called *whipping*. If the force-displacement relation is linear, the dynamic issue can be solved in the frequency domain. Transformed operator.

3. OTHER LEVELS OF ANALYSIS

In the first years of application of the finite element method for designing vessels, the biggest problem was the calculation power. In addition, the finite element analysis on the entire ship involved the creation of a mathematical model of large dimensions, therefore the analysis could have errors and their source was difficult to discover. This is the reason why, simulations were not conducted on the whole ship, but on ship modules, consisting usually of maximum 3 compartments. These modules are analyzed and optimized separately.

The process can take a very long time, but in this way, issues which may pass unnoticed, can be discovered if we analyze the entire model. In order to take account of the interaction of a module with the rest of the structure, various techniques have been developed.

Due to the difficulties and uncertainties in determining the interactions between modules, recently the entire ship began to be modeled with finite elements. The continuous improvement of computer hardware and specific software come to support these approaches. At the level of main elements and at local level, a dynamic analysis is performed only if required significantly by sources that cannot be avoided, such as propellers and main engines. In most cases, only a modal analysis is conducted in order to avoid resonance with the vibration sources.

On the other hand, there are some cases where dynamic analysis is required. We are talking about ships with relatively flexible structure that may be powerfully required by the springing phenomenon; these vessels typically operate at high speeds and have powerfully flared edges. This includes also container ships.

4. CONCLUSIONS

Structural design of a ship involves formulating a mathematical model that can estimate as accurately as possible the way it behaves in loads stressing it. According to the adopted program with finite elements, the model is discretized and submitted to the loading with external forces and bindings.

The results are subject to safety criteria (in order to certify the strength of the structure) and optimization, so that the response of the structure to the loading action would optimally correspond to one or more objectives.

The continuous expansion of markets and the development of industry in recent years have not been possible without a stable and increasingly diversified shipping network (sea and river), conducted under conditions of maximum protection of the crew life, the environment and the capital invested. Because of these aspects, the issues of design and strength calculation of the ship structures have always remained important and current, of great interest to ship owners and classification and shipbuilding companies and stuck to the attention of engineers and researchers dealing with design, construction and shipping issues.

5. REFERENCES

[1]. ALINA ION, - *" Research on the calculation of a container ship structural resistance to wave oscillations„* Phd thesis; 2014

[2]. ALINA ION, PAUL BOCĂNETE, RODICA IONELA ȚICU, *„The modern design of naval structures"* Analele Universității Maritime din Constanta, România, Vol. 20 – 2013, ISSN 1844-5381

[4]. ARGYRIS J., KELSEY A., *Sovremënye metody rasčjota složynyh statičeskih neopredelimyh sistem*, trad. din engl., redactor *Filin A. P.*, Sudostroenie, Leningrad, 1961

[5]. ANSYS Structural Aanalysis Guide ,ANSYS ,INC Canonsburg,PA,1997

[6]. ANSYS, Mechanical User Guide, Release 14.5, 2012

[6] BAARHOLM, G. S., AND MOAN, T**.,** *Efficient estimation of extreme long-term stresses by considering a combination of longitudinal bending stresses,* J. MarineScience and Technology, Vol. 6, Issue 3, 122–134, 2002

[7] BARKANOV, E**.,** *Introduction to finite element method*, Institute of Materials and Structures, Riga, 2001

[8]. BEARDS, C. F., *Engineering vibration analysis with application to control systems*, Arrowsmith Ltd, Londra, 1995

[9]. BATHE K.-J., *Finite element procedures in*

engineerng analysis, Prentice-Hall, New Jersey, 1982;
[10]. BEARDS, C. F., *Engineering vibration analysis with application to control systems*, Arrowsmith Ltd, Londra, 1995
[11]. BATHE K.-J., *Finite element procedures in engineerng analysis*, Prentice-Hall, New Jersey, 1982 1 *Beards, C.F., Engineering vibration analysis with application to control systems*, Arrowsmith Ltd, Londra, 1995
[12]. BESCHEA N., *Rezistența materialelor – capitole speciale*, Editura Didactică şi Pedagogică, Bucureşti, 1971
[13]. ZIENKIEWICZ O. C., *The Finite Element Method in Engineeting Science*, McGraw Book Company, London, 1972
[14]. ZIENKIEWICZ O.C., TAYLOR R.L., *The finite element method*, vol I, Butterworth - Heinemann, Oxford, 2000;
[15]. ZIENKIEWICZ O.C., TAYLOR R.L., The Finite Element Method for Solid and Structural Mechanics, Sixth Edition, 2005

THE ARCHITECTURE OF SOFTWARE SHIP POWER V1.0

[1]XHAFERAJ BLENARD, [2]LAPA KRISTOFOR, [3]DUKAJ AGRON

[1,2]Department of Naval and Mechanical Engineering, University of Vlora "Ismail Qemali", Vlore, Albania
[3]Department of Maritime Science, University of Vlora "Ismail Qemali", Vlore, Albania

ABSTRACT

Use of software has spread more and more in all application areas, becoming more and more relevant and critical for the development of design process of engineering product. Also in new design of ships the use of software is an important element for the development of the project with quality and on time. Prediction of power and resistance of the ship is one of the most important components of ship design process.

The purpose of this paper is to present the architecture of the computer program, Ship Power V1.0, for the prediction of resistance and power of the ship. The software predicts resistance and power, as well as the resistance coefficient and power propulsion factor.

The software is written in Visual basic, taking in consideration the requirement of quality of ISO 9126. The current version of software configuration is based on MARIN regression analysis models, but it is, also, conceptualized to include easily other regression analysis models, to further enhance its range of application. The program gives a detailed report and graphical representation of effective resistances and power versus speed. Ship Power can be used, with satisfactory results, during the early stage of ship design process for a rapid prediction of resistance and power, or to carry out the optimization of principal dimensions, in order to find the best solution.

Keywords: *Resistance, Power, Ship Design, Regression Analysis.*

1. INTRODUCTION

Ship design process requires the recognizing as soon as possible of resistance and power, needed in the conditions of maximum displacement, so that the ship can advance with the required navigational speed. Consequently, in early stages of ship design process is needed a rapid assessment of some hydrodynamic quality, specially the power and resistance. Importance of first and fast determination of resistance and power, from the early stages of ship design, is emphasized in the relevant literature of ship design. [1],[2],[3].

Current practice of naval hydrodynamic design also wildly uses mathematical models. Developments in field of computers and programming have facilitated the work with very long and sophisticated mathematical models.

The estimation of propulsive power enables the estimation of size and weight of propulsion plant, as well as estimates for fuel consumption and operating costs. One of the options available for ship designer to determinate the resistance and power are the models based on regression analysis.

Ship resistance prediction based on statistical regression methods has been a subject of some interest for a number of years. In literature there are statistical methods, such as Holtrop and Holtrop-Mennen methods; Van Oortmersen's method, Savitsky method, etc., that enable the assessment of resistance and power of ship in early design stage. These statistical methods are based on the traditional naval architectural parameters of hull form; for example, block coefficient, longitudinal centre of buoyancy, prismatic coefficient, etc.

Most of these methods include a large number of variables and mathematical operators. During the application these methods can be associated with errors, which are transmitted step by step, thereby affecting on the accuracy of the final result. Some of these methods, because of their complexity, are tedious and consume a very long time, if applied manually. All these problems may be passed if the calculations of resistance and power, by theoretical models, will be realized with help of computers and computer programs.

In market there are advanced computer programs which enable predictions of resistance and power, but for their application these software generally require the development of the detailed geometry of ship. Recently in the Department of Naval Architecture and Marine Engineering at University of Vlora (Albania) has started the work for the development of an integrated computer program, which will be able to evaluate, according to a certain level of accuracy, the propulsive characteristics of a wide range of ships during the early design stages. The first version of this software has been developed taking into account the requirements of the International Quality Standard ISO/IEC 9126 of software product. ISO 9126 not prescribe specific quality requirements, but defines a general framework for the evaluation of software quality and that this is in fact one of its strengths as it is more adaptable and can be used across many computer systems. Its characteristics may be applicable to every kind of software, including computer programs and data contained in firmware.

The main objective set for the development of this program have been that the software be easy to use, minimize the difficulties and the required computation time, provide estimates with a satisfactory accuracy, provide estimates for various combinations of data; assist the user step by step.

The program performs calculations, within a range of speeds and a whatsoever step, declared by the user, without limit on the number of speeds for the calculations. The program gives a detailed report of the components of resistance, coefficients of resistance, power and propulsive factors. These reports can be

generated either in printed or in electronic format, according to the format chosen by the user. Likewise, the program represents graphically the results of calculations of resistance and power in function of speed. The program is developed in "Visual Basic", and the reports of calculations are realized by the help of the "Crystal Reports".

2. MATERIAL AND METHODS

2.1 The software quality. ISO norms

According ISO 9126 the software quality is defined as the totality of features and characteristics of a software product that bear on its ability to satisfy stated or implied needs. The quality of a software product concerns characteristics relating to different points of view. The characteristics of software quality are defined as "internal", "external" and "of use". The internal characteristics relate to the intrinsic quality of the software as, for example, its modularity, complexity, understandability, defectiveness, compliance to standard etc. The characteristics of internal qualities can affect the external characteristics and these on those of use. The model that best represents the various characteristic of software quality, is that described by ISO / IEC 9126.The original model defined the following six quality characteristics of software product (see also Figure 1). [4],[5].

- Functionality – A set of attribute that bear on existence of a set of functions and their respective properties. The functions are those that satisfy stated or implied needs.
- Reliability - A set of attribute that bear on the capability of software to maintain its level of performance under stated conditions for a stated period of time.
- Usability – A set of attribute that bear on the effort needed for use, and on the individual assessment of such use, by a stated or implied set of users.
- Efficiency – A set of attribute that bear on the relationship between the level of performance of the software and the amount of resources used, under stated conditions.
- Maintainability- A set of attribute that bear on the effort needed to make specified modifications.
- Portability – A set of attribute that bear on the ability of the software to be transferred from one environment to another.

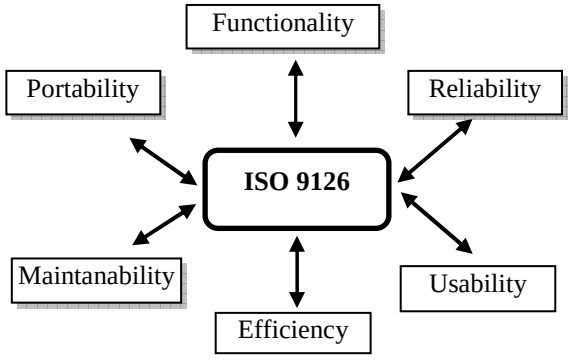

Figure 1 The Model of ISO 9126 [4],[5]

These six characteristics are further subdivided into a number of sub-characteristics (see Table1).

These characteristics and sub characteristics are taken in consideration during the development of Ship Power V 1.0.

Table 1. Characteristics and sub characteristics of ISO 9126 [4], [5], [6]

Characteristic	Sub-characteristic	Explanation
Functionality	Suitability	Can software perform the tasks required?
	Accurateness	Is the result as expected?
	Interoperability	Can the system interact with another system?
	Security	Does the software prevent unauthorized access?
Reliability	Maturity	Have most of the faults in the software been eliminated over time?
	Fault tolerance	Is the software capable of handling errors?
	Recoverability	Can the software resume working and restore lost data after failure?
Usability	Understandability	Does the user comprehend how to use the system easily?
	Learn ability	Can the user learn to use the system easily?
	Operability	Can the user use the system without much effort?
	Attractiveness	Does the interface look good?
Efficiency	Time Behaviour	How quickly does the system respond?
	Resource Utilization	Does the system utilize resources efficiently?
Maintainability	Analyzability	Can faults be easily diagnosed?
	Changeability	Can the software be easily modified?
	Stability	Can the software continue functioning if changes are made?
	Testability	Can the software be tested easily?
Portability	Adaptability	Can the software be moved to other environments?
	Install ability	Can the software be installed easily?
	Conformance	Does the software comply with portability standards?
	Replace ability	Can the software easily replace other software?
All characteristics	Compliance	Does the software comply with laws or regulations?

2.2 The operational model of the software

The first and very important element in development of any applicative software is the determination of theories and models which are available in literature. After determining the available models is important to assess the suitability of these methods regarding the accuracy of the results, scope of application, disadvantages and facilities of these methods related to programming.

In determining the mathematical model, that has served as the core of the program, we have had in mind that the mathematical model must be reliable, take into consideration a great number of resistance and propulsive components factors and be easy to modify and improve.

Ship resistance prediction based on statistical regression methods has been a subject of some interest for a number of years. Early work by Scott in the 1970s [1], resulted in methods for predicting the trial performance of single- and twin-screw merchant ships. The theme of statistical prediction was then taken up by Holtrop and Mennen in a series of papers (1977, 1978, 1982, 1988). [1]. Bibliographic researches realized in technical literature indicate that among the mathematical models available the models developed by MARIN (Holtrop & Mennen, 1982; Holtrop 1984) are widely accepted for the estimations of resistance and power at early stages of ship design. [1], [2] These models are the most models used for displacement hulls ($Fn_V \leq \approx 2$). [5]. Also the formats of these models are ideal for computer programming and the mathematical equations of these models include a wide range of parameters.

Holtrop and Mennen model is a complex, physical based model, where the final coefficients were obtained by regression analysis of 334 model tests conducted at MARIN. [1],[2],[7],[8],[9].

Besides the high degree of accuracy that these models have, compared with others models, the mathematical models developed by Marin have also other advantages as they allow the evaluation of the influence of bulbous bow; evaluation of the influence of bow thrusters; evaluation of the influence of different stern types, evaluation of the influence of different half angles of entrance of the waterline.

All these advantages have made the MARIN model as the model chosen to constitute the heart of the developed program. Also the others procedures that are planned to be implemented in the developed program will be formatted around these models.

The model as implemented in the current version of Ship Power calculates the total resistance according the following formula:

$$R_T = R_F(1+k_1) + R_W + R_B + R_{TR} + R_{APP} + R_A + R_{AIR} + R_{MARGIN} \quad (1)$$

Frictional resistance (R_F) is calculated according the ITTC – 1957 formula. Depending on the specific conditions, the form factor (1 + k), appendages resistance (R_{APP}), wave resistance (R_W), additional resistance due to a bulbous bow (R_B), additional pressure resistance due to the immersed transom (R_{TR}), the model ship correlation resistance (R_A) are calculated as in Holtrop (1984) and in Holtrop and Mennen (1982). Air resistance (R_{Air}) is calculated as in Van Manen and Van Oossanen. (1988). Additional resistance for meteorological conditions (R_{Margin}) in the current version of the program is simply calculated as a percentage addition of the resistance in calm seas.

In its current version, all propulsion factors w, t, η_R are calculated as in Holtrop (1984) and in Holtrop and Mennen (1982).

Calculations of resistance coefficients, power, propeller propulsion force, hull efficiency, and quasi propulsive efficiency are realized according the following formulas.

$$C_{XX} = \frac{R_{XX}}{0{,}5 \cdot \rho \cdot S \cdot V^2} \quad (2)$$

$$T = \frac{R_T}{(1-t)} \quad (3)$$

$$\eta_H = \frac{(1-t)}{(1-w)} \quad (4)$$

$$\eta_D = \eta_0 \cdot \eta_H \cdot \eta_R \quad (5)$$

$$P_E = R_T \cdot V \quad (6)$$

$$P_T = T \cdot V \quad (7)$$

$$P_D = \frac{P_E}{\eta_D} \quad (8)$$

Each component of resistance is expressed in function of speed and hull shape parameters. This particular model applies to displacement mono hulls with characteristics, in the range $0.55 \leq Cp \leq 0.85$; $3.90 \leq L/B \leq 14.9$; $2.10 \leq B/T \leq 4.00$; $0.05 \leq Fn \leq 1.00$. [3]. The MARIN model gives results very close to real results if it is applied in the case of tankers, bulk carriers, trawlers, coaster, tugs, containerships, destroyer, cargo liner, roll on roll of, car Ferries. In each case the model has a defined range of the values of Fn, B / T, L/B and Cp.

Before the completion of calculations, in function of ship type, speed and geometric parameters, the program verifies and selects the method of calculation. For Froude numbers up to 0.4 the program follows the calculations of resistance and propulsion factors as described in Holtrop and Mennen (1982), while for Froude numbers above 0.4 the program follows the calculations of resistance and propulsion factors as described in Holtrop (1984).

The program is structured in modular form, where each component of the resistance and propulsion factor is calculated according to an individual procedure and the final result is taken as the sum of the results derived from each procedures. Such a setup provides a better localization of possible problems that may arise during the development of the code, and facilitates modifications in future. Each procedure is tested

individually, providing first the accuracy of evaluation of each component and then the whole result.

Particular attention has been given to the interface of the program, because a well-designed interface pleasant and consonant to the cultural environment in which the product is used has a lot of relevance for end users and is a very important element for the use of the software.

In this first version of program, additional power and resistance for the effects of operational conditions, sea state and fouling, is obtained simply as an increase in percentage of resistance and power in calm seas, where the user simply needs to declare the value of this increase. For the calculation of wind resistance in this version of software is not developed any special evaluation procedure, but it can be included by the user in the percentage increase of resistance and power. In other versions of the program, is intended that this resistance will be evaluated in greater detail.

Before the implementation of calculations the program verifies, if all the necessary data are declared and if these data are written in an appropriate manner. In all cases of irregularities the program signals the user for the problem, creating him the possibility for necessary correction.

In Figure 2 is presented a simplified flow chart of the program.

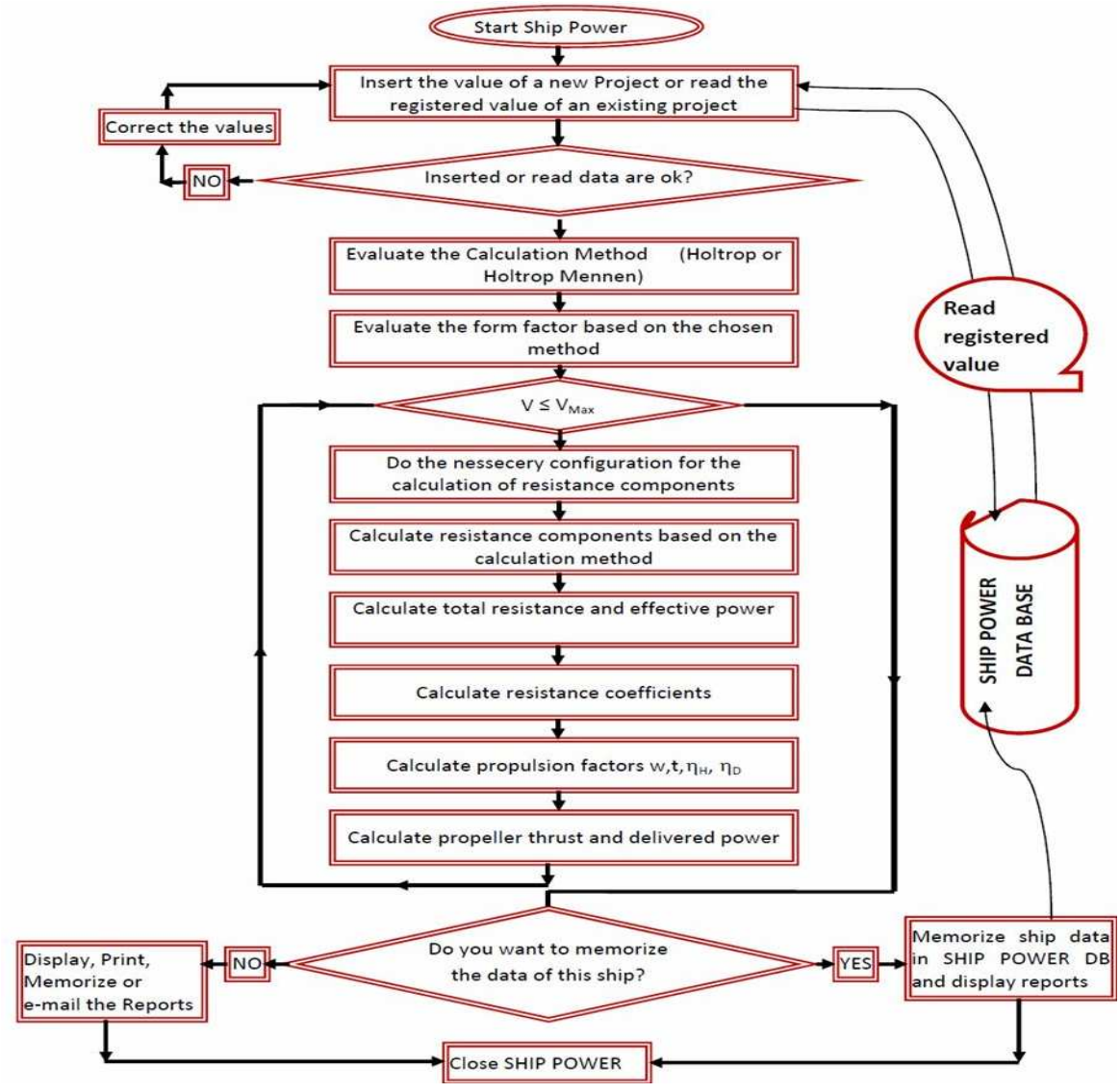

Figure 2 The simplified flow chart of "Ship Power"

3. RESULTS AND DISCUSSION

3.1 Software Interfaces

The software has two main interfaces, a first interface for the input of general data and a second interface that can be customized in function of the relevant computational procedure. Again, such a setup provides a better localization of possible problems that may arise during the development of the code, and facilitates modifications in the future.

The software has five menus that are activated and deactivated in function of the graphic interfaces in which we are working. The five menus are all active only when the software works with personalized interface. The menus of Ship Power are File, Edit, Configuration, Reports and Language menus. In the current version the

software operates with graphical interface in Albanian and English.

3.1.1 General Data Interface of Ship Power V1.0

This graphic interface has five main blocks and two buttons "Continue" and “Cancel”. The main blocks of this interface are; Ship; Ship Type; Propulsion type; Propeller Data and General Data. (sea figure 3).

The block "The Ship" is a block in which the user completes the general identification data of the ship, such as name, flag, ship-owner and IMO number.

The block "Ship Type" is a block in which the user selects the ship type and its categorization, by clicking in the respective option and combo box.

The block "Propulsion Type" is a block in which the user can selects the type of propulsion by clicking in one of the options boxes located in this block, i.e. if it is a single screw ship with a traditional stern, single screw ship with an open stern and twin screw ship.

The block "Propeller Data" is a block in which the user can declare (if known) the propeller data, such as the diameter, the expanded area ratio (AE/A0), the pitch ratio (P/D) and the open efficiency η0. When the propeller data are not known we can activate the option "propeller data are not known" and the program automatically disables the entry of data for the diameter, the expanded area ratio, the pitch ratio and the open efficiency η_0.

The block "Main data" is a block in which the user can declare the main ship data, as ship lengths, breadths, draughts and ship navigational speed.

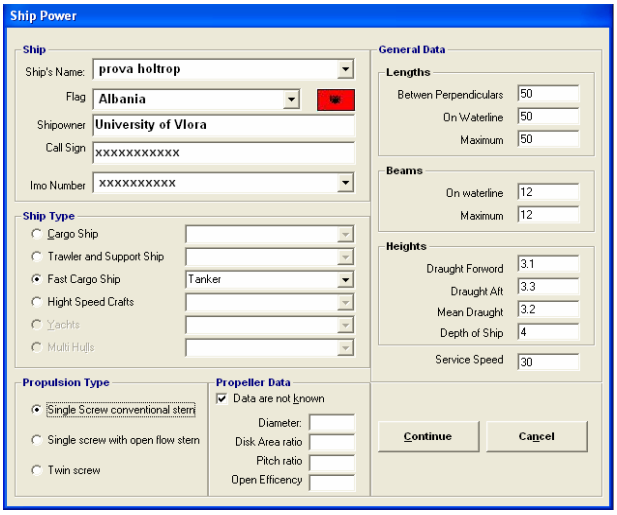

Figure 3 General Data Interface of Ship Power V1.0.

During all working time, in this graphic interface, the software signals the possible irregularities. When all the required data are completed in this graphic interface the user must click on the “Continue” button in order that Ship Power can continues with others procedures. If any of the data is not completed properly, or when it is not quite completed, the program indicates the stated problem, by giving to user the opportunity to make necessary corrections. Once the program verifies that all data are well completed “Ship Power” continues with further procedures.

3.1.2 Interface of customized data

This graphic interface has four main blocks that are; Ship Hull; Form Feature; Water Environment; Appendages Modelling and Speed Range, sea figure 4. This graphic interface allows the user to declare others data, needed for program execution.

The block "Ship Hull" is composed of two other sub-blocks, “Main Particulars” and “Form Features”. This block has several options that allow the user to personalize the ship in consideration and interact with Ship Power, enabling the software to take, or not to take, in consideration some certain parameters and characteristics.

The sub-block “Main Particulars” is a block in which the user can declare the coefficients of form of the hull and the LCB position. The basic data, such as length of waterline, breadth of waterline, draught forward and draught aft, are imported from the previous interface and can be modified in this interface, if the user considers necessary. The sub-block "Form Features" is a block in which the user can declare other feature of the ship under investigation such as the characteristics of stern and bow.

The block “Water Environment" is a block in which the user can declare water characteristics such as, temperature, density and viscosity. Default the software takes in consideration the standard characteristics of water defined by ITTC.

The "Speeds Range” block is a block in which the user can declare, minimum and maximum values of speed and also the step of speeds for which the calculations will be performed.

The block "Modelling Appendages" is a block in which the user can model the hull appendages, in order that “Ship Power” can evaluate the appendages resistance as the sum of resistance of individual appendages or to calculate this resistance as a percentage of viscous resistance.

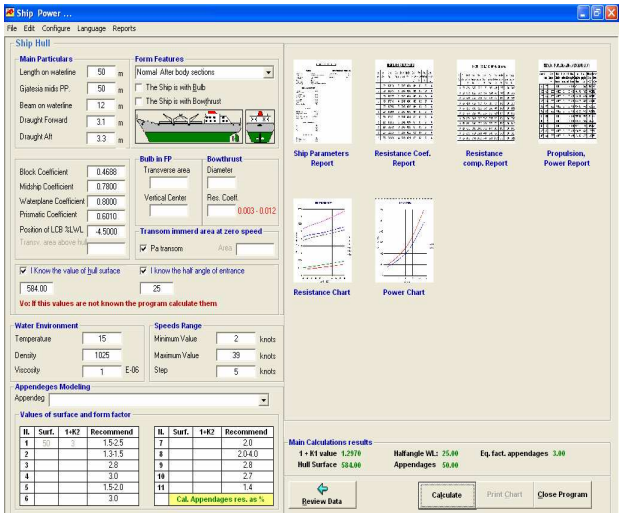

Figure 4 Customized interface of “Ship Power V 1.0”.

3.1.3 Ship power reports and charts.

The reports of calculation for each speed and graphical representation of calculations can be displayed under the menu Report. Reports compiled by the program are: resistance report, report of resistance coefficients, report of propulsion parameters and report of general parameters of the ship. All these reports can be printed in paper format, or can be saved in electronic form for further processing. The graphs constructed from the program are: graph of effective and delivered propeller power in function of speed and graph of resistance components in function of speed.

The report of resistance includes for each speed results of calculation for the frictional resistance, residual resistance, total resistance, wave resistance, viscous resistance, model ship correlation resistance, appendages resistance and air resistance.

The report of resistance coefficients includes for each speed the results of calculation for the coefficients of frictional resistance, residual resistance, total resistance, wave resistance, viscous resistance, model ship correlation resistance.

The report of propulsion factors includes for each speed the results of calculation for wake fraction, thrust deduction fraction, relative rotative efficiency, ship hull efficiency, quasi propulsive efficiency, propeller thrust, effective power and delivered power.

3.2 Software Validation.

As required by ISO standards (ISO 9126 and ISO 9001) the developed program certainly requires to be verified in order to ensure its validity. The verification of this software, as we have stated in previous sections, has started upon the early development of the code. Stage by stage each of the developed procedures is verified by running the program and comparing the output results of the program with results available in literature. As a reference for verifications of the program we have obtained the data presented as in Holtrop (1984). The main ship data, obtained as in Holtrop (1984), are presented in Table 2.

For the realization of calculations of resistance and power the user must start the program and choose from the "File" menu to create a new project (or to open an existing project, if it is an existing project examined before by Ship Power). After this it is necessary to complete the relevant data of the ship in the graphic interface opened by the program.

Results of the calculations performed by the program are compared with the results of calculations presented in Holtrop (1984). Below are presented comparison of results obtained by the program with those available in literature.

Summary of the reports of resistance, propulsion and resistance coefficients generated by the program are presented in Tables 3, 4, 5. Graphical representations of the results of calculations of power and resistance components in function of speed are presented in figure 5 and figure 6. Results obtained by the program are compared with results presented in Holtrop (1984). In table 6 are presented these comparisons.

Table 2. Main Characteristics as in Holtrop (1984).

Main Ship characteristics		Main Ship characteristics	
Length on waterline, LWL	50.00 m	Appendages area, S_{APP}	50.0 m2
Breadth moulded, B	12.00 m	1+k2	3
Draught moulded on F.P, T_F	3.10 m	Transom area, A_T	10.0 m2
Draught moulded on A.P, T_A	3.30 m	Stern parameter, C_{stern}	0.0
Displacement volume, ∇	900 m3	Midship coefficient, C_M	0.78
Longitudinal center of buoyancy, LCB	4.5 % A	Waterplane coefficient, C_{WP}	0.80

Table 3. Resistance components calculated in speed range 25-35 knots, speed increment 2 knots.

V knots	RF	RR	RT	RW	RV	RA	RAPP	RB	RTR
25	80,091	523,733	656,143	475,119	103,878	31,748	20,571	0	24,827
27	92,508	555,431	708,729	512,498	119,983	37,030	23,761	0	15,458
29	105,758	573,036	748,678	539,367	137,169	42,720	27,164	0	2,257
31	119,837	599,532	798,964	563,940	155,429	48,815	30,780	0	0
33	134,736	629,932	854,592	589,915	174,753	55,317	34,607	0	0
35	150,451	663,289	914,608	618,604	195,135	62,225	38,643	0	0

Table 4. Resistance coefficients calculated in speed range 25-35 knots, speed increment 2 knots.

V Knots	CF	CR	CT	CW	CV	CA
25.00	0.001618	0.010581	0.012199	0.010100	0.002099	0.000641
27.00	0.001602	0.009620	0.011223	0.009145	0.002078	0.000641
29.00	0.001588	0.008604	0.010191	0.008132	0.002059	0.000641
31.00	0.001575	0.007877	0.009452	0.007410	0.002042	0.000641
33.00	0.001562	0.007304	0.008866	0.006840	0.002026	0.000641
35.00	0.001551	0.006837	0.008388	0.006376	0.002011	0.000641

Table 5. Propulsion factor calculated in speed range 25-35 knots, speed increment 2 knots

V Knots	w	t	ηR	ηH	ηD	Total thrust T (N)	Effective Power PE (KW)	Delivered Power PD (KW)
25.00	0.03802	0.05408	0.98	0.98	0.68	693,653.44	8,438.00	12,422.97
27.00	0.03792	0.05408	0.98	0.98	0.68	749,245.55	9,843.40	14,493.53
29.00	0.03783	0.05408	0.98	0.98	0.68	791,477.56	11,168.47	16,446.08
31.00	0.03775	0.05408	0.98	0.98	0.68	844,638.35	12,740.59	18,762.68
33.00	0.03768	0.05408	0.98	0.98	0.68	903,447.15	14,506.88	21,365.49
35.00	0.03761	0.05408	0.98	0.98	0.68	966,893.62	16,466.60	24,253.49

Table 6. Comparison of calculation results of “Ship Power V1.0” with results presented in Holtrop (1984).

V knots	R_W (kN)		Diff.	R_T (kN)		Diff.	T (kN)		Diff.
	Ref.[2]	Program	%	Ref.[2]	Program	%	Ref.[2]	Program	%
25	475	475,1	0,03	662	656,14	-0,89	699	693,653	-0.76
27	512	512,4	0,10	715	708,73	-0,88	756	749,245	-0.89
29	539	539,3	0,06	756	748,77	-0,96	799	791,477	-0.94
31	564	563,9	-0,01	807	798,63	-1,04	853	844,638	-0.98
33	590	589,9	-0,02	864	854,59	-1,09	913	903,477	-1.04
35	618	618,6	0,10	925	914,61	-1,12	978	966,893	-1.13

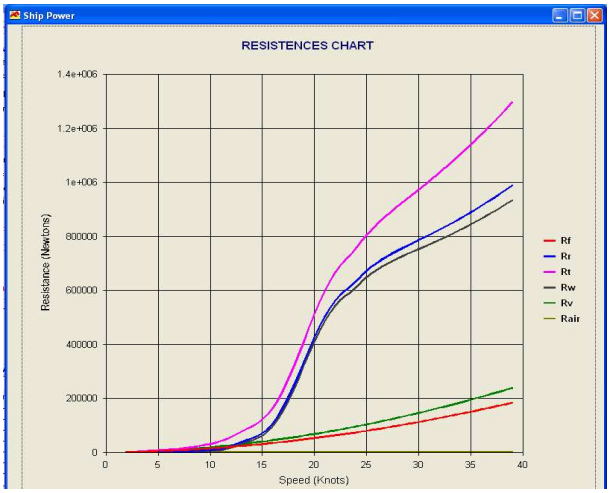

Figure 5 Graph of resistance components vs. speed, generated by the program. (Appendages resistance included at R_T)

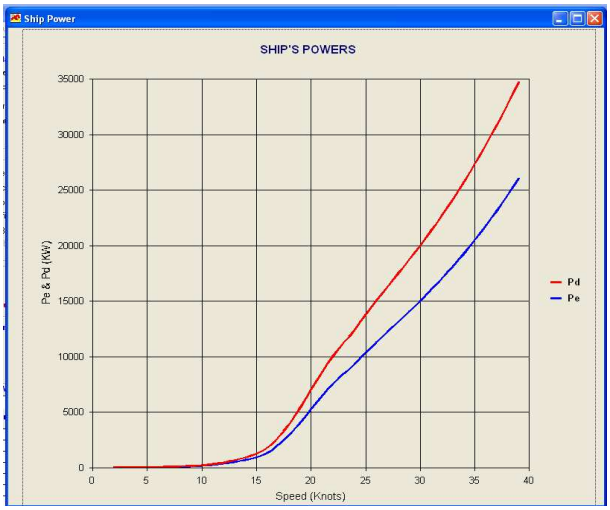

Figure 6 Graph of power vs. speed, generated by the program

4. CONCLUSIONS

In this paper we have briefly described the structure of the program developed for the calculations of resistance and power of ship in early design stage. For the calculation of resistance and power the program needs only the main characteristics of the ship and not the development of detailed geometry of ship. The program is written in visual Basic and designed to run on any computer. The program is written taking in consideration the principal requirements of ISO 9126.

The program is simple to use and assists the user step by step by creating the possibility of modifications in real time. The overall accuracy of this program is similar with the accuracy of the models available in literature. Even though nowadays exist many others reliable software or programs to calculate and predict the resistance and power of ship, this program is also reliable and can be used like other existing and well-known programs. The program should be seen as a good tool to reduce design iterations and ensure that the hull form, which is tank tested, is as close to the final hull as possible. The program could be used to qualitatively compare the merits of a series of hull forms and the output from the program will only be as good as the input at early design stage.

5. REFERENCES

[1]. THE MARITIME ENGINEERING REFERENCE BOOK – *A guide to Ship Design, Construction and Operation- Anthony Molland*, ISBN 978 0 7506 – 8987 8, 2008

[2]. SHIP DESIGN AND CONSTRUCTION Vol.1 - SNAME, 2004

[3]. APPUNTI DI PROGETTO DELLA NAVE – Prof. Giuglio Russo Krauss

[4]. INTERNATIONAL STANDART ISO 9126

[5]. ABRAN, A., KHELIFI, A., SURYN, W., & SEFFAH, A.. *Usability Meanings and Interpretations in ISO Standards*. Software Quality Journal, 11(4), 325-338, 2003

[6]. CHUA, B., DYSON L.. *Applying the ISO 9126 model to the evaluation of an e-learning system*

[7]. HOLTROP, J., MENNEN, G. G. J. *"An Approximate Power Prediction Method*," International Shipbuilding Progress, Vol. 29, No. 335, pp 166-170, 1982

[8]. HOLTROP, J. "*A Statistical Re-Analysis of Resistance and Propulsion Data*," International Shipbuilding Progress, Vol. 31, No. 363, pp - 272-276, 1984

[9]. VAN MANEN, J.D, VAN OOSSANEN., *"Resistance", Principles of Naval Architecture*, Volume II, chapter V, pp-29-34, S.NA.M.E, 1988

SECTION II
MECHANICAL ENGINEERING AND ENVIRONMENT

COMPARATIVE ANALYSIS OF THE OPTIMIZED AND UNOPTIMIZED DOUBLE BOTTOM STRUCTURE

CRISTEA ANISOARA-GABRIELA

"Dunarea de Jos" University of Galati, Faculty of Naval Architecture, Romania

ABSTRACT

This paper shows the effects of variable stresses acting on structures, the positioning modes of stress raisers, as well as the determination of stress concentration factor and the establishment of some cracking scenarios in order to determine the main characteristics of the crack.

Keywords: *concentration factor, the J-integral, stress intensity*

1. INTRODUCTION

Fatigue analysis is performed on some connecting elements, joining elements, within a set of structures of high volume. Verification of fatigue strength for some structural elements is made through the two methods:

- The method of the cumulative damage factor D, that is based on the criterion issued by Palmgren - Miner by designing the stress curves – S-N cycles.

- The method of allowable values for the variation of maximum stresses, at extreme loads (Domnişoru, L., 2002).

In order to satisfy the criterion of resistance proposed by Palmgren - Miner, the cumulative damage factor obtained through calculation must be smaller than 1, $D \leq 1$.

Determination of the cumulative damage factor (D) represents the linear summation of individual damages of all intervals considered in the period of stress.

In principle, these stress raisers or "HOT SPOT" appear in the connection areas, in areas with holes, soldering, addition of material, etc.

In practice, this problem is solved by applying a stress concentration factor (SCF), of stress resulting from the analysis.

Determination of stress concentration factor by standard relations or through the use of some finite element programs, which explicitly calculate this factor, is done by selecting an appropriate geometric area.

Figure 1 shows the position of the stress raiser and distance t that represents the dimension of an element of digitization of the structure.

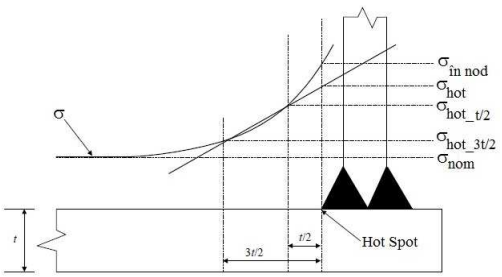

Figure 1 Position of the stress raiser ("HOT SPOT"), (ABS, 2010)

where:

σ_{hot} - represents stress value in the most stressed area (in concentration – hot spot). It must be taken into consideration that the effects caused by the possible soldering, addition of material or welding are not taken into account in determining stress, but the overall effect of the geometry of the structure is taken into the calculation of the nominal stress;

σ_{nom} - represents nominal stress, in a cross-section or in a local area, but away from the concentration and the area where the crack may occur. Nominal stress value is not influenced by the geometric effects or any soldering, additions, etc.;

σ_{innod} - represents maximum stress at welding. Maximum stress value includes the stress of the raiser (hot spot - σ_{hot}), as well as stress from welding, additions of material.

To calculate stress concentration factor, the following aspects must be taken into account:

- Digitization: it must be fine so as to capture as accurately as possible the effect of stress in the area considered dangerous;

- The type of element: it is recommended to membrane and plate type (Shell) or solid (brick - in case of volume elements), and digitization must be quadrilateral;

- The dimension of the digitization element: in the area of the stress raiser the dimension of the element is recommended to be $t \times t$. The dimension of an element of digitization, in the case of the plate-like element, should be approximately equal to the thickness of the plate in the proximity of the concentration, Figure 1;

- The ratio between the length and width of the element of digitization: as a rule, a ratio of 1: 1 is preferred in the area of the stress raiser, a ratio of 1:3 is preferred outside the concentration and ratio should not exceed 1:5 in the rest of the structure;

- Determination of stress: it is based on a linear extrapolation system.

Formula (1) allows calculating stress in the most stressed point, determining by the use of linear extrapolation, stress concentration factor for each location considered dangerous.

$$\sigma_{hot} = 1.5\sigma_{0.5t} - 0.5\sigma_{1.5t} \quad (1)$$

2. DETERMINATION OF STRESS CONCENTRATION FACTOR USING FEM

Due to stress variation in case of fatigue strength analysis, the possible influences of stress raisers and how they modify fatigue strength values must be taken into consideration.

In the first step in the analysis of cracks, stress concentration areas were determined for each model, separately.

The second step is the simulation of two cases of production and extension of the crack, resulting in the calculation of the intensity factor K at the tip of the crack and the J-integral.

Following the global analysis, the position of stress raisers can be noticed. (Figure 2)

In order to determine stress concentration factor, the area of technological cutouts in the double bottom reinforcements (DB), with a radius of the technological cutout of 200 mm, was taken into consideration.

In order to analyze this concentration factor for the models presented, one radius of fillet with different loads namely of a force of 25 kN ÷ 75 kN was discussed.

- Case 2D - R_200_unoptimized;
- Case 2D - R_200_optimized.

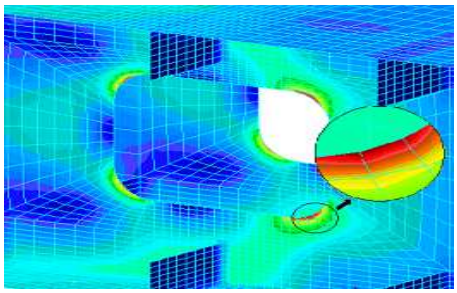

Figure 2 Highlighting stress raisers, cut-out detail Structure R_200

When fatigue strength due to stress variation is analyzed, the possible influences of stress raisers and how they modify fatigue strength values should be considered.

In this case, determination of this stress concentration factor was done by two different methods of digitization: fine and coarse, applying the methodology described above and using the formula (1).

2.1 Coarse digitization- Structure R_200_unoptimized

In this case, structure R_200 was finely and coarsely digitized (Figure 3).

For a fine digitization of the structure (Figure 3a), the dimension of the element is approximately 8 mm in the area of technological cutout, and for a coarsely digitized structure (Figure 3b), the dimension of the element is approximately 4 mm.

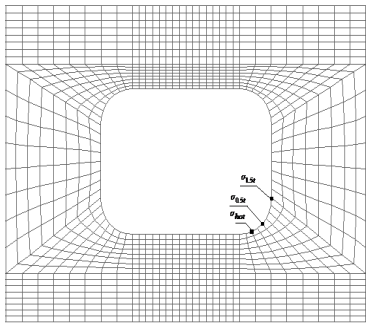

a) Finely

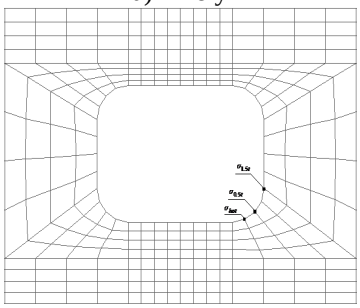

b) Coarse

Figure 3 Digitization in case of Structure R_200

Stresses were selected from the area adjacent to the stress raiser at 0.5t and respectively 1.5t (Table 1).

Table 1 Determination of the concentration factor SCF_{coarse} – Structure R_200_unoptimized

Quota to extract stress	**Force [kN]**	**Stress value [MPa]**
0.5t	**25**	176.459
1.5t		74.083
The value of SCF_{coarse}		**227.65**
0.5t	**50**	352.918
1.5t		148.166
The value of SCF_{coarse}		**455.29**
0.5t	**75**	529.378
1.5t		222.249
The value of SCF_{coarse}		**682.94**

Stress concentration factor for different loads was carried out by interpolating stresses at 0.5t and 1.5t, respectively (Figures 4, 5, 6).

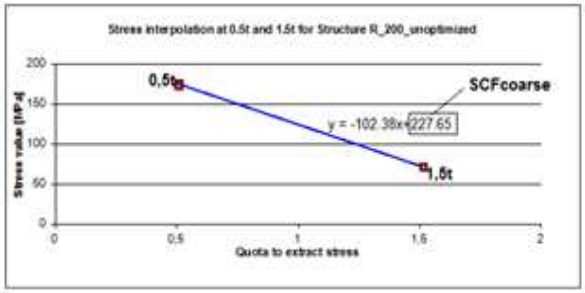

Figure 4 Stress interpolation at 0.5t and 1.5t for Structure R_200_unoptimized (a force of 25 kN)

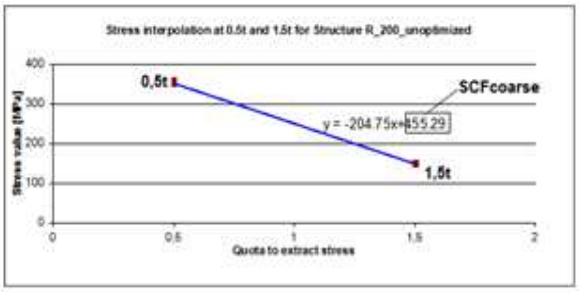

Figure 5 Stress interpolation at 0.5t and 1.5t for Structure R_200_unoptimized (a force of 50 kN)

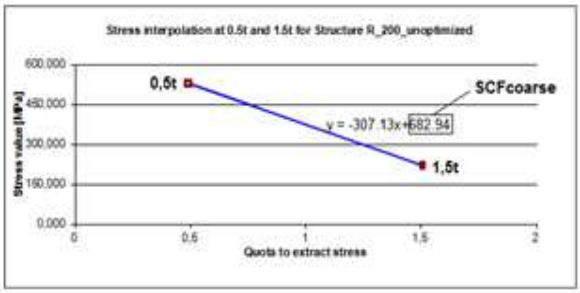

Figure 6 Stress interpolation at 0.5t and 1.5t for Structure R_200_unoptimized (a force of 75 kN)

2.2Fine digitization - Structure R_200_unoptimized

Following numerical analysis, stress values at 0.5t and 1.5t were extracted, resulting in the value of stress concentration factor (Table 2).

Table 2 Determination of the concentration factor SCF_{fine} – Structure R_200_unoptimized

Quota to extract stress	Force [kN]	Stress value [MPa]
0.5t	25	188.741
1.5t		58.334
The value of SCF_{fine}		**253.94**
0.5t	50	377.483
1.5t		116.668
The value of SCF_{fine}		**507.89**
0.5t	75	566.224
1.5t		175.002
The value of SCF_{fine}		**761.84**

Stress concentration factor for various loads was obtained by interpolating stresses at 0.5T and respectively 1.5T (Figures 7, 8, 9).

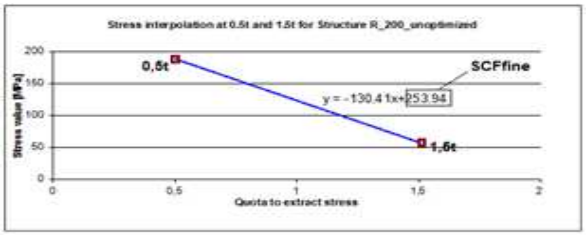

Figure 7 Stress interpolation at 0.5t and 1.5t for Structure R_200_unoptimized (a force of 25 kN)

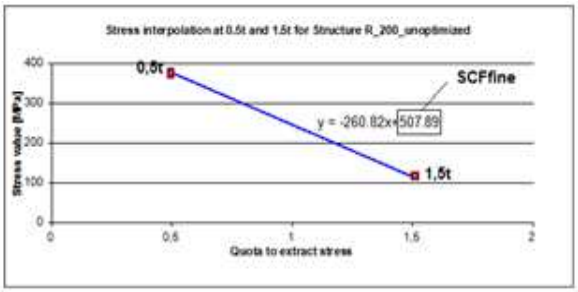

Figure 8 Stress interpolation at 0.5t and 1.5t for Structure R_200_unoptimized (a force of 50 kN)

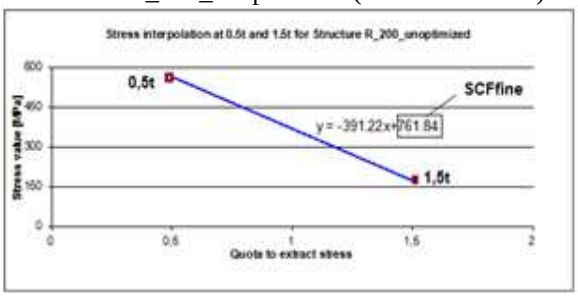

Figure 9 Stress interpolation at 0.5t and 1.5t for Structure R_200_unoptimized (a force of 75 kN)

2.3 Coarse digitization - Structure R_200_optimized

Stresses were selected from the area adjacent to the stress raiser at 0.5t and respectively 1.5t (Table 3).

Table 3 Determination of the concentration factor SCF_{coarse} – Structure R_200_optimized

Quota to extract stress	Force [kN]	Stress value [MPa]
0.5t	25	168.6095
1.5t		73.9405
The value of SCF_{coarse}		**215.94**
0.5t	50	335.886
1.5t		147.881
The value of SCF_{coarse}		**429.89**
0.5t	75	503.829
1.5t		221.821
The value of SCF_{coarse}		**644.83**

Stress concentration factor for various loads was carried out by interpolating stresses at 0.5T and respectively 1.5T (Figures 10, 11, 12).

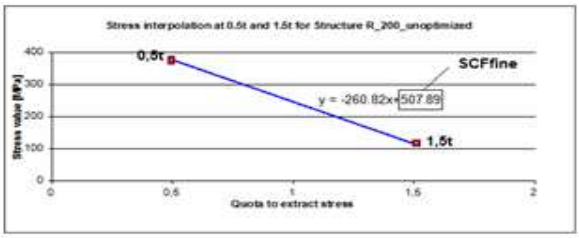

Figure 8 Stress interpolation at 0.5t and 1.5t for Structure R_200_unoptimized (a force of 50 kN)

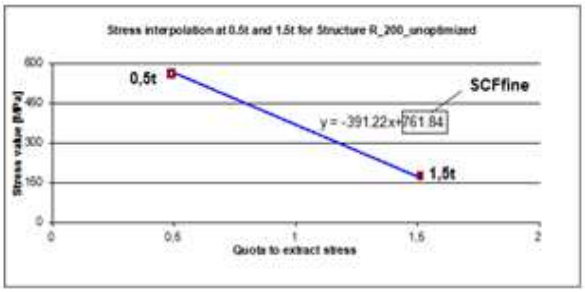

Figure 9 Stress interpolation at 0.5t and 1.5t for Structure R_200_unoptimized (a force of 75 kN)

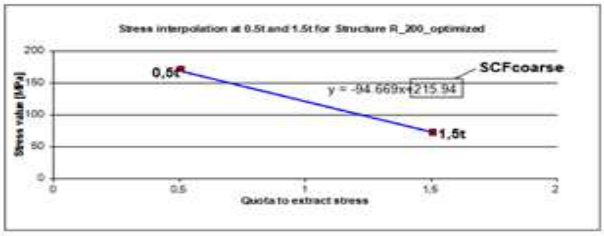

Figure 10 Stress interpolation at 0.5t and 1.5t for Structure R_200_optimized (a force of 25 kN)

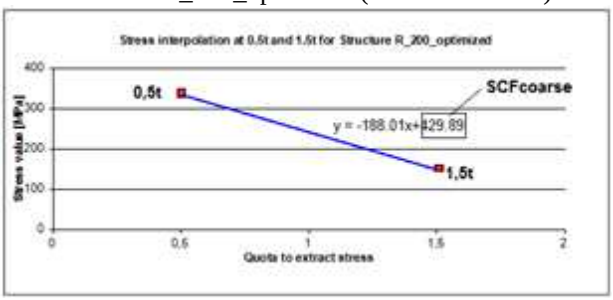

Figure 11 Stress interpolation at 0.5t and 1.5t for Structure R_200_optimized (a force of 50 kN)

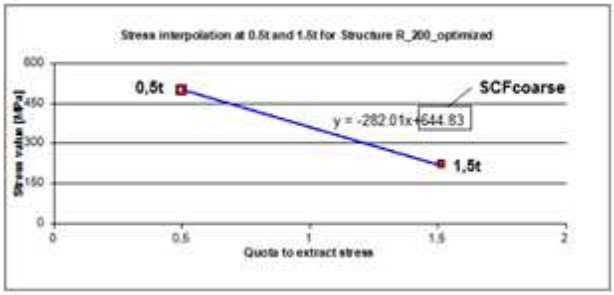

Figure 12 Stress interpolation at 0.5t and 1.5t for Structure R_200_optimized (a force of 75 kN)

2.4 Fine digitization - Structure R_200_optimized

Following numerical analysis, stress values at 0.5t and 1.5t were extracted, resulting in the value of stress concentration factor (Table 4).

Table 4 Determination of the concentration factor SCF_{fine} – Structure R_200_optimized

Quota to extract stress	**Force [kN]**	**Stress value [MPa]**
0.5t	**25**	195.496
1.5t		61.0842
The value of SCF_{fine}		**262.7**
0.5t	**50**	390.992
1.5t		122.168
The value of SCF_{fine}		**525.4**
0.5t	**75**	586.488
1.5t		183.253
The value of SCF_{fine}		**788.11**

Stress concentration factor for various loads was carried out by interpolating stresses at 0.5T and respectively 1.5T (Figures 13, 14, 15).

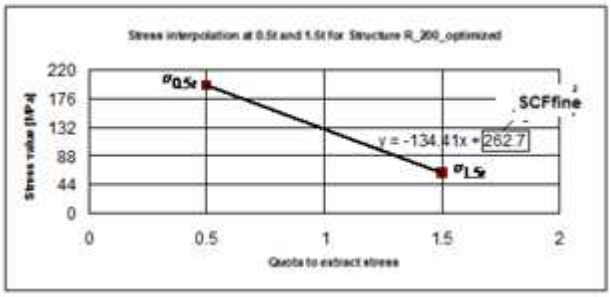

Figure 13 Stress interpolation at 0.5t and 1.5t for Structure R_200_optimized (a force of 25 kN)

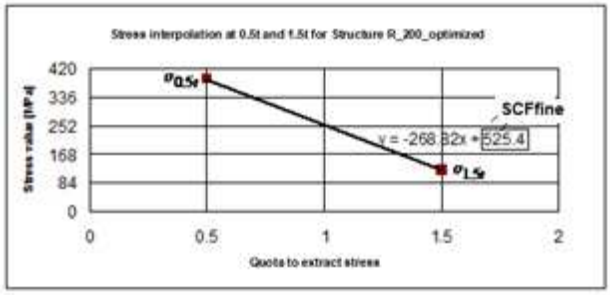

Figure 14 Stress interpolation at 0.5t and 1.5t for Structure R_200_optimized (a force of 50 kN)

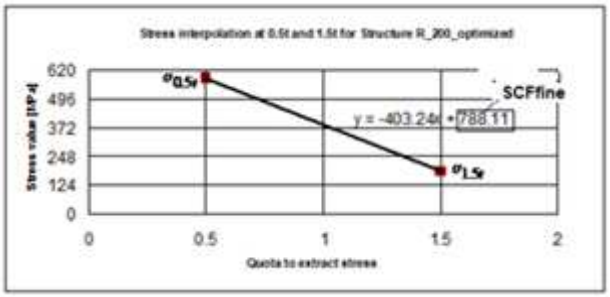

Figure 15 Stress interpolation at 0.5t and 1.5t for Structure R_200_optimized (a force of 75 kN)

Since in finite element analysis, precision depends on the digitization adopted, it results as it can be also noticed in Table 5 that, in case of fine digitization, stress concentration factor resulted was higher than in case of coarse digitization (Figure 16).

Table 5 Comparing the results in the two cases of digitization

Structure	**Force [kN]**	**SCF_{fine}**	**SCF_{coarse}**	**Deviations [%] SCF_{coarse} / SCF_{fine}**
R_200_unoptimize	**25**	253.94	227.65	10.35%
	50	507.89	455.29	10.36%

d	**75**	761.84	682.94	10.36%
R_200_optimized	**25**	262.7	215.94	17.80%
	50	525.4	429.89	18.18%
	75	788.11	644.83	18.18%

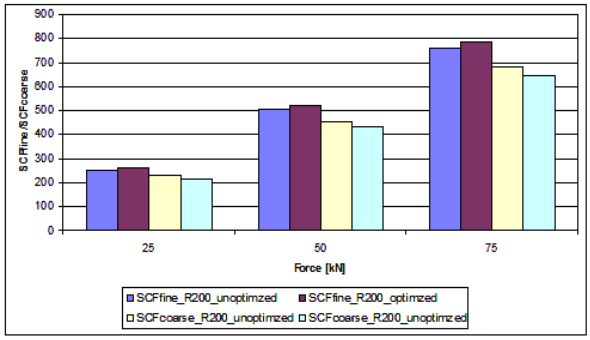

Figure 16 Results for both structures unoptimized/optimized in the cases with fine digitization and coarse digitization

3. EMERGENCE AND EXTENSION OF CRACKS IN TECHNOLOGICAL CUTOUTS AREA OF DOUBLE BOTTOM REINFORCEMENT (DB). DETERMINATION OF PARAMETERS SPECIFIC TO CRACKS PROPAGATION

For crack propagation, stress field must release deformation energy. When variation of the deformation energy, due to the extension of the crack, is greater than the energy needed to increase the area of the crack, crack propagates. Most of this energy is consumed for moving the deformed area from the tip of the crack.

Analysis of stress at the tip of the crack is carried out by the determination of some values such as stress intensity factor at the tip of the crack K_I, K_{II} and the J-integral that generally characterize the evolution of the crack.

The critical value of J integral can be determined and defined by similarity with crack extension force that represents in this case the limit at which crack extension may occur.

$$J(\alpha) \geq J_{cr}. \qquad (2)$$

Relation 2 states that a crack develops only if the potential energy released by crack extension is greater than the energy required for the formation of free surfaces.

The assessment of stress intensity factor K contains all the information on external load and the geometry of the body containing a crack.

Based on numerical calculations performed, the results obtained were summarized in charts which highlighted the variation of J integral as well as variation of the stress intensity factor K.

Verification of J integral value can be done with the relationship:

$$J = \frac{K^2}{E}. \qquad (3)$$

where:

K - represents stress intensity factor;

E - represents the modulus of elasticity of the material.

Afterwards, the numerical calculation of J integral and stress intensity factor K is carried out.

Then, the dependence of J integral is determined depending on the length of the crack for each structure separately.

In order to determine stress intensity factor K and the J-integral, the area of technological cutouts in double bottom reinforcements (DB), with the radius of fillet of 200 mm was considered.

To analyze the production and propagation of cracks for the models presented only one radius of fillet with different loads namely of a force of 25 kN ÷ 75 kN was discussed.

- Case 2D - Structure R_200.

In both cases, digitization was carried out using PLANE 2D type finite element (for the floor) and SHELL 4T type finite elements for the rest of the elements that are part of the double bottom structure (DB).

The material considered in numerical modeling is isotropic with material properties:

$E = 2.1 \cdot 10^5$[MPa], $\upsilon = 0.3$, $\rho = 7800 - 7900$ [Kg/m^3].

The numerical calculation has been carried out under static loading. Model loading was carried out by introducing an experimentally determined load.

In the first step of the analysis of cracks, stress concentration areas were determined for each model, separately.

Following this step, three cases of production and extension of the crack were simulated resulting in the calculation of the intensity factor K at the tip of the crack and the J-integral.

3.1 Emergence and extension of cracks in Structure R_200_unoptimized. Determination of parameters specific to crack propagation

Figure 17, shows the position of the stress raiser following numerical analysis.

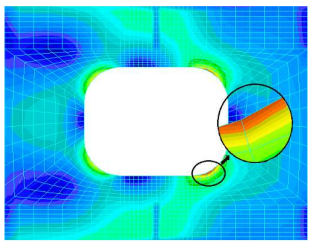

Figure 17 Model with concentrators emphasis 2D analysis – Structure R_200_unoptimized

As shown in Figure 6.1, stress raiser occurs in the connection area and does not have a gradual shift, what makes this portion to be prone to cracking.

a) SCENARIO I

Scenario I (Figure 18) consists of the initiation of a crack with the length equal to a digitization element.

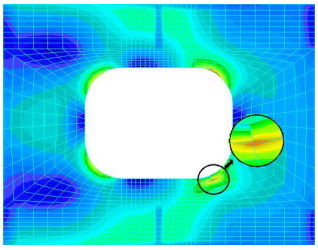

Figure 18 Scenario I of cracking 2D analysis – Structure R_200_unoptimized

The results obtained both for the J-integral and for intensity factor K are shown in Table 6.

Table 6 Scenario I of cracking – Structure R_200_unoptimized

Scenario I	Force [kN]	Module I		Module II	
		J [N/mm]	K [N·mm$^{0.5}$]	J [N/mm]	K [N·mm$^{0.5}$]
	25	15.069	1778.9	10.319	1472.1
	50	60.274	3557.8	41.275	2944.1
	75	135.62	5336.6	92.869	4416.2

b) SCENARIO II

This scenario considered a continuous propagation of the crack, the length of the crack being directed on two elements of digitization (Figure 19).

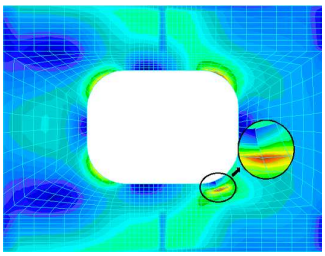

Figure 19 Scenario II of cracking 2D analysis – Structure R_200_unoptimized

The results obtained both for the J-integral and for intensity factor K are shown in Table 7.

Table 7 Scenario II of cracking – Structure R_200_unoptimized

Scenario II	Force [kN]	Module I		Module II	
		J [N/mm]	K [N·mm$^{0.5}$]	J [N/mm]	K [N·mm$^{0.5}$]
	25	23.783	2234.8	-5.9285	1115.8
	50	95.132	4469.6	-23.714	2231.6
	75	214.05	6704.5	-53.357	3347.4

3.2 Emergence and extension of cracks in Structure R_200_optimized. Determination of specific parameters to crack propagation

The optimized structure has a radius of technological cutout of 200 mm (sheet thickness 11.5 mm) where the same steps for the determination of the parameters specific to crack propagation will be followed.

a) SCENARIO I

Scenario I consists of the initiation of a crack with the length equal to a digitization element.

The results obtained both for the J-integral and for intensity factor K are shown in Table 8.

Table 8 Scenario I of cracking – Structure R_200_optimized

Scenario I	Force [kN]	Module I		Module II	
		J [N/mm]	K [N·mm$^{0.5}$]	J [N/mm]	K [N·mm$^{0.5}$]
	25	16.074	1837.2	10.262	1468
	50	64.295	3674.5	41.046	2935.9
	75	114.66	5511.7	92.354	4403.9

b) SCENARIO II

In this scenario the length of the crack is directed on two elements of digitization.

The results obtained both for the J-integral and for intensity factor K are shown in Table 9.

Table 9 Scenario II of cracking – Structure R_200_optimized

Scenario II	Force [kN]	Module I		Module II	
		J [N/mm]	K [N·mm$^{0.5}$]	J [N/mm]	K [N·mm$^{0.5}$]
	25	25.380	2308.7	-6.7906	1194.2
	50	101.52	4617.3	-27.162	2388.3
	75	228.42	6926	-61.115	3582.5

4. NUMERICAL PROCESSING OF RESULTS IN THE ANALYSIS OF EMERGENCE AND EXTENSION OF CRACKS IN DOUBLE BOTTOM STRUCTURE. 2D ANALYSIS

The results obtained were summarized in charts which highlighted the variation of J integral and stress intensity factor K depending on the length of the crack.

Table 10 shows the results of the J-integral in the area of technological cutouts in double bottom reinforcements (DB).

Table 10. The J-integral for the structures of the two structures - unoptimized/optimized

Structure	Force [kN]	J-integral [N/mm]	
		Scenario I	Scenario II
R_200_unoptimized	**25**	25.387	17.854
	50	101.55	71.418
	75	228.49	160.69
R_200_optimized	**25**	26.335	18.590
	50	105.34	74.359
	75	237.02	167.31

Figures 20 and 21 show the variation of J integral depending on the radius of fillet and load capacity on the length of an element (scenario I), respectively on the length of two elements (scenario II).

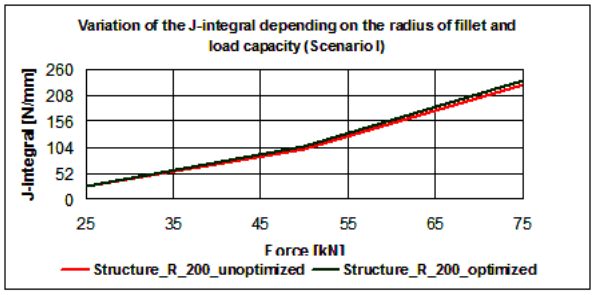

Figure 20 Variation of the J-integral depending on the radius of fillet and load capacity (Scenario I)

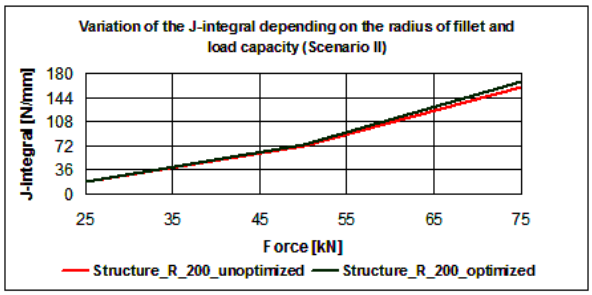

Figure 21 Variation of the J-integral depending on the radius of fillet and load capacity (Scenario I)

Tables 11 and 12 show the values of stress intensity factor K_I and K_{II}, for each step of the extension of the crack.

Table 11 Stress intensity factor K_I for both structures

Structure	Force [kN]	Stress intensity factor K_I [N·mm$^{0.5}$]	
		Scenario I	Scenario II
R_200_unoptimized	25	1778.9	2234.8
	50	3557.8	4469.6
	75	5336.6	6704.5
R_200_optimized	25	1837.2	2308.7
	50	3674.5	4617.3
	75	5511.7	6926.0

Table 12 Stress intensity factor K_{II} for both structures

Structure	Force [kN]	Stress intensity factor K_{II} [N·mm$^{0.5}$]	
		Scenario I	Scenario II
R_200_unoptimized	25	1472.1	1115.8
	50	2944.1	2231.6
	75	4416.2	3347.4
R_200_optimized	25	1468	1194.2
	50	2935.9	2388.3
	75	4403.9	3582.5

Stress intensity factors K_I and K_{II} at the tip of the crack give a picture of the structure where crack is considered. In case of 2D cracks (Figures 22, 23, 24 and 25), variation of, respectively depending on the length of the crack, is shown.

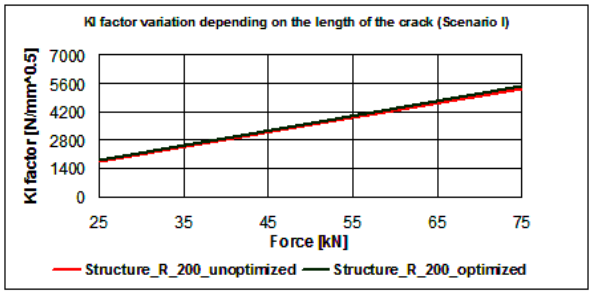

Figure 22 K_I factor variation depending on the length of the crack (Scenario I)

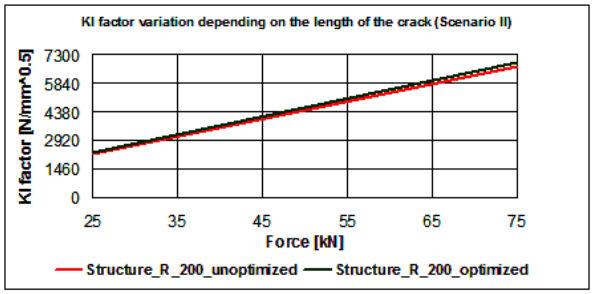

Figure 23 K_I factor variation depending on the length of the crack (Scenario II)

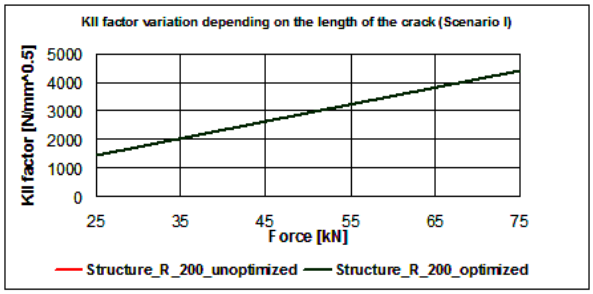

Figura 24 K_{II} factor variation depending on the length of the crack (Scenario I)

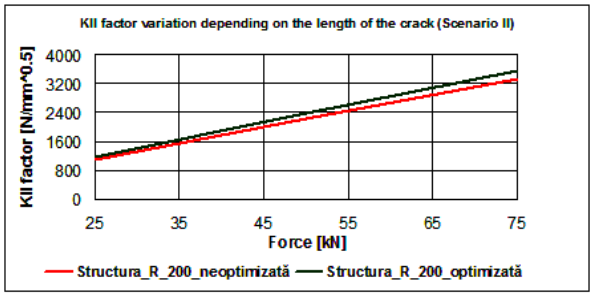

Figure 25 K_{II} factor variation depending on the length of the crack (Scenario II)

5. CONCLUSIONS

Determination of the modes of cracking necessary for the extension of the crack was an important point in evaluating and determining damages that occur during operation in structures made of steel.

Most times, the analysis of the emergence and extension of cracks can be achieved only by using numerical and experimental methods.

As can be seen in Table 11 (K_I) compared to Table 12 (K_{II}), K_I factor has the highest values. Therefore, the possibility of cracking most likely to occur is the opening.

6. REFERENCES

[1] American Bureau of Shipping (ABS), Guide for - Spectral-based fatigue analysis for floating production, storage and offloading (FPSO) installations, Section 7, Structural Modeling Analysis, 2010.

[2]. Dumitru, I., Marşavina, L., *Elemente de mecanica ruperii*, - curs - Univ. "Politehnica" Timişoara, 2000.

[3] Goanță, V., Palihovici V., *Calculation of J-Integral by the Analysis of Finite Elements*, Buletinul Institutului Politehnic Iaşi, Tomul XLV(IL), fasc. 1-2, p. 241-248, 1999.

[4] Hadăr A., Constantinescu I.N., Gheorghiu H., Coteț C.E., *Modelare şi modele pentru calcule în ingineria mecanică*, Editura PRINTECH, Bucureşti, 2007.

[5] Irwin, G.R., *Relation of stresses near a crack to the crack extension force*, Proc. 9th Int. Congr. Appl. Mech, Vol. VIII: 245-251, University of Brussels, 1957.

[6] Rice J.R., *"A path independent integral and the approximate analysis of strain concentration by notches and cracks"*, J. Appl. Mech., 35: 379-386, 1968.

[7] Wang, Q. and J.S. Arora, *Int. J. for Num. Methods In Engineering*, - 2006 in press.

[8] ***SWCM, SolidWorks Cosmos/M FEM Program User Guide, Dassault Systems SolidWorks Corporation, 2008.

EXERGETIC ANALYSIS OF THE HEAT PUMP USED TO RECOVER ENEGY RESOURCES WITH LOW THERMAL POTENTIAL

[1] DIACONESCU IOANA, [2] GRIGORESCU LUIZA

[1,2] "Dunarea de Jos"University from Galati

ABSTRACT

Exergy efficiency increases are subject to theoretical limitations, which identify the maximum attainability, and practical limitations, which further limit efficiency.

The paper presents the results of an applicable research where the aim was to establish the real energy efficiency of the heat pump for industrial practices to recovery energy resources with low thermal potential.

Also, this paper put on users' disposal useful information referring to the exergy efficiency calculation for different heat pumps working conditions.

Keywords: *Efficiency, exergy, heat pump, qualitative analysis, recovery processes, secondary energy resources*

1. INTRODUCTION

We conventionally assess energy systems using energy, which is based on the first law of thermodynamics which states the principle of energy conservation. But energy analysis has many weaknesses that can be overcome with an alternative thermodynamic analysis method. Exergy analysis, based on the second law, has several advantages over energy analysis. For instance, more meaningful efficiencies are evaluated with exergy analysis since exergy efficiencies always measure approach to ideality, while inefficiencies are better described with exergy analysis in terms of magnitude, type, cause and location. Exergy methods can also play a role in improving environmental and economic performance. When all facets of exergy are taken together, it is observed that exergy is a powerful tool for understanding and improving the efficiency of processes and systems, and helping achieve sustainable development. For these reasons and others, exergy analysis has been increasingly applied over the last several decades, to improve efficiency, economic and environmental performance. Exergy analysis can be applied to assess and improve energy systems, as well as other systems like ecological systems. In this article, we examine the role of as a tool for efficiency, with the objective of increasing appreciation and utilization of exergy methods.

Here, we describe exergy and its application [1] through exergy analysis. The breadth of energy systems assessed with exergy analysis is presented. The ties between exergy and economics, the environmental implications of exergy and the links between exergy and recovery energy processes are described. Finally, an illustrative example of applications of exergy analysis is presented heat pump for industrial practices based on recovery energy resources with low thermal potential.

2. EXERGY ANALYSIS

Exergy analysis [1,2] involves the application of exergy concepts, balances and efficiencies to evaluate and improve energy and other systems. Exergy flows through at all points in a process or system are examined. Many suggest that devices are best evaluated and improved using exergy analysis with or in place of energy analysis. Energy analysis has inherent difficulties as it considers only quantities of energy and ignores energy quality, which is continually degraded during real processes. Exergy analysis overcomes many of these problems. Many exergy applications have been reported over several decades, and extensive bibliographies assembled, including Goran Wall's compilation at http://exergy.se. In addition, a journal devoted to exergy, International Journal of Exergy, was established several years ago by Inderscience. Applications of exergy reported include:

- Conventional and alternative electricity generation.
- Engines and combustion.
- Transportation, e.g., land, air and water.
- Heating and cooling and cogeneration.
- Petrochemical processing and fuels production.
- Chemical processes, e.g., distillation and desalination.
- Metallurgical processes, e.g., smelting.
- Energy storage, e.g., in batteries and thermal storages.

2.1 Exergy

Exergy is defined as the maximum work which can be produced by a flow or system as it is brought to equilibrium with a reference environment, and can be viewed as a measure of energy usefulness or quality.

Exergy is consumed during real processes due to irreversibilities, and conserved during ideal processes. Exergy quantities are evaluated relative to a reference environment [1,2], which has zero exergy and is in stable equilibrium, with all parts at rest relative to one another. Chemical reactions can not occur between environmental components. The reference environment acts as an infinite system (a sink and source for heat and materials), and experiences only internally reversible processes in which its intensive state (i.e., temperature

To, pressure Po, chemical potentials for each of the *i* components present) remains constant. These properties in part determine the exergy of a flow or system.
Exergy efficiency increases are subject to theoretical limitations, which identify the maximum attainability, and practical limitations, which further limit efficiency. Theoretical limitations establish an upper limit. To assess the potential for increased efficiency, theoretical limits must be clearly understood. Lack of clarity on this issue has in the past often led to confusion, in part because energy efficiencies generally are not measures of how nearly the performance of a process or device approaches the theoretical ideal. The consequences of such confusion can be very significant. For example, resources have at times been directed towards increasing the energy efficiencies of devices that in reality were efficient and had little potential for improvement, while devices have not been targeted for improved efficiency, even though the difference between the actual and maximum theoretical efficiencies, which represents the potential for improvement, has been large. Practical limitations acknowledge that no process can be ideal, And that the goal when selecting energy sources and utilization processes is not to achieve maximum efficiency, but rather to achieve an optimal trade-off between efficiency and such factors as economics, sustainability, environmental impact, safety and societal and political acceptability. This optimum is dependent on many factors, which can be altered to favour increased efficiency via government financial incentives for efficient technologies and disincentives for low-efficiency alternatives through special taxes and regulations.

2.2 Exergy and Environmental Impact

Exergy applications are increasing in environment and ecology. Many suggest that the impact of energy resource utilization on the environment and the achievement of increased resource-utilization efficiency are best addressed with exergy. Although the exergy of an energy form or a substance is a measure of its usefulness, exergy is also a measure of its potential to cause change. The latter point suggests that exergy may be, or provide the basis for, an effective measure of the potential of a substance or energy form to impact the environment. The most appropriate link between the second law of thermodynamics and environmental impact has been cited as exergy, in part because it is a measure of the departure of the state of a system from that of the environment [1]. The exergy of a system depends on the states of both the system and the environment. This departure is zero only when the system is in equilibrium with its environment. Relations between exergy and the environment may reveal the underlying fundamental patterns and forces affecting changes in the environment, and help efforts to address environmental damage. Tribus and McIrvine [1,3] suggest that performing exergy analyses of the natural processes occurring on the earth could form a rational foundation for ecologically planning because it would indicate the disturbance caused by large-scale changes. The author introduced relationships between exergy and environmental impact [1,3], which are illustrated approximately in figure 1 as a function of process exergy efficiency.

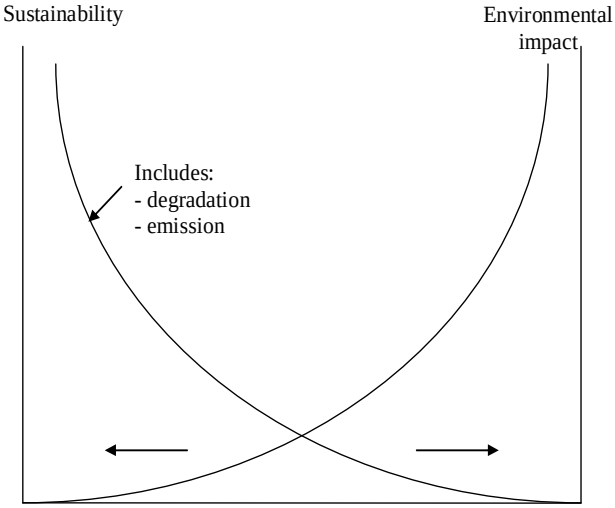

Figure 1- Process exergy efficiency

3. EXERGETIC EFFICIENCY OF HEATING PROCESSES

Exergetic efficiency may be define as ratio of heat exergy E_Q which is delivered to the warm source and combustion exergy E_B which is necessary for generating heat Q, so:

$$\xi = \frac{E_Q}{E_B} \tag{1}$$

and

$$E_Q = Q\frac{T_R - T_m}{T_R} \tag{2}$$

where:
T_R is warm source temperature (K)
T_m is environment temperature (K)
E_B is combustion heat (J)

If we are taking into account the device's quntitative analysis (energy loss), we can define the device efficiency:

$$\eta = \frac{Q}{E_B} \tag{3}$$

$$\text{so } E_Q = \eta \cdot E_B \cdot \frac{T_R - T_m}{T_R} \tag{4}$$

$$\text{and } \xi = \eta \cdot \frac{T_R - T_m}{T_R} \tag{5}$$

For small power plant the usual average value of efficiency is between 0.7 and 0.9 [3]. In situation when t_R=20°C and t_m=-15°C exergetic efficiency ξ is between 0.084 and 0.107.

In case of heating with electrical resistance, electrical energy W will be produced with an efficiency:

$$\eta_e = \frac{W}{E_B} \quad (6)$$

Because the whole electrical energy is changed in heat (W=Q) exergy efficiency for this kind of heating became:

$$\xi_E = \eta_e \cdot \frac{T_R - T_m}{T_R} \quad (7)$$

For η_e=0.35 and the same temperature conditions exergy efficiency is ξ_E=0.042. Is very clear that electrical heating is not a proper method economical and technical speaking. So, electrical heating is better to be removed with heat pump, in all the situations and technological processes.

4. EXERGETIC BALANCE OF PROCESSES WITH HEAT PUMP

For qualitative analysis of process with pump heat we considered the scheme figure 2.

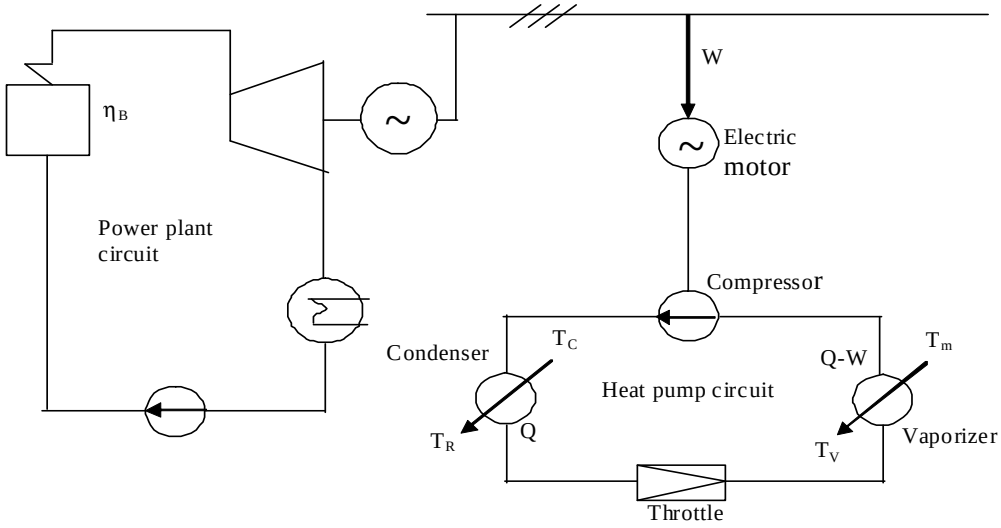

Figure 2- Heat pump scheme used for exergetic analysis

In figure 3 the exergetic balance of the heat pump process is shown.

In the ideal process (zero losses) the energy of the compressor electric motor equals the exergy of heat Q (E_Q).

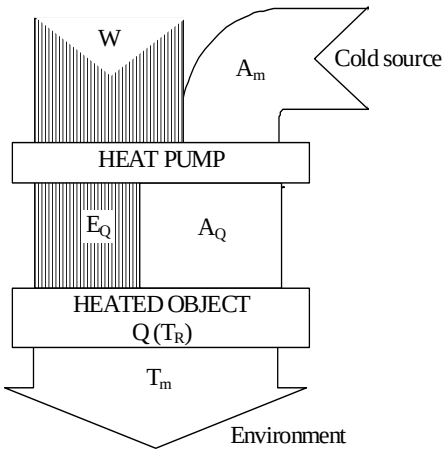

Figure 3- Sankey diagram of the process

In the real process two types of loss affect the process quality ($W>E_Q$):

- Mechanic and electric losses of the heat pump driving system ($\eta_m \cdot \eta_e$). The internal irreversibility of the process must be considered also (η_i).
- The external irreversibility of the process as result of the finite temperature difference of the heat transfer process over the condenser and vaporizer ($\xi_{\Delta T}$).

For the real process conditions $T_C > T_R$; $T_m > T_V$; $\eta_i < 1$ it means that $\xi_{\Delta T} < 1$.

For a correct comparison between heat pump and the other heating processes we must taking into account that electrical energy is produced into a power plant with an efficiency $\eta_e = W/E_B$ and in this situation the exergy efficiency of the heat pump process (ξ_{PC}) became:

$$\xi_{PC} = E_C/E_B = W/E_B * Q/W * E_Q/Q = \eta_i \xi_{\Delta T} \quad (8)$$

If is considered that in condenser and vaporizer heat transfer processes are running at the constant temperatures:

$$\xi_{\Delta T} = Q/W \cdot E_C/Q = Q/W \cdot (W - E_V)/Q \quad (9)$$

where E_V is lost exergy in condenser and vaporizer heat transfer processes, and

$$E_V = QT_m\left(\frac{1}{T_R}-\frac{1}{T_C}\right)+(Q-W)T_m\left(\frac{1}{T_V}-\frac{1}{T_m}\right) \quad (10)$$

If the process follows Carnot conditions:

$$\frac{Q}{W}=\left(\frac{T_C}{T_C-T_V}+\frac{1-\eta_i}{\eta_i}\right)\eta_i\eta_m\eta_{el} \quad (11)$$

and

$$\xi_{\Delta T}=\eta_i\eta_m\eta_{el}\left(\frac{T_C}{T_C-T_V}+\frac{1-\eta_i}{\eta_i}\right)\frac{T_R-T_m}{T_m} \quad (12)$$

5. HEAT TRANSFER INFLUENCE

The heat exchange through the condenser is directly proportional with temperature difference [2] :

$Q \sim (T_C - T_R) \sim (T_R - T_m)$,

so $(T_C - T_R) / (T_R - T_m) = K = const$ (13)

$Q \sim T_V / T_C \sim (T_R - T_m)$; $T_V / T_C \sim (T_m - T_V)$, so

$$\frac{T_m-T_V}{T_R-T_m}\cdot\frac{T_C}{T_V}=V=const \quad (14)$$

K and V are two constants that characterize qualitative behaviour of condenser and vaporizer. Considering all these, the exergetic efficiency of heat pump became:

$$\xi_{PC}=\eta_e\eta_m\eta_{el}\eta_i\left[\frac{1+(V+K)\cdot\left(1-\frac{T_m}{T_R}\right)}{1+(V+K)}+\frac{1-\eta_i}{\eta_i}\cdot\left(1-\frac{T_m}{T_R}\right)\right] \quad (15)$$

The analysis of function $\zeta_{PC} = f(V+K, T_R - T_m)$ allow us to reach the conclusions that:

- heat pump works in good conditions for $T_R - T_m = (10 – 30)\ ^oC$;
- for low environment temperatures heat pump exergetic efficiency increase.

6. LIMITING VALUES OF HEAT PUMP EFFICIENCY

By definition, the heat pump efficiency is:

$$\varepsilon = Q / W \quad (16)$$

Using relations 11 and 16 results:

$$\varepsilon=\eta_m\eta_{el}\eta_i\left[\frac{1+(V+K)\left(1-\frac{T_m}{T_R}\right)}{(1+V+K)\left(1-\frac{T_m}{T_R}\right)}+\frac{1-\eta_i}{\eta_i}\right] \quad (17)$$

Setting limiting conditions regarding the fuel consumption that means fuel amount used by power plant to produce heat Q equals fuel amount used to produce electric energy W for driving the heat pump compressor, and heat pump thermal charge is Q, the following relation can be written:

$$\varepsilon_{min} = \eta_B / \eta_e \quad (18)$$

7. CONCLUSIONS

One of the conclusions is that the heat pump is good to be used when $\varepsilon > \varepsilon_{min}$, because in this situation is a proper fuel consumption.

Making a graphical and experimental analysis of function $\varepsilon_{PC} = f(V+K, T_R - T_m)$ some conclusions regarding the heat pump efficiency limits were drawn:

-is recommended $\varepsilon > 2.6$ for the units with power plant in cogeneration;

- is recommended $\varepsilon > 2$ for the units with power plant;
- is recommended $\varepsilon > 1$ when heat pump replaces electric heating.

8. REFERENCES

[1] ROSEN, M.A., *Exergy as a Tool for Sustainability*, 3rd IASME/WSEAS Int. Conf. on Energy & Environment, University of Cambridge, UK, February 23-25, 2008

[2] CARABOGDAN, GH., BADEA, A., LECA, A.,sa, *Industrial thermal equipments (Instalatii termice industriale)*, Culegere de probleme, vol.II, Ed. Tehnica , Bucuresti, 1989

[3] SVENSSON, K., *Heat pump technologies*, TAPPI Press, Vol. 79, p.1-5, 2011

THEORETICAL AND EXPERIMENTAL RESEARCH ON THE RHEOLOGY OF THE MATERIALS' COUPLE WITH COMPOSITE STRUCTURE

[1]GRIGORESCU LUIZA, [2]DIACONESCU IOANA

[1,2]*„Dunarea de Jos" University, Galati, Romania*

ABSTRACT

The paper is a simplified hypothetical model of a tire made up of a toroidal flexible membrane, of inherent rigidity zero where there is a gas under a certain pressure p, in contact with a flat stable running path. Then actual operation is presented, with intense dynamic loads, where this approximation cannot be used even for an ideal tire. The real tire is not an ideal membrane without inherent rigidity but has a certain thickness, a certain rigidity which in rubber is not particularly linear when subjected to combined deformation of compressive and flexural tensile strength and adds to the additional nonlinear components making the elastic force expression become more complicated and difficult to formulate. Rubber is not perfectly elastic and it has plastic and viscous components, making that in addition to the elastic conservative forces even when they are not linear, to occur dissipative forces corresponding to plasticity and viscosity. Considering the path as real, therefore deformable, the foregoing considerations for the tire deformation are also valid for the path deformation. In addition, between the tire and the road/path, on the contact ellipse surface appear dry-type friction forces. All this leads to a very complex rheological model that cannot be approached separately for the tire or for the path but only for the assembly of the two elements.

Keywords: *rheology, tire, material's couple, friction, composite structure.*

1. INTRODUCTION

The rheology of a body considered isolated is a purely abstract, idealized concept. If we consider that rheology describes the behavior of a body subjected to stress, it automatically appears the need to have at least one other body that produce this stress. According to the principle of action and reaction in Newtonian mechanics, at the interaction between two bodies, the stress in the contact area act at the same intensity and direction on each body, so both bodies are subject to stress. Since there are no non-deformable bodies, the stress behavior means summation of the behavior of each body, the mathematical models that must describe the rheology of each body cannot be properly used unless conceived as torque models where important are not only the mechanical characteristics of each body but also their shape and size. It is easy to see that, for example, the same spherical body in interaction with another cylindrical body will deform quite differently if interacting with another flat body, the so-called contact patch shall have different sizes and shapes when the same forces are applied. Not only the spherical body is deformed but also the bodies it reacts with, i.e. cylindrical or flat bodies in the example above. Even if the deformations of one of the bodies are smaller and thus may be neglected, especially at static stress, this is no longer valid for dynamic stresses where the intensity of the stress is greater as the body is less deformable and where forces in the contact area are no longer transmitted instantly throughout the body.

As the most obvious example of the rheology of materials is the torque of a motor vehicle tire and the road surface/path. The tire is a very complex composite structure, consisting of a mixture of elasto - plastic material (usually natural or synthetic rubber), textile or metal inserts, and last but not least, the gas under pressure which provides a certain form and size. The rheological characteristics of each component are known, highly non-linear characteristics, but to assemble all of these features onto the whole tire it would be to reconstruct the characteristics of a material by assembling the characteristics of the atoms that compose it and still it would not be accurate. On the other hand, the path can be made of concrete, asphalt or simply compacted ground. Here too all the features of any material are known, and they are strongly nonlinear too, but if it should be found the tire –path couple characteristics, all this is of no help. One is to model the deformation of a rubber body under the action of a laboratory device, and other is to act upon the body with a real element such as the path which is different from the laboratory device in terms of shape, size, characteristics, and particularly dynamic action.

Therefore a vehicle tire and the road/path together form a purely individually deformable geometric assembly, dimensional and rheological under the influence of external efforts, the shape and size of the contact surface depending on the shape, dimensions, mechanical properties and deformation of the two components. The deformation of each component lead to internal reactions which, in general, can consist of all types of mechanical forces known such as elastic plastic viscous and dry friction. A very brief analysis can show that these forces are far from linear, which complicates any attempt to develop and solve a rheological model as close as possible to reality. The complexity of deformation is so high that makes it, very difficult to develop a rheological model if only theoretical, leading to the necessity of experiments to provide information on possible rheological models. With this conviction, we initiated a series of research whose results will be shown below.

2. ASSUMPTIONS

From the very beginning it will be deemed that no internal reaction which occurs after the tire deformation has a linear characteristic. If we considered a simplified hypothetical model of a tire made up of a toroidal flexible membrane, of inherent rigidity zero where there is a gas under a certain pressure p, in contact with a flat stable running path, Figure 1, a simple calculation shows that the relationship between the force F and deflection δ cannot be linear.

The force F is taken up by a reaction which is obtained by applying pressure p on the elliptic contact surface with the semi-axes a and b, i.e.

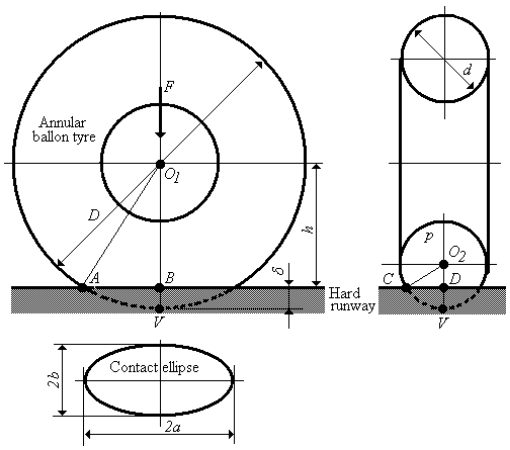

Figure 1 The simplified tire

$$F = p\pi ab \tag{1}$$

From triangles O_1AB and O_2CD it is found that

$$a = AB = \sqrt{\delta(D-\delta)} \tag{2}$$

$$b = CD = \sqrt{\delta(d-\delta)} \tag{3}$$

Where from

$$F = p\pi\delta\sqrt{(D-\delta)(d-\delta)} \tag{4}$$

From (4) it is seen that even in the case of an ideal tire, of the simplest form, which is on a dimensionally stable running track/path, the force F relation,which is an elastic force, is a nonlinear function of the deformation δ. Only for very small deformations so that δ is negligible compared to d and D, respectively, $\delta << D, \delta << d$ and only by such approximation it can be considered that the elastic reaction of the tire is described by a linear expression of the form:

$$F = p\pi\delta\sqrt{Dd} \tag{5}$$

But in actual operation, with intense dynamic loads, this approximation cannot be used even for an ideal tire as the above. The real tire is not an ideal membrane without inherent rigidity but has a certain thickness, a certain rigidity which in rubber is not particularly linear when subjected to combined deformation of compressive and flexural tensile strength and adds to the force provided by (4), additional nonlinear components making the elastic force expression become more complicated and difficult to formulate. Rubber is not perfectly elastic and, like any real deformable material, it has plastic and viscous components, making that in addition to the elastic conservative forces even when they are not linear, to occur dissipative forces corresponding to plasticity and viscosity. Considering the path as real, therefore deformable, the foregoing considerations for the tire deformation are also valid for the path deformation. In addition, between the tire and the road/path, on the contact ellipse surface appear dry-type friction forces. All this leads to a very complex rheological model that cannot be approached separately for the tire or for the path but only for the assembly of the two elements. The development of research in this regard considers the following assumptions:

1) The internal forces of the tire-path assembly opposing the action of the external are elastic, plastic, viscous and dry friction forces dependent nonlinearly on the deformation of the assembly in the contact area;

2) The components that cause elastic, plastic, viscous and dry friction forces in environments subject to deformation will be considered as connected in parallel because they produce effects each of them undergoing the same deformation

3) Resultant of the internal forces (reaction forces) is found, as any coupling in parallel, by adding the elastic, plastic, viscous and dry friction forces

4) The resultant is oriented toward the center of the tired wheel, being normal onto the path as it is before deformation

5) The deformation in the contact area is the result of joint deformation of both tire and path and will be considered as a whole, without separating it into separate deformations corresponding to the tire and the path.

The rheological model developed will be substantiated both theoretically and experimentally, the experiment being also the instrument that determines the actual values of the coefficients of the analytical expressions. From the assumptions stated above, the fourth is far from the real situations by failing to consider the reactions in the path plane (plane perpendicular to the wheel beam direction in the contact point), that appear in the startup or braking the vehicle, when driving on sloping or uneven road. We accepted this simplifying assumption to test a particular rheological model valid only to stresses on the normal direction and to conduct a simple accurate experiment which, if it will prove effective, can be extended to any other stress.

3. THE EXPRESSION OF THE REACTION FORCES

As shown above the reaction forces characterize the tire- path assembly and depend nonlinearly on the joint deformation δ. These forces occur only when the tire presses on the path/road, being identifiable by the fact that the position h of the vehicle wheel center O_1 to the undeformed road surface is smaller than the outer radius of the tire, D / 2, Figure 1, the remaining forces being null. This alone makes the internal reaction forces to be non-linear by the discontinuity introduced by the value of h = D / 2, which is illustrated in the form of writing

$$F = \begin{cases} F(\delta) & \text{if } h \le D/2 \\ 0 & \text{if } h > D/2 \end{cases} \quad (6)$$

and presented in figure 2.

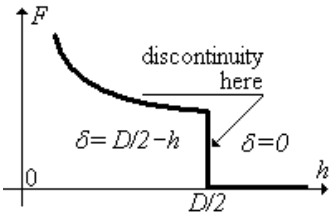

Figure 2 The gap of tire inside reaction

It is also known that the elastic, conservative forces oppose deformation while dissipative forces which include the dry friction and viscous forces oppose the deformation rate. Also the plastic deformation forces, being also dissipative forces, will resist the deformation rate. The expressions of these forces can take various forms. After several tests it was found that the more realistic is the polytropic writing so that we have:

- For the elastic force, $F_{el,}$ dependent on deformation, and resisting deformation

$$F_{el} = \begin{cases} -C_{el}|\delta|^{x_{el}} SGN(\delta) & \text{if } h \le D/2 \\ 0 & \text{if } h > D/2 \end{cases} \quad (7)$$

- For the plastic deformation force, F_{pl}, dependent on deformation and resisting deformation rate

$$F_{pl} = \begin{cases} -C_{pl}|\delta|^{x_{pl}} SGN(\dot{\delta}) & \text{if } h \le D/2 \\ 0 & \text{if } h > D/2 \end{cases} \quad (8)$$

- for the viscous friction force F_v, dependent on the deformation rate and resisting the deformation rate

$$F_v = \begin{cases} -C_v|\dot{\delta}|^{x_v} SGN(\dot{\delta}) & \text{if } h \le D/2 \\ 0 & \text{if } h > D/2 \end{cases} \quad (9)$$

In the above expressions SGN function is the "sign" function in the well known truth table

$$SGN(x) = \begin{cases} +1 & \text{if } x > 0 \\ 0 & \text{if } x = 0 \\ -1 & \text{if } x < 0 \end{cases} \quad (10)$$

and "-" sign in front of each expression (7) - (9) show formally that there are forces that oppose deformation or deformation rate. The dot above deflection δ shows that it is the deformation rate, ie. $\dot{\delta} = d\delta/dt$.

Although deflection δ cannot be negative as formulated in Figure 2, we preferred the writing mode for the relations uniformity. As regards the viscous friction, the deformation rate may be negative or positive and model writing is compulsory for a polytrope function when the value of the frictional force is independent of the sense of the deformation rate. If the viscous friction values would depend on the sense of this rate, the writing would have the form

$$F_v = \begin{cases} -C_{v1}|\dot{\delta}|^{x_{v1}} SGN(\dot{\delta}) & \text{if } h \le D/2 \text{ şi } \dot{\delta} > 0 \\ -C_{v2}|\dot{\delta}|^{x_{v2}} SGN(\dot{\delta}) & \text{if } h \le D/2 \text{ şi } \dot{\delta} < 0 \\ 0 & \text{dacă } h > D/2 \end{cases} \quad (11)$$

but in viscous homogeneous isotropic and continuous environments, the viscous friction value can be considered not dependent on the sense of the rate /speed.

As for the dry friction force, dependent on the amount of deformation δ which in turn the amount of normal force depend on, its expression is similar to the plastic deformation force and can be included in it. On a closer analysis it is found that even the plastic deformation is a deformation where strong internal dry friction force occurs thus preventing the return to original shape after removal of the forces that produced the deformation, so that the inclusion of the two forces into the same expression can be considered correct

In conclusion, the internal reaction forces can be written grouped as conservative forces, ie the elastic force of the form given by (7), who opposes to the deformation and as dissipative forces under the form of internal friction forces opposing the internal friction force F_{fr} opposing to the deformation rate given by:

$$F_{fr} = \begin{cases} -\left(C_{pl}|\delta|^{x_{pl}} + C_v|\dot{\delta}|^{x_v}\right) SGN(\dot{\delta}) & \text{if } h \le D/2 \\ 0 & \text{if } h > D/2 \end{cases} \quad (12)$$

4. THE DETERMINATION OF THE REACTION FORCES COEFFICIENTS AND EXPONENTS

To determine the coefficients and exponents that appear in equations (7) and (12) use is made of a simple experiment but with the appropriate precision to meet the desired goal. A real tire wheel, having mass M is dropped from a height h_1 on a flat surface of the real running path, Figure 3. After the partially elastic collision with the path surface, the tire wheel will rise to

height h_2. Considering the origin of the time when the wheel is allowed to fall freely the moment when the wheel reaches the height h_2 represents the time during descent-ascent movement, t_u.

Very important is to know the values h_1, h_2 *and* t_u, because their determination accuracy influencing the outcome. In order to find them, the following additional equipment was resorted to: next to the ruler graduated in mm was placed (actually a saw tape, unfolded) and the experiment was filmed with a digital camera, recording at normal speed of 25 frames / second. By analyzing the video frame by frame on a normal PC using the utility "Ulead VideoStudio 10", the values of h1 and h2 could be measured, then viewing the photograms with the utility used the moment t_u was found. Such analysis does not take much time as the motion takes 2 seconds, and no more than 50 frames have to be studied.

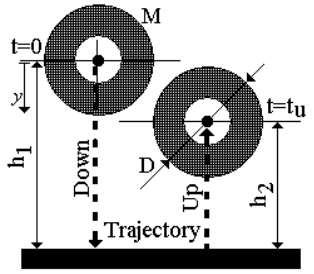

Figure 3 The experiment

Another important element is the number of experiments performed with the same wheel so that the results are less influenced by measurement errors and take into account the existence of the three types of reaction forces. The experiment must carry out deformations with different values for the same deformation rate and deformation at different deformation rates.

Getting deformation with different values at the same rate of deformation is possible if the wheel falls from the same height h_1 but have different masses M. In this way, the deformation will be different, but the impact with the running path is made vertically at the same speed, so that at least the initial deformation conditions of speed are the same.

Getting different deformation rates is possible if the wheel falls from different heights h_1. Thus there are two independent parameters of the experiment, ie wheel mass and fall height. The theory according to which is minimized the effect of the measurement errors leads to 6 experiments planned as follows.

For each parameter we consider two values, M_1, M_2, h_{1-1}, h_{1-2}, which in terms of geometric forms is a rectangle with a parameter on each side and the four corners would be all possible combinations of the values of the two parameters, Figure 4. The experiment should be carried out for the four values above plus twice the rectangle center M_c values h_{1-c}, a total of 6 determinations being required. If we follow the influence on the three parameters, for example the two above plus the pressure p in the tire, the three parameters would form as a parallelepiped with eight corners, requiring a total of 10 experimental determinations resulting from the 8 corners plus twice the values in the center of the parallelepiped. It goes without saying that in the latter case it is necessary to correct the expressions (7) and (12) for the pressure to appear as an independent variable.

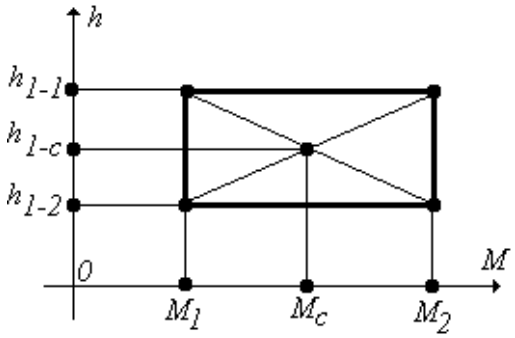

Figure 4 The experiment planning

For the purpose of the experiment the vertical coordinate *y* will have the origin in the center of the wheel which is the initial height h_1 and will be positive downward, Figure 3. Equation of the vertical motion of the wheel results by applying the principle of d'Alembert and separating the forces opposing the movement from those which favor the movement

$$M\ddot{y}+\begin{cases}\left(C_{pl}|\delta|^{x\,pl}+C_v|\dot{\delta}|^{x\,v}\right)SGN(\dot{\delta})+C_{el}|\delta|^{x\,el}\,SGN(\delta) & \text{if } y\geq h_1-D/2\\ 0 & \text{if } y<h_1-D/2\end{cases}=Mg \qquad (13)$$

With initial conditions: $y=0$, $\dot{y}=0$. The solution of equation (13) is considered the numerical function $y=f(t)$ (minus $h=f(t)$), assuming that we know the concrete values of the coefficients and exponents. Deflection δ will be expressed in this case as

$$\delta=D/2-(h_1-y) \qquad (14)$$

And the deformation rate $\dot{\delta}$ can be found, taking into account (14), by

$$\dot{\delta}=\frac{d\delta}{dt}=\dot{y} \qquad (15)$$

But in reality, the values of the coefficients and exponents of the equation (13) are not known precisely

these are true unknowns of the problem. In reality we know the tire data (diameter, mass, internal pressure) and the six experiments, therefore we know the following:
- The values of pressure *p* and the diameter *D*, constant for a given real tire;
- The values of variable parameters such as the mass and drop height *M* and h_1, under the form of two-dimensional array $M_i, h_{1-i}, i=1,2,\cdots,6$;
- The values measured for h_2, t_u, under the form of two-dimensional array $h_{2-i}, t_{u-i}, i=1,2,\cdots 6$.

As a way of working to find the coefficients and exponents of the relations (7) --- (9) it will be applied the mean square deviation minimizing method applied numerically to the solutions of equation (13). The basic idea is that, by trials, to find the values for the coefficients and exponents such that the solution of equation (13) on the the values of h_2 şi t_u have smallest deviations from the experimentally measured values. The concrete working algorithm using the numerical analysis in an original software includes the following steps:

1) The user chooses for each unknown value to be found, i.e. for $C_{pl}, x_{pl}, C_v, x_v, C_{el}, x_{el}$, an interval where their true value is supposed to be. Let these intervals be known through concrete values for each margin, which we denote
$C_{pl1}, C_{pl2}, x_{pl1}, x_{pl2}, C_{v1}, C_{v2}, x_{v1}, x_{v2}, C_{el1}, C_{el2}, x_{el1}, x_{el2}$;

2) Each interval is divided into a number *n* of equidistant subintervals. Thus a network of nodes of six independent dimensions is formed, corresponding to the six coefficients and exponents, of the form $C_{pli}, x_{pli}, C_{vi}, x_{vi}, C_{eli}, x_{eli}, i=1,2,\cdots n$;

3) The differential equation (13) is numerically solved in all possible combinations formed on the above node network, therefore 6^n solutions are needed. Every solution begins with the initial conditions given above and stops when the value $\dot{y}$ is canceled for the second time, ie when the wheel reaches its maximum height after the collision denoted by $h_{2calculated}$ (first cancellation occurs at the start of the climb race, on the impact with the running path, the second cancellation occurs at achieving the maximum height).

4) For each of the 6^n values $C_{pl}, x_{pl}, C_v, x_v, C_{el}, x_{el}$ are record and the values $h_{2\,calculated}$ and $t_{u\,calculated}$ resulted from each solution;

5) For the 6^n cases is calculated the mean square deviation *S* using the known formula

$$S=\sqrt{\frac{\sum_{i=1}^{6}\left(h_{2i}-h_{2\,calculated}\right)^2}{6}} \qquad (16)$$

And it is found for which group of values $C_{pl}, x_{pl}, C_v, x_v, C_{el}, x_{el}$ the deviation is minimum. The values of the coefficients and exponents $C_{pl}, x_{pl}, C_v, x_v, C_{el}, x_{el}$ which are for to the min. square deviation characterizing the rheologic model proposed.

A very complicated issue occurs though. If, for example, for a certain coefficient, be it C_{pl}, the search interval lies between the values $C_{pl1}=0$ and $C_{pl2}=10000$, to finally obtain sufficiently accurate value it would be necessary to divide it into minimum *n=100* subintervals 100. With six unknown values for which all intervals are divided into 100 subintervals it follows that equation (13) should be solved $6^{100}\approx 6{,}53\cdot 10^{77}$ times, which would take very much time even for the age of the Universe. For a simple comparison, our Universe has an estimated age of 10^{15} years which means about $3{,}16\cdot 10^{22}$ seconds. And if solving took only a thousandth of a second to a node, the complete resolution would enormously exceed the age of our universe. In spite of this, the problem has the solution. Instead of 100 subintervals or more it will be chosen only 6, maximum 7 subintervals, which reduces the number of solutions to " only " 46656, max 279 936, which does not last very long (tens of seconds) on a typical computer. The problem of accuracy is solved by filling the above algorithm by the following steps:

- Solving equation (13) for the 6 and 7 subintervals the value of the coefficients and exponents were divided into; $C_{pl}, x_{pl}, C_v, x_v, C_{el}, x_{el}$
- After retaining from the 6 or 7 values the group of values for $C_{pl}, x_{pl}, C_v, x_v, C_{el}, x_{el}$ which minimizes the standard deviation are intervals are created in which to look for the solution which in turn will minimize the deviation. These intervals will have the ends formed of the adjacent values to $C_{pl}, x_{pl}, C_v, x_v, C_{el}, x_{el}$ found above;
- The new intervals are divided in turn into the 6 or 7 subintervals and the algorithm described above is applied;
- The process continues until no minimum deviation decreases significantly ie until the difference between two measurements of minimum deviation is less than the value required for accurate determination; as well it may be required a number of reversals of the iterative process, I prefer to choose up to 8 --- 10 reversals.

In this way the problem of accuracy and length of solving is also dealt with, requiring a maximum of 2,239,488 of solutions to equation (13) instead of about $6{,}53\cdot 10^{77}$ solutions.

If we are only interested in the rheology of the tire it can be used in experiment a practically rigid running path such as a slab of concrete or cast iron of very large mass. If we are only interested in the soil rheology, instead of a tire it can be used a wheel as rigid as possible. But the results will not be correct and will not allow summation of the two cases because they do not account for the fact that deformations are from both

bodies. Only if both - the tire and wheel - are deformable the rheology of the pair tire - wheel can be obtained.

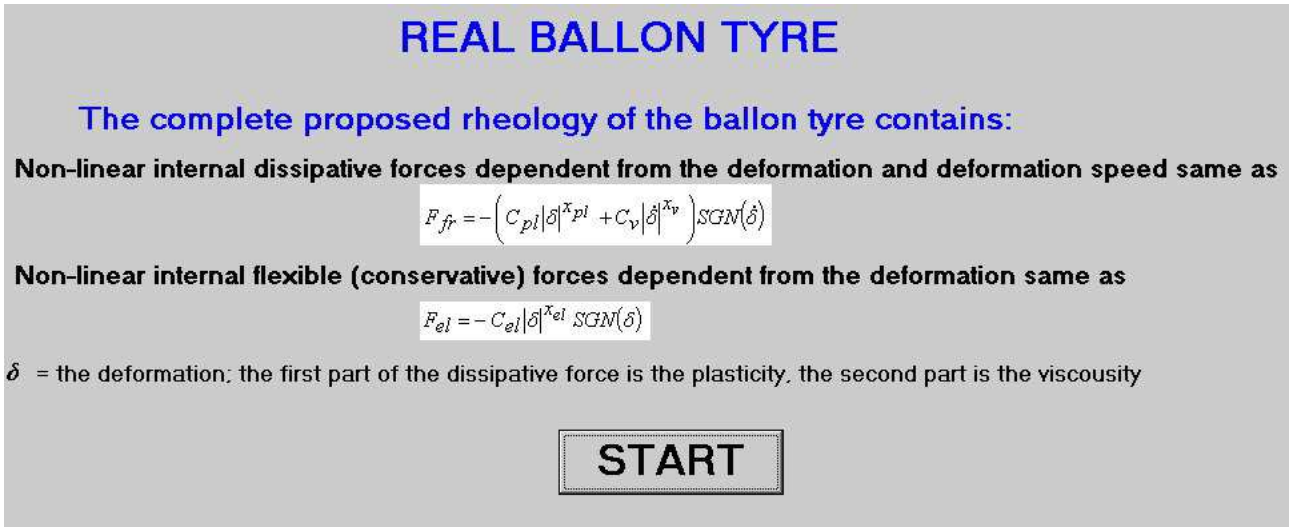

Figure 5 Print screen of software for coefficients and exponents calculation

We have shown above that the final value of the coefficients and exponents are under the condition that the standard deviation (16) is minimum. As parameter to determine this deviation the height h_2, was chosen taking into account the calculated and measured values. But the experiment and the differential equation also provide a parameter, namely the time t_u which has also the great importance in the determination. Given this, there are several possibilities of calculation:

$$S = \lambda_1\sqrt{\frac{\sum_{i=1}^{6}\left(h_{2\,i} - h_{2\,calculated}\right)^2}{6}} + \lambda_2\sqrt{\frac{\sum_{i=1}^{6}\left(t_{u\,i} - t_{u\,calculated}\right)^2}{6}} \quad (17)$$

a) To calculate a standard mixed and weigthed deviation of the form (17) with λ_1 and λ_2 weighing coefficients between 0 and 1so that $\lambda_1 + \lambda_2 = 1$. Computer tests have shown that this variant fails to provide additional accuracy while making the calculation time longer;
b) let us calculate the standard deviation only depending on a single parameter, either h_2 or t_u and the other parameter is used to decide which type of expression of internal forces is closer to reality. After testing it was determined that the most accurate results are obtained using h_2 for finding the values and t_u for choosing the type of expression. Thus it was found that the expressions presented here, the of polytropic type, best fit (small inaccuracies resulting from values t_u) in comparison with other expressions of polynomial, exponential, or combinations type.

5. PRACTICAL RESULTS

Details of the structure of the tire (number of insertions, the thickness of the layers, the cross-sectional shape and the like) or of the running path (trademark, thickness, etc.) have no relevance. Their knowledge can only have archival value, they cannot be taken over by the physical and mathematical model of the pair/torque rheology.

The model so developed, of actual values for the empirical coefficients, will only be a model for strictly the individual pair of experiments that have been conducted. Changing the tire pressure, its size, the running path (eg asphalt) another rheological model of the new pair will be obtained. And precisely this is highlighted in the paper: any material pair will have their own rheology, we shall call it pair rheology and characterizes only one couple actually. The advantage of this approach is to obtain a precise and reproducible rheological model as long as the couple remains the same.

In the experiment conducted to determine the coefficients and exponents from the relation (13) which actually describe the mathematical model of the dynamic rheology, we chose what we had available, namely a wheel tire Opel Corsa 1300 type 185/70 R14 Continental company, internal pressure 2 bar on a concrete runway. Additional data may be found at the company but, as I mentioned, they are of no value.

For processing we have developed specialized software in the Delphi 6 which, provides a screen page as shown in Figure 5 and after START it requires the actual data of the experiment, Figure 6.

After running the software the results are visible as shown in Figure7.

A comparison of the calculated values using the model described by (13) is shown in Figure 8.

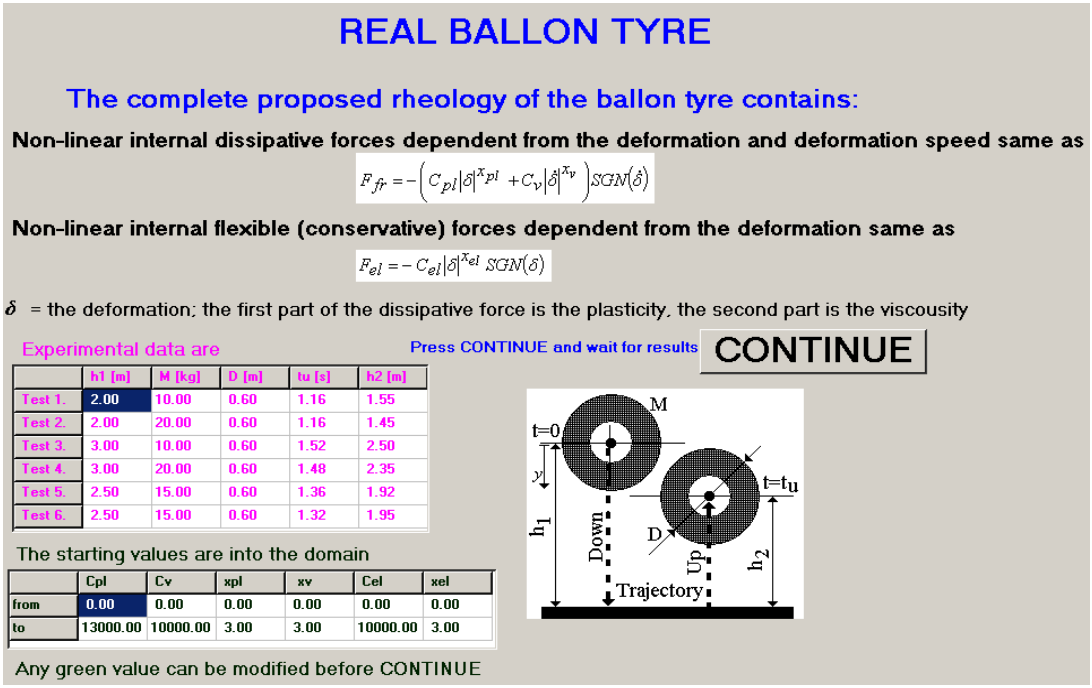

Figure 6 Print screen with practical values of the experiment

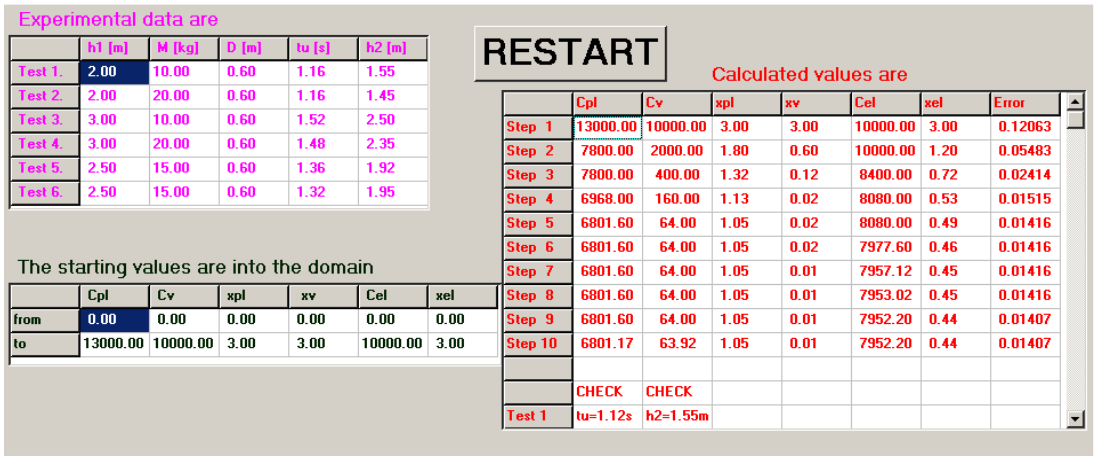

Figure 7 After running software results

6. CONCLUSIONS AND RHEOLOGICAL TESTS OF OTHER MATERIALS

We have shown that the method presented above allows finding the tire behavior only to radial strain. For strains in other directions, such as transverse or tangential, the method described in principle remains the same. All six experiments are needed, but organized differently. Instead of the wheel falling onto the tire to collide with a hard surface, the wheel remains at rest in a non-deformable area (or negligible deformation) and it is allowed to fall on it, transverse to the tire, a deformable body, hard and heavy of mass M, Figure 9.

On the tire other devices may be attached as well to allow collision to tangential direction or any direction of interest. A more refined variant of the transversal load testing, applicable also to tangential strains is shown in Figure 10, for which another physical -mathematical model must be developed due to the combination of radial load with the transversal or tangential ones and the movement of the wheel in both directions, vertically and horizontally, and its forced rotation at collision and free rotation after the collision. Since the physico-mathematical model must include also the rotation of the wheel, the moment of inertia about the axis of rotation during the experiment must be known - or measured.

Using an experiment like that described in Figure 9 under the mathematical formalism discussed in Chapter 3 of this paper, we can determine the rheological characteristics of materials with a very complex behavior due to internal forces of different natures caused by the deformations, such as different types earth, asphalt, concrete, composites, rubber, plastics and more similar ones.

Calculated values are							
	Cpl	Cv	xpl	xv	Cel	xel	Error
Step 10	6801.17	63.92	1.05	0.01	7952.20	0.44	0.01407
	CHECK	CHECK					
Test 1	tu=1.12s	h2=1.55m					
Test 2	tu=1.16s	h2=1.47m					
Test 3	tu=1.48s	h2=2.49m					
Test 4	tu=1.48s	h2=2.34m					
Test 5	tu=1.32s	h2=1.94m					
Test 6	tu=1.32s	h2=1.94m					

Figure 8 The calculated values for the rise time t_u and the height h_2

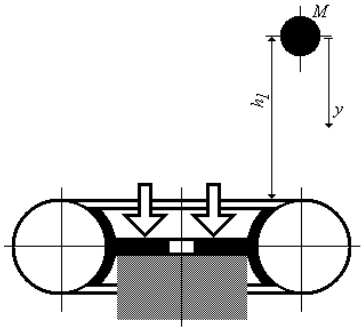

Figure 9 The determination of tire behaviour on transversal direction

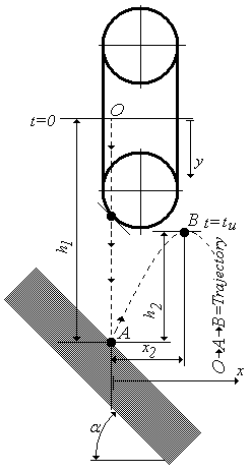

Figure 10 The mixed, radial and transversal application test

7. REFERENCES

[1] Debeleac, C., Oproescu Gh., *Non-linear behaviour of a soil campaction equipment.* 5th International Vilnius Conference KORSD-2009, Lithuania, September 30 – October 3, 2009, ISBN 978-9955-28-482-6

[2] Cauteş, Gh., Oproescu, Gh., *Dinamica sistemelor mecanice neliniare*. Editura CEPROHART, Brăila, 2003, ISBN 973-7909-03-8

[3] Cauteş, Gh., Oproescu, Gh., *Analiza dinamică a sistemelor elastice neliniare prin simulare numerică*. Editura CEPROHART, Brăila, 2004, ISBN 973-7909-08-9

[4] Cauteş, Gh., Oproescu, Gh., *Analiza vibraţiilor sistemelor cu neliniarităţi fizice* Editura CEPROHART, Brăila, 2004, ISBN 973-7909-07-0

[5] Năstac, S., Oproescu, Gh., *About damages identification methods at MDOF dynamic systems.* Academia Română, Academia de ştiinţe tehnice, SISOM 2008 and Sesion of the Commission of Acoustics, Bucharest, 29-30 may 2008

[6] Oproescu, Gh., Cauteş, Gh., *Metode numerice şi aplicaţii*. Editura TEHNICA-INFO, Chişinău 2005, ISBN 9975-63-254-8

[7] Oproescu, Gh., Năstac, S., *The modeling of the dissipative solidly media for the waves*. Academia Română, Academia de ştiinţe tehnice, SISOM 2008 and Sesion of the Commission of Acoustics, Bucharest, 29-30 may 2008

[8] Oproescu, Gh., Debeleac, Gh., *Classic and Modern in the Simulation of the Dynamical Behavior of the Technical Systems*. Workshop cod proiect CNCSIS – UEFISCSU 194 "Modelarea reologica avansata in conceptie micro-si macrostructurala a sistemelor compozite din neopren pentru izolarea bazei la socuri si vibratii", Braila, 17-18 nov. 2008, ISBN 978-973-8132-68-9

[9] Oproescu, Gh., *Self made modern measurement equipments, easy and ever-available*. Annals of Oradea University, volume VIII (XVIII), may 2009, ISSN 1583-0691, pg. 772-777

[10] Oproescu, Gh., Carmen Debeleac. *New trends in simulation of dynamic behaviour of the technical systems*. 5th International Vilnius Conference KORSD-2009, Lithuania, September 30 – October 3, 2009, ISBN 978-9955-28-482-6.

MODELLING THE HEAT RELEASE IN HIGH SPEED DIESEL ENGINES

MAHRAN DAWWA, PAUL BOCANETE

Constanta Maritime University, Constanta, Romania

ABSTRACT

Heat release phenomenon is considered one of the most important factors that affect the characteristics of diesel engine. Hence, modeling the heat release rate is an important step for modeling the whole combustion process in diesel engines, and for predicting the engine performance, in-cylinder temperature, and emissions specially NOx emissions which are so linked to the in-cylinder temperature at the premixed phase of combustion. Depending on the nature of the heat release and the nature of combustion process in the diesel engines combustion chamber many models have been developed in an effort for modeling the actual heat release in a relative short time with a satisfied accuracy. This work shed light on the ignition delay period, the phases of combustion process in diesel engines, and on two main important models which used for modeling the heat release in diesel engines, the vibe model and Watson et al model.

Keywords: *diesel engine, heat release, double vibe function, Watson function.*

1. INTRODUCTION

This paper discusses the modelling of heat release in diesel engines by the use of different functions. The heat release in diesel engines is linked directly to the mass fraction of fuel which burned during the combustion process, so the higher heat release rate means the shorter combustion period, actually the burning of fuel inside the engine cylinders is incomplete and imperfect combustion it should be distinguished between the different types of combustion, complete, perfect, incomplete, and imperfect combustion. The products of complete combustion are only carbon dioxide and fuel vapour, however this type of combustion is hypothetical type and it cannot be obtained whether air ratio greater, equal, or smaller than one.

2. HEAT RELEASE PHASES

Due to the nature of the Diesel fuel and the nature of mixture formation inside the cylinder of diesel engines the mixture formation and the combustion process cannot be considered as a separate or independent from each other, because of the mixture formation has a large impact on the combustion process. Hence, the combustion process in diesel engines can be divided into three phases, the first phase is called premixed combustion, this phase corresponds to the period of high pressure increase speed, and in diesel engines this phase is accompanied with noise which is which it is the result of high pressure increase speed. And it lasts for only a few crank angle degrees the rate of burning during this phase is generally high.

The second phase is the diffusion combustion (main combustion), this phase starts once the fuel and air mixture which formed during the ignition delay have been started to burn, the fuel injection continues during this phase, and the mixture formation continues by series of processes atomizing, vaporizing, and mixing the fuel with hot compressed air, this series of processes influences the combustion process and the emissions formation including NOx formation. The mixture formation process controls the diffusion phase. The end of the diffusion phase generally is determined by reaching the maximum temperature of in-cylinder gases.

The third phase or called post-combustion (late-combustion) corresponds to the “tail” of the combustion, third phase occurs at late period of the diesel engine expansion stroke, the combustion continues even though the injection process has completed, flame jet transforms into pockets of air-fuel mixture that surrounded by the flame because no addition fuel injected into the combustion chamber, which causes the decreasing of pressure and temperature in the combustion chamber, which leads in its turn to reduce chemical reactions speed.

The third phase also depends on the injection system characteristics such as the speed of nozzle needle closure, a quick closure leads to form high speed fuel parcels which combust in the same sequence of diffusion combustion, differently a slow closure leads to low speed fuel parcels with lack of oxygen, this phenomenon causes the increase in soot emissions formation.

3. HEAT RELEASE MODELS

The heat release rate is given at each crank angle by empirical equations which will be explained as follows.

3.1 Double Vibe model

Vibe function provided by “Vibe” (1970). This equation is used to model the mass fraction of burned fuel as a function of crank angle, in other words this equation is described the total heat release rate inside the combustion chamber, vibe function is based reaction kinetic consideration [3]. In other words formation of radicals is proportional to the amount of injected fuel which means the more fuel injected the more radicals formed, and formation of radicals is inverse proportional to the increase of fuel that is available to combustion,

$$\frac{dm_{fuel}^{+}}{dt} = k \cdot m_{fuel} \text{, and } dm_{fuel}^{+} = -\mu \cdot dm_{fuel}$$

$$\frac{Q_{chem}(\varphi)}{Q_{chem.tot}} = 1 - \exp\left[-\alpha \left(\frac{\varphi - \varphi_{soc}}{\Delta\varphi_{CD}} \right)^{m+1} \right] \quad (1)$$

Where: φ is crank angle degree between the start and the end of combustion, the entire amount of heat release is calculated from calculation the fuel mass that injected in one engine cycle multiplied by lower heating value of diesel.

$$Q_{f,total} = m_{fuel} \cdot lhv \quad (2)$$

By deviating the total heat release rate from the degree of crank angle

$$\frac{dQ_{chem}}{d\varphi} = \alpha \cdot Q_{chemtot} \cdot (m+1) \cdot \left(\frac{\varphi - \varphi_{soc}}{\Delta\varphi_{CD}} \right) \cdot \exp\left[-\alpha \left(\frac{\varphi - \varphi_{soc}}{\Delta\varphi_{CD}} \right)^{m+1} \right] \quad (3)$$

The heat release also can be modeled a as double vibe function, the idea of the double vibe function is to replace the simple vibe heat release rate model with more sophisticated model of two Vibe functions, for making the heat release model more suitable for real combustion process and make a division between premixed and mixing-controlled phases.

$$\frac{dQ_{f,1}}{d\varphi} = Q_{f,1} a (m_1 + 1) \cdot \left(\frac{\varphi - \varphi_{SOC,1}}{\Delta\varphi_{CD},1} \right)^{m_1} \cdot \exp\left[-\alpha \left(\frac{\varphi - \varphi_{SOC,1}}{\Delta\varphi_{CD,1}} \right)^{m_1+1} \right] \quad (4)$$

Where: φ is crank angle degree between the crank angle that corresponds to the start of combustion and crank angle that corresponds to the end of premixed phase.

$$\frac{dQ_{f,2}}{d\varphi} = Q_{f,2} a (m_2 + 1) \cdot \left(\frac{\varphi - \varphi_{SOC,2}}{\Delta\varphi_{CD,2}} \right)^{m_2} \cdot \exp\left[-\alpha \left(\frac{\varphi - \varphi_{SOC,2}}{\Delta\varphi_{CD,2}} \right)^{m_2+1} \right] \quad (5)$$

Where: φ is crank angle degree between the crank angle that corresponds to the end of premixed phase and the crank angle that corresponds to the end of combustion. By taking into consideration the proportion of released heat for premixed and diffusion phases as follows. $Q_{f,1} = xQ_{f,gas}$, and $Q_{f,2} = (1-x)Q_{f,gas}$

$$\frac{dQ_f}{d\varphi} = \frac{dQ_{f,1}}{d\varphi} + \frac{dQ_{f,2}}{d\varphi} \quad (6)$$

Where Parameters m_1 and m_2 indicate respectively the shape of premixed and diffusion phases of combustion. Increasing the parameter m_1 leads to increase the released heat during the premixed phase and to reduce the released heat during the diffusion phase. In the contrast increasing the parameter m_2 leads to decrease the released heat during the premixed phase and to increase the released heat during the diffusion phase. Parameter x is the phase proportionality factor which determines the amount of released heat in each phase. With regard to parameter a it is linked to the total conversion coefficient ($\eta_{conv,total}$), the influence of the parameter is complicated, it affects the amount of released heat during the premixed combustion phase, parameter a becomes larger with $\eta_{conv,total}$ increase, also the combustion terminates earlier for larger $\eta_{conv,total}$. However, the value of parameter a varies from 2.995 for $\eta_{conv,total} = 0.950$, to 6.908 for $\eta_{conv,total} = 0.999$ more data about this model in [8], [3]

In order to get the most accurate result from using the vibe function a heat release rate pre-calculation must be carried out to determine the three parameters of vibe function, start of combustion, combustion duration, and the shape parameters. Anyhow in this study the shape parameters will determined and fixed for all engine regime work on the other hand for, the determination of the start of combustion the following equation is used:

$$\varphi_{SOC} = \varphi_{SOI} + \tau_{id} \quad (7)$$

The combustion duration depends on the air-fuel ratio and on the speed and given by the following equation

$$\Delta\varphi_{CD} = \Delta\varphi_{CD,A} \left(\frac{\lambda_A}{\lambda} \right)^{a_{CD}} \left(\frac{n}{n_A} \right)^{b_{CD}} \quad (8)$$

Where: the index A means initial operating point of the engine. The shape parameter will not be implemented in this work.

3.2 Watson et al model:

This model considered a good model for modeling the heat release in diesel engines especially for the first phase of combustion, by the use of two functions for modeling the heat release the first function is used to model the premixed heat release phase, and the second function is used for modeling the diffusion phase. Hence, the mass of burned fuel by the total fuel mass with injected per cycle can be written by the use of the two functions as follows [7]:

$$\frac{m_{b,f}}{m_{tot}} = \beta f_1 + (1-\beta) f_2 \quad (9)$$

Where: β is the phase proportionality factor which determines the heat release for each phase given as $\beta = 1 - \frac{a\phi^b}{\tau_{id}^c}$, $0. < a < 0.95$, and $0.25 < b < 0.45$ are empirical constants.

The first function that describes the premixed phase is given as:

$$f_1 = 1 - \left(1 - t'^{K_1}\right)^{K_2} \quad (10)$$

The second function for the diffusion phase is given as:

$$f_2 = 1 - \exp\left(1 - K_3 t'^{K_4}\right) \quad (11)$$

Where: $t' = \frac{\varphi - \varphi_{SOC}}{\Delta\varphi_{CD}}$, $K_1 = 2 + 1.25 \cdot 10^{-8} (\tau_{id} N)^{2.4}$, $K_2 = 5000$, $K_3 = \frac{14.2}{\phi^{0.644}}$, and $K_4 = 0.79 K_3^{0.25}$ are empirical coefficients.

4. RESULTS AND DISSCUSION

In this section the result of modelling naturally aspirated Hino W04D high speed marine diesel engine will be discussed, the model have been done by the using of MATLAB program. The fuel system is direct injection system, bore and stroke dimensions are 104mm, and 118 mm respectively, the total displacement is 4.009 L, and the compression ratio is 17.9.

At 1600 rpm and 150 N.m the figure 1 shows, changing the value of parameter m_1 affects the peak of the rate of heat release at the premixed phase, which will affect the accuracy of prediction the engine parameters specially the peak pressure and the amount of NOx emissions that forms inside the combustion chamber.

It can be noticed that decreasing the value of m_1 will increase the peak of heat release and on the contrary increasing m_1 value will decrease the rate of heat release peak. As will as it can be noticed that the peak of released heat occurs earlier by decreasing the value of parameter.

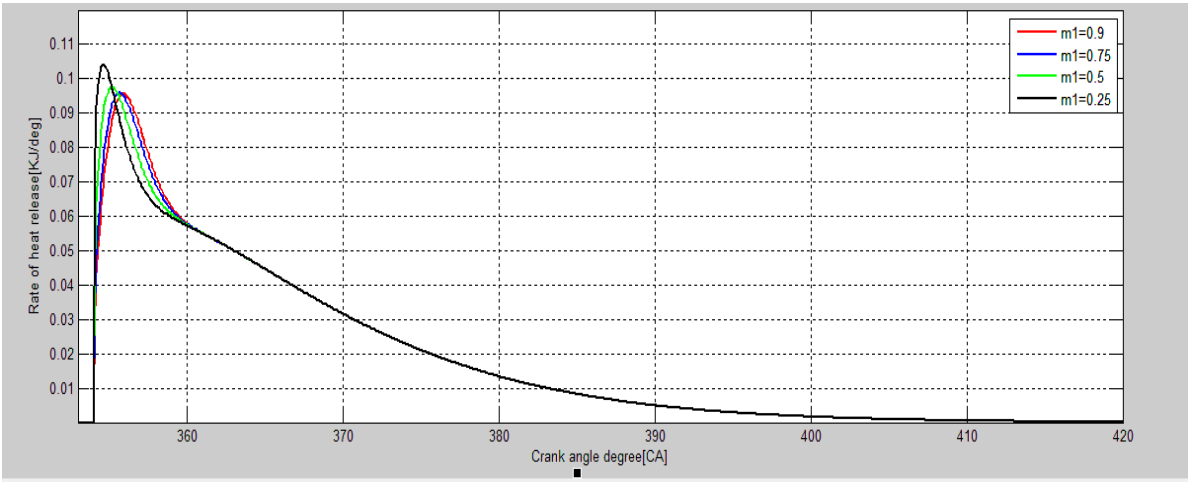

Figure 1 The effect of parameter m_1 on the rate heat release

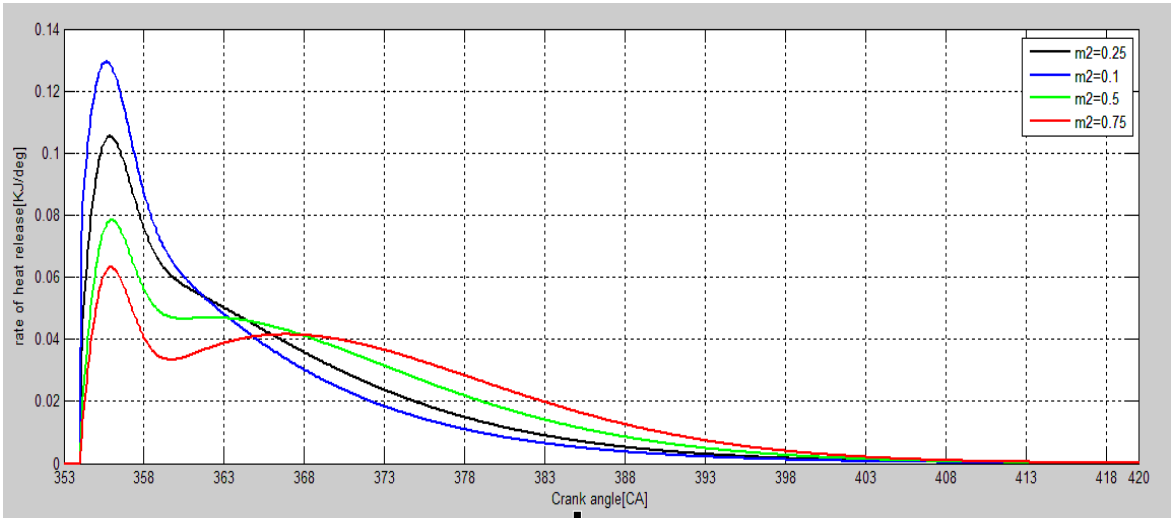

Figure 2 The effect of parameter m_2 on the rate of heat release

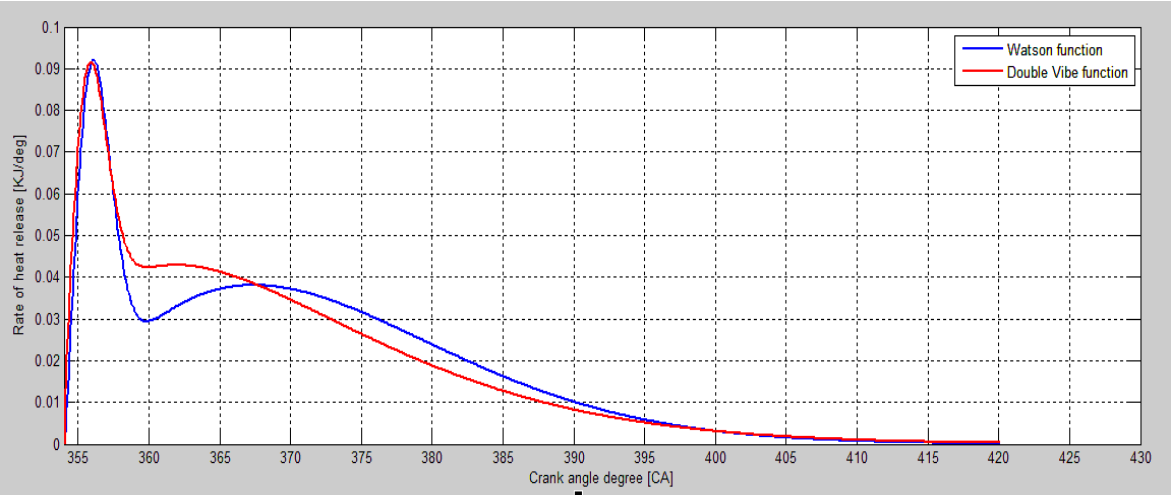

Figure 3 The rate of heat release

The figure 2 shows the effect of changing parameter m_2 on the profile of the rate of heat release by using Vibe function, as we notice the effects of changing the parameter m_2 are larger and affects the rate of heat release throughout the combustion period specially at the diffusion phase, and by increasing the value of parameter m_2 the heat release during the diffusion phase will be increased

Figure 3 shows the difference between the results of using Vibe and Watson models, after the peak of rate of heat release the mount of rate of heat release by using Watson function is less the by using Vibe function, on the other hand there is another peak of rate of heat release during diffusion phase by using Watson model which considered as shortcoming of this function when it use for modeling modern diesel engines.

5. CONCLUSIONS

In order to model the combustion process in high speed marine diesel engines, it can be relied on using Vibe and Watson models for modeling the rate of heat release because they give satisfied results especially at premixed phase during a relative short time. This paper showed the importance of choosing the accurate parameters for using Vibe function on modeling the rate of heat transfer in diesel engines. The error which occurs from using inaccurate parameters for both functions causes unacceptable results, so the most important step for modeling the rate of heat release by numerical models is to determine the functions parameters to ensure accurate modeling process.

6. REFERENCES

[1] B. Venkateswara Rao, G. Amba Prasad Rao, Prediction of Heat Release Patterns for Modeling Diesel Engine Performance and Emissions, Department of Mechanical Engineering, National Institute of Technology, India, 2012

[2] Constantine D. Rakopoulos, Evangelos G Giakoumis, Diesel Engine Transient Operation Principles of Operation and Simulation Analysis, London, 2009

[3] Günter Merker, Christian Schwarz, Gunnar Stiesch, Frank Otto, Simulating Combustion Simulation of Combustion and Pollutant Formation for Engine-Development, Berlin, 2006

[4] Gunter Merker, Christian Schwarz, Rudiger Teichmann Combustion Engines Development Mixture Formation, Combustion, Emissions and Simulation, Berlin, 2012

[5] Gunnar Stiesch, Modeling Engine Spray and Combustion Processes, Berlin, 2003

[6] Jamil Ghojel, Damon Honnery b, Heat release model for the combustion of diesel oil emulsions in DI diesel engines Department of Mechanical Engineering, Monash University, Florida, 2005

[7] John B. Heywood Internal Combustion Engine Fundamentals, Newyork, USA, 1988

[8] Klaus Mollenhauer, Helmut Tschoeke, Handbook of Diesel Engines, Berlin, 2010

[9] Lino Guzzella, Christopher H. Onder, Introduction to Modeling and Control of Internal Combustion Engine System, Berlin, 2010

[10] P, Lakshminarayanan, Yogesh V.Aghav, Modeling Diesel Combustion, New York 2010

NUMERIC GEOMETRY OPTIMIZATION OF AN WED FOR DUCT PRESSURE ANGLE, LENGTH AND RADIUS

[1]MARTINAS GEORGE, [2]ARSENIE ANDREEA, [3] LAMBA MARINEL-DANUT

[1, 2 ,3]*Constanta Maritime University, Romania*

ABSTRACT

The Wake Equalizing Duct (WED) device must be customized to fit to the afterbody of the ship in terms of performing its supposed function as Duct Pressure Angle, Length and Radius. The Designer is therefore placed in the front of multiple geometric solutions from between he has to make a choice. A given geometry of a WED device is taken and via Design Optimization the geometry of the duct was refined so that better results are achieved with a smaller and more compact WED. A rational choosing approach by involving the numeric optimization of the geometry of the WED in order to select the best fitted WED to perform the best in order to achieve some predefined parameters is targeted in this papers. The pressure on ships designers to achieve both reduced fuel costs and reduced emissions by optimizing the hull and propeller has never been higher. Being one of the key strategic business goals for ship owners and operators, the reduction of fuel cost becomes essential; and furthermore a variety of recent legislations require owners and operators to move towards the reduction of emissions from ships of SOx, NOx and CO. There has been great interest in the potential to enhance the performance of existing vessels through retrofit of devices to the hull, in parallel to the performance improvement of new built vessels.

Keywords: *Finite Volume Analysis; Geometry Optimization; Design Explorer; Maritime Ships; Wake Equalizing Duct.*

1. INTRODUCTION

The reduction of fuel cost has always been one of the key strategic business goals for ship owners and operators. In the current climate of high oil prices, the reduction of fuel costs becomes essential; and furthermore a variety of recent legislations require owners and operators to move towards the reduction of emissions from ships of SOx, NOx and CO.

Hence the pressure on designers to achieve both reduced fuel costs and reduced emissions by optimising the hull and propeller has never been higher. In parallel to the performance improvement of new built vessels, there has been great interest in the potential to enhance the performance of existing vessels through retrofit of devices to the hull. A wide range of concepts has been proposed, many of which involve modification or control of the flow in the vicinity of the propeller. The interest in these devices arises with increasing oil price. These devices are commonly called “energy saving devices (ESD)” and sometimes “retrofitting technologies” although many can be considered for new designs as well.

In any case for instance the WED device must be customized to fit to the afterbody of the ship in terms of performing its supposed function. The Designer is therefore placed in the front of multiple geometric solutions from between he has to make a choice. This paper is intended to help the Designers to have a rational choosing approach by involving the numeric optimization of the geometry of the WED in order to select the best fitted WED to perform the best in order to achieve some predefined parameters.

The claims may not give details as to the conditions under which the savings have been achieved and/or how the savings have been calculated and/or measured. Furthermore,the magnitude of the savings may well be within the range of uncertainties and measurement errors on the full-scale vessel. Consequently, cautious operators may well be skeptical about the validity of the figures being presented to the market, and it is absolutely reasonable and necessary for a buyer to verify independently the amount of savings before any investment on an ESD or ESDs.

The savings look very attractive to ship operators, for instance a saving of 7-9% from installation of a wake equalising duct (Schneekluth, 1986, Schneekluth (WED) and Bertram, 1998) or 8-9% from a combination of wake equalising duct and pre-swirl fins (Mewis, 2008, Mewis, 2009). In general, the negative aspects of the devices include the considerable cost of installation, and also the reported reluctance of manufacturers to guarantee the claimed savings.

2. MODEL OF THE SHIP - CAD AND FINITE VOLUME ANALISYS (FVA

The goal of this paper is to calculate via software Ansys 13^{TM} the best geometric solution for a WED device. It is known that a poor design of the WED is not only improving the overall efficiency of the vessel but may have an adverse impact failing to achieve its purpose.

The model has as departure point a real portcontainer as seen below, with the following parameters:

- Length *L*- [m]- 173,
- Breadth *B*- [m]- 25,
- Draught *T*- [m]- 9.50,
- Diameter *D*- [m]- 5,
- Number of blades *Z* – 6,
- Propeller RPM-120, Average Speed-16 knots (7 m/s)

In order to have a starting point for the simulation, first of all the afterbody was firstly CAD generated with the WED device attached, and all the parameters for fluid flow were calculated accordingly. From that point on the Ansys

Design Explorer was involved in order to optimize the geometry.

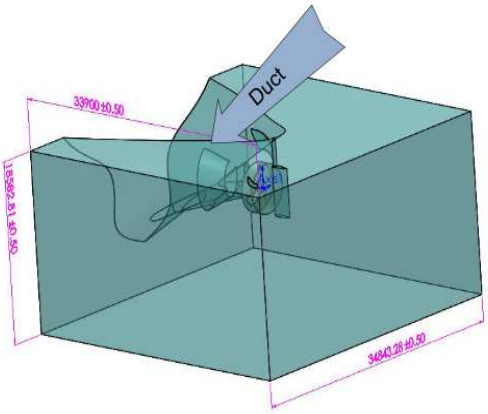

Fig.1 CAD geometry with WED

In order to provide more details on the geometry of starting model of the WED device and the optimization input parameters, the below figure is shown, with dimensions in [mm]:

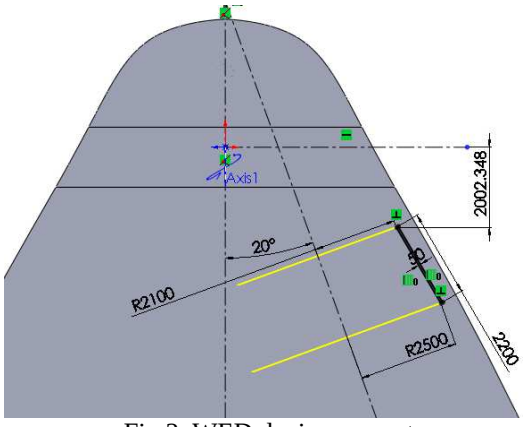

Fig.2 WED device geometry

5 input geometric parameters were defined as follows:

Table 1-Input geometric parameters

	Name	Type	Lower limit	Upper limit
P1	Angle (Minimize)	Continuos	14 [degree]	22 [degree]
P2	Duct Length (Minimize)	Continuos	1980 [mm]	2420 [mm]
P3	Small radius (Minimize)	Continuos	1600 [mm]	2250 [mm]
P4	Bigger cone radius (Minimize)	Continuos	2250 [mm]	2750 [mm]
P5	Distance from the propeller (Minimize)	Continuos	1800 [mm]	2200 [mm]

The fluid domain was divided in two: the fluid domain which is surrounding the afterbody having the relative velocity on Oz axis of 7 m/s and the Propeller fluid domain with CFX option of “frozen Rotor” where the fluid is moving circularly around OZ axis with 120 RPM. In between these two domains interfaces were established. The other boundary conditions were inlet, outlet and openings as shown below:

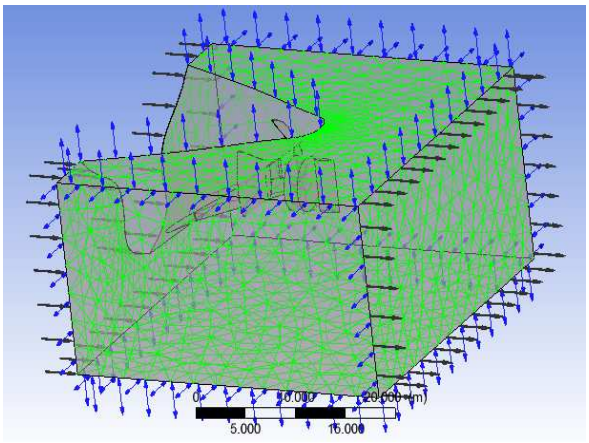

Fig. 3-Boudary Conditions

In order to make clear some important surfaces, three control planes were defined as follows:

- Control plane number 1 (P1) placed at 1200 mm above the propeller axis and coplanar with the two WED devices axis;
- Control plane number 2 (P2) which is including the propeller axis;
- Control plane number 3 (P3) placed at 1500 mm away from the propeller domain;
- Target Plane which is in fact one of the propeller domain interfaces as below:

Taking into account the above defined control planes as output parameters needing to be optimized were defined as being the Average fluid velocity passing through the Target Plane (suspected to improve the propeller efficiency-the bigger the better) and the average pressure on the inside of the WED device (suspected to increase the drag-the smaller the better):

Table 2. Output parameters

ID	Parameter Name	Starting Value	Unit
P6	VelocityTarget (maximize)	14.769	m s^-1
P7	PressureDuct (minimize)	89874	Pa

3. CFA SIMULATION AND OPTIMIZATION RESULTS

After reaching the convergence of the given starting models, and going through Design Explorer Module, 27 design points were calculated in order to define the response surfaces of the project:

Table 3-Design Points

Name	P1 - Angle (deg)	P2 – Duct Length (mm)	P3 – Small radius (mm)	P4 – Biggerr adius (mm)	P5 – Distance from propeller (mm)
1	18	2200	1925	2500	2000
2	14	2200	1925	2500	2000
3	22	2200	1925	2500	2000
4	18	1980	1925	2500	2000
5	18	2420	1925	2500	2000
6	18	2200	1600	2500	2000
7	18	2200	2250	2500	2000
8	18	2200	1925	2250	2000
9	18	2200	1925	2750	2000
10	18	2200	1925	2500	1800
11	18	2200	1925	2500	2200
12	16.867	2137.7	1832.9	2429.2	2056.7
13	19.133	2137.7	1832.9	2429.2	1943.3
14	16.867	2262.3	1832.9	2429.2	1943.3
15	19.133	2262.3	1832.9	2429.2	2056.7
16	16.867	2137.7	2017.1	2429.2	1943.3
17	19.133	2137.7	2017.1	2429.2	2056.7
18	16.867	2262.3	2017.1	2429.2	2056.7
19	19.133	2262.3	2017.1	2429.2	1943.3
20	16.867	2137.7	1832.9	2570.8	1943.3
21	19.133	2137.7	1832.9	2570.8	2056.7
22	16.867	2262.3	1832.9	2570.8	2056.7
23	19.133	2262.3	1832.9	2570.8	1943.3
24	16.867	2137.7	2017.1	2570.8	2056.7
25	19.133	2137.7	2017.1	2570.8	1943.3
26	16.867	2262.3	2017.1	2570.8	1943.3
27	19.133	2262.3	2017.1	2570.8	2056.7

Taking each and every design points to be calculated via CFA, the output parameters to be optimized are shown below:

Table 4.Output calculated parameters for each design points

Name	P6 – Velocity Target (m s^-1)	P7 – Pressure Duct (Pa)
1	14.518	1.0123E+05
2	14.75	99999
3	14.514	1.0294E+05
4	14.553	1.02E+05
5	14.482	1.0077E+05
6	14.527	1.033E+05
7	14.541	97174
8	14.561	97907
9	14.581	1.0307E+05
10	14.556	1.0094E+05
11	14.571	1.0135E+05
12	14.65	1.015E+05
13	14.596	1.0155E+05
14	14.574	1.008E+05
15	14.543	1.0136E+05
16	14.6	98976
17	14.539	99788
18	14.563	98563
19	14.576	99455
20	14.595	1.0255E+05
21	14.553	1.0314E+05
22	14.547	1.0218E+05
23	14.514	1.0297E+05
24	14.588	98469
25	14.577	1.0143E+05
26	14.57	1.0046E+05
27	14.558	1.0152E+05

The software is automatically selecting the maximum and minimum calculated values of output parameters as below:

Table 5-Minimum and maximum output parameters

	Minimum value	Maximum value
P6 - VelocityTarget (m s^-1)	14.478	14.784
P7 - PressureDuct (Pa)	67648	1.4648E+05

By judging the above minimum and maximum value of the pressure inside the duct, the difference is 20 folds which is clearly making a difference between a good and a poor design.

By setting the goals of maximization or minimization defined above for all the parameters, at the end of the optimization process three best candidates will be generated:

Table 6. The three best candidates

	P1 - Angle (degree)	P2 – Duct lenght (mm)	P3 – Small radius (mm)	P4 – Bigger con radius (mm)
Candidate Point 1	14.164≈ 14 degree	2049≈ 1050 mm	2081.8≈ 2080 mm	2330.3≈ 2330 mm
Candidate Point 2	14.644	1997.4	2242.3	2282.3
Candidate Point 3	15.284	1988.8	2028.3	2295.1

P5 – Distance from the propeler (mm)	P6 – Velocity Target (m s^-1)	P7 – Pressure Duct (Pa)
2159.4≈ 2160 mm	14.78	98351
2005.4	14.756	94591
2154.7	14.702	1.0633E+05

Here once again the Designer is called to make a decision, we choose the first candidate having three stars to the most of the parameters.

In order to have an overall idea on the influence of each and any input parameter has on the output parameter, the sensitivity charts and response surfaces are the best aids for judgment. Since the possible combinations are many, only few response surfaces are given below.

- **Duct Pressure-Duct Angle and Duct Length Response Surface**

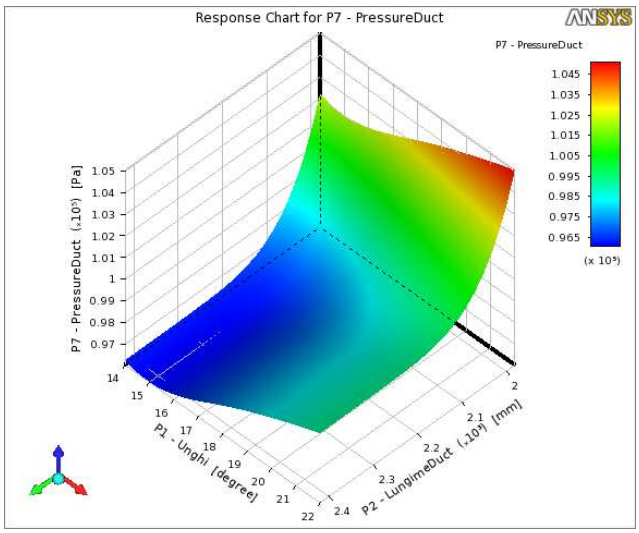

Fig.4 Duct Pressure-Duct Angle and Duct Length Response Surface

From the above chart one may imply that the duct Angle has a bigger influence than the Length of the duct over the Pressure inside the duct, which is somehow in line with a common sense hypothesis. The smaller the angle is and the bigger the length is then the smaller the inside pressure will be.

- **Duct Pressure-Duct Angle and Duct Small Radius Response Surface**

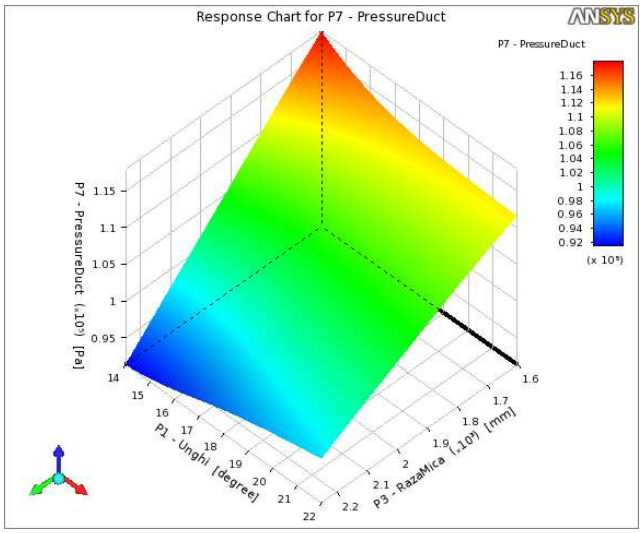

Fig.5 Duct Pressure-Duct Angle and Duct Small Radius Response surface

The pressure inside the duct will be smaller as the angle is smaller and the small radius will be smaller.

- **Velocity over the Target Surface-Duct Angle and Duct Length Response Surface**

The smaller the Duct angle (near 14 degrees) and the Length is, the bigger the velocity of the fluid on the target surface will be.

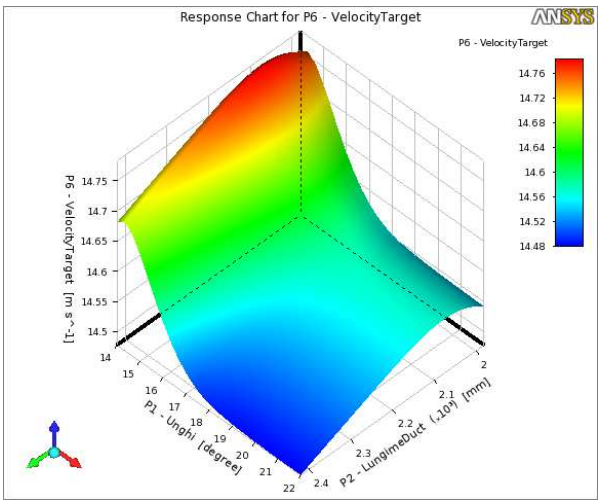

Fig.6 Duct Pressure-Duct Angle and Duct Small Radius Response surface

In order to place all the influences on a single chart, the sensitivity chart is used as below:

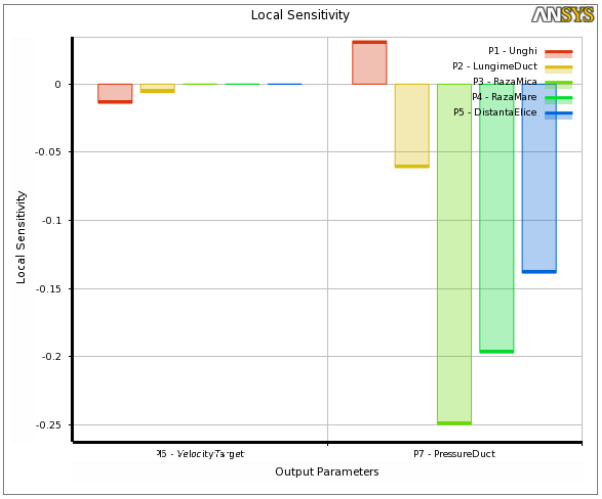

Fig.7 Sensitivity chart

Finally if one wants to visualize the effect of the optimized input parameters, we can recalculate the model with these new optimized parameters for geometry resulting for the output parameters the following figures:

- **The influence of optimized parameters on the velocity through the target surface**

By analyzing the figures below, one may see that the shape of the velocity fields on the upper zone of the propeller is more extended, so that the optimized version is “pushing” more fluid on this zone.

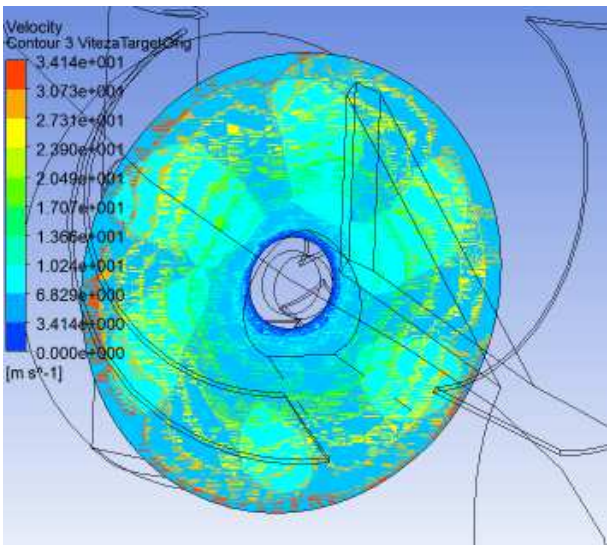

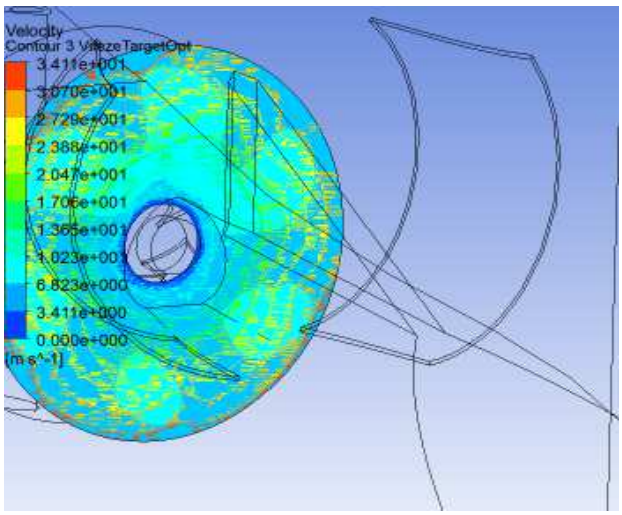

Fig.8 The starting model and the optimized model velocities

- **The influence of optimized parameters on the pressure inside the duct**

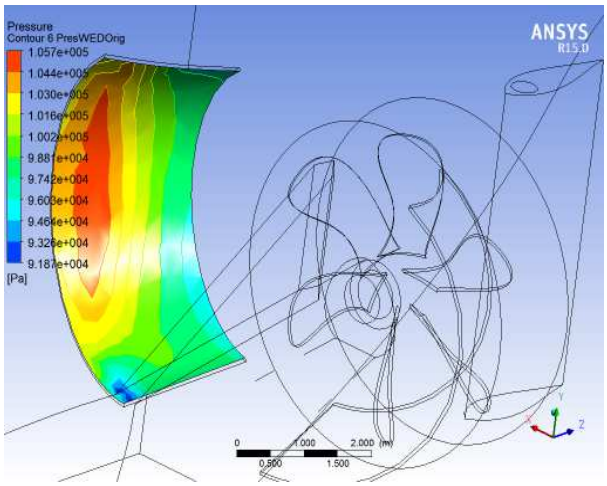

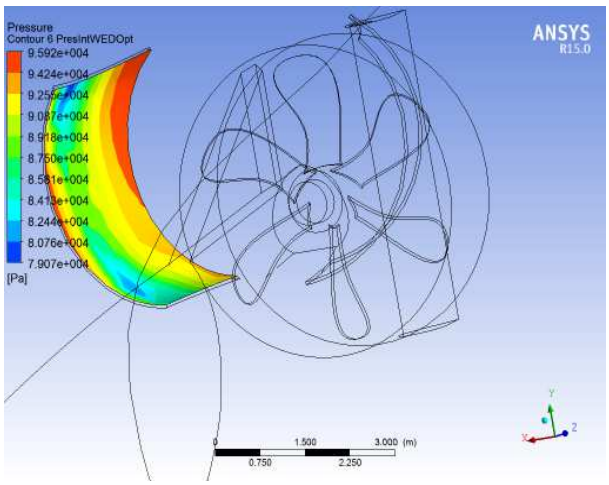

Fig.9 The starting model and the optimized model duct pressures

The starting model has a bigger (red colored) pressure fields on the inside the duct whereas the optimised version has smaller and placed at the outlet zone of the duct pressure fields, which is an indication that the inside pressure and the drag is then diminished for the optimized version.

4. CONCLUSIONS

The wake equalizing duct (WED) is one of the most commonly used energy saving devices for improving the propulsion performance of a ship; and reducing the propeller-excited vibrations and viscous resistance forces.

In this paperwork a given geometry of a WED device is taken and via Design Optimization the geometry of the duct was refined so that better results are achieved with a smaller and more compact WED considering **Duct Pressure Angle, Length and Radius**. In doing so, the Designer is assisted by numeric optimization methods to choose from only three final candidates instead of several thousands in order to provide the best fitted WED geometry for a given ship afterbody.

5. REFERENCES

[1] H.J. Heinke, K. Hellwig-Rieck, “Investigation of Scale Effects on Ships with a Wake Equilizing Duct or with Vortex Generator Fins”, Second International Symposium on Marine Propulsors, Hamburg, Germany, 2011.

[2] E. Huse, “Effect of Afterbody Forms and Afterbody Fins on the Wake Distribution of Single Screw Ships”, NSFI Report No.R31-74,1974.

[3] J.Carlton, Marine Propellers and Propulsion, Butterworth Heinemann, Oxford, 2007.

[4] H.Schneekluth and V. Bertram, Ship Design for Efficiency and Economy, Butterworth-Heinemann, Oxford, 1998.

[5] E. Korkut, “A case study for the effect of a flow improvement device (a partial wake equalizing duct) on ship powering characteristics”, Ocean Engineering, 2005.

[6] F. Celik, “A numerical study for effectiveness of a wake equalizing duct,” in Ocean Engineering, 2007.

[7] J. Friesch, C. Johannsen, “Propulsion optimization tests at high Reynolds numbers”, SNAME Transactions 102, 1994, pp. 1–21.

[8] ITTC 1999, “Final report of the specialist committee on unconventional propulsors“, 22nd International Towing Tank Conference, Seoul, Korea and Sanghai, China, 1999.

[9] A.Y. Odabasi, P.A. Fitzsimmons, "Alternative methods for wake quality assessment", Int. Shipbuilding Prog., 25(282), 1978.

AN EXPERIENCE IN REFRIGERATION CALCULATION CARRIED OUT BY FUTURE MARINE ENGINEERS IN CMU

MEMET FEIZA

Constanta Maritime University, Romania

ABSTRACT

An important educational outcome of the Undergraduate Studies Programme belonging to Naval Electromechanics Faculty in Constanta Maritime University (CMU) is the ability to design a component or a system specific for marine technologies. In CMU, students are introduced in refrigeration technology due to the discipline entitled "Marine Refrigeration Plants", which they take in the 7th semester of their higher education.

This paper highlights the manner in which our students are achieving competencies in evaluating the performance of vapor compression systems in terms of Coefficient of Performance (COP).

Such kind of experience enables the understanding of basic concepts and principles which rule this type of technology

Keywords: *marine engineering, refrigeration, competencies, students.*

1. INTRODUCTION

An engineering curriculum is successful if it ensures engineering design skills gained during its undergraduate engineering programs (Abu-Mulaweh, Al Arfaj, 2012).

The curricula specific for Naval Electromechanics Faculty in Constanta Maritime University (CMU) aims to offer to its students a proper framework able to develop their self confidence, to gain specific competencies and to assess the level of their scholarly.

As an important provider of services to the shipping sector, CMU has generated its study programmes according to STW and national authorities requirements, under IMO Model Courses for Navigation and Marine Engine specialisations (Stan, 2011).

Educational outcomes of a Marine Engineering curriculum might be summarised as (Deng et al, 2003):

- the student will acquire requested competencies in fundamental education in fields of mechanical engineering applied in marine technologies;
- the student will be able to prove its competencies in experimental testing, error analysis, data acquisition, laboratory safety, instrumentation and report conceive;
- the student will show computer competency in solving different engineering problems.

Our future graduates should have a strong theoretical and practical background which will support their professional carrier in Marine Engineering and will generate motivation for future professional development.

Competencies that an employee in Marine Engineering sector should demonstrate can be depicted in Figure 1 (Williams, Mui Hua, 1999).

Curricula in Constanta Maritime University contains the course entitled "Marine Refrigeration Plants", which is delivered for students enrolled in Undergraduate Studies Programme, Naval Electromechanics Faculty, year IV, during one semester, the seventh, for 47 hours.

This discipline is in accordance with competence A-III/1-4.1

Basic construction and operation principles of machinery systems and with Appendix 3 from STW, IMO Model Course 7.04 – Marine Engineering at Operational Level.

It is also in accordance with the number of hours requested by IMO Model 7.02 – Marine Engineering at Managerial Level Competence, A-III/2-7.02 (Mitu, 2014).

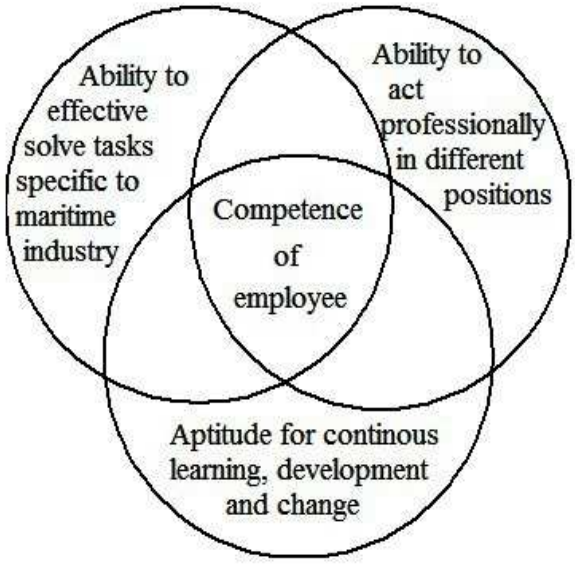

Figure 1 Competencies gained by a professional in Marine Engineering throught education

This paper deals with the manner in which students in CMU are familiarised with calculation experience specific for vapour compression refrigeration plants, more specific with the determination of Coefficient of Performance (COP).

2. MATERIALS AND METHODS

Teaching syllabus of the discipline called Marine Refrigeration Plants replies to a plan able to reveal outcomes, as seen in Figure 2 (Terry et al, 2002).

The following deals with an example of marine refrigeration design experience, namely with the evaluation of COP for a given vapour compression refrigeration cycle.

A simple vapour compression refrigeration systems contains the elements seen in Figure 3.

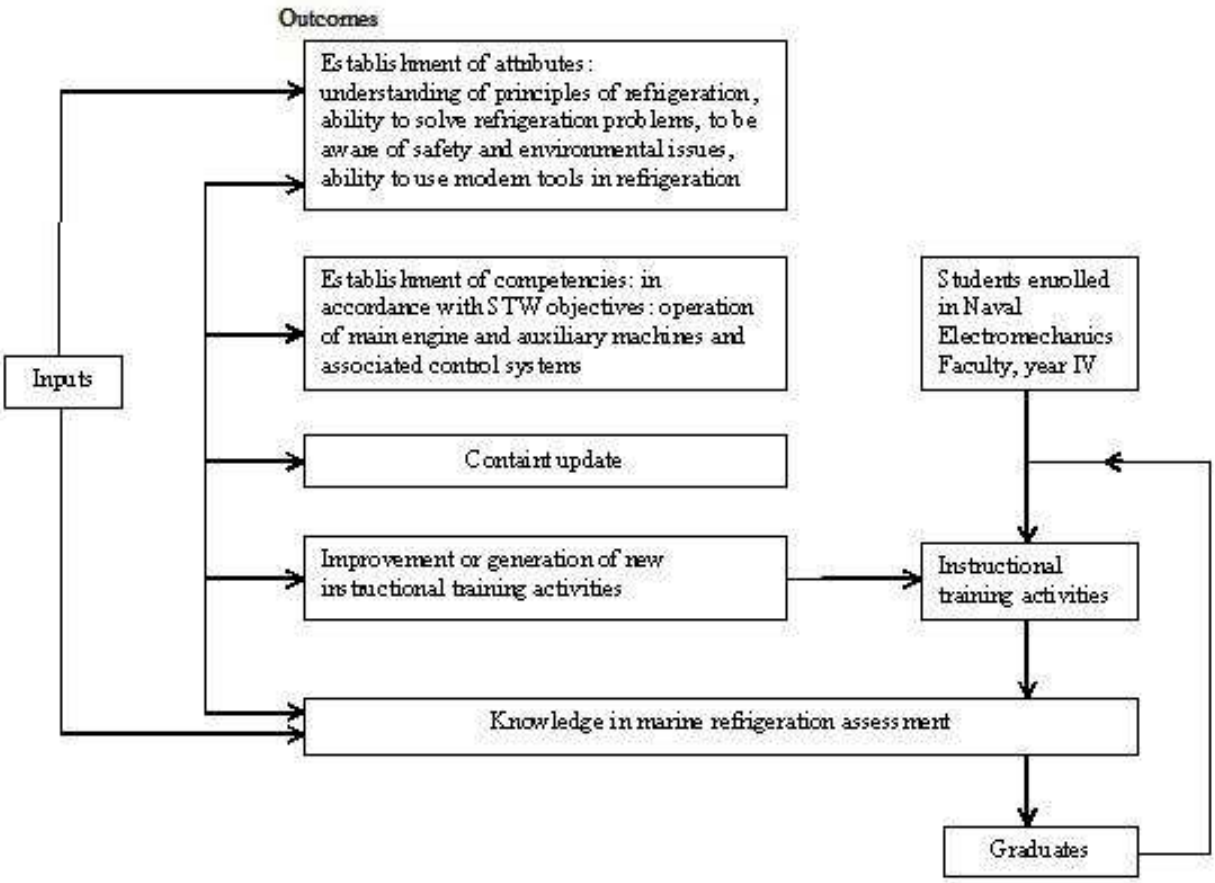

Figure 2 Outcomes of marine refrigeration education

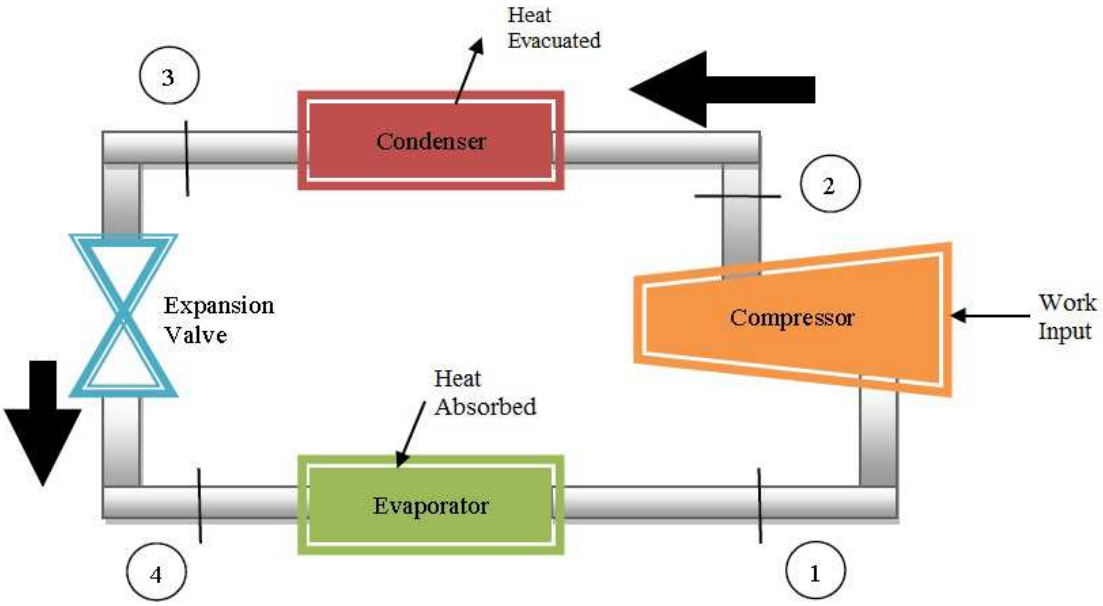

Figure 3 Simple vapor compression refrigeration system

The cycle starts when low pressure and temperature vapours of refrigerant enter in the compressor where are compressed, resulting high pressure and temperature superheated vapours.

These vapours will be led into the condenser where are turned into refrigerant liquid by evacuating heat to the environment, during an isothermal-isobaric process.

Resulted liquid presents high pressure and temperature and for this reason is directed into the expansion valve where its pressure is lowered to the evaporation pressure, by keeping the enthalpy constant.

The refrigerant enters then into the evaporator where it is turned into vapours at pressure and temperature constant, by heat absorption.

The refrigerant compressor is a thermal device that needs energy input to increase the pressure of refrigerant vapours.

The condenser and the evaporator are two basic heat exchangers in the refrigeration plant. They consist of coils of pipe where refrigerant gives up its latent heat to the surrounding (sea water) – in case of the condenser and absorbs latent heat of vaporisation from the medium (air, water or brine) which should be cooled – in case of the evaporator.

The expansion valve might be met also under the title of throttling valve or refrigerant control valve.

A part of the refrigerant liquid evaporates as it passes through the expansion valve, but the most part is vaporised in the evaporator of the system.

The mixture of the liquid and gas going out the expansion valve is also known as “flash gas”.

Assumptions made for an ideal vapour – compression cycle are as follows:

- the main components of the system are designed as open systems and work under steady–state, steady–flow process;
- heat exchangers are considered to be constant pressure devices and irreversibilities are ignored inside them;
- there are no changes in kinetic and potential energies across devices;
- there are no frictional pressure drops;
- there are no heat losses to the surroundings;
- compression processes is at constant entropy.

The equations of thermal calculus of the cycle are given in the following:

- specific cooling effect:

$$q_o = h_1 - h_4 \quad (1)$$

- specific work input:

$$l_k = h_2 - h_1 \quad (2)$$

- specific heat evacuated at the condenser:

$$q_C = h_2 - h_3 \quad (3)$$

where h – enthalpy.

- refrigerant mass flow:

$$\dot{m} = \frac{\dot{Q}_o}{q_o} \quad (4)$$

where Q_o – cooling effect.

- heat flow rate in the condenser:

$$\dot{Q}_C = \dot{m} \cdot q_C \quad (5)$$

- power input to the compressor:

$$P_K = \dot{m} \cdot l_K \quad (6)$$

- Coefficient of Performance:

$$COP = \frac{\dot{Q}_o}{P_K} \quad (7)$$

3. RESULTS AND DISCUSSION

Calculation is done in the case of a vapour compression cycle working in the same conditions but using two different refrigerants: R134a and NH_3, both of them often used in marine refrigeration.

Considered working conditions are (Şerban et al, 2012):

- temperature in the cooling space: 3^oC;
- temperature of water at condenser inlet: 20^oC;
- cooling effect: 100 kW.

Results of thermal calculus are presented in Table 1.

Table 1. Results of thermal calculus of the refrigeration cycle

	Cycle working with R134a	Cycle working with NH_3
q_o, kJ/kg	149,58	1100,33
l_K, kJ/kg	28,06	176,7
q_C, kJ/kg	177,64	1277,03
$\dot{m}$, kg/s	0,67	0,09
$\dot{Q}_C$, kW	119,02	114,93
P_K, kW	18,80	15,90
COP	5,32	6,29

From environmental protection point of view, using NH_3 as a refrigerant is more profitable than using R134a because it has null GWP (Global Warming Potential).

Table 1 offers the possibility to the students to compare these two refrigerants from thermodynamic point of view.

Using NH_3 in the refrigeration systems leads to higher values of the specific work input, higher values for specific cooling effect, which reveals lower values for the mass flow, and a better performance of the cycle, seen in the higher values of COP.

4. CONCLUSIONS

This paper described an outcome of an Undergraduate Marine Engineering course, named Marine Refrigeration Plants, delivered in CMU/Naval Electromechanics Faculty.

As the basic measurement indicator of a Marine Engineering Program outcome is that graduates prove abilities in design for different areas of study, it was presented such kind of experience when talking about marine refrigeration plants.

Starting with the plant description, it is continued with introduction of specific equations and calculus in certain conditions.

Comparative calculation will supply to the student informations on advantages and drawbacks of one solution or other.

5. REFERENCES

[1] ABU-MULAWEH, H.I., AL-ARFAJ, A.A., *Engineering design experience of an undergraduate thermodynamics course*, World Transactions on Engineering and Technology Education, Vol.10, No.1, pp.77-81, 2012

[2] DENG, Z.T. et al, *Evaluation of assessment tools for outcome based engineering courses*, Proc. of 2003 American Society for Engineering Education Annual Conference and Exposition, Session 1566, pp.8, 2003

[3] MITU, D.E., *Education regarding green refrigerants in CMU*, Journal of Marine Technology and Environment, Vol.2, pp.87-92, 2014

[4] STAN, L., *Implementation of the 1995 STCW Convention in Constanta Maritime University, Human Resources and Crew Resource Management, Marine Navigation and Safety of Sea Transportation*, The 9 the International Symposium on Navigation Trans-Nave, Gdynia, 15-17 June, 2011.

[5] SERBAN, Al. CHIRIAC, Fl., NASTASE, G, *Instalatii frigorifice, Aplicatii si problem rezolvate*, Ed. Agir, Bucuresti, ISBN: 978-973-720-425-7, 2012

[6] TERRY, R.E. et al, *Definition of student competencies and development of an educational plan to assess student mastery level*, Int. J. Engage. Ed. Vol.18, No.2, pp.225-235, 2002

[7] WILLIAMS, S., MUI HUA, T., *A competency based approach to Polytechnic Education for the learning ape*, MERA-ERA Conference: Educational Challenges in the New Millennium, 1-2 December, Malacca, Malaysia, 9 pp, 1999.

AN ORIGINAL METHOD TO EVALUATE THE ELASTIC CONSTANTS OF THE ELASTIC SUPPORTS USING THE METHOD OF INITIAL PARAMETERS

[1]OANTA M. EMIL, [2]AXINTE TIBERIU, [3]DASCALESCU ANCA-ELENA

[1,2]Constanta Maritime University, [3]'Politehnica' University of Bucharest, Romania

ABSTRACT

Elasticity of the supports is usually disregarded by the structural analysts, who want to create a simple model of a given structural phenomenon. However, there are certain situations when the accuracy of the results depends on the consideration of the elastic supports. In the paper is presented a method to consider the elastic supports in analytic models. Thus, there is assumed a linear dependency between a given reaction and the according displacement, in this way being possible to consider a spring directed along that given reaction. There is also interesting to study the effect of the elastic supports onto the calculus methodology used within the method of initial parameters which offers laws of variations of the displacement and of the rotation along a straight bar. Beside these aspects, some other questions still remain regarding the methods used to evaluate the elasticity of the supports.

Keywords: *Elastic supports, elastic constants, method of initial parameters, calculus methodology.*

1. INTRODUCTION

Analytic models in structural mechanics are based on a set of so-called 'classic' hypotheses or assumptions. These hypotheses were very useful in an age of technological development, when the instrument employed to perform the calculi was not very evolved. Some assumptions may be considered axioms, such as the punctual application of the concentrated forces which, theoretically, may lead to an infinite contact pressure, aspect which is disregarded. Another example concerns the small displacements hypothesis, which offers a simple theoretical set of relations, [6], and [9]. However, beside their inherent lack of accuracy, the hypotheses were very useful to create models of most of the structural phenomena, models which lead to an important industrial progress. In the next sections are presented aspects regarding the theoretical context and the elasticity of the supports.

2. THEORETICAL CONTEXT

The nowadays modern computation instruments may be used in several directions in the analytical modelling field.

One of the important directions is to automatize the calculus for certain, well defined models which solve a given problem. Regarding the calculus of the displacements, the method of initial parameters was the best choice to calculate the laws of variation of the displacement and of the rotation along a straight beam. Several ideas regarding the most effective, general and parameterized algorithm to calculate the displacements were studied [5]. Finally, the algorithm was implemented in an original software application consisting of more than 11000 computer code lines, [8]. It is important to notice that once a model is implemented, the resulting parameterized software solves completely that given problem. It is also important that the resulting software to have a high degree of connectability with other software applications. To conclude, the method of initial parameters was employed to create the algorithm of some original software applications, but none of them include the concept of 'elastic support'.

The elastic supports may be identified in many structural models, being important to evaluate the elasticity of the supports. Their use may offer more accuracy of the model, together with a higher complexity of the algorithm. The solution to deal with the higher complexity is to implement the according algorithm.

Consequently, the second direction is to create software instruments for the more complex and more accurate computer based models which consider the elasticity of the supports. The rigid supports are often mentioned as simplified versions of the elastic supports, [7]. However, there is no coherent theory which systematically considers the elasticity of the supports in the deduction of the calculus analytical relations.

If the influence of the supports must be explicitly considered, there may be carried out experiments, [3], the results being used to calibrate the theoretical model, [4], which therefore includes accurate models of the elastic supports.

In this context, we investigate the influence of the elastic supports onto the theoretical aspects that are used to deduce analytical relations. The next section is dedicated to the definition of the simplest elastic supports.

3. DEFINITION OF THE ELASTIC SUPPORTS

Let us consider the types of supports for plane problems presented in figure 1. As it can be noticed, in the upper area of the figure there are the elastic supports and in the lower part there are their simplified, rigid versions. In order to have a relative simple model of the elastic supports, we consider a linear dependency between the elastic reaction, force or moment, and the given displacement or rotation. This linear function is graphically symbolized by a coil (helicoidal) spring positioned along the elastic force / moment. In this way,

the elastic constant of the spring is actually the elasticity of the support along that given direction.

The relations between the general elastic reactions (forces or moments) and the according displacements / rotations are:

$$\begin{cases} H_{X\,i} = k_{u_X\,i} \cdot u_{X\,i} \\ V_{Y\,i} = k_{u_Y\,i} \cdot u_{Y\,i} \\ V_{Z\,i} = k_{u_Z\,i} \cdot u_{Z\,i} \end{cases} \quad \begin{cases} M_{X\,i} = k_{\varphi_X\,i} \cdot \varphi_{X\,i} \\ M_{Y\,i} = k_{\varphi_Y\,i} \cdot \varphi_{Y\,i} \\ M_{Z\,i} = k_{\varphi_Z\,i} \cdot \varphi_{Z\,i} \end{cases}, \qquad (1)$$

where, by k there are denoted the elastic constants of the support.

As it can be noticed, for the rigid supports the according displacements are zero. In this case the elasticity of the supports is disregarded.

There are several approaches regarding the way how the elasticity of the supports may be considered in the subsequent calculi.

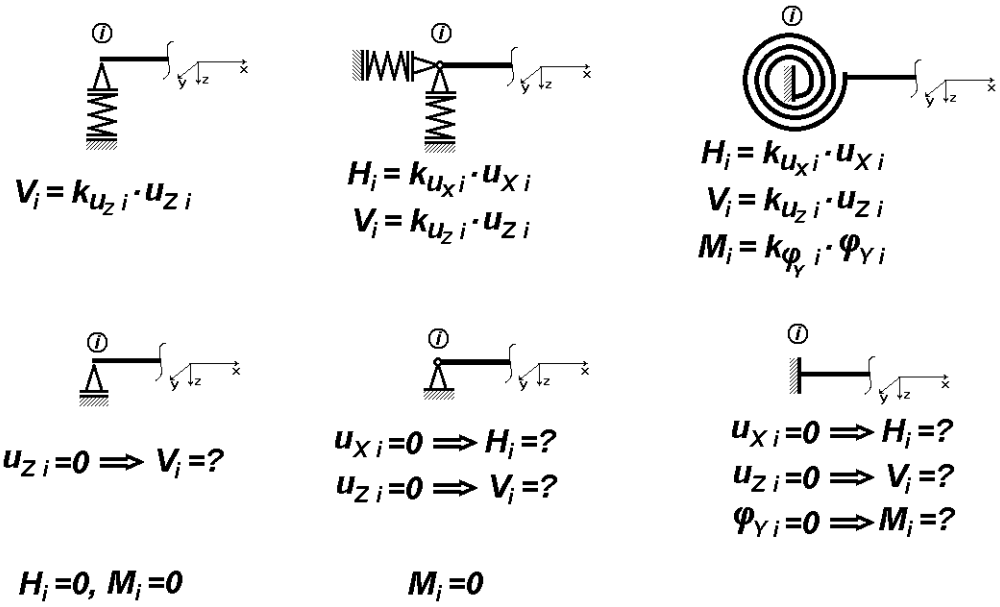

Figure 1 – Definition of the elastic supports for plane problems

For most of the physical bodies, the elastic displacements are small. Therefore, the solids loaded by external forces have small changes of theirs shapes. This hypothesis is known as the initial dimensions preservation assumption. According to this hypothesis, the static equilibrium relationships may be set by considering the initial non-displaced shape of the structure, when the points in which the external forces are located are not displaced. The calculus which considers the non-displaced structure is designated as the first order calculus. The second order calculus takes into account the small displacements hypothesis, and the static equilibrium relations may be set by considering the displaced shape of the structure. The third order calculus disregards the small displacements hypothesis, all the displacements being considered large, and the static equilibrium equations are set for the displaced state of the structure.

As it can be noticed in figure 1, by considering the elasticity of the supports it is possible to use the second order calculus or the third order calculus if a problem requires this type of approach.

The following study is focused on the method of initial parameters, widely used for the calculus of the displacements.

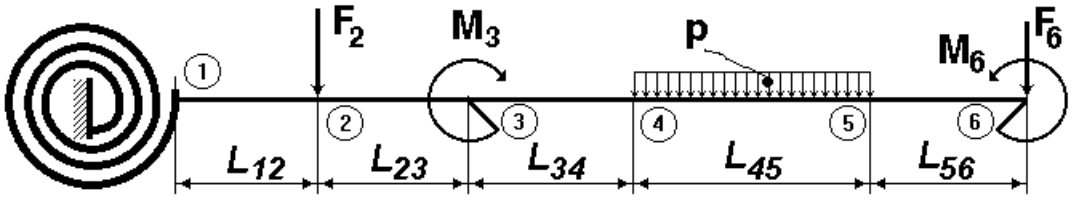

Figure 2 – Calculus scheme of the method of initial parameters for an elastic built-in support

4. THE METHOD OF INITIAL PARAMETERS AND THE ELASTIC SUPPORTS ISSUE

Let us consider the theoretical model presented in figure 2, [1] pg. 151-157, [2] pg. 398. As it can be noticed, in section no. 1, we have an elastic built-in support. In order to write the laws of variation of the shear force, bending moment, rotation and of the displacement we use Heaviside's function

$$H(x-x_j)=\begin{cases}0, & x<x_j\\ +\frac{1}{2}, & x=x_j\ ,\ \forall x_j\\ 1, & x>x_j\end{cases} \quad (2)$$

which is represented in the following figure.

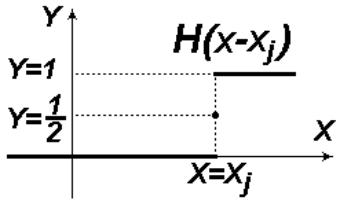

Figure 3 – Heaviside's function

We denote the x_i coordinate of each section as:

$$x_i=\sum_{i=2}^{6}L_{i-1,i}\ . \quad (3)$$

The law of variation of the shear force is:

$$T_Z(x)=V_1\cdot H(x)+(-F_2)\cdot H(x-x_2)+ +(-p)\cdot(x-x_4)\cdot H(x-x_4)+ +p\cdot(x-x_5)\cdot H(x-x_5) \quad . \quad (4)$$

The law of variation of the bending moment is:

$$M_Y(x)=M_1\cdot H(x)+V_1\cdot x\cdot H(x)+ +(-F_2)\cdot(x-x_2)\cdot H(x-x_2)+ +M_3\cdot H(x-x_3)+ +(-p)\cdot\frac{(x-x_4)^2}{2}\cdot H(x-x_4)+ +p\cdot\frac{(x-x_5)^2}{2}\cdot H(x-x_5) \quad . \quad (5)$$

The differential equation of the neutral fiber is:

$$(E\cdot I_Y)\cdot\frac{d^2u_Z(x)}{dx^2}=(E\cdot I_Y)\frac{d\varphi_Y(x)}{dx}=-M_Y(x) \quad (6)$$

After the integration, it results the law of variation of the rotation:

$$(E\cdot I_Y)\cdot\frac{d\,u_Z(x)}{dx}=(E\cdot I_Y)\cdot\varphi_Y(x)= =(E\cdot I_Y)\cdot\overbrace{\varphi_{Y1}}^{\text{integration constant}}\cdot H(x)-M_1\cdot x\cdot H(x)- -V_1\cdot\frac{x^2}{2}\cdot H(x)+F_2\cdot\frac{(x-x_2)^2}{2}\cdot H(x-x_2)- -M_3\cdot(x-x_3)\cdot H(x-x_3)+ +p\cdot\frac{(x-x_4)^3}{6}\cdot H(x-x_4)- -p\cdot\frac{(x-x_5)^3}{6}\cdot H(x-x_5) \quad . \quad (7)$$

Integrating the previous equation, it results the law of variation of the displacement:

$$(E\cdot I_Y)\cdot u_Z(x)=(E\cdot I_Y)\cdot\overbrace{u_{Z1}}^{\text{integration constant}}\cdot H(x)+ +(E\cdot I_Y)\cdot\overbrace{\varphi_{Y1}}^{\text{integration constant}}\cdot x\cdot H(x)-M_1\cdot\frac{x^2}{2}\cdot H(x)- -V_1\cdot\frac{x^3}{6}\cdot H(x)+F_2\cdot\frac{(x-x_2)^3}{6}\cdot H(x-x_2)- - M_3\cdot\frac{(x-x_3)^2}{2}\cdot H(x-x_3)+ +p\cdot\frac{(x-x_4)^4}{24}\cdot H(x-x_4)- -p\cdot\frac{(x-x_5)^4}{24}\cdot H(x-x_5) \quad . \quad (8)$$

The unknowns of the problem are u_{Z1}, φ_{Y1}, V_1, M_1, being necessary 4 equations to create a compatible and determinate system of equations.

We consider the following boundary conditions:

a) at the rightmost end of the beam, for $x=x_6$, the shear force is:

$$T_Z(x_6)=F_6\ ; \quad (9)$$

b) at the rightmost end of the beam, the bending moment is:

$$M_Y(x_6)=M_6\ ; \quad (10)$$

c) at the leftmost end of the beam, if there would be a built-in support, the vertical displacement will be zero, i.e. $u_Z(x=0)=0$. In our case the displacement cannot be set to a given value. However, for an elastic built-in support, relations (1) are connecting the displacements to the internal forces and moments. The according relation is:

$$V_{Z1}=k_{u_Z1}\cdot u_{Z1}\ ; \quad (11)$$

where $V_{Z1}=V_1$ may be deduced using relation (9), i.e.

$$V_1=F_2+p\cdot(x_5-x_4)+F_6\ ; \quad (12)$$

d) at the leftmost end of the beam, if there would be a built-in support, the rotation will be zero, i.e. $\varphi_Y(x=0)=0$. For an elastic built-in support the according relation is:

$$M_{Y1}=k_{\varphi_Y1}\cdot\varphi_{Y1}\ ; \quad (13)$$

where M_{Y1} may be deduced using relation (10), i.e.

$$M_1=-V_1\cdot x_6+F_2\cdot(x_6-x_2)-M_3+ +\frac{p}{2}\cdot(x_5-x_4)\cdot(2\cdot x_6-x_5-x_4)+M_6 \quad . \quad (14)$$

So, it results that if we know the elastic constants of the built-in support, k_{u_Z1} and k_{φ_Y1}, we are able to calculate the initial displacement using relation (11) and the initial rotation using relation (13).

It is interesting to evaluate the method to solve this problem if we do not know the elastic constants. This

means that we have two more unknowns, $k_{u_Z 1}$ and $k_{\varphi_Y 1}$. In this way we need some additional information which may be offered by some experimental studies. Let us suppose that we are able to measure the vertical displacements in sections 2 and 3. This means that we have the equations

$$u_{Z2} = (E \cdot I_Y) \cdot u_Z(x_2) = (E \cdot I_Y) \cdot \overbrace{u_{Z1}}^{\text{integration constant}} + \\ + (E \cdot I_Y) \cdot \overbrace{\varphi_{Y1}}^{\text{integration constant}} \cdot x_2 - M_1 \cdot \frac{x_2^2}{2} - V_1 \cdot \frac{x_2^3}{6} \quad (15)$$

$$u_{Z3} = (E \cdot I_Y) \cdot u_Z(x_3) = (E \cdot I_Y) \cdot \overbrace{u_{Z1}}^{\text{integration constant}} + \\ + (E \cdot I_Y) \cdot \overbrace{\varphi_{Y1}}^{\text{integration constant}} \cdot x_3 - M_1 \cdot \frac{x_3^2}{2} - V_1 \cdot \frac{x_3^3}{6} + \cdot \quad (16) \\ + F_2 \cdot \frac{(x_3 - x_2)^3}{6}$$

In this way we are able to add two more relations for the additional unknowns, $k_{u_Z 1}$ and $k_{\varphi_Y 1}$. Thus, we obtain a compatible and determinate system of equations. In this particular case we notice that using conditions (9) and (10), we deduce the unknown reactions V_1 and M_1. Then, using relations (15) and (16) we calculate u_{Z1} and φ_{Y1}. So far, using this information there may be deduced the laws of variation of the shear force, of the bending moment, of the rotation and of the displacements. However, if the loads are modifying their values, new experimental measurements of the u_{Z2} and u_{Z3} displacements are required. In order to avoid this situation it is easier to calculate the elastic constants of the built-in support using relations (11) and (13).

Calculus of the elastic constants $k_{u_Z 1}$ and $k_{\varphi_Y 1}$ using the results of an experimental study may be considered the calibration of the model. It is interesting to relate the number of displacements measured experimentally to the elastic supports of a structure.

5. CASE STUDY – A STATICALLY INDETERMINATE SYSTEM

Let us consider the case of a statically indeterminate system, figure 4. The system has an elastic built-in support at its leftmost end and an elastic simple support along its length. We must conceive the optimal method to solve the problem, i.e. if there are necessary additional information and what the information consist of.

We shall not follow the solving pattern presented for the previous case study, which offers the minimum amount of information, relevant for the method of the initial parameters in the context of the elastic supports. For now, we shall simply follow the balance unknowns vs. equations in order to establish the best strategy to solve this type of problem.

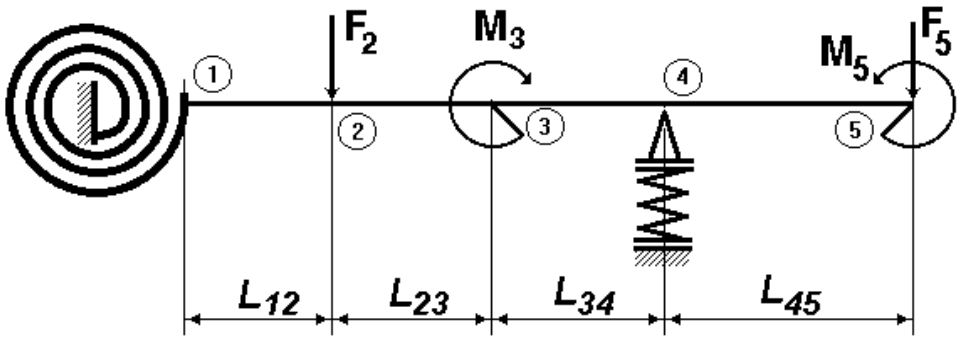

Figure 4 – Case study: statically indeterminate system which uses elastic supports

The law of variation of the shear force, similar to relation (4), includes the following unknowns: V_1 and V_4. The law of variation of the bending moment, similar to relation (5), uses the unknowns V_1, V_4 and M_1. After the first integration of the neutral fiber equation, it results the law of variation of the rotation, similar to relation (7), which uses the following unknowns: V_1, V_4, M_1 and φ_{Y1}. Next, integrating this equation it results the law of variation of the displacement which uses the following unknowns: V_1, V_4, M_1, φ_{Y1} and u_{Z1}. To conclude, there are 5 unknowns and we must identify 5 equations in order to create a compatible and determinate system of equations.

First two equations are taking into account the boundary conditions in the rightmost end, similar to (9) and (10), i.e. $T_Z(x_5) = F_5$ and $M_Y(x_5) = M_5$. Because we have a statically indeterminate system, unknowns V_1, V_4 and M_1 cannot be calculated using the aforementioned two relations.

In order to match the number of equations to the number of unknowns, we conclude that there are still needed 3 equations. These equations must be coherent to the type of unknowns, i.e. there cannot be equations regarding only the reactions (forces and moment). The upmost level which takes into account all the unknowns

regards the displacements. Moreover, there are common experimental instruments for the measurement of the displacements. In this way, if we are able to experimentally measure the displacements in 3 distinct points along the beam, it results that the system of equations is compatible and determinate.

6. METHODOLOGICAL ASPECTS

Let us suppose that the elastic constants of the supports are unknown.

For the problem presented in figure 2 there are two elastic constants, therefore are required two displacements experimentally measured. For the problem presented in figure 4 there are three elastic constants and consequently three displacements resulted from experimental studies are required.

A first conclusion is that for each elastic constant which is unknown, there is required a displacement on that given direction. For instance, we have the following distinct classes of unknowns for which there are required distinct experimental measurements of the according displacements:

1. u_X , axial loads for which $H_{X\,i} = k_{u_X\,i} \cdot u_{X\,i}$;
2. φ_X , torsion for which $M_{X\,i} = k_{\varphi_X\,i} \cdot \varphi_{X\,i}$;
3. u_Y , flexure for which $V_{Y\,i} = k_{u_Y\,i} \cdot u_{Y\,i}$;
4. u_Z , flexure for which $V_{Z\,i} = k_{u_Z\,i} \cdot u_{Z\,i}$.

Once the according systems of equations are compatible and determinate, the problem of the displacements is completely solved. The next stage is to calculate the elastic constants, using relations (1).

At this point, we are allowed to suppose that the elastic constants of the supports are known, so we can solve similar problems for other values of the loads (external distributed force, forces and moments). The subsequent variants of models do not require experimental measurements once the elastic constants are known.

Starting from this theory we identify the following method: we create a parameterized general model with various forces and with elastic supports. We conceive and run experimental studies in order to measure displacements which allow us to define compatible and determinate systems of equations which, once they are solved, we calculate the elastic constants of the supports. All the following low-complexity models, for which some of the external loads may be nil, are solved without the use of the experimental studies. In this way, we are able to create a coherent and accurate analytic model of a real structural phenomenon, based on the first order calculus. However, a higher order calculus approach must take into account our theory and our method previously presented.

Another interesting aspect regards the significance of the 'node' related data. For instance, each section in the problems presented in figures 2 and 4 may be identified and classified in several classes.

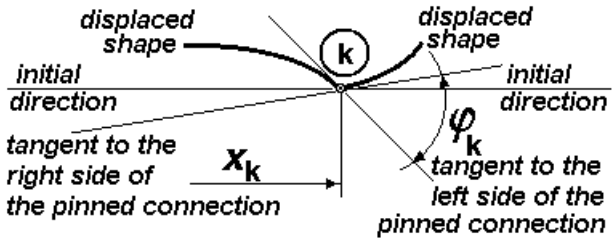

Figure 5 – Variation of the rotation (slope) in an internal pinned connection

Let us analyze relation (1). We identify three classes of information: forces and moments, generalized displacements in the elastic supports and the elastic constants. This means we have 18 nodal parameters. Beside these parameters, according to figure 1, there are certain displacements supposed to be nil. The general aspect of the aforementioned remark is that the displacements may have a given value, nil or non-zero for some given constraints (given values of the displacements in some certain points). This means another 6 nodal parameters. Moreover, if in a section we have a concentrated moment, or a concentrated force, the value on the right side of the section must take into account the sudden variation of the shear force or of the bending moment, produced by the these concentrated loads. Same situation occurs when we deal with an internal pinned connection, for which the slope on the right side is different with respect to the slope on the left side, case presented in figure 5, [1] pg. 156, [2] pg. 400. This means that the sudden variation of the rotation may be also identified as a nodal parameter, which may be an unknown in the first stage of the solving process. The only notion which may not have a sudden variation is the displacement, this means that the beam is not in collapse, so we have the continuity of the topmost variable, i.e. the displacements. This means we have additional 4 nodal parameters. So far, we were able to count 28 nodal parameters, to say nothing about the geometrical coordinates which identify the node, the flag parameters and the data used to connect the adjacent nodes.

To conclude this section regarding the nodal parameters, we state that a computer based model may be rationally and optimally designed if an abstract data type is conceived, based on the aspects previously presented. Moreover, this concept regarding the allocation of some significant information to a given node may lead to a meta-level of understanding in the design of the computer based models in engineering.

7. CONCLUSIONS

The paper is an endeavor to identify general patterns in computer based models in engineering.

A major aspect concerns the elastic supports, widely used in the real life, their elasticity being disregarded by the hypotheses on which are based the so-called 'classic' theories. By considering them, we have more accurate models. The paper offers a methodology to solve problems and to design analytical models based on the use of the elastic supports.

A second aspect regards the parameters which may be assigned to a node which belongs either to an analytical model, or to a numerical model (which may be based on either the finite element method, or the finite difference method). This is a long run concern of the author and a general solution regarding a general abstract data type would be very useful for the easily design and development of computer based models in engineering.

The elastic supports issue is a very interesting problem and additional solutions may be imagined using both the theoretical aspects and the experimental studies.

8. ACKNOWLEDGEMENT

Ideas regarding the computer based instruments in applied elasticity are the result of the models developed in the framework of the MIEC2010 bilateral Ro-Md research project, Oanta, E., Panait, C., Lepadatu, L., Tamas, R., Constantinescu, M., Odagescu, I., Tamas, I., Batrinca, G., Nistor, C., Marina, V., Iliadi, G., Sontea, V., Marina, V., Balan, V. (2010-2012), "Mathematical Models for Inter-Domain Approaches with Applications in Engineering and Economy", MIEC2010 - Bilateral Romania-Moldavia Scientific Research Project, under the supervision of the National Authority for Scientific Research (ANCS), Romania, that is the follow-up of the ID1223 scientific research project: Oanta, E., Panait, C., Nicolescu, B., Dinu, S., Pescaru, A., Nita, A., Gavrila, G., (2007-2010), "Computer Aided Advanced Studies in Applied Elasticity from an Interdisciplinary Perspective", under the supervision of the National University Research Council (CNCSIS), Romania.

Ideas regarding the application of the results for maritime structures are the outcome of the models developed in the framework of the scientific research study 'Development of computer assisted marine structures', Emil Oanta, Cornel Panait, Ghiorghe Batrinca, Alexandru Pescaru, Alexandra Nita, Feiza Memet, which is a component of the RoNoMar project, 2010.

9. REFERENCES

[1] BUZDUGAN, G. *Rezistenta materialelor* (Editia a IX-a revizuita), Editura Tehnica, Bucuresti, 1970.

[2] KUMBETLIAN, G. *Rezistenta materialelor*, vol. 2, Centrul de multiplicare al Institutului de Marina Civila Constanta, Constanta, 1992.

[3] OANTA, E.; TARAZA. D. *Experimental Investigation of the Strains and Stresses in the Cylinder Block of a Marine Diesel Engine*, Paper SAE 2000-01-0521, 2000 SAE International Congress and Exposition, Detroit, Michigan, March 6-9, 2000, ISSN 0148-7191.

[4] OANTA, E. *PhD Thesis: FEM Study of the Stresses and Strains in the Block Cylinder of the Internal Combustion Engines*, 442 pages, 86 letters of support, 105 reviewers, 2001, 'Politehnica' University of Bucharest, The Faculty of Mechanical Engineering; Promoter: Prof. Dr. H. C. Eng. Constantin Arama, Member of the Romanian Science Academy.

[5] OANTA, E. *Comparison Between the 'By-Hand' Calculus and the Automatic Computing for the Method of Initial Parameters Applied for Hulls*, Annals of Constanta Maritime University, Pg. 167-172, ISSN 1582-3601, Constanta, 2002.

[6] OANTA, E.; NICOLESCU, B., *An original approach in the computer aided calculus of the large deflections*, Analele Universității Maritime Constanța, România, 2003, Year IV, Vol. 5, pag. 53-58, ISSN 1582-3601.

[7] OANTA, E. *Rezistenta Materialelor - curs si aplicatii*, 422 pag, Editura Fundatiei "Andrei Saguna", Constanta, 2004, ISBN 973-8146-38-0.

[8] OANTA, E.; PANAIT, C.; BATRANCA, G.; PESCARU, A.; NITA, A.; MEMET, F. *Development of Computer Assisted Marine Structures*, 130 pag, Editura Nautica, Constanța, 2012, ISBN 978-606-8105-70-3, 629.5.

[9] OANTA, E. *Approximations in structural analytical studies*, Constanta Maritime University Annals, 2012, Year XIII, Volume 18, ISSN 1582-3601, pag. 129-134.

[10] OANTA, E.; PANAIT, C.; AXINTE, T.; DASCALESCU, E. *Instrumente software originale folosite ca interfețe în cadrul modelelor hibride din ingineria mecanică*, Buletinul AGIR No. 4 / 2014, ISSN-L 1224-7928, Online: ISSN 2247-3548, http://www.agir.ro/buletine/2151.pdf.

AN ORIGINAL METHOD TO MEASURE THE ELASTICITY OF THE SUPPORTS USING A SHOCK LOADING AND THE STRAIN GAGE TECHNOLOGY

[1]OANTA M. EMIL, [2]AXINTE TIBERIU, [3] DASCALESCU ANCA-ELENA

[1,2]Constanta Maritime University, [3]'Politehnica' University of Bucharest, Romania

ABSTRACT

The accuracy of the analytical models of the structural phenomena may be improved if some of the simplifying hypotheses are disregarded, being replaced with more sophisticated and more precise approaches. In this way, the elastic supports which may be found in all the real phenomena were modelled as rigid supports. If we want to use elastic supports in our models, which may be theoretically defined as coil (helicoidal) springs, we must conceive experimental methods to measure their elastic constants. The paper presents an original method to measure the elastic constant of a support using a shock loading whose effects are measured using the strain gage technology. In this way, there is measured the elastic displacement of the elastic support under various loads, the ratio between the reaction and the displacement being the elastic constant of that given support. Beside this information, there may be also evaluated the damping effects due to the elastic support. The method may be tested in laboratory conditions, being able to be generalized for real, field conditions, if necessary.

Keywords: *Elastic supports, elastic constants, strain gage technology, damping factor.*

1. INTRODUCTION

Analytical models are usually based on a set of assumptions provided by the so called 'classic' theory. These simplifying hypotheses are useful for the modelling of many real phenomena where the accuracy is not a special issue. For these simple case studies there is not required an advanced instrument to perform the calculi, such as an original or a commercial software application. However, there are cases when more accurate results are necessary, so new approaches are needed.

Regarding the structural studies, the elastic supports considered within a model may improve the accuracy of the results. The main problem regards the measurement of the elastic constants of the supports, theoretically defined as coil (helicoidal) springs.

2. PREVIOUS EXPERIMENTAL WORK REGARDING THE SHOCK / DYNAMIC LOADINGS

There are many practical situations when shock loadings are produced: crash loads, explosions, firing a weapon, impact and others.

Shock loadings are producing an overload expressed by the shock load multiplying factor, which according to [1] pg. 414, it may be defined as

$$\psi = \frac{\sigma_{shock\ \ loading}}{\sigma_{statical\ \ loading}} \ . \qquad (1)$$

By default, the effects of the shock loadings are considered to be in the linear-elastic range of the stress-strain diagram of the material.

For complex loadings and complex calculus domains it is difficult to create theoretical (analytical and numerical) models of the shock loading phenomena, so there are very useful experimental studies, most of them based on the strain gage technology, which is able to record maximum values of the dynamic strains, [2], [3] and [4]. In these experimental studies there were not considered elastic supports of the structure subjected to shock loading. The statical loads were not considered, the experimental study being carried out simply for the verification of the stresses produced by the dynamic loading and it was not followed by the creation of a theoretical model (analytical or numerical).

A case study when the influence of the elastic supports onto the state of strains and stresses produced by variable loads is given in [6], the experimental study being presented in [5].

As it can be noticed in figure 1, several types of boundary conditions and models of the elastic supports were tested. Each model is producing a given state of strains which is variable in time according to the periodical loads produced into the internal combustion engine, (ICE).

In order to calibrate the finite element model of the block of cylinders belonging to the ICE, experimental studies were carried out in order to have the variation of the strains in points R1 and R5 in several steady state conditions of the ICE.

There was studied the best match between the results of the theoretical model and of the experimental studies, being analysed millions of values produced by the experimental measurement, for various steady state conditions of the ICE.

Finally, there were selected the models of the supports whose influence was very similar to the influence of the real supports, in this way the theoretical model being calibrated.

A description of the hybrid model conceived for this study and of the subsequent studies is given in [8], together with directions to be followed in the development of the interfaces necessary to design an actual hybrid model.

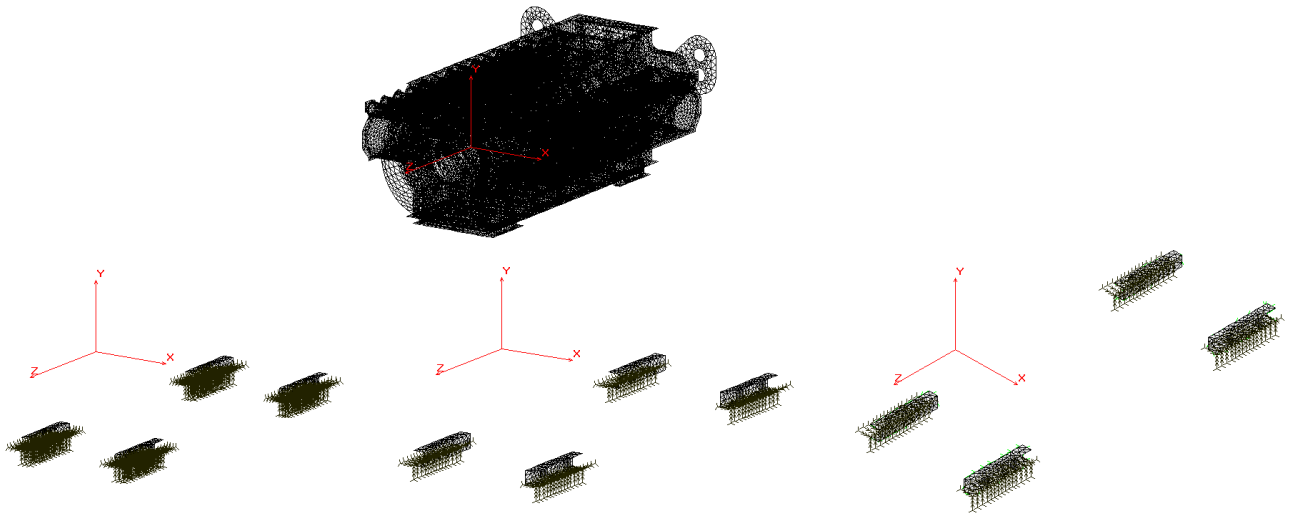

Figure 1 – FEM tests regarding the elasticity of the supports of an internal combustion engine

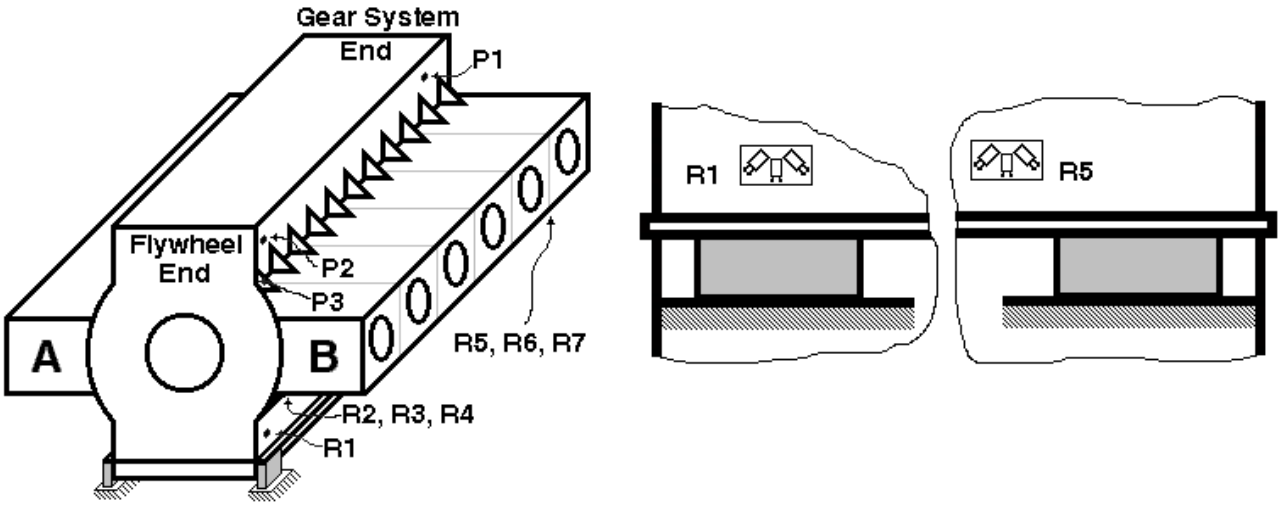

Figure 2 – Experimental study regarding the strains in the adjacent area of the supports of an internal combustion engine in running conditions

3. SETUP OF THE EXPERIMENT

Let us consider a theoretical case study, the experimental setup being presented in figure 3. As it can be noticed, an object of mass m falls from height H in the midsection of a beam. The bar has a pinned support at its left end and a simple support on its right end. In the left drawing the supports are rigid, meanwhile in the right drawing the supports are elastic. The elastic supports are drawn as coil (helicoidal) springs, their elastic constant being the unknowns of our study. The beam has a rectangular cross section of height h and width b. The according geometrical characteristics of the cross section are:

$$I_Y = \frac{b \cdot h^3}{12},\ W_Y = \frac{b \cdot h^2}{6} \qquad (1)$$

The force applied in static conditions is the weight of the object which falls:

$$F = m \cdot g \qquad (2).$$

The reactions produced by this static force are:

$$V_1 = V_5 = F \frac{L_{35}}{L_{13} + L_{35}} = \frac{F}{2}. \qquad (3)$$

At distance a with respect to the supports, in sections 2 and 4, we bond the R_1, R_2, R_3 and R_4 strain gages, which are installed in a full-bridge arrangement. The grid of the strain gages is along the length of the beam, i.e. along the principal directions.

In sections 2 and 4 the bending moment produced by force F is:

$$M_{Y2} = M_{Y4} = V_1 \cdot a = (m \cdot g) \cdot a. \qquad (4)$$

The maximum normal stress on the topmost and bottommost surfaces of the beam, on which the strain gages are bonded, is:

$$\sigma_2^{M_Y} = \frac{M_{Y2}}{W_Y} = E \cdot \varepsilon_{M_Y} \qquad (5).$$

In this way we have a connection between the strains which are measured in sections 2 and 4 and the mass of the object which falls.

Relations (1) ÷(5) may be used for the both types of supports, rigid and elastic.

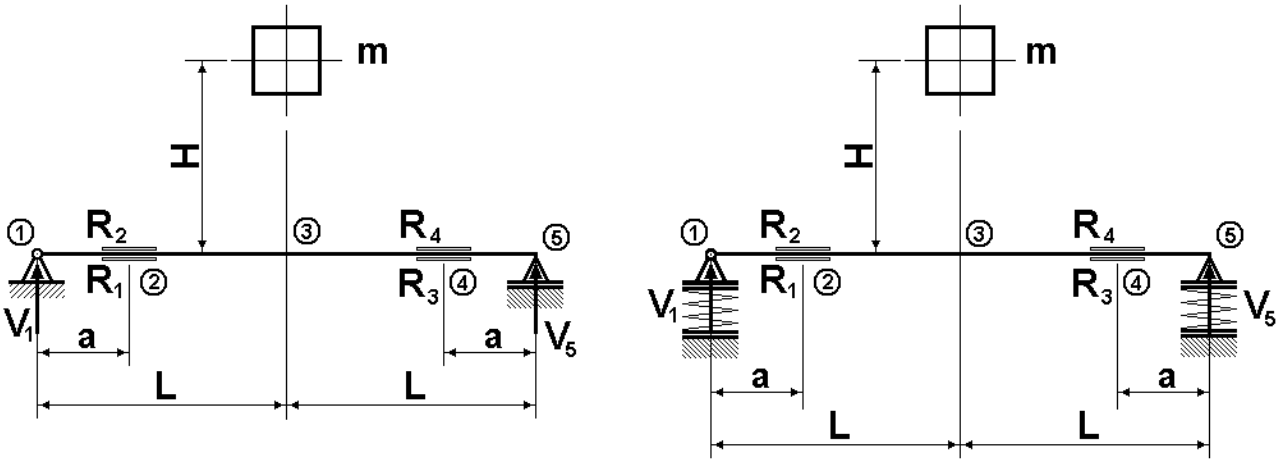

Figure 3 – Setup of the experimental study

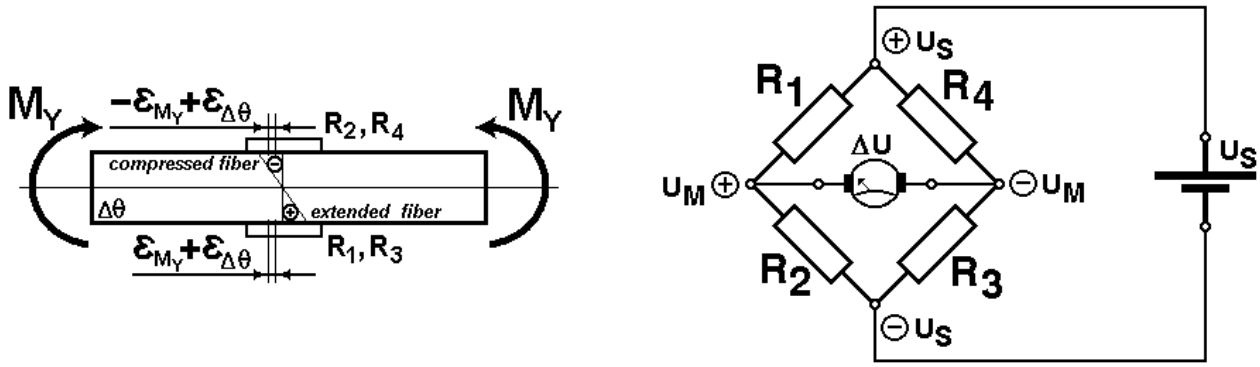

Figure 4 – Strains which are measured by the R_i strain gages and their locations in the Wheatstone bridge

4. CALCULUS RELATIONS

Let us consider only the R_1 and R_2 strain gages, located in section 2. Both strain gages are measuring the mechanical strain given by the mechanical load and the apparent strain given by the temperature variation during the experiment, which is considered a parasitic effect.

The strain gages are located in adjacent sides of the Wheatstone bridge, so their effects are subtracted one from the other. The according output signal of the Wheatstone bridge, denoted ε_{WB} is:

$$\begin{array}{ll} \textbf{(+)} & \varepsilon_{R_1} = \varepsilon_{M_Y} + \varepsilon_{\Delta\theta} \\ \textbf{(-)} & \varepsilon_{R_2} = -\varepsilon_{M_Y} + \varepsilon_{\Delta\theta} \\ \hline \varepsilon_{WB} = \varepsilon_{R_1} + \varepsilon_{R_2} = & 2\cdot\varepsilon_{M_Y} \end{array}$$

It results that for a half-bridge arrangement the strain measured by the Wheatstone bridge is

$$\varepsilon_{WB} = 2\cdot\varepsilon_{M_Y} . \tag{6}$$

For a full bridge arrangement we have

$$\varepsilon_{WB} = 4\cdot\varepsilon_{M_Y} . \tag{7}$$

The stress in this section for a full bridge arrangement is

$$\sigma_2^{M_Y} = \frac{V_1\cdot a}{\left(\frac{b\cdot h^2}{6}\right)} = E\cdot\frac{\varepsilon_{WB}}{4} . \tag{8}$$

The reaction is

$$V_1 = E\cdot\left(\frac{b\cdot h^2}{24\cdot a}\right)\cdot\varepsilon_{WB} . \tag{9}$$

The shock load multiplying factor for rigid supports is

$$\psi_{rigid} = 1+\sqrt{1+\frac{2\cdot H}{u_{Z\ static\&rigid}}} . \tag{10}$$

The displacement in section 3 under a static load for rigid supports is

$$u_{Z\ static\&rigid\ 3} = \frac{1}{3\cdot E\cdot I_Y}\cdot F\cdot\frac{L_{13}^2\cdot L_{35}^2}{L_{13}+L_{35}} . \tag{11}$$

If $L_{13} = L_{35} = L$, it results the relation

$$u_{Z\ static\&rigid\ 3} = \frac{F \cdot L^3}{6 \cdot E \cdot I_Y}. \quad (12)$$

The shock load multiplying factor for elastic supports is

$$\psi_{elastic} = 1 + \sqrt{1 + \frac{2 \cdot H}{u_{Z\ static\&elastic\ 3}}}. \quad (13)$$

Using the previous relation, we express $u_{Z\ static\&elastic\ 3}$ with respect to $\psi_{elastic}$ and it results

$$u_{Z\ static\&elastic\ 3} = \frac{2 \cdot H}{\psi_{elastic} \cdot (\psi_{elastic} - 2)}. \quad (14)$$

The $u_{Z\ static\&elastic}$ is

$$u_{Z\ static\&elastic\ 3} = u_{Z\ static\&rigid\ 3} + u_{Z\ elastic\ support\ 1}. \quad (15)$$

According to the definition of the shock load multiplying factor

$$\sigma_{2\ elastic}^{M_Y} = \psi_{elastic} \cdot \sigma_{2\ static}^{M_Y}, \quad (16)$$

and it results

$$\psi_{elastic} = \frac{\sigma_{2\ elastic}^{M_Y}}{\sigma_{2\ static}^{M_Y}} = \frac{E \cdot \varepsilon_{M_Y\ elastic}}{E \cdot \varepsilon_{M_Y\ static}} = \frac{\varepsilon_{WB\ elastic}}{\varepsilon_{WB\ static}}. \quad (17)$$

The strain in static conditions is

$$\varepsilon_{M_Y\ static} = \frac{\sigma_2^{M_Y}}{E} = \frac{M_{Y\ 2\ static}}{E \cdot W_Y} = \frac{V_1 \cdot a}{E \cdot W_Y},$$

$$\varepsilon_{M_Y\ static} = \frac{F \cdot a}{2 \cdot E \cdot W_Y} = \frac{\varepsilon_{WB\ static}}{4}. \quad (18)$$

In this case the output signal of the Wheatstone bridge is

$$\varepsilon_{WB\ static} = \frac{2 \cdot F \cdot a}{E \cdot W_Y}. \quad (19)$$

From relation (17) it results

$$\psi_{elastic} = \frac{\sigma_{2\ elastic}^{M_Y}}{\sigma_{2\ static}^{M_Y}} = \frac{M_{Y\ elastic\ 2}}{M_{Y\ static\ 2}} = \frac{V_{1\ elastic}}{V_{1\ static}}, \quad (20)$$

where $V_{1\ static}$ is given by relation (3).

Moreover, using the previous relations we are able to calculate the damping effect, this is the ratio between the shock load multiplying factor for the rigid supports and the shock load multiplying factor for the elastic supports, i.e. $\frac{\psi_{rigid}}{\psi_{elastic}}$.

5. NUMERICAL EXAMPLE

We use the geometrical information given in section 3 and in figure 3, together with $\varepsilon_{WB\ static}$, $\varepsilon_{WB\ shock,rigid}$ and $\varepsilon_{WB\ shock,elastic}$. By $\varepsilon_{WB\ static}$ we mean $\varepsilon_{WB\ static\&rigid}$.

Using relation (19) and (2) it results the mass of the object,

$$m = \frac{E \cdot W_Y}{2 \cdot a \cdot g} \cdot \varepsilon_{WB\ static}. \quad (21)$$

For the shock loading, the shock load multiplying factor is given by relation (17).

Figure 5 – Device which was initially designed to measure the effects of a shock loading

$u_{Z\ static\&rigid\ 3}$ is given by relation (12) in which we replace (2) and (21) and it results

$$u_{Z\ static\&rigid\ 3} = \frac{L^3}{6 \cdot a \cdot h} \cdot \varepsilon_{WB\ static}. \quad (22)$$

Using (14) we calculate $u_{Z\ static\&elastic\ 3}$, and from relation (15) it results

$$u_{Z\ elastic\ support\ 1} = u_{Z\ static\&elastic\ 3} - u_{Z\ static\&rigid\ 3}. \quad (23)$$

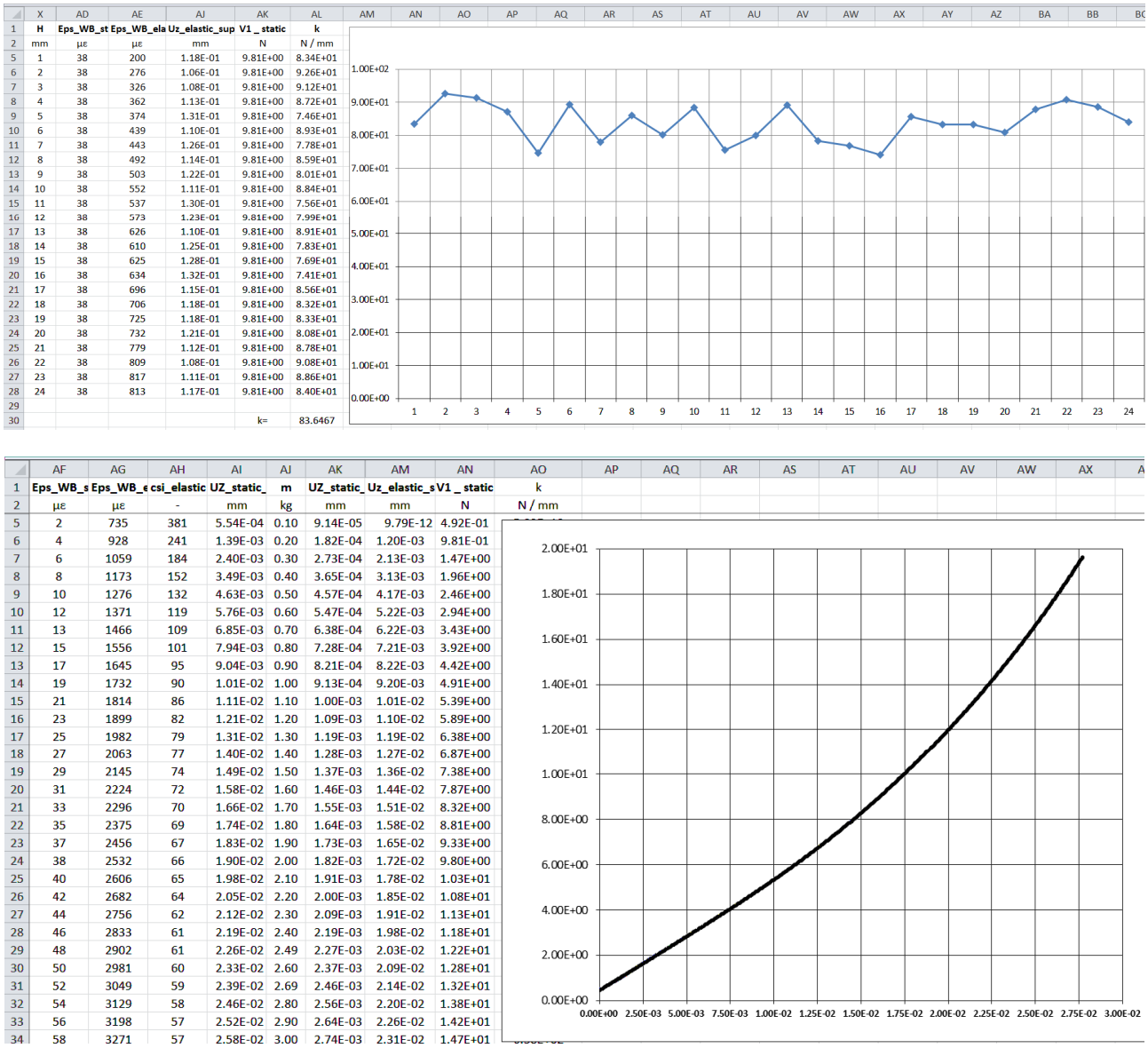

H	Eps_WB_st	Eps_WB_ela	Uz_elastic_sup	V1 _ static	k
mm	με	με	mm	N	N / mm
1	38	200	1.18E-01	9.81E+00	8.34E+01
2	38	276	1.06E-01	9.81E+00	9.26E+01
3	38	326	1.08E-01	9.81E+00	9.12E+01
4	38	362	1.13E-01	9.81E+00	8.72E+01
5	38	374	1.31E-01	9.81E+00	7.46E+01
6	38	439	1.10E-01	9.81E+00	8.93E+01
7	38	443	1.26E-01	9.81E+00	7.78E+01
8	38	492	1.14E-01	9.81E+00	8.59E+01
9	38	503	1.22E-01	9.81E+00	8.01E+01
10	38	552	1.11E-01	9.81E+00	8.84E+01
11	38	537	1.30E-01	9.81E+00	7.56E+01
12	38	573	1.23E-01	9.81E+00	7.99E+01
13	38	626	1.10E-01	9.81E+00	8.91E+01
14	38	610	1.25E-01	9.81E+00	7.83E+01
15	38	625	1.28E-01	9.81E+00	7.69E+01
16	38	634	1.32E-01	9.81E+00	7.41E+01
17	38	696	1.15E-01	9.81E+00	8.56E+01
18	38	706	1.18E-01	9.81E+00	8.32E+01
19	38	725	1.18E-01	9.81E+00	8.33E+01
20	38	732	1.21E-01	9.81E+00	8.08E+01
21	38	779	1.12E-01	9.81E+00	8.78E+01
22	38	809	1.08E-01	9.81E+00	9.08E+01
23	38	817	1.11E-01	9.81E+00	8.86E+01
24	38	813	1.17E-01	9.81E+00	8.40E+01
				k=	83.6467

Eps_WB_s	Eps_WB_ε	csi_elastic	UZ_static_	m	UZ_static_	Uz_elastic_s	V1 _ static	k
με	με	-	mm	kg	mm	mm	N	N / mm
2	735	381	5.54E-04	0.10	9.14E-05	9.79E-12	4.92E-01	
4	928	241	1.39E-03	0.20	1.82E-04	1.20E-03	9.81E-01	
6	1059	184	2.40E-03	0.30	2.73E-04	2.13E-03	1.47E+00	
8	1173	152	3.49E-03	0.40	3.65E-04	3.13E-03	1.96E+00	
10	1276	132	4.63E-03	0.50	4.57E-04	4.17E-03	2.46E+00	
12	1371	119	5.76E-03	0.60	5.47E-04	5.22E-03	2.94E+00	
13	1466	109	6.85E-03	0.70	6.38E-04	6.22E-03	3.43E+00	
15	1556	101	7.94E-03	0.80	7.28E-04	7.21E-03	3.92E+00	
17	1645	95	9.04E-03	0.90	8.21E-04	8.22E-03	4.42E+00	
19	1732	90	1.01E-02	1.00	9.13E-04	9.20E-03	4.91E+00	
21	1814	86	1.11E-02	1.10	1.00E-03	1.01E-02	5.39E+00	
23	1899	82	1.21E-02	1.20	1.09E-03	1.10E-02	5.89E+00	
25	1982	79	1.31E-02	1.30	1.19E-03	1.19E-02	6.38E+00	
27	2063	77	1.40E-02	1.40	1.28E-03	1.27E-02	6.87E+00	
29	2145	74	1.49E-02	1.50	1.37E-03	1.36E-02	7.38E+00	
31	2224	72	1.58E-02	1.60	1.46E-03	1.44E-02	7.87E+00	
33	2296	70	1.66E-02	1.70	1.55E-03	1.51E-02	8.32E+00	
35	2375	69	1.74E-02	1.80	1.64E-03	1.58E-02	8.81E+00	
37	2456	67	1.83E-02	1.90	1.73E-03	1.65E-02	9.33E+00	
38	2532	66	1.90E-02	2.00	1.82E-03	1.72E-02	9.80E+00	
40	2606	65	1.98E-02	2.10	1.91E-03	1.78E-02	1.03E+01	
42	2682	64	2.05E-02	2.20	2.00E-03	1.85E-02	1.08E+01	
44	2756	62	2.12E-02	2.30	2.09E-03	1.91E-02	1.13E+01	
46	2833	61	2.19E-02	2.40	2.19E-03	1.98E-02	1.18E+01	
48	2902	61	2.26E-02	2.49	2.27E-03	2.03E-02	1.22E+01	
50	2981	60	2.33E-02	2.60	2.37E-03	2.09E-02	1.28E+01	
52	3049	59	2.39E-02	2.69	2.46E-03	2.14E-02	1.32E+01	
54	3129	58	2.46E-02	2.80	2.56E-03	2.20E-02	1.38E+01	
56	3198	57	2.52E-02	2.90	2.64E-03	2.26E-02	1.42E+01	
58	3271	57	2.58E-02	3.00	2.74E-03	2.31E-02	1.47E+01	

Figure 6 – Results of the calculi performed in a spreadsheet software

According to relation (20), it results

$$V_{1\,elastic} = \psi_{elastic} \cdot V_{1\,static} = \psi_{elastic} \cdot \frac{m \cdot g}{2}, \qquad (24)$$

where m is given by relation (21).

Using the above relations, there may be conceived an algorithm which may be implemented, either by the use of a programming language, or using a spreadsheet application.

The device which may be used to perform the measurements is presented in figure 5. The strain gages may be connected to a SYSTEM6000 data acquisition equipment in order to have a data acquisition chain. This device was created as a practical application within a university graduation project about 25 years ago and it was conceived to measure only the effects of the shock loadings, not the effects of the elastic supports.

By adding a layer of rubber under its supports, we redesign the device to be able to measure the effect of the elastic constants of the supports.

The measurement based on this device must take into account the following hypotheses (sources of inaccuracy):

- the mass falls right in the midsection of the bar;
- the height H is precisely measured;
- the sections 2 and 4 are precisely located at the same distance, a, with respect to the ends of the bar;
- the elastic constants of the both supports have the same value (thickness, composition and elastic behavior of the both layers of rubber);
- the strain gages are precisely aligned to the principal directions.

Based on these sources of inaccuracy, there were drawn conclusions regarding the redesign of some parts of the device, the stages to be followed during the experimental measurements and regarding the methods to process the results.

Experimental data reduction may be done, either for the same mass, m, together with several heights, H, case presented in the upper part of figure 6, or for several

masses, this case being presented in the bottommost part of figure 6. In this case it was simulated an elastic non-linear support. There was also simulated a certain degree of randomness of the simulated experimental data. This proves that our theory is able to generate a practical method to measure the elastic behavior of the supports.

Other calculi were also performed regarding the maximum normal stress, to verify if they are in the linear-elastic range of stresses and the damping effect due to the elastic supports.

6. CONCLUSIONS

The paper presents two case studies regarding the effect of the elastic supports. The first study solves a practical problem requested by industry: an internal combustion engine on elastic supports in running conditions, [5], [6], being presented the knowhow regarding the elastic supports issue. The second study presents an original theoretical approach regarding the measurement of the elastic constants of the supports in laboratory conditions. The theoretical aspects are followed by the presentation of the method employed to perform the calculi and two case studies regarding the simulated experimental data reduction. The assembly *theory plus method*, validates the original approach to measure the elasticity of the supports using shock loading and the strain gage technology.

The principles of this original method may be also used for field experiments.

7. ACKNOWLEDGMENTS

Ideas regarding the computer based instruments in applied elasticity are the result of the models developed in the framework of the MIEC2010 bilateral Ro-Md research project, Oanta, E., Panait, C., Lepadatu, L., Tamas, R., Constantinescu, M., Odagescu, I., Tamas, I., Batrinca, G., Nistor, C., Marina, V., Iliadi, G., Sontea, V., Marina, V., Balan, V. (2010-2012), “Mathematical Models for Inter-Domain Approaches with Applications in Engineering and Economy”, MIEC2010 - Bilateral Romania-Moldavia Scientific Research Project, under the supervision of the National Authority for Scientific Research (ANCS), Romania, that is the follow-up of the ID1223 scientific research project: Oanta, E., Panait, C., Nicolescu, B., Dinu, S., Pescaru, A., Nita, A., Gavrila, G., (2007-2010), "Computer Aided Advanced Studies in Applied Elasticity from an Interdisciplinary Perspective", under the supervision of the National University Research Council (CNCSIS), Romania.

Ideas regarding the application of the results for the maritime structures are the outcome of the models developed in the framework of the scientific research study ‘Development of computer assisted marine structures’, Emil Oanta, Cornel Panait, Ghiorghe Batrinca, Alexandru Pescaru, Alexandra Nita, Feiza Memet, which is a component of the RoNoMar project, 2010.

8. REFERENCES

[1] BUZDUGAN, G. *Rezistenta materialelor* (Editia a IX-a revizuita), Editura Tehnica, Bucuresti, 1970.

[2] KUMBETLIAN, G., MAIER, V., POPA, G., NICULESCU, C., CALANCEA, N., OANTA, E. *Masurari tensometrice în conditii speciale*, Academia Navala Constanta, 'A XVIII-a Conferinta de Mecanica Solidelor', Sectia III - Mecanica navei si a structurilor navale, 09-11 iunie 1994, Pag. 198-202.

[3] KUMBETLIAN, G., PERIDE, N., et all. *Determinarea experimentala a tensiunilor în punctele considerate periculoase la produsul cal. 130 mm*, Simpozionul National de Tehnica Marina - TEHMAR '96 - Centrul de cercetari stiintifice al marinei militare, 3-4 octombrie 1996.

[4] KUMBETLIAN, G., PERIDE, N., et all. *Analiza tensiunilor in conditii de soc*, Al VII-lea Simpozion National de Tensometrie cu participare internationala, Universitatea din Suceava, 17-19 octombrie 1996, Vol. 1, Pag. 41-46.

[5] OANTA, E.; TARAZA. D. *Experimental Investigation of the Strains and Stresses in the Cylinder Block of a Marine Diesel Engine*, Paper SAE 2000-01-0521, 2000 SAE International Congress and Exposition, Detroit, Michigan, March 6-9, 2000, ISSN 0148-7191.

[6] OANTA, E. *PhD Thesis: FEM Study of the Stresses and Strains in the Block Cylinder of the Internal Combustion Engines*, 442 pages, 86 letters of support, 105 reviewers, 2001, ‘Politehnica’ University of Bucharest, The Faculty of Mechanical Engineering; Promoter: Prof. Dr. H. C. Eng. Constantin Arama, Member of the Romanian Science Academy.

[7] OANTA, E., PANAIT, C., LAZAROIU, G., RAICU, A., AXINTE, T., DASCALESCU, A.E. *Conceiving a Hybrid Model of a Weighting Device*, ATOM-N 2014 - The 7th edition of the International Conference "Advanced Topics in Optoelectronics, Microelectronics and Nanotechnologies", 21-24 August 2014, Constanta, Romania.

[8] OANTA, E.; PANAIT, C.; AXINTE, T.; DASCALESCU, E. *Instrumente software originale folosite ca interfete în cadrul modelelor hibride din ingineria mecanică*, Buletinul AGIR No. 4 / 2014, ISSN-L 1224-7928, Online: ISSN 2247-3548, http://www.agir.ro/buletine/2151.pdf

ANALYSIS OF INTERVENTION METHODS IN CASE OF ACCIDENTAL POLLUTION WITH OIL PRODUCTS

[1]PARASCHIV SPIRU, [2]PARASCHIV LIZICA-SIMONA

[1, 2] *"Dunarea de Jos" University of Galati, Romania*

ABSTRACT

Combating the pollution with hydrocarbons includes preventive methods but also intervention methods.

In present worldwide, are used five methods to combat the pollution with hydrocarbons. Using either of these methods involve a number of factors such as: weather limit conditions, technical features of intervention equipment, boundary conditions on the state of the pollutant and a number of advantages and disadvantages depending on the type of method chosen.

Keywords: *pollution incident, oil dispersion, marine equipment.*

1. INTRODUCTION

The magnitude of a pollution event is given by the quantity of oil spilled or that are going to be spilled from the sources presented before [1]. The method used in the intervention is determined in first place by the severity of the pollution incident.

In this context according to OPRC Convention/1990 were established the following levels of severity based on the quantities that have been spilled:

- Minor marine pollution (level 1) <7 tons;
- Average marine pollution (level 2) from 7 tons up to 700 tons;
- Major marine pollution (level 3) more than 700 tons;

For each pollution level there is a method of intervention as:

- for level 1 and level 2 exists local plans of actions with the involvement of the polluter or local authorities;
- For level 2 pollution where local authorities are outweighed by the situation and for level 3 pollution are activated the national structures designated as law requires.

An analysis on the three levels of pollution depending on the sources that caused it is necessary to make a hierarchy of pollution risk areas.

Although they are rare, in general context when they appear, major pollution (more than 700 t) can seriously affect the environment, economy, and the health of population and social frame [3].

The number of accident involving oil spills bigger than 700 t in the last 43 years indicates the fact that, from 1970 until present, in oceans or seas water from the whole world there have been spilled about 5, 75 million tons of oil products [2]. However, from this data, we can take a positive conclusion highlighted by the decreasing number of accidents worldwide, due to international regulations that are applied by most countries in the world.

The data provided by international sources show that, on global plan, the number of oil spills produced by marine ships decreased by 60% in the last 25 years [4].

2. METHODS USED IN CASE OF MARINE POLLUTION WITH OIL PRODUCTS

In present there are known five types of intervention techniques as follows:

- Natural degreasing;
- The transfer of goods in storage barges;
- Dispersion in the water body;
- The concentration and recovery of oil products from the water surface;
- Setting the hole site on fire

The methods of recovery and control of the pollutant are in general the first used [5]. Specific equipment include a series of floating barriers that are meant to stop the fast dispersion of the pollutant, machinery and ships specially designed for the recovery of the pollutant (ex. Skimmers) and also natural and synthetic absorbent materials.

There are also used special containers for transient storage of pollutant.

Figure 1 Dam limiter from Danube Eco 1 ship

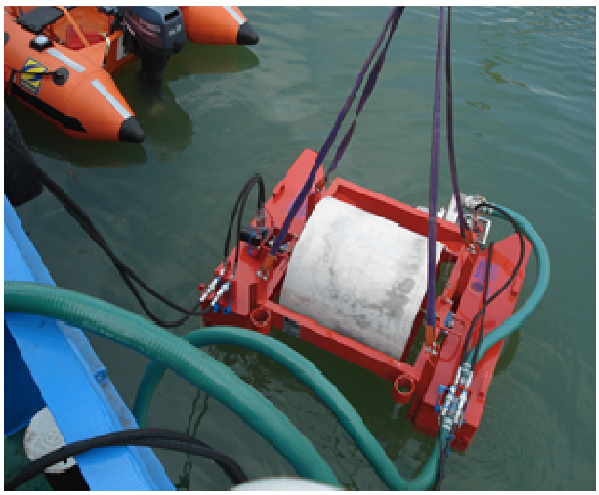

Figure 2 The skimmer from Danube Eco 1 ship

Figure 3 Spray ramp for chemical dispersion in water volume

Figure 4 Exercise with limitation dam from Danube Eco 1 ship

Absorbent materials that are used are insoluble and are able to recover the liquid pollutant either by absorption or adsorption, or by both processes, and they are able to retain up to 50% of the pollutant. To be effective this materials need to be oleophile (to be able to retain oil) and in the same time to be hydrophobic (the materials can't absorb water), and water-insoluble at a rate of at least 70%.

From the point of view of their origins this materials can be included in three base categories: natural organic, inorganic natural and synthetic.

The natural organic materials can absorb a pollutant quantity from 3 to 15 times their own weight, but some of them have the disadvantage that they absorb a quantity of water which can result in more rapid sinking of them, which largely prevents their collection.

Chemical and biological methods are used along with mechanical methods. There can be used some substances that either disperse the pollutant, or ensure its agglutination. These methods are useful in the attempt to prevent the pollution of coasts, lagoon areas, wet lands or other sensitive ecosystems. In the same areas, some biological agents that enable a more quick eliminations of pollutant.

Biological agents are either chemical compounds that stimulate the activity of microorganisms that destroy the pollutant, or microorganisms that accelerate the process of natural biodegradation. Bioremediation technologies refer to dispersion actions of fertilizers or microorganisms (bacteria and fungi) in the pollutant mass that increase the rate of natural decay rate of the pollutant.

Physical methods are mainly used for cleaning coastal zones. The natural processes such as oxidation, evaporation and biodegradation, may be characteristic for the beginning of pollutant elimination process but they are usually to slow to return to a normal state of environment.

Physical methods involving removal of residual waste, the use of some absorbent materials, washing with pressurized liquids and the removal of the affected soil layer may accelerate the process of natural decontamination.

3. MODELING THE MOVEMENT OF THE POLLUTANT IN MARINE ENVIRONMENT

In the modelling of pollutant dispersion in the marine environment we used GNOME (General NOAA Operational Modelling Environment) modelling program [7].

Input data in the program are:
- Type and quantity of spilled pollutant
- Weather conditions
- The place and moment of the accident

Data obtained:
- Dispersion vector of the spill
- The surface affected by the spill
- Localization of the spill at a given moment
- An estimative path in time
-Front movement

The model was made for a 5000 m^3 oil spill with a wind speed of 10 m/s from NNE.

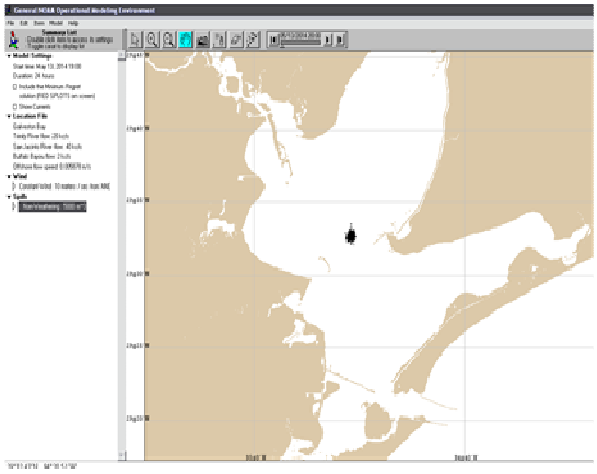

Figure 5 Evolution of a 5000 m^3 oil spill after 3 hours

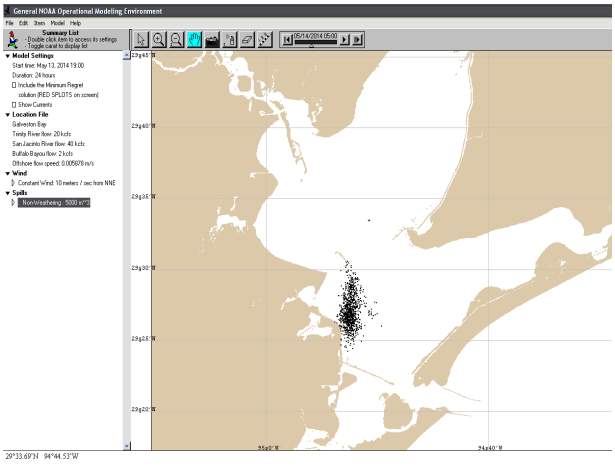

Figure 8 Evolution of 5000 m^3 oil spill after 12 hours

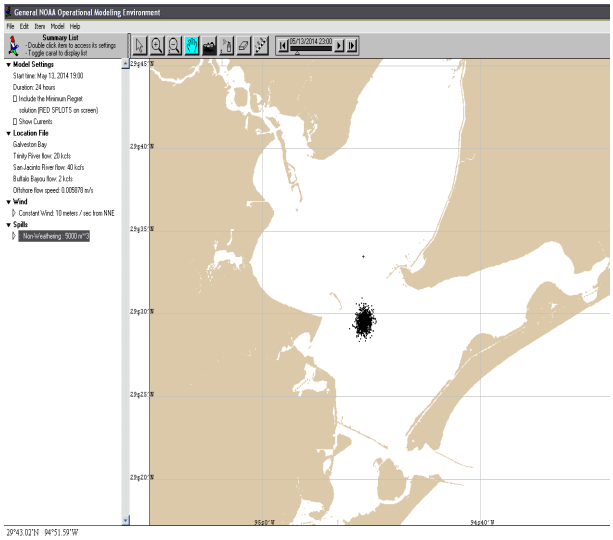

Figure 6 Evolution of 5000 m^3 oil pill after 6 hours

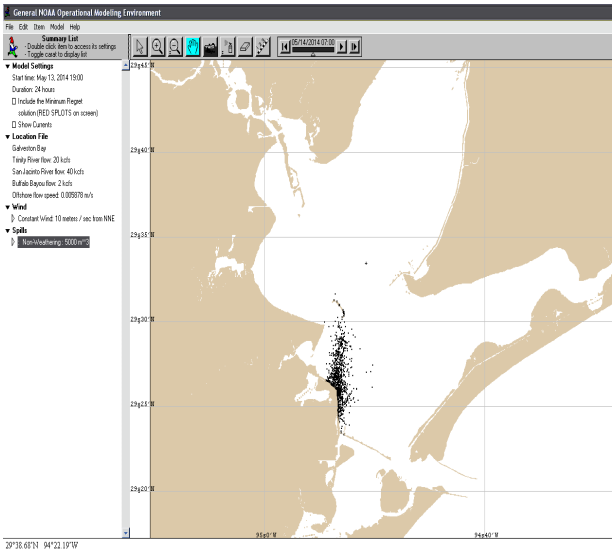

Figure 9 Evolution of 5000 m^3 oil spill after 15 hours

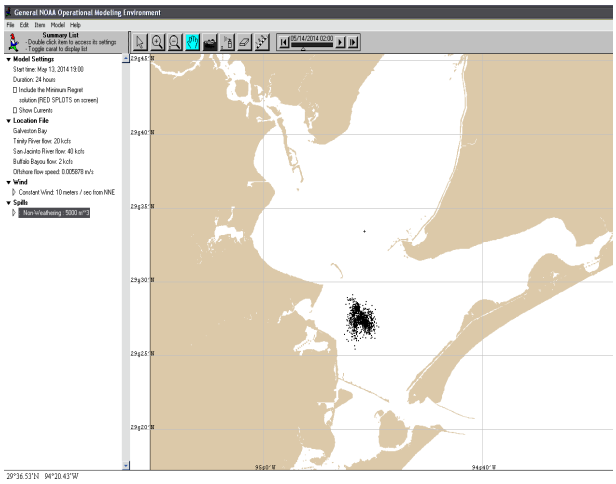

Figure 7 Evolution of 5000 m^3 oil spill after 9 hours

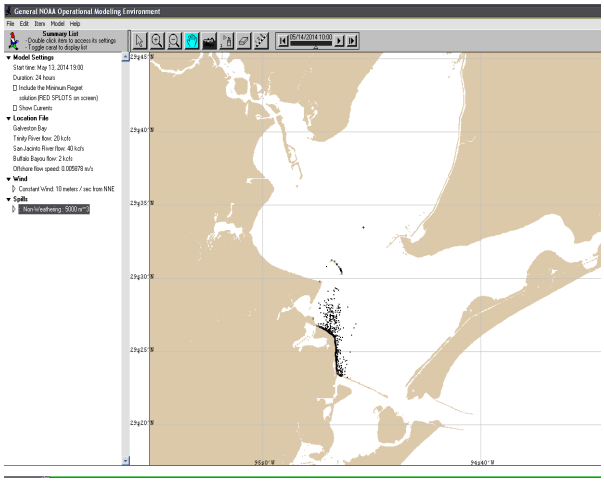

Figure 10 Evolution of 5000m3 oil spill after 18 hours

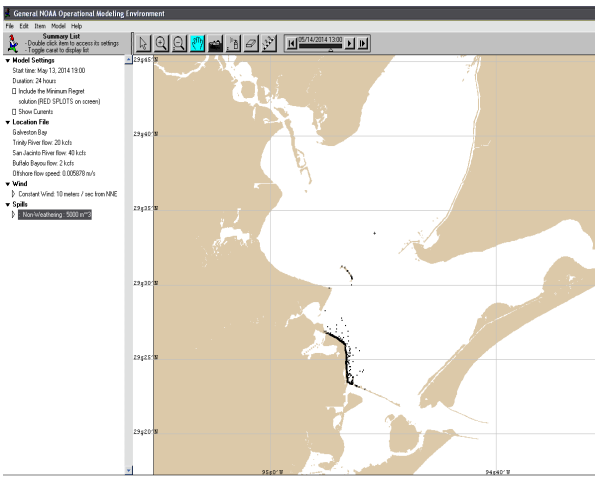

Figure 11 Evolution of 5000 m^3 oil spill after 21 hours

4. CONCLUSIONS

Accidental oil spills in marine environment have a significant economic impact for the activities carried out on shore but also for the activities that exploit the marine resources.

The presence of oil products on the surface of the marine environment cause physical, biological and social consequences.

The oil spread on the surface of marine environment is subject to specific physical-chemical evolution, depending on the nature and the oceanic conditions. By dispersing, emulsifying and dissolving oil in marine environment alters water quality, by concentrating and accumulation in sediments and in marine creatures.

The experience earned from different intervention situations, shows that every pollution event is unique, and because of this it doesn't exist a single efficient system that can cover all the situations that may occur practically on sea and that being said, the best result can be obtained only by combining the methods.

5. REFERENCES

[1] ORNITZ B. E., CHAMP M. A., *Oil Spills First Principles: Prevention and Best Response*, Elsevier Science Ltd, Amsterdam, Netherlands, 2002

[2] NOAA, OIL SPILL, *Case Histories/1967-1991 – Summaries and Significant U.S. and International Spills*, Report HMRAD 92-11, Hazardous Materials Response and Assessment Division, Seattle, Washington, U.S.A., 1992

[3] BOLOGNESI, C., PERRONE, E., ROGGIERI, P., SCIUTTO, A., *Bioindicators in monitoring long term genotoxic impact of oil spill: Haven case study*, Marine Environmental Research 62, S287–S291. 2006

[4] BURGHERR, P., *In-depth analysis of accidental oil spills from tankers in the context of global spill trends from all sources*, Journal of Hazardous Materials 140, 245–256, 2007

[5] KIRBY, M.F., LAW, R.J., *Pollution Response in Emergencies – Marine Impact Assessment and Monitoring (PREMIAM)*, In: Conference Proceedings, Interspill, Marseille, May 12–14, 2009

[6] LESCHINE, T.M., *Oil spills and the social amplification and attenuation of risk*, Spill Science & Technology Bulletin 7, 63–73, 2002

[7] http://response.restoration.noaa.gov/gnome

DESIGNING A HYBRID WIND / PV POWER SYSTEM TO SUPPLY ELECTRICITY FOR A PUBLIC BUILDING

PARASCHIV SPIRU

"Dunarea de Jos" University of Galati, Romania

ABSTRACT

The paper presents a procedure for sizing a hybrid system with which it will examine annual performance photovoltaic hybrid power system considering wind-renewable resources available. The hybrid system, which includes PV panels, wind turbines, inverter and batteries, has been designed to provide a building with energy consumption of 319.7 kWh/day, given that renewable energy resources of the site are: solar radiation the 1700Wh / m2 / day and an average speed of wind of 3.43 m/s.

Keywords: *wind energy, solar energy, hybrid system*

1. INTRODUCTION

A hybrid power system consists usually of two or more renewable energy sources used together to increase the efficiency of the system.

Renewable energy resources such as solar and wind power alternative offers clean and economically competitive to conventional energy generation in areas where wind and solar radiation are available.

Wind power and solar energy that used independently as energy sources are less reliable due to their random change, but by combining them to produce electricity they complement each other by daily and seasonal variation.

By implementing systems that combine two energy sources may become more reliable and could lead to a lower cost system based on renewable potential.

Renewables do not produce emissions and benefits the environment and combat local pollution. The main objective of using renewable energy is to reduce emissions of greenhouse gases.

The development of renewable energy sources as a significant energy resource and clean is a major global energy policy objective, in the context of sustainable development, aimed to increase the security of energy supply, protects the environment and the development of commercially viable energy technologies. In the current context characterized by an alarming increase of pollution caused by energy production from fossil fuels is becoming increasingly important to reduce dependence on these fuels.

Wind energy has already proven to be a very good solution to the problem of global energy. Using renewable resources is addressed not only produce energy, but the particular way of generating reformulated model of development through decentralization sources. Wind energy in particular is among the forms of renewable energy that lends itself to small-scale applications.

According to experts in renewable energy a small electric system that combines wind technology with PV offers several advantages over the two systems individually. In many locations, wind speed is low in summer, and the sun has the most power. Instead the wind is much stronger in winter, when the sun has less power. Since the periods of maximum efficiency for the two systems are different, a hybrid system can produce more energy when you need it.

2. THE BUILDING'S ELECTRICITY CONSUMPTION

The PV and wind turbines generate electricity for energy supply and excess energy is stored in batteries and used to power when the energy generated is not enough. Battery charge controllers maintain battery voltage within specific voltage and eliminate the over discharge regimes or overload. Inverters convert the DC power generated in AC for AC consumers.

Electricity will be produced by wind turbines in combination with photovoltaic panels to cover the consumption of the building as shown in Table 1.

Table 1 Electricity demand of the building

Consumers	Power [W]	h/day	Quantity	kWh/day	kWh/month (20 working days)
Energy saving light bulb	15	8	100	12	360
Fluorescent light bulb	20	8	50	8	240
Refrigerator	1000	5	4	20	600
Vacuum cleaner	1500	2	1	3	90
Air conditioning	2000	5	9	90	2700
Printer	35	1	7	0,2	7,4
PC	350	8	65	182	5460
Total	5020			319,7	9592,35

3. GEOGRAPHIC LOCATION OF THE BUILDING ANALYZED

Figure 1 present the geographical location and meteorological data required for photovoltaic hybrid system design / wind.

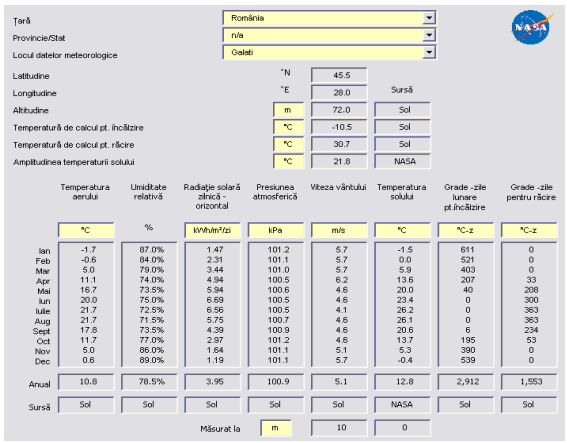

Figure 1 The geographical and meteorological data

Meteorological data presented in Figure 1 were measured at a height of 10 m above the ground. Wind speed at roof height is usually significantly higher than wind speed measured at anemometer height for wind system design wind speed values were recalculated for the height of 25 m above the ground (height of the building), which is the height of their installation.

The variation of the wind speed v, depending on the height h:

$$\frac{V}{V_0} = \left(\frac{h}{h_0}\right)^{\alpha}$$

V_0 - wind speed at anemometer high, [m/s]

α - Characteristic coefficient of the location, α = 0.25

Table 2 Wind speed in the analyzed location

	V[m/s]at 10 m	V[m/s] at 25 m
January	5.7	7.1
February	5.7	7.1
March	5.7	7.1
April	6.2	7.7
May	4.6	5.7
June	4.6	5.7
July	4.1	5.1
August	4.6	5.7
September	4.6	5.7
October	4.6	5.7
November	5.1	6.4
December	5.7	7.1

Figure 2 Building Presentation analyzed

4. CHARACTERISTICS OF WIND SYSTEM

The building is located in a favorable area in the directions N, NE of the building is not located other buildings with a height greater than it is shown in Figure 3.

Figure 3 Overview of the roof of the building

Surfaces that are placed wind turbines are oriented as follows: one side is oriented north with a length of 40 m, it will be located on 10 wind turbines AVX1000 the second side is oriented east with a length of 20 m, on this will by placed five wind turbines. In total 15 wind turbines will be installed with a nominal power of 15 kW.

The main features of this type of wind turbine are shown in Table 3.

Table 3 The main features of a wind turbine AVX1000

Characteristic	value
Rated	1 kW
Generator starting speed	2.2 m/s
Rated speed	6.5 m/s
Maximum wind speed	60 m/s
Protection for wind speed	Automatic
Rotor diameter	1.83 m
Blade number	5
Suport height	1.6 m
Turbine weight	60 kg

5. WIND SYSTEM DESIGN

Choosing an appropriate model wind turbine is very important. For a typical wind turbine characteristic

output power can be assumed so as to start generating at startup speed v_c generator output and the power increases linearly with the increase of wind speed v_c until rated wind speed v_r. Rated power PR is produced when the wind speed varies from v_r to wind speed at which wind turbines are closed for safety reasons.

The power produced by wind turbines can be simulated as follows:

$$P_w = \begin{cases} P_N \cdot \dfrac{v - v_c}{v_R - v_c} & (v_c \le v \le v_R) \\ P_N & (v_R \le v \le v_F) \\ 0 & (v < v_c \ sau \ v > v_F) \end{cases}$$

For small wind turbines, wind speed startup is relatively smaller, and wind turbines can operate easily even when the wind speed is not very high.

The system must to provide the energy needed for 2 days even if we have no supply of energy from wind turbines, solar panels or from the grid.

Because the building is already equipped with batteries needed they will be used for connecting solar hybrid system / wind. For the system to have a good range it is composed of a number of 48 batteries of type Sunlight SVT1500 - 2V / 1500Ah, the 2x24 configuration and 2x batteries connected in series (2x24) connected in parallel (Figure 4). These batteries are part of a wide reliable for heavy duty applications. Designed to support up to 1,200 cycles for a 100% discharge, but can reach 4500 cycles for a discharge rate of only 30%.

Figure 4 Group batteries

6. CHARACTERISTICS OF PHOTOVOLTAIC SYSTEM

The building is located in a favorable area, in the direction E, S, W is not placed other buildings with a height greater than it, so the photovoltaic modules will not be shaded all day.

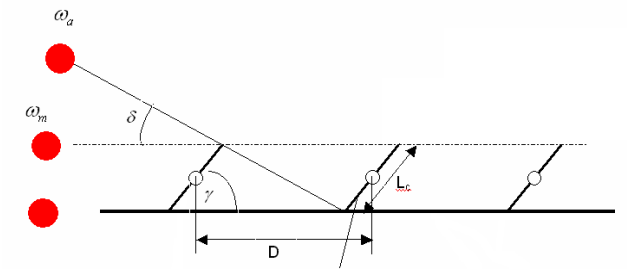

Figure 5 Layout rows of photovoltaic modules

Figure 6 The area available for placement of photovoltaic panels

The relationship used to determine the distance between rows of collectors is:

$$D = \sin(\delta + \gamma)\frac{L_c}{\sin(\delta)}$$

Where:

δ - Declination of the sun

Lc - module height

δ - inclination angle of the modules

Declination depends on the day and month of the year and is calculated with Cooper's formula:

$$\delta = \frac{23.45}{180} \cdot \sin\left(2 \cdot \frac{284 + n}{365}\right)$$

n - The number of days elapsed since the beginning of the year

The inclination angle of PV panels is considered γ = 30 ° for maximum seasonal operation thereof between the months of April to September.

$$D = 3{,}101 \ m$$

The length available for placement of modules is 18.4 m and the number of rows of PV modules will be six.

The number of PV modules mounted on a single row is:

$$N_p = \frac{L - 2 \cdot b}{b} = 30$$

Total number of PV panels to be installed:

$$N_m = N_p \cdot N_s - 2 \cdot 20 = 140$$

Selected PV module is USP 150, with maximum power of 150 W.

Figure 7 Overview of the hybrid wind / photovoltaic system

The maximum power output of PV system will be:

$$P_{PV} = N_p \cdot N_s \cdot P_m \cdot \eta_o \cdot \eta_p$$

$$P_{PV} = 18,952\,kW$$

Total power produced by the hybrid system considering that wind turbines and PV modules operate at nominal power would be:

$$P_T = P_W + P_{PV}$$

$$P_T = 33,952 \quad kW$$

For the period April to September is considered that the PV modules operate at rated power for 6 h / day, and wind turbines operate at a capacity of 0.65 for 8 h / day. Daily total power supplied by the hybrid system in April-September period will be:

$$P_T^V = P_W^V + P_{PV}^V$$

$$P_T^V = P_W^N \cdot \eta_W \cdot \tau_W + N_p \cdot N_s \cdot P_m \cdot \eta_{PV} \cdot \eta_o \cdot \eta_p \cdot \tau_{PV} \left[kWh/day\right]$$

Where:

- η_W - Wind system capacity
- η_{PV} - PV system capacity
- τ_W - FUNCTIONING duration of wind turbines
- τ_{PV} - FUNCTIONING life of the PV system

$$P_T^V = 218,943 \quad kWh/day$$

For the period from October to March is considered as PV modules operate at a capacity of 0.1 for 3 h / day and wind turbines operating at rated power for 9 h / day. Daily total power supplied by the hybrid system during October-March will be:

$$P_T^I = P_W^I + P_{PV}^I$$

$$= P_W^N \cdot \eta_W \cdot \tau_W + N_p \cdot N_s \cdot P_m \cdot \eta_{PV} \cdot \eta_o \cdot \eta_p \cdot \tau_{PV} \quad \left[kWh/zi\right]$$

$$P_T^I = P_W^I + P_{PV}^I = 215,685\ kWh/zi$$

Total power from the hybrid system during a year will be:

$$P_T^{an} = 78833,04\ kWh/an$$

7. RENEWABLE ENERGY DEFICIT

Renewable energy deficit Ed, is the difference between the energy needed ER and energy collected from wind and solar sources and delivered EP:

$$E_d = E_R - E_P$$

For the summer energy deficit will be:

$$E_D = 319,7\ kWh/day$$

$$E_d^V = 100,757\,kWh/day$$

For the winter energy deficit will be:

$$E_D = 229,7\ kWh/day$$

$$E_d^V = 14,015\ kWh/day$$

The contribution of renewable energy provided by the hybrid wind / PV system is shown in Figure 8:

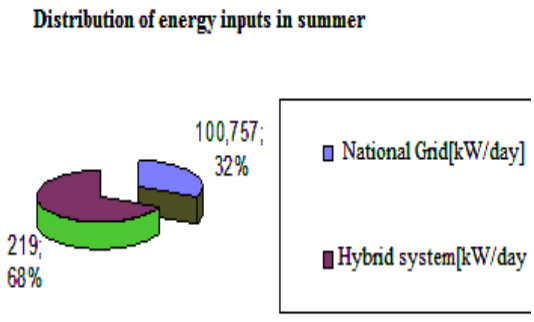

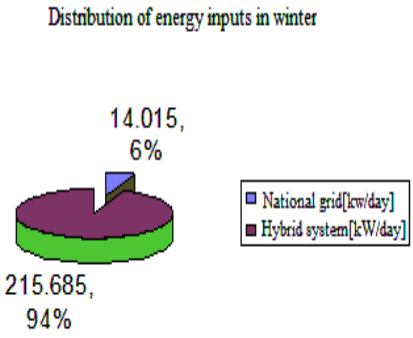

Figure 8 The contribution of renewable energy

8. GREENHOUSE GAS EMISSIONS REDUCTIONS ANALYSIS

The net annual reduction of GHG emissions when using the proposed hybrid wind / photovoltaic system is shown in Table 4:

Table 4 The net annual reduction of GHG emissions

Net emissions of GHG tCO_2	
Monthly net emissions GHG tCO_2	7,194
Net annual emissions GHG tCO_2	86,331
Annual net reduction of GHG emissions	
Reducing GHG emissions tCO2 in summer	29,557
Reducing GHG emissions tCO2 in winter	25,067
Reducing the gross annual GHG emissions tCO2	54,624
Net annual GHG emissions tCO2 by integrating hybrid system	31,706
Gross annual reduction of GHG emissions tCO2 is equivalent to: - 21956,4 Liters of petrol unused - 112,32 Unused oil barrels - 18,36 Tons of waste recycled	

9. FINANCIAL ANALYSIS

For hybrid system wind / PV studied, the annual cost of the system is composed of the annual capital cost Ca, Cr and annual replacement cost of annual maintenance cost Cm. The annual cost of the system can be expressed in terms of four main components: the cost of PV modules, wind turbines, batteries and connecting auxiliary equipment):

$$C_a = \underbrace{\left(C^a_{PV} \cdot PV + C^a_W \cdot W + C^a_{Ac} \cdot Ac + C^a_{Ec} \cdot Ec\right)}_{C_a} +$$

$$+ \underbrace{C^r_{Ac} \cdot (Ac)}_{C_r} + \underbrace{\left(C^m_{PV} \cdot PV + C^m_W \cdot W + C^m_{Ac} \cdot Ac + C^m_{Ec} \cdot Ec\right)}_{C_m}$$

The costs of equipment used in this study, presented below are just estimates, following the final evaluation of the project to be implemented discounts dimension corresponding application.

The lifetime of the project is considered 25 years.

$$C_a = 7597{,}8 \; Euro/an$$

The cost of electricity generated by the hybrid system wind / PV is:

$$C_e = \frac{C_a}{P_T^{an}} = 0{,}09637 \, Euro/kWh$$

4. CONCLUSIONS

The main advantage of wind energy is zero emissions of pollutants and greenhouse gases, because it does not burn fuel.

Other advantages are that wind is a "fuel" free, inexhaustible, abundant and independent of political sensitivities. The turbines are installed quickly and easily and reliable with an availability of 98%. However, the use of wind turbines has a number of disadvantages.

Initially, an important disadvantage of wind energy production was rather high price of energy production and relatively low reliability of the turbines. In recent years, however, the production cost per unit of electricity fell sharply, reaching the figures of the order 3-4 cents per kilowatt hour, improving the technical parameters of the turbine.

A practical disadvantage is the variation in wind speed. Many places on Earth cannot produce enough electricity using wind power, wind energy and therefore not viable in any location.

By installing turbines on the parapet of the building, the manufacturer claims that the turbines will have wind speeds 15% higher, which results in 50% more energy compared to capture wind turbines mounted on the tower.

5. REFERENCES

[1] MIRON V., PARASCHIV L. S., PARASCHIV S., "*Transfer de căldură*", Editura Fundației Universitare "Dunărea de Jos" din Galați, 2006, ISBN (10) 973-627-284-2.

[2] MOCANU C. B., PANAIT T., PARASCHIV S., TASMA D., *"Energy analysis by numerical simulation from a family home"*, Constanta Maritime University Annals, 2012, an 13, vol. 17, 115 – 120

[3] MOCANU C. B., PARASCHIV S., PANAIT T., JORGE MARTINS, TASMA D., *"Evaluation of solar fraction for a passive solar system"*, Constanta Maritime University Annals, 2012, an 13, vol. 17,
121 - 124
[4] PARASCHIV S., ION V. ION, PARASCHIV L. S., *"Thermodynamic performance for the solar collector of a micro-combined cooling, heating and power system"*, Environmental Engineering and Management Journal - EEJM, September 2011, Vol.10, No. 9, pp. 1311-1317
[5] PARASCHIV L. S., PARASCHIV S., ION V. ION, *"Experimental and theoretical analyses on thermal performance of a solar air collector"*, *Environmental* Engineering and Management Journal, August 2014, Vol.13, No. 8, pp. 1965 – 1970
[6] PARASCHIV S., PARASCHIV S.., ION V. ION, *"A mathematical model for the estimation of daily sunshine duration*", 2007, MOCM14-VOL.1, ISSN 1224-7480, pp.189-192
[7] PARASCHIV S., MOCANU C. B., PARASCHIV S., *"Domestic solar water heating potential in the south eastern region of Romania"*, Constanta Maritime [8] University Annals, 2012, an 13, vol. 18, 139-142
PARASCHIV S., MOCANU C. B., PARASCHIV S., *"Analysis of residential photovoltaic energy systems"*, Constanta Maritime University Annals, 2012, an 13, vol. 18, 143 – 147

SAVING ENERGY IN BUILDINGS THROUGH THERMAL INSULATION

PARASCHIV SPIRU

"Dunarea de Jos" University of Galati, Romania

ABSTRACT

This paper analyzes the impact of thermal insulation on heat demand of a house in the SE of Romania. Can be noticed that by insulating the exterior walls of the building can reduce heat flux transmitted through them about 5 times and therefore the total losses by exterior walls about 25-40% depending on the glazing surface of the building and the materials of walls are made.

Keywords: *energy efficiency solutions, thermal insulation, building insulation*

1. INTRODUCTION

Energy efficiency reduces energy consumption and eliminates energy waste. Energy saving is the most effective and simplest way to reduce the consumption of primary resources and reduce emissions of greenhouse gases. Consequences of emissions reduction by decreasing energy consumption are: increasing air quality, health and life.

European Commission recommends new targets to climate and energy policies: 40% reduction in greenhouse gas emissions by 2030 compared to 1990.

EU could save by 2020, 20% of current consumption, which means 20 billion per year.

In accordance with Directive 31/2010 / EU on the energy performance of buildings, they are responsible to 40% of total energy consumption in the European Union.

Therefore, reducing energy consumption and use of renewable energy in the buildings sector constitute important measures needed to reduce the Union's energy dependency and greenhouse gas emissions.

2. THE CLIMATE IN GALATI COUNTY

The energy consumption of a building depends on external and internal factors. External factors are climatic features of the site parameters: air temperature, wind speed, sunshine, humidity. Designing buildings and afferent installations is based on statistical average values of climatic parameters for a specific period of the year (day, month, heating season) values obtained from observation durations for decades. These values are standardized conventional air temperature and wind speed to sunlight, humidity and air temperature, etc.).

In this sense for a home located in Galați, the climate is temperate-continental, with an average annual temperature of 10˚C, with a range between 0 ° C in winter and -28˚C, and in summer between 15C and 35˚C. Due to its location in the city of Galați winds are quite common from the N-NE and S-SE

3. THE STRUCTURE AND LOCATION OF THE BUILDING

The building is located in the city of Galati, is located at ground level and has two bedrooms, a bathroom, a living room, a kitchen and a lounge. The house was built for the needs of a family of four, with the area of 64.42 m^2.

Effective areas of the building on each camera are presented in Table 1.

Table 1 Surface house

	Area [m^2]	Height [m]
Hall	12,5	2,6
Bathroom	4,2	
Kitchen	7,92	
Bedroom 1	9,91	
Bedroom 2	11,9	
Living room	17,99	
Total area	64,42 [m^2]	

Galati is located in the eastern part of Romania, southern extremity of the Moldova plateau at 45˚27 'north latitude, respectively 28˚02' east longitude. Located on the left bank of the Danube, covers an area of 241.5 km2, at the confluence of Siret (west) and Prut (east).

4. INCREASING THE ENERGY EFFICIENCY OF HOUSING BY THERMAL INSULATION

The sealing elements of the buildings are roof and exterior walls. They are made from opaque glazing elements. Glass elements that provide natural lighting assure much lower thermal protection than the opaque, so their share in the entire closure assembly is limited to what is necessary to ensure natural lighting.

To ensure an efficient thermal protection are used insulating materials. The thickness of the insulating material directly influences thermal protection. Increasing the thickness reduce heat loss and thus reduce the heating power required and therefore fuel

consumption. At the same time, increasing the thermal insulation leads to increased cost. Embodied energy is the energy consumed as fuel or electricity to produce materials used in that construction, from raw material to its finished form, and for transportation.

Also enhancing thermal protection construction is necessary for reducing harmful emissions, in particular carbon dioxide, which emphasizes the global greenhouse effect and increase comforts.

According to the norm [20], the thermal insulation of buildings aims:

• ensure proper thermal environments in enclosed spaces;

• eliminating the risk of condensation on the inner surface of building elements;

• avoid the accumulation of water in the structure of the building elements as a result of condensation of water vapor in their structure;

• reducing energy consumption in operation.

There are a number of building blocks which must be provided with a certain amount of insulation. These are:

• elements that separates the external environment of the indoor environment, with different temperatures;

• the internal bounding partitioning for closed space with operating temperatures that differ by more than 5 ° C.

5. THERMAL INSULATION OF PLANE WALL

Heterogeneous plane wall flanked by two known temperature fluids:

Consider a plane wall consists of "5" layers perpendicular to the direction of heat flow bounded two known temperature fluids, tf1, and $t_{f2} \cdot \left(t_{f1} > t_{f2}\right)$.

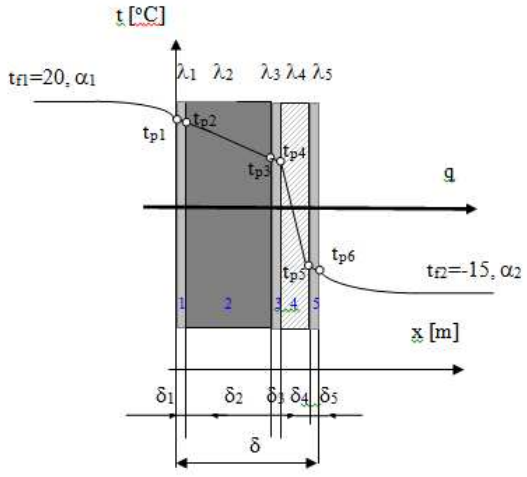

Figure 1 Insulated wall

Initial data for calculation are:

hot air temperature	$t_{f1} = 20°C$
convection coefficient	$\alpha_1 = 9\ W/m^2K$
cold air temperature	$t_{f2} = -15°C$
convection coefficient	$\alpha_2 = 28\ W/m^2K$
Layer "1" - internal plaster:	$\delta_1 = 20\ mm$
	$\lambda_1 = 0,988\ W/mK$
Layer "2" - concrete plate:	$\delta_2 = 250\ mm$
	$\lambda_2 = 1,51\ W/mK$
Layer "3" - plaster support:	$\delta_3 = 10\ mm$
	$\lambda_3 = 0,988\ W/mK$
Layer "4" - thermal insulation:	$\delta_4 = 50\ mm$
	$\lambda_4 = 0,04\ W/mK$
Layer "5" - plaster exterior:	$\delta_5 = 20\ mm$
	$\lambda_5 = 0,988\ W/mK$

The complex process of heat transfer can be broken down into simple processes:

$$q_1 = \alpha_1 \cdot \left(t_{f1} - t_{p1}\right) \quad (1)$$

$$q_2 = \frac{t_{p1} - t_{p2}}{\frac{\delta_1}{\lambda_1}} \quad (2)$$

$$q_3 = \frac{t_{p2} - t_{p3}}{\frac{\delta_2}{\lambda_2}} \quad (3)$$

$$q_4 = \frac{t_{p3} - t_{p4}}{\frac{\delta_3}{\lambda_3}} \quad (4)$$

$$q_5 = \frac{t_{p4} - t_{p5}}{\frac{\delta_4}{\lambda_4}} \quad (5)$$

$$q_6 = \frac{t_{p5} - t_{p6}}{\frac{\delta_5}{\lambda_5}} \quad (6)$$

$$q_7 = \alpha_2 \cdot \left(t_{p6} - t_{f2}\right) \quad (7)$$

Considering the condition of unidirectional heat flow:

$$q_1 = q_2 = q_3 = ... = q_n$$

It is obtained:

$$q = \frac{t_{f1} - t_{f2}}{\frac{1}{\alpha_1} + \sum \frac{\delta_i}{\lambda_i} + \frac{1}{\alpha_2}} = \frac{t_{f1} - t_{f2}}{R_{s1} + \sum R_{ti} + R_{s2}} = \\ = k \cdot \left(t_{f1} - t_{f2}\right)\left[W / m^2\right] \quad (8)$$

Unde:
k - - total heat transfer coefficient

$$k = \frac{1}{\frac{1}{\alpha_1} + \sum_1^5 \frac{\delta_i}{\lambda_i} + \frac{1}{\alpha_2}} = \frac{1}{R_{s1} + \sum_1^5 R_{ti} + R_{s2}} \left[W / m^2 K\right] \quad (9)$$

Temperatures on the lateral and contact surfaces of the wall:

$$t_{pi} = t_{f1} - q \cdot \left(\frac{1}{\alpha_1} + \sum_1^{n-1} \frac{\delta_i}{\lambda_i}\right)[°C] \quad (10)$$

$$R_{s1} = \frac{1}{\alpha_1}, \quad R_{t1} = \frac{\delta_1}{\lambda_1}, \quad R_{t2} = \frac{\delta_2}{\lambda_2}, \quad R_{t3} = \frac{\delta_3}{\lambda_3},$$

$$R_{t4} = \frac{\delta_4}{\lambda_4}, \quad R_{t5} = \frac{\delta_5}{\lambda_5}, \quad R_{s2} = \frac{1}{\alpha_2}$$

$$q = \frac{t_{f1} - t_{f2}}{R_{s1} + \sum R_{ti} + R_{s2}} \quad (11)$$

Temperature on the lateral and contact surfaces of the wall when insulation is mounted is calculated as:

$$t_{p_1} = t_{f_1} - q \cdot R_{s_1} \ [°C] \quad (12)$$

$$t_{p_2} = t_{f_1} - q \cdot (R_{s_1} + R_{t_1}) \ [°C] \quad (13)$$

$$t_{p_3} = t_{f_1} - q \cdot (R_{s_1} + R_{t_1} + R_{t_2}) \ [°C] \quad (14)$$

$$t_{p_4} = t_{f_1} - q \cdot (R_{s_1} + R_{t_1} + R_{t_2} + R_{t_3}) \ [°C] \quad (15)$$

$$t_{p_5} = t_{f_1} - q \cdot (R_{s_1} + R_{t_1} + R_{t_2} + R_{t_3} + R_{t_4}) \ [°C]$$

$$t_{p_6} = t_{f_2} + q \cdot R_{s_2} \ [°C] \quad (17)$$

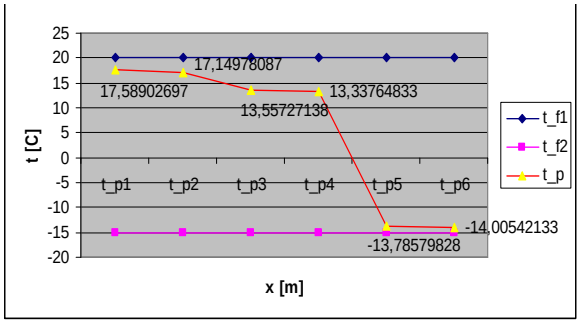

Figure 2 Variation of temperatures on lateral and contact surfaces of the wall when insulation is placed on exterior

Determination of temperature on lateral and contact surfaces of the wall in the case of un-insulated wall

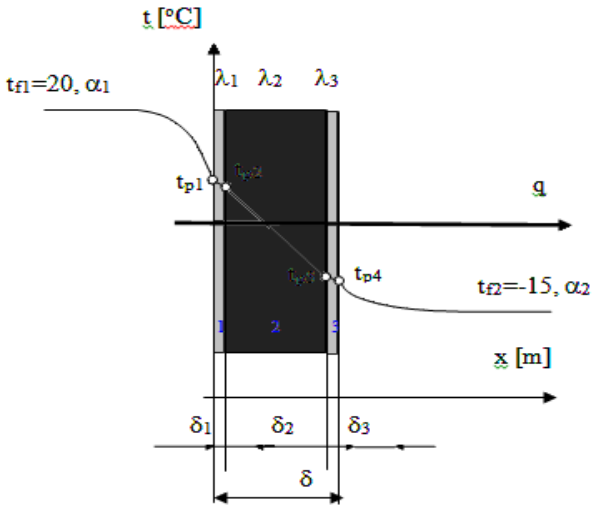

Figure 3 Un-insulated wall

Initial data for calculation are:
- The hot air temperature tf1 = 20°C and convection coefficient α_1 = 9 W/m^{2}K;
- Cold air temperature t_{f2} = -15°C and convection coefficient α_2 = 28 W/m^{2}K;
- Layer "1" - plaster interior: δ_1 = 20 mm and λ_1 = 0.988 W / mK;
- Layer "2" - concrete plate: δ_2 = 250 mm and λ_2 = 1.51 W / mK;
- Layer "3" - plaster support: δ_3 = 10 mm and λ_3 = 0.988 W / mK.

Temperature on the lateral and contact surfaces of the un-insulated are:

$$t_{p_1} = t_{f_1} - q \cdot R_{s_1} \ [°C] \quad (18)$$

$$t_{p_2} = t_{f_1} - q \cdot (R_{s_1} + R_{t_1}) \ [°C] \quad (19)$$

$$t_{p_3} = t_{f_1} - q \cdot (R_{s_1} + R_{t_1} + R_{t_2}) \ [°C] \quad (20)$$

$$t_{p_4} = t_{f_2} + q \cdot R_{s_2} \ [°C] \quad (21)$$

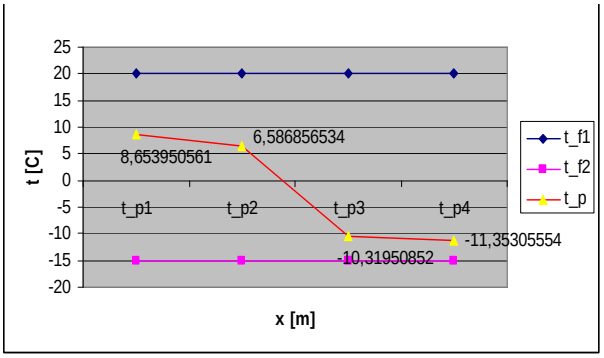

Figure 4 Variation of temperatures on lateral and contact surfaces of the wall un-insulated

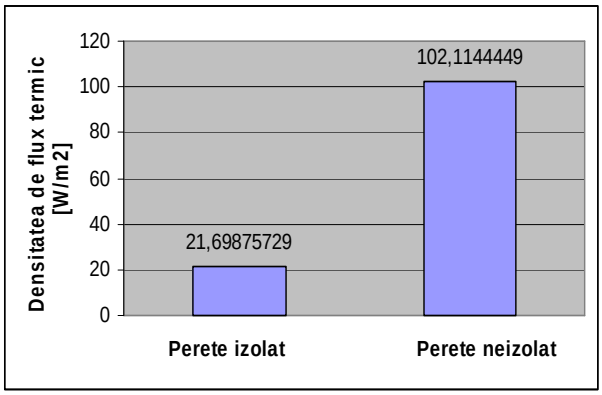

Figure 5 Variation of heat flux density for the isolated and un-insulated wall

After analysis, it can be seen that insulating the external walls of the building will improve thermal efficiency by reducing heat flux density and reducing thus the amount of heat lost.

6. CONCLUSIONS

A properly installed insulation reduces heating and cooling costs by reducing heat loss and gain through the building envelope.

Isolation of the house is the most effective way to reduce energy bills and make your home a living space warmer and more comfortable. You can save about 25% on heating bills and at the same time will increase the price if you decide to sell or to rent the house by receiving an energy performance certificate (EPC).

Insulation protects your home against cold in the winter and excess heat in summer, and may even reduce noise pollution. Most isolation techniques are cheaper and their cost is recovered in less than five years.

5. REFERENCES

[1] HARRESTRUP M. , SVENDSEN S., *Full-scale test of an old heritage multi-storey building undergoing energy retrofitting with focus on internal insulation and moisture*, Building and Environment, Volume 85, February 2015, Pages 123–133

[2] NUNO P., MANUEL D. P., JOSÉ D. S., JORGE B., *Comparative environmental life cycle assessment of thermal insulation materials of buildings*, Energy and Buildings, Volume 82, October 2014, Pages 466–481

[3] UNIBEN Y., AYIKOE T., AMBROSE D., LEIF G., *Effects of different insulation materials on primary energy and CO2 emission of a multi-storey residential building*, Energy and Buildings, Volume 82, October 2014, Pages 369–377

[4] ZHAOSONG F., NAN L., GUOZHI L., YANQI H., *The effect of building envelope insulation on cooling energy consumption in summer*, Energy and Buildings, Volume 77, July 2014, Pages 197–205

[5] MIRON V., PARASCHIV L. S., PARASCHIV S., "*Transfer de căldură*", Editura Fundației Universitare "Dunărea de Jos" din Galați, 2006, ISBN (10) 973-627-284-2.

[6] MOCANU C. B., PANAIT T., PARASCHIV S., TASMA D., "*Energy analysis by numerical simulation from a family home*", Constanta Maritime University Annals, 2012, an 13, vol. 17, 115 – 120

[7] MOCANU C. B., PARASCHIV S., PANAIT T., JORGE MARTINS, TASMA D., "*Evaluation of solar fraction for a passive solar system*", Constanta Maritime University Annals, 2012, an 13, vol. 17, 121 - 124

[8] PARASCHIV S., ION V. ION, PARASCHIV L. S., "*Thermodynamic performance for the solar collector of a micro-combined cooling, heating and power system*", Environmental Engineering and Management Journal - EEJM, September 2011, Vol.10, No. 9, pp. 1311-1317

[9] PARASCHIV L. S., PARASCHIV S., ION V. ION, "*Experimental and theoretical analyses on thermal performance of a solar air collector*", *Environmental* Engineering and Management Journal, August 2014, Vol.13, No. 8, pp. 1965 – 1970

STRESS AND STRAIN ANALYSIS OF HEAVE PLATES

[1]SCURTU IONUT-CRISTIAN, [2]ONCICA VALENTIN [3]GARCÍA DÍAZ IGNACIO, [4]BABIUC BOGDAN

[1]Constanta Maritime University, [2,4]"Mircea cel Batran" Naval Academy, Romania, [3]Technical University Of Cartagena, Spain

ABSTRACT

This paper presents the analysis of WindFloat's heave plate using the finite elements method. It will be draw a cylinder with a hexagonal heave plate at one end using sizing technology of the WindFloat. Heave plates are realised according to the technical prospects of the designer. The stress and deformation analysis will use the finite element analysis software Solidworks for different heave plate configuration.

With Solidworks, the analysis program, will show the behaviour of the heave plate submerge in the water during heave motion. A comparative study between different configurations is presented.

Keywords: *finite element method, Solidworks, heave plate, WindFloat.*

1. INTRODUCTION

A floating wind turbine, like WindFloat, is an offshore wind turbine added to a tri-column semisubmersible in order to unlock high wind energy potential in water depths more than 60 m.

WindFloats are semisubmersibles structures designed to support turbine weight and environmental loadings according to sea characteristics. This type of structure is designed and patented by *Principle Power*. These structures are developed to float in the sea far away of the coast (offshore) because the winds in these areas are more consistent and stronger due to the absence of topographic features that disrupt wind flow. For this reason it must be most stable as is possible including stability elements to improve the dynamic stability as heave plates.

WindFloats consist in a tri-column triangular semisubmersible platform with the wind turbine positioned on one of the three columns or in the middle of the triangle depending on design. The triangular platform is then "moored" using asymmetric mooring [5] system consisting of four lines, two of which are connected to the column supporting the turbine, figure 1.

To get the hull-trim the structure used a ballast system, this system shift water between each of the three columns. This permit to the platform maintain even keel while producing the maximum amount of energy. Also, the floating structure must provide enough buoyancy to support the weight of the turbine and to restrain pitch, roll and heave motion within acceptable limits [6].

Figure 1 presents the main elements of a complete floating wind turbine, whit the wind float equipped with heave plates and the mooring system and the turbine positioned on one of the three columns [1].

2. PROBLEM DESCRIPTION

It is necessary to attain movements in a restricted limits with the intention of generate the maximum amount of energy. This is achieve by increasing the damping factor, so in order to create a huge damping factor for these movements, they are equipped with hexagonal heaves plates that use a principle called "added mass", it creates a resistant area to the movements of water at the bottom of the structure.

Damping force is generated by the vortex shedding at the thin edges of the heave plate, and there is a close relationship between the heave plate thickness and the damping force.

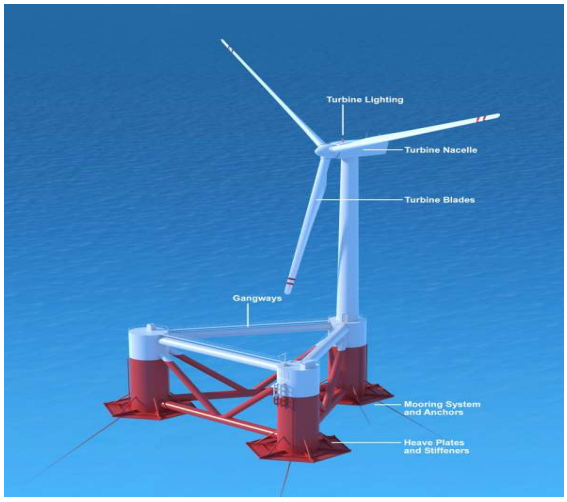

Fig. 1 Floating wind turbine [2]

The research on the optimization of hydrodynamic performance for heave plates is scarce. The shapes and geometry are very important; **L.Tao and Thiagarajan (2003)** investigated the hydrodynamics of a vertical heaving cylinder with a single disk attached to the kell. The effects of the geometry of the dick, such as aspect ratio (thickness / Diameter heave plate) and diameter ratio (Diameter heave plate/ Diameter column), the recommendation os a spar hull and disk geometry was made to achieve optimum heave response [2].

SHEN Wen-jun (2011) studied the optimize shape of a heave plate [3] and **L. Tao (2007)** studied the spacing between the heave plates to lead the maximum damping and added mass [4], but this project is about the analysis of stress and strain of a heave plate with different configuration of stiffener. In each case is added

stiffener in order to see the displacements and the von Misses stress distribution due to the movement of the structure in the heave, this movement creates a hydrodynamic pressure at the top of the heave plate, that must be consider because these can be important loads. Also seeing it as a cyclic load, the fatigue aspect must be considered.

The structure is made from naval steel, also the heave plates are made in the same material. The main particulars of the WindFloat floater are present below.

Table 1 Particulars of WindFloat Floater

	Unit	Value
Column diameter	m	10
Length of heave plate edge	m	15
Draft	m	17
Thickness of heave plate	m	0.1

3. PROBLEM SOLUTION. ANALYSIS OF THE DISPLACEMENT AND STRAIN OF THE WINDFLOAT'S HEAVE PLATE

For the case study we analysed using the finite element method, with the software SolidWorks, the heave plate of a single column, the diameter of the column is 10 [m], the diameter of the circumscribed circle of the heave plate is 35 [m] and a thickness of 0.1 [m] as is presented in table 1. In this paper we will analyse the displacements and the von Mises Stress creates because of the influence of a pressure on top of the heave plate with a value of 50000 [N/m^2] due to the hydrodynamics pressures. The material used is naval steel with the characteristics presented in table 2.

Table 2 Material characteristics

Elastic modulus	2.10E+11	N/m^2
Poisson's ratio	0.28	NA
Shear modulus	2.35E+10	N/m^2
Mass density	7700	kg/m^3
Thermal expansion coefficient	1.30E-05	/Kelvin

To study heave plates with finite element analysis it was performed a statically analysis that was going through following steps:

1. 3D modelling as specified dimensional geometry.
2. Establish the boundaries conditions as a fixture surface, in this case will be the surface of the column.
3. Addition of the acting pressure on the top surface of the heave plate and the value calculated by the formula of dynamic pressure:

$$P = \rho \cdot \frac{V^2}{2}$$

4. Selection of material defined previously.
5. Run the calculated program, it will do a meshing automatically and then solve the equations using the finite element method.
6. Access the results of the analysis, confirming that the displacements of the structure are correct.
7. Plot the results as images and data files.

3.1. Analysis of the hexagonal heave plate 1st stiffener configuration

This configuration consists in only the plate, without any stiffener as is shown in Figure 2.

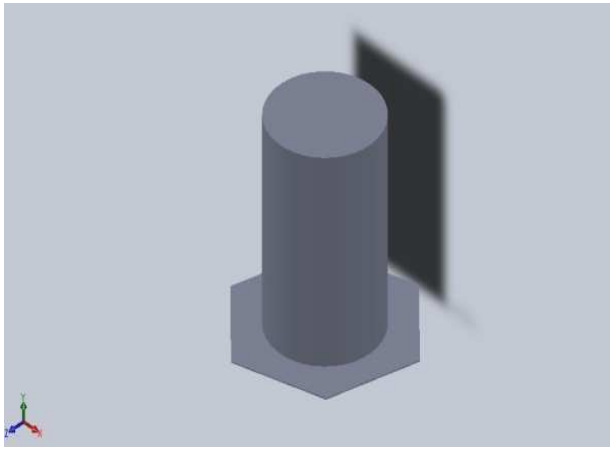

Fig. 2 Heave plate - 1st Configuration

With the purpose of achieve the analysis for the heave plate with this configuration, it was applied the load as is shown in Figure 3 with the deformed shape, it consists in one constrain at the column's exterior surface. The pressure is applying on the top surface of the heave plate as a hydrodynamic pressure generated by the movement of the column with a considered heave motion with velocity of 10 [m/s], the structure is floating in fresh water (1000kg/m^3), so the hydrodynamic pressure is:

$$P = \rho \cdot \frac{V^2}{2} = 1000 \cdot \frac{10^2}{2} = 50000\ N/m^2$$

The determined pressure pressure produce a deformed shape as is shown in Figure 3:

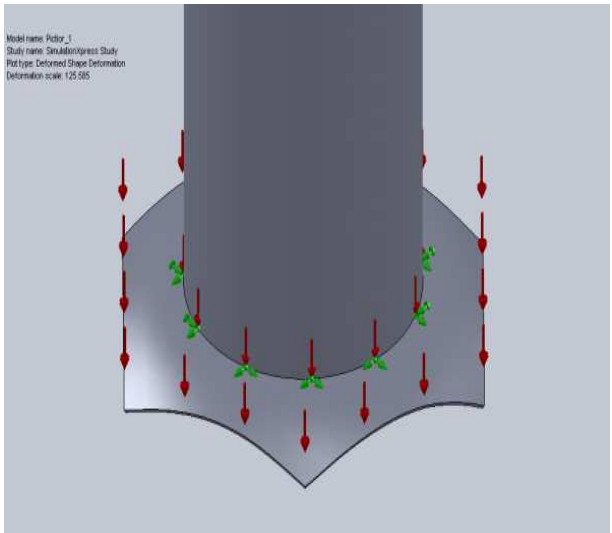

Fig. 3 Deformed shape - 1st Configuration

In this case the maximum deformation the value of **0.01362 [m]** and these occur at the outer corners as is shown in Figure 4.

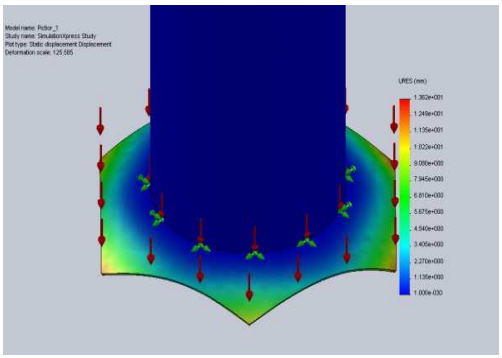

Fig.4 Maximum deformation – 1st configuration

The igure 5 present the von Mises stress distribution for the heave plate, in this case the greater stress is **3.69558e7 [N/m^2]** and it location is in the edge of union between the column and the heave plate.

Table 1 - 1st Configuration - Maximum values

	Location	**Value**
Displacement [m]	Corners	0.01362
Von Mises stress [N/m^2]	Edge of union	3.6956E+07

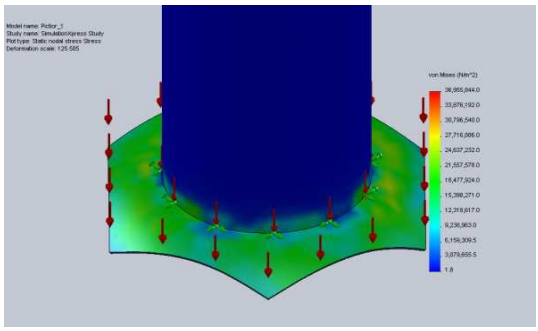

Fig. 5 Von Mises stress distribution – 1st configuration

3.2. Analysis of the hexagonal heave plate 2nd stiffener configuration

This configuration consists in a grating of stiffener as is shown in Figure 6.

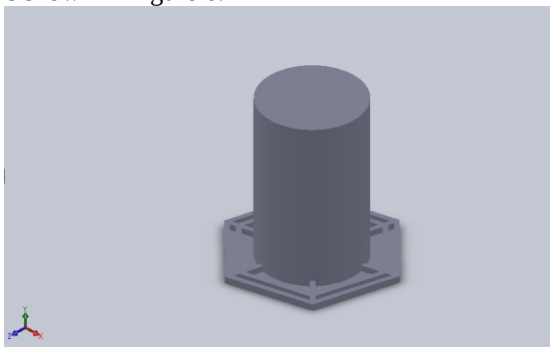

Fig. 6 Heave plate – 2nd Configuration

To analyse this second configuration, it shall apply the same charging scheme as in the other case the deformation shape after this is shown in figure 7.

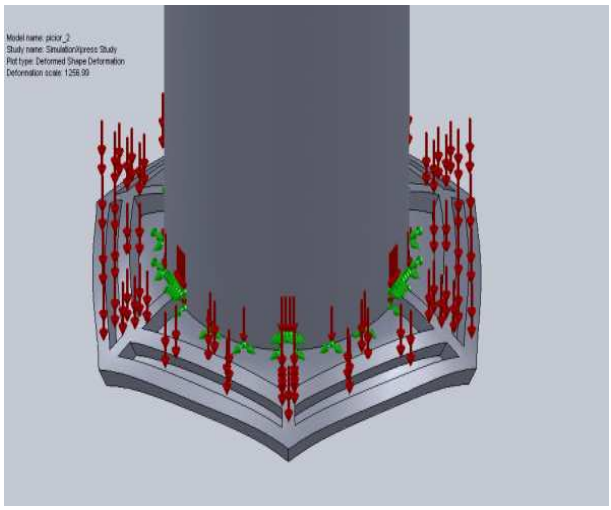

Fig.7 Deformed shape – 2nd configuration

In this case the maximum deformation the value of **0.001371 [m]** and these occur at the outer corners as in the first configuration, but its value is **ten times less**, this is shown in Figure 8.

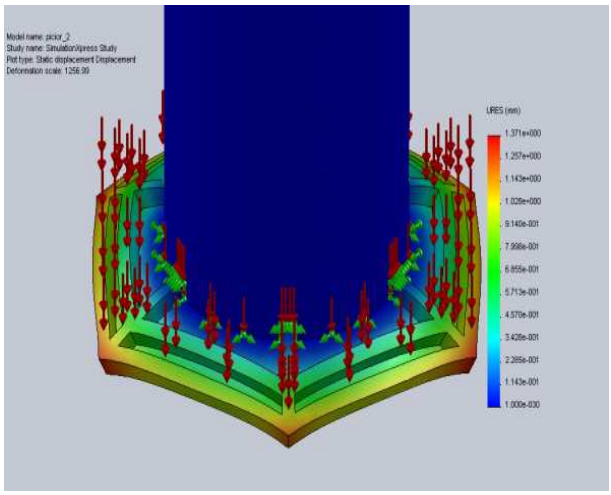

Fig. 8 Maximum deformation – 2nd configuration

Following the analysis of the second configuration we observed that the Von Mises Stress distribution is in the union of the column with the stiffeners. The value of the maximum stress is **3.5409e7 [N/m^2]**, so close to the first configuration value. The results are plotted in figure 8.

Table 2 - 2nd Configuration - Maximum values

	Location	**Value**
Displacement [m]	Corners	0.00137
Von Mises stress [N/m^2]	Edge of union	3.54090E+07

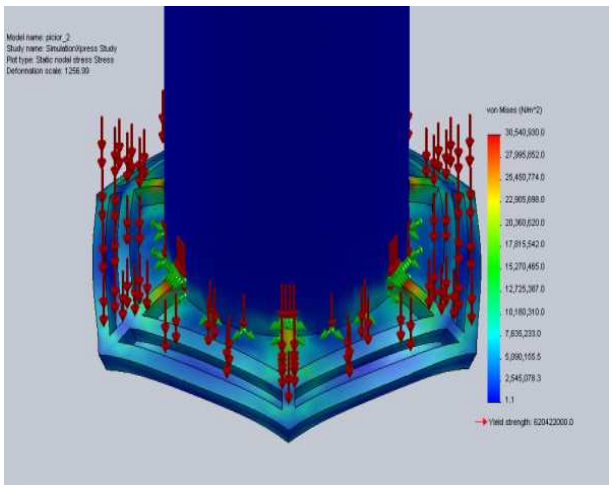

Fig. 8 Von Mises stress distribution – 2nd configuration

3.3. Analysis of the hexagonal heave plate 3rd stiffener configuration

In this configuration is added a bar between the corners and the column as is shown in Figure 9.

Fig. 9 Heave plate – 3rd Configuration

Applying the same hydrodynamics loads as in the other cases, the deformation with this configuration has many changes as is shown in Figure 10.

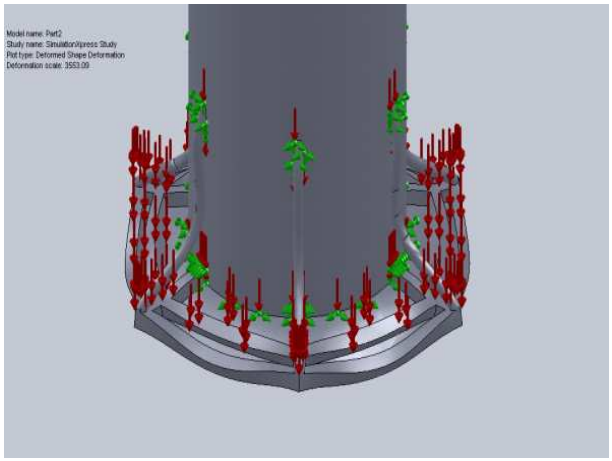

Fig.10 Heave plate – 3rd Configuration

It can appreciate that the corners stays approximately in the same position, while the bars and the middle of the segment are the points where the maximum displacement happen. The values of these displacements are the smaller, the corners have a displacement of 0.0002 [m] and the middle of the segment 0.0004 [m] and the maximum displacement value occurs in the middle of the bars and it is 0.00056 [m].

Table 3 - 3rd Configuration - Maximum values

	Location	**Value**
Displacement [m]	Corners	0.00056
Von Mises stress [N/m^2]	Top of bars	1.5885E+07

In the analysis of the third configuration we observed that the Von Mises Stress distribution is in the union of the column with the bars and the value of the maximum stress is **1.58854e7 [N/m^2]**, also there is a high stress on the bottom of the bars, at the union with the heave plate as it shown at Figure 12.

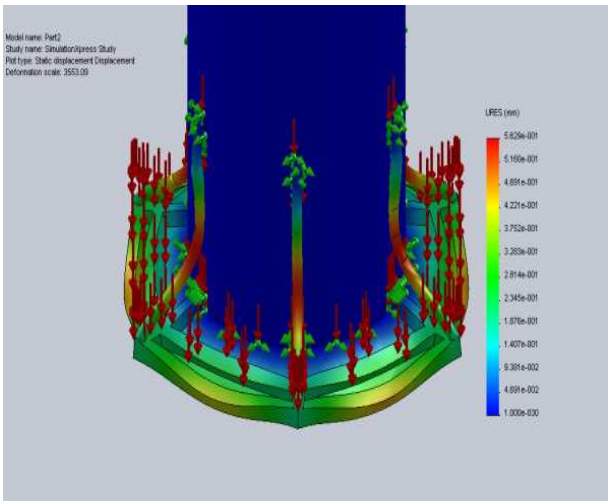

Fig. 11 Maximum deformation – 3rd configuration

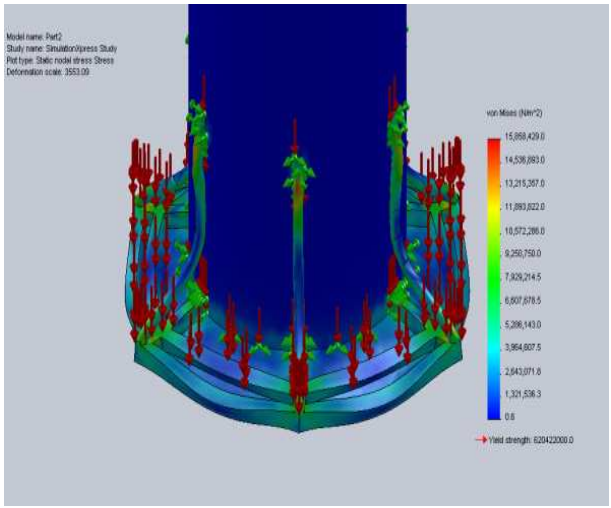

Fig. 12 Von Mises stress distribution – 3rd Configuration

4. CONCLUSIONS

The analysis performed on the three different configurations had the result that the last configuration performs better the strains creating less deformation and stresses on the heave than the other two configurations.

In every case the structure is subjected on the considered hydrodynamic pressure of 50000 [N/m^2] and all data presented for each case can be used in further fatigue analysis because in offshore environment loads direction alternates. Considering stresses values, the last configurations must resist better than the other two. The point of stress concentration on the two firsts configuration is on the union between the column and heave plate. For the third configuration it has less points of stress concentration and the lines of stress can flow through the bars, and this is the reason because the third configuration is secure than the other two.

Using the finite element method to determinate the sustainability is a fast and highly efficient, thus with is producing a significant reduction of effort and design, material, and is reinforced by the research presented here.

5. REFERENCES

[1] Dominique Roddier, Christian Cermelli, Alexia Aubault and Alla Weinstein. *WindFloat: A floating foundation for offshore wind turbines.* Principle Power, Inc., Seattle, Washington, USA. June 2010.

[2] Rui Zhang. *Comparative study on dynamic responses of a semi-submergible wind turbine using a simplified aerodynamic model and a BEM model.* Norwegian University of Science and Technology. Sping 2013

[3] Anghelache Diana, Cristea Simona-Andra, Iacob Nicolae. *Stress and Strain analysis of a tower crane arm.* University "Dunarea de Jos Galati". Engineering Faculty of Braila, 2014.

[4] Tao, L., Thiagarajan, K.., *Low KC flow regimes of oscilating sharp edges, I: vortex shedding observation.* Applied Ocean Research 25. 2003

[5] SHEN Wen-jun, TANG You-gang and LIU Li-qin. *Research on the Hydrodynamic Characteristics of Heave Plate Structure with Different Form Edges of A Spar Platform.* Tianjin University, China, 2011.

[6] L. Tao, B Molin, Y.M. Scolan, K. Thiagarajan. *Spacing effects on hydrodynamics of heave plates on offshore structures.* Griffith university, Australia, Engineering School of Marseille, France, School of oil and Gas Engineering, Australia. June 2007.

STUDY OF OFFSHORE STRUCTURE DESIGN RELATED TO ANSYS STRESS, DISPLACEMENT AND VIBRATION MODES

[1]SCURTU IONUT-CRISTIAN, [2] PRICOP MIHAIL, [3]BABIUC BOGDAN

[1]*Constanta Maritime University,* [2,3]*"Mircea cel Batran" Naval Academy, Romania*

ABSTRACT

In this paper it is shown a comparison between five Windfloat's constructive configuration types using the same basic structure provided by the designer. The entire structure was realized in Solid works software using the execution drawings from the designer, and the static structural analysis was made using Mechanical Ansys Parametric Design Language Solver from Ansys software.

The main scope was to obtain numerical results which allowed us to show the influence of the dynamic pressure over each construction configuration type.

Keywords: *windfloat, configuration, stress and displacement, vibration modes.*

1. INTRODUCTION

The offshore structure industry has been growing at a fast rate since its inception half century ago. In water depths where bottom-mounted towers are not feasible to capture the wind energy above the sea, the perfect solution is a floating structure that allows the turbine to be mounted on and to generate electricity using that kind of energy.

This structures are semi-submersible which can support a wind turbine, and are designed to float far away from mainland where the wind is stronger and more abundant in the absence of landforms. In the offshore areas, the marine and ocean currents are very powerful and the waves are taller than those of the shore. Those two factors have a major impact on structure dynamic stability.

The structure has a triangular shape with three columns with a ballast system inside them. The wind turbine is positioned on one of those columns which are kept together by four horizontal pipes. In the space between two columns and the pipes which held them, the structure present some reinforcement elements of different construction configurations. The semi-submersible structure described above has enough buoyancy to support the wind turbine, and to keep the motion of roll, pitch, and heave within acceptable limits[1].

In the Figure 1 is an operating floating structure with a wind turbine mounted on one of its column.

Figure 1 Floating wind turbine

2. PROBLEM DESCRIPTION

Offshore structures are built to withstand the environmental forces during operation in waters depths more than 40 meters. In the same time a structure like WindFloat will be subjected to operational forces and vibrations caused by the wind turbine. The present paper will study the reinforcement elements of different construction configurations.

All existing structure types will be analysed using Ansys software to solve static structural differences and vibration modes. The present analyses is based on values presented in table 1 and table 2, values extracted from Windfloat project[1][2]. All calculations will be done using the magnitude of the horizontal impact force given by Allsop[3] for random waves.

Table 1. Windfloat geometrical configuration

Geometrical specification	Unit	Value
Column diameter	m	10
Draft	m	17
Column center to center	m	46
Thickness of pipes	m	0.1
Operating depth	m	<40

Table 2. Mass distribution for structure

		Unit	Value
Displacement		t	4640
Coordinate of the center of gravity	x_G	m	34.28
	y_G	m	0
	z_G	m	4.70
Radius of giration	R_x	m	34.9
	R_y	m	34.7
	R_z	m	26.5

3. PROBLEM SOLUTION

3.1. Offshore 3D designs in Solidworks

Solidworks software will be used to draw the tri-dimensional designs for the three column semi-submersible structure.

All configuration studied in this paper are: D, K, V, Y and Z, and will be realized as .step model in order to be exported in Ansys software. The entire semi-submersible structure was designed in Solidworks software with each reinforcement configuration as shown in figures 2-6.

Differences in mass and configuration will give a different response to environmental and operational loads. All models will be analysed in Ansys to obtain differences between structures[4][5].

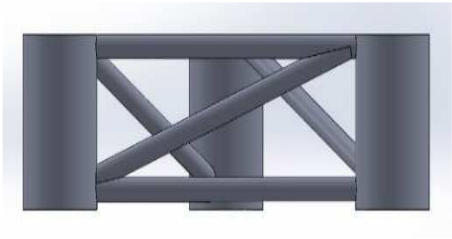

Figure 2 "D" construction configuration

Figure 3 "K" construction configuration

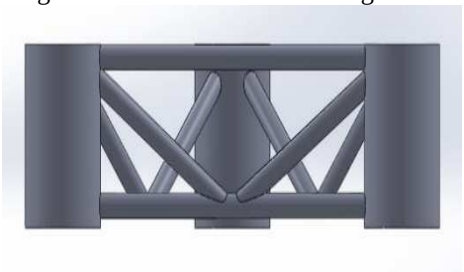

Figure 4 "V" construction configuration

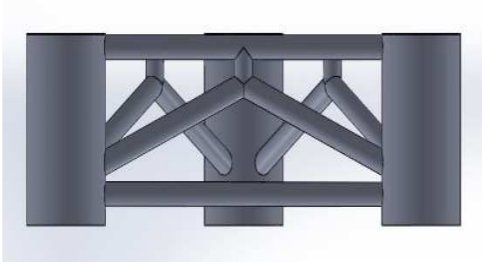

Figure 5 "Y" construction configuration

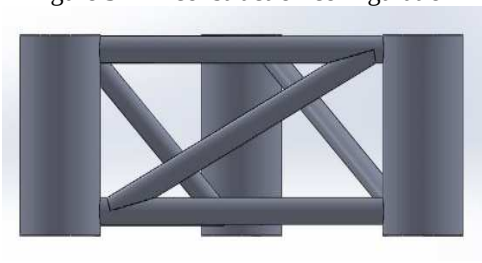

Figure 6 "Z" construction configuration

All geometrical dimensions of the structures presented in Figures 2-6 are according to the actual dimensions of construction of the WindFloat project, presented already in table 1 and table 2. The material used is naval steel with E=200GPa and ρ=7850 kg/m3. All structures are made identically, the only differences are those reinforcements designs which can make the entire structure stronger or weaker[6].

3.2. Calculation of impact forces

A large data of information was investigated by Allsop and ot. in 1996 on different structure geometries to predict horizontal wave forces on vertical breakwaters. The relative wave height Hsi/d has been found to most significantly influence the wave forces nondimensional by the water depth. All forces were given at a 1/250 level thustaking the mean out of the highest two waves (500 waves per test were measured). [3]Themagnitude of the horizontal impact force can then be estimated from:

$$F_{h,1/250} = 15 * \rho_W * g * d^2 * (H_{si}/d)^3$$

This formula has been derived from data sets with a 1:50 foreshore slope and checked againstother slopes where it also seems to fit the data very well. To show the accurate of the presented equation, above is a graphic in figure 7, which represent the relative force plotted vs. relative wave height and comparison to calculation method given by equation [7].

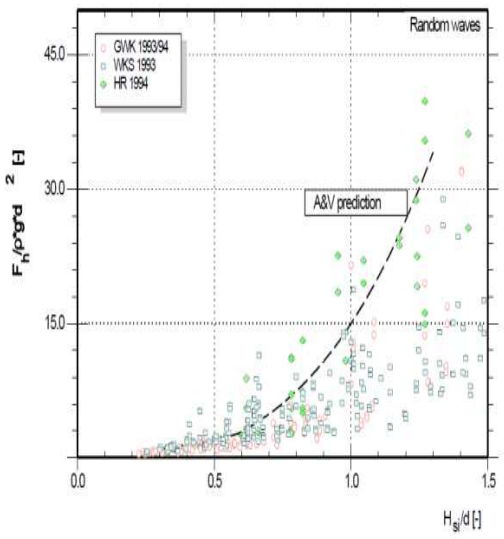

Figure 7 Relative wave force Fh, max/(Dgd2) plotted vs. relative wave height Hsi/d

In Ansys static analysis we will use a estimated force of 30 kN according to presented data of Black Sea environment.

3.3. Software stress and displacement analysis

Ansys static structural module presented in Figure 8 will import each .step file previously created and will generate required stress and displacement values according to presented data. The result are correctly calculated when all seven part point from Ansys static structural module are checked with green, as shown in Figure 8 and the project model is defined as in Figure 8. All results will be extracted from Solution >Total deformation and Solution>Equivalent stress.

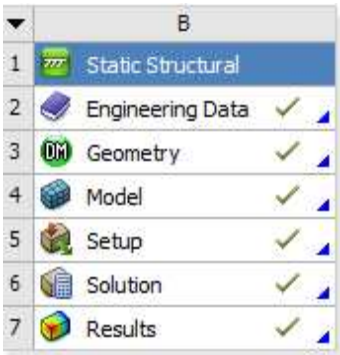

Figure 7 Ansys static structural module

In Ansys static structural module settings, we give the general details of the simulation, choose the fixed support faces, and the last settings are for the pressure (size, direction, etc.). After all the settings are done we can ask the program to give multiple solution based on the settings provided. In Figure 8 are shown all this steps and the solutions that we are interested in: total deformation and equivalent stress (von-Mises)[8].

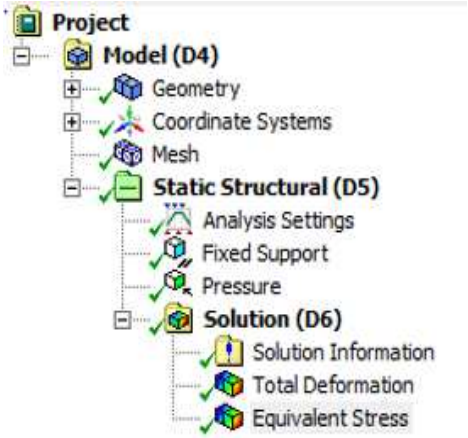

Figure 8 Ansys static structural settings

Results from Ansys static structural analyses are summarized in table 3.

Table 3. Results from Ansys static structural analyses

Designs	Maximum stress [N/mm^2]	Maximum displacement [mm]
Z	2.61e4	0.047833
V	1.58e4	0.064712
K	1.69e4	0.036980
D	2.36e4	0.032587
Y	3.37e4	0.025987

As it is shown in table 3, the maximum stress in N/mm^2 in present at the structure with Y design. The order of designs after maximum stress si V, K, D, Z, and Y. The V design is the most common used design in structures as those in this study. The stress is presented in the joint of the horizontal pipes with the main cylinder, and for that reason the stress presented in in design in very low. In K design in almost the same situation as in V design. Those two designs are opposite each other. When de design start to complicate the structure, in every extra joint points it is present an extra stress which make the structure weaker at wave pressure.

When we talk about displacement the order of the designs is Y, D, K, Z, and V. The Y design is the most complicated (three pieces) and is more solid and keeps the structure more fix. The V, Z and K designs are very simple and because of this reason, structures with those designs are used mostly in calm environmental with small wave and low pressure. The constructor, based on this analysis, can decide what kind of structure he want depending of the environmental conditions where the structure with its turbine operate.

3.4. Software modal analysis

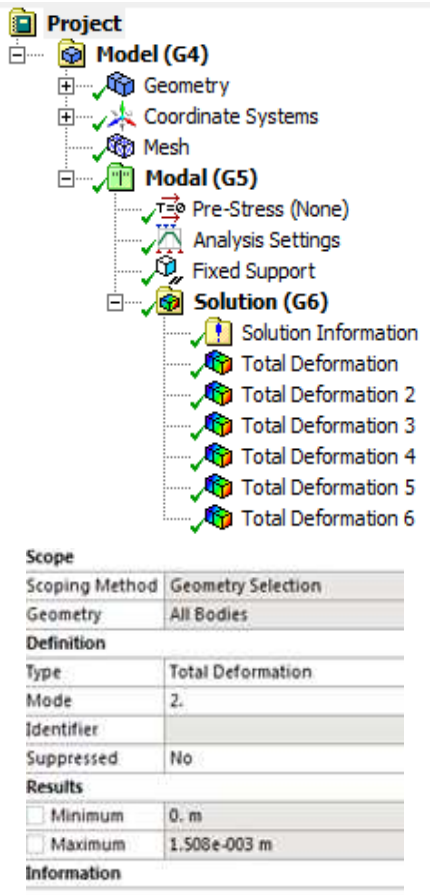

Figure 9 Ansys modal settings

In Ansys modal settings, the first step is to give the analysis settings of simulation and then choose the fixed support faces. After all the settings are done, based on the settings provided we can see how the structure behave at different frequency. In figure 9 are shown all this steps and the solutions that we are interested in: total deformation [9].

Tabel 4. Total deformation of the structure

Design	Y`	Z	V	D	K
Total deformation 1	7.63e-004 m	5.56e-003 m	2.06e-003 m	6.32e-003 m	2.21e-003 m
Total deformation 2	8.45e-004 m	4.98e-003 m	1.53e-003 m	5.56e-003 m	1.54e-003 m
Total deformation 3	7.21e-004 m	5.05e-003 m	1.70e-003 m	5.20e-003 m	1.78e-003 m
Total deformation 4	1.29e-003 m	4.36e-003 m	2.70e-003 m	4.88e-003 m	2.93e-003 m
Total deformation 5	1.13e-003 m	3.99e-003 m	2.17e-003 m	4.61e-003 m	2.18e-003 m
Total deformation 6	1.05e-003 m	4.21e-003 m	2.11e-003 m	4.70e-003 m	2.20e-003 m

After we run six frequency tests on every structure, the most problematic frequency for D design we had at total deformation 1, the value of 6.32e-003 m. With Y design, a problem is at total deformation 4 as is shown in figure 10, the value of 1.29e-003 m. The order of designs based on maximum deformation is D, Z, K, V and Y as we can see in table 4 [10].Every structure had a different behave at different frequencies and a total deformation at one of that. The D design had highest values from all the shapes and the best design with less deformation from all is Y design. The other construction configurations had entry value, and again the constructor is the only who decide in what kind of environmental he use a specific design based on this kind of study.

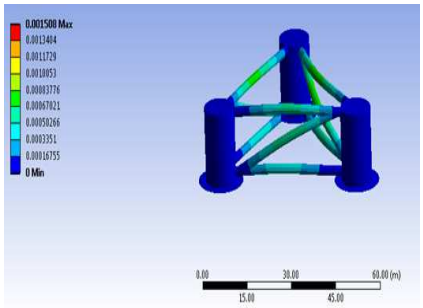

Figure 10 Total deformation 4 of Y design at 5.3654 Hz

In the Figure 10 it is shown the behave of Y design at a frequency of 5.3654 Hz. This design has the lowest deformation from all construction configuration and is recommended in ruthless environmental.

4. CONCLUSIONS

The analysis on this six designs of offshore structures raise big problems when the constructor had to choose the perfect structure design for a specific environmental because he had three minimal condition to perform an action. For stress and displacement a force of 30 kN was used and all data provided for each design can be used for further analysis in different offshore environmental. Considering stress values, the structure with the best behaviour had a V design, the structure with best displacement had a Y design, and the structure with the minimum deformation based on the specific frequency had a Y design. According to the analysis performed on all structures, we can see that the structure with Y design had the best response for the worse Black Sea environmental. The more complicated the design is, the more strong the entire structure became. Every extra pipe joined to the structure raise the construction price and for that reason the turbine mounted on it must have a very good yield.

5. REFERENCES

[1] DOMINIQUE RODDIER, CHRISTIAN CERMELLI, ALEXIA Aubaultand Alla Weinstein. *WindFloat: A floating foundation for offshore wind turbines.* Principle Power, Inc., Seattle, Washington, USA. June 2010.

[2] RUI ZHANG. *Comparative study on dynamic responses of a semi-submergible wind turbine using a simplified aerodynamic model and a BEM model.* Norwegian University of Science and Technology. Sping 2013

[3] ALLSOP, N.W.H.; VICINANZA, D.; MCKENNA; J.E. (1996): *Wave forces on vertical andcomposite breakwaters. Strategic Research Report. Hydraulic Research Wallingford*, SR 443, Wallingford, U.K

[4] ANGHELACHE Diana, Cristea Simona-Andra, IacobNicolae. *Stress and Strain analysis of a tower crane arm.* University "Dunarea de Jos Galati". Engineering Faculty of Braila, 2014.

[5] TAO, L., THIAGARAJAN, K.., *Low KC flow regimes of oscilating sharp edges, I: vortex shedding observation.* Applied Ocean Research 25. 2003.

[6] DOBROT Oana-Mirela, MOCANU Costel-Iulian, *Study of the destruction influence of elements from offshore platform leg on stress and vibration mode.* University "Dunărea de Jos" of Gala□i, 2014.

[7] SHEN Wen-jun, TANG You-gang and LIU Li-qin. *Research on the Hydrodynamic Characteristics of Heave Plate Structure with Different Form Edges of A Spar Platform.* Tianjin University, China, 2011.

[8] L. TAO, B MOLIN, Y.M. SCOLAN, K. THIAGARAJAn. *Spacing effects on hydrodynamics of heave plates on offshore structures.* Griffith University, Australia,
Engineering School of Marseille, France, School of oil and Gas Engineering, Australia. June 2007.

[9] COOKER, M.J.; PEREGRINE, D.H. (1990): *A model for breaking wave impact pressures.* Proceedings International Conference Coastal Engineering (ICCE), ASCE, Delft, TheNetherlands, no. 22, Volume 2.

[10] MCCONNELL, K. (1998): *Revetment systems against wave attack - a design manual*.London, U.K.: Thomas Telford.

SECTION III
ELECTRONICS, ELECTRONICAL ENGINEERING AND COMPUTER SCIENCE

PRACTICAL ASPECTS REGARDING THE ROBOT ARM

[1]BONCATA IONUT, [2]NEGUT ALIN, [3]HNATIUC MIHAELA

[1,2]Electronics and Telecommunication, "Mircea cel Batran" Naval Academy, [3]Constanta Maritime University, Romania

ABSTRACT

The inventions using computing systems are 3D printers. These devices can replicate many things of diverse materials. In this way, the prostheses which are very expensive can be accessible for all the people. After the prosthesis is built it can be controlled by several means, can have diverse functions, parameters or cost. One method to control and command a hand prosthesis made with the help of a 3D printer is by using an intelligent glove presented in this paper.

Keywords: *3D printer, prosthesis, microcontroller, flex sensors*

1. INTRODUCTION

One of the most dynamic areas in robotics is the robotic arms. They're best known for their use in industry, where they are used because of their speed and accuracy, and have features such as welding and assembling components. Another section of development is the humanoid arms, which are similar to the human body. The most complicated things are handmade, and that's why it must reproduce as many human hand actions. The human arm reproducing is not as simple as it seems, muscular and skeletal structure of the hand provides a unique and unrivaled steady hand. It's stable and accurate but also fast and flexible. The imitation of the models has named biomimetics or biomimicry [1]. The terms biomimetics and biomimicry come from Ancient Greek and a closely related field is bionics. The adapted systems based on imitation are evolved in last time. Biomimetics has given rise to new technologies inspired by biological solutions at macro and nanoscales. Humans have looked at nature for answers to problems throughout our existence. Nature has solved engineering problems such as self-healing abilities, environmental exposure tolerance and resistance, hydrophobicity, self-assembly, and harnessing solar energy.

The prosthesis is an artificial device that replaces a missing body part, which may be lost through trauma, disease, or congenital conditions. Prosthesis devices are based on many algorithms, have various methods to move and to be build. This kind of devices are developed using interdisciplinary knowledge and researches.

The innovation of this century is 3D printers which can replicate many objects without much knowledge from the user. Using this device we are going to build a hand controlled by an intelligent glove. An intelligent glove is a device operated by the human hand based on the flex sensors which command the actuators.

InMoov is a 3D printed robot. The idea was to create an open source robot which was capable of doing more complex motions than other robots. Its skin, joints, gears and other parts of InMoov are 3D printed [2,3,4].

But in addition to the technology used to create the robot, the designer's determination and ingenuity were unmatchable.

Gael Langevin started building a life-size animatronic robot using a 3D printer in 2012. He did not have experienced in robotics, and his initial plan was simple: to build a robot arm. The process went very smooth, so he continued building the upper body, including head, shoulders, brain and vocal commands for the future InMoov robot.

The hand plans were designed in Blender, printed using 3D Touch printer, and made out of ABS. This project is based on the above example, introducing new ideas in manufacturing and motion. In this case, the robot arm is controlled through a smart glove by an operator. The system was both physically and electrically made.

2. BUILDING THE ROBOT HAND

2.1. Choosing the components for the robot system

The robot hand, built in the laboratory, is operated using a sensor glove. The moves made by the person who's wearing the glove are sent to the robot hand.

The implementation was done in several stages. First of all, the idea was to find and use components that would not cause connection and configuration problems. The block diagram for operating the hand is shown in Fig.1.

Thus, were acquired [5,6,7]:

- Arduino Uno development board to process the signal of glove and to command the robot hand [8]
- 5 Flex Sensors 4.5" for acquired the fingers movement of the operator
- 5 mg955 actuators to command the robot hand
- Plastic ABS (Acrilonitril-Butadien-Stiren) – for making the hand itself [9]
- Screws, wires, pins, resistors, various materials to build the mechanical part of the robot hand [10].

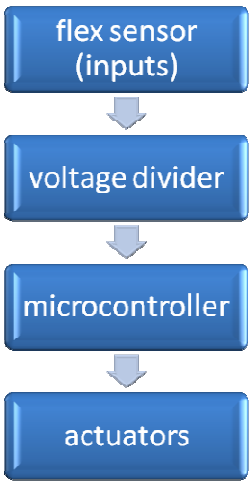

Figure 1 Block diagram of the robot hand system

2.2 Hand plans

We would download the plans for different components from http://www.thingiverse.com/thing: 17773.

For making the hand, we would print the following parts:

- Fingers: Auriculaire3.stl, Index3.stl, Majeure3.stl, ringfinger3.stl, thumb5.stl
- Palm: WristsmallV3.stl, WristlargeV3.stl
- Wrist: robpart1.stl
- Lower forearm: robpart2V2.stl, robpart5V2.stl
- Actuator support: RobServoBedV4.stl, RobCableFrontV1.stl, RobCableBackV2.stl
- Upper forearm: robpart3V3.stl, robpart4V3.stl (These are just covers; they are not entirely necessary)

All the programs are sending to the 3D printer to build the robot hand. This model is a first prototype for the hand prosthesis which are learned to move itself using the adaptive algorithms.

2.3 Printing and assembling of the hand

A 3D printer was used for printing the parts and they were all built with 2 layers, with 15% filling and no stand (already included in plan).

For fingers, standard printing resolution was used and low-res for the wrist and arm parts (Fig.2).

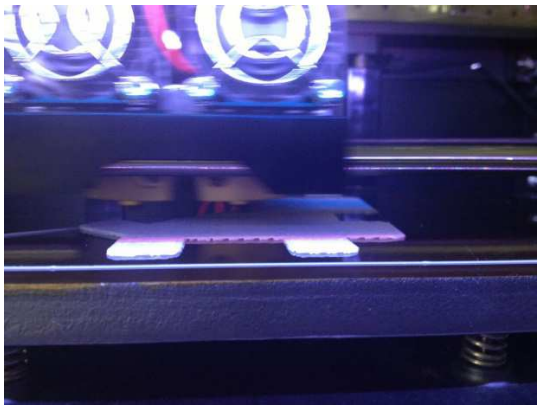

Figure 2 WristlargeV3 palm printing

High breaking point fishery thread was used for the "tendons". They go through the fingers, the palm, all the way down until the mg955 actuator (Fig.3).

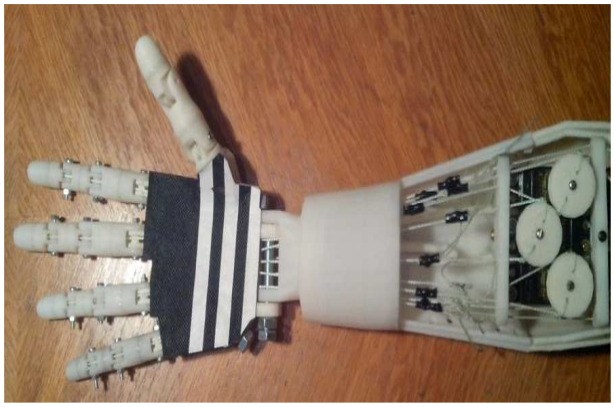

Figure 3 The robot hand part

The robot arm is controlled by an operator using the intelligent glove, with flex sensors on each finger which convert the movements into electrical signals which enter the arm's control board (Fig.4).

Figure 4 Sensor glove with the flax sensors

In order to work with Arduino, the flex sensors are connected in a circuit. Flex sensors are variable resistors and that's why the signal enters the voltage divider (Fig.5).

The change in resistance can be measured using the change in voltage between the resistors. This change wich is an analog voltage is read by the Arduino, using its analog inputs.

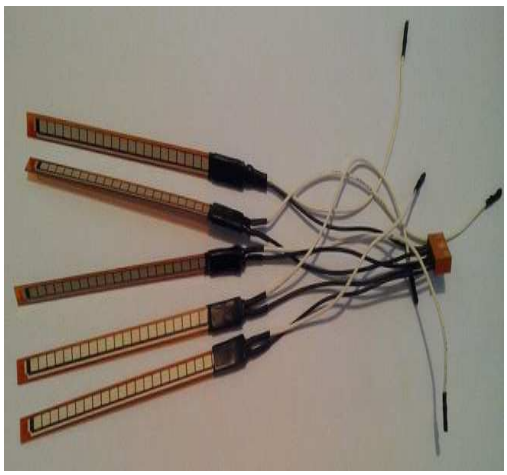

Figure 5 Flex sensors with wires attached to their pins

System connection is made using the block diagram Fig.1 and the electrical scheme Fig.6.

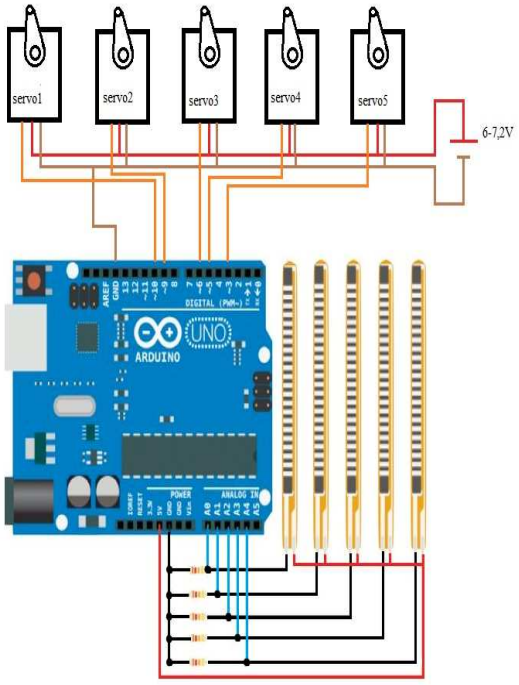

Figure 6 Electrical scheme of the command and control system

The actuators' wires connect to Arduino's PWM.

Actuators are powered by a variable voltage self-protected power supply. Voltage can vary from 0 to 18V, but for an optimal result, 7V would do. Arduino is powered by a 9V battery.

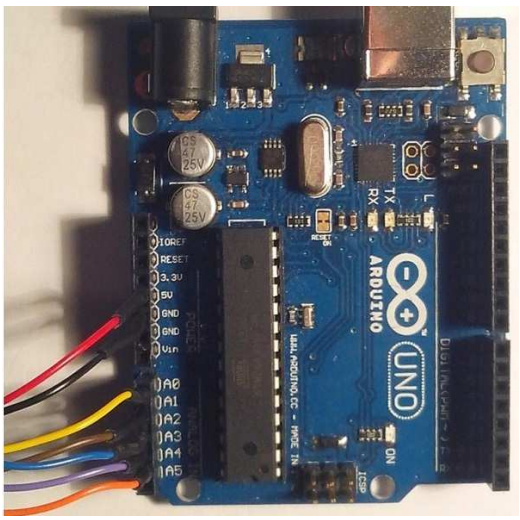

Figure 7 Glove-Arduino connections

The AVR microcontroller is programmed in Arduino's IDE. There's a bootloader in every microcontroller, for interfacing and running the apps.

Arduino program has 2 sections: setup (run at startup/reset) and loop (it goes in cycles, as long as the board is powered).

The final system robot arm – glove is shown in the Figure below.

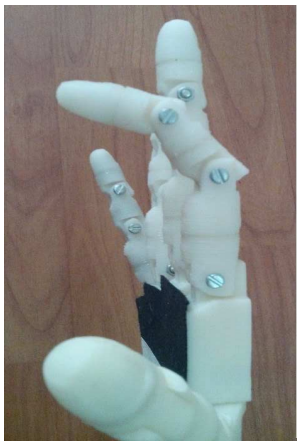

Figure 8 Prosthesis and intelligent glove

3. RESULTS AND CONCLUSIONS

After the experiment, there were the following results.

During the first test, the relationship between sensor resistance and fingers angle was measured. It was found that the index, middle, ring and little finger had about the same input value from the flex sensors and almost the same bending angle. On the other side, the thumb was limited in motion to the other finger and therefore the gathered data was smaller.

For testing purposes, 3 positions were used: fully extended, half flexed and flexed. Every motion was analyzed and every finger's angle has been noted. It turns out that in the fully extended position, there was a slight difference between operator's and robot's finger.

The biggest difference was in the half flexed stand, but it didn't affect its behavior. The least difference was noticed during flexed position.

This means that there's a relationship in these proportions, which can be the subject of further study. This type of robot control using only the human hand can have tons of applications, both in medical domain and industry. The prosthesis can be accessible by many social categories of people, because of its manufacturing method.

4. REFERENCES

[1] http://www.reading.ac.uk/biomimetics/origins.htm
[2] http://www.inmoov.fr/ (French made 3D robot)
[3] http://www.iai.fzk.de/www-extern-kit/fileadmin/Image_Archive/Hochdurchsatz/biosignal/publikationen/control_zit01.pdf
[4] SILVESTRO MICERA, JACOPO CARPANETO, and STANISA RASPOPOVIC., *Control of Hand Prostheses Using Peripheral Information*, IEEE REVIEWS IN BIOMEDICAL ENGINEERING, VOL. 3, 2010,
[5] http://www.unb.ca/conferences/mec/_resources/docs/silvestro-micera-keynote-papers/micera2010-ieee-rbme.pdf
[6] http://mindtrans.narod.ru/hands/hands.htm
[7] http://itp.nyu.edu/physcomp/sensors/Reports/Flex
[8] http://www.electrical4u.com/servo-motor-servo-mechanism-theory-and-working-principle/#Servo-Motor-Theory
[9] http://www.arduino.cc/
[10] http://www.inmoov.fr
[11] http://www.shadowrobot.com/products/dexterous-hand, HyperLynx Thermal user guide, march 2014

A PARABOLIC-HYPERBOLIC MODEL USABLE IN ELECTROMAGNETICS

[1]COSTEA MARIUS-AUREL, [2]CARLAN MILTIADE

[1]Lumina -The University of South- East Europe, [2]S.C. Formenerg S.A., Romania

ABSTRACT

The paper presents a phenomenological analysis from a statistical-mathematical point of view, of the interrelation of three quantities: the magnetic potential depending of the electrical current and the air-gap. The magnetic potential was determined through numerical simulations considering different values for the electrical current and the air gap corresponding to a E-E type, DC fed electromagnet. To this purpose, the FEMM 2D program was used for non-linear media in stationary conditions. For the case under study, we propose a parabolic-hyperbolic dependence. This analysis is precedeed by the validation of the accuracy of test data, operation confirmed by the Shapiro – Wilk concordance test, specific to this kind of statistical distribution. Also, the correlation coefficient associated to data included in the statistical sample and those obtained using the regression equation highlights their high similarity, hypothesis also proven by another indicator – Hamming distance – concept related to fuzzy logic.

Keywords: *Electromagnet, non-linear media, magnetic potential, regression coefficient quantile, correlation coefficient ratio, Hamming distance.*

1. INTRODUCTION

The assumed model is supported by the phenomenological evolution of the three quantities important for this analysis: the magnitude of the magnetic potential increases when the magnitude of the current increases and decreases when the air gap increases. The volume of the primary data sample is of 140 entries, but the sample used for this analysis consist of nine entries, approximately 6,4% of the entire sample. The actual entries that have been used are presented in table 1.

2. CASE STUDY

2.1. Determining the magnetic potential

Let there be a DC fed electromagnet [1]-[3]. The magnetic field is produced by a coil consisting of 470 windings consumes a maximum current of 2 A. The magnetic field problem can be solved using the finit element method. To this purpose, the FEMM 2D software was used considering non-linear media and stationary conditions. The equations of the magnetic field behaviour in stationary regime are:

$$rot\overline{H} = \overline{J} \tag{1}$$

$$div\overline{B} = 0 \tag{2}$$

$$\overline{B} = \mu(\overline{H} + \overline{M}), \tag{3}$$

where $\overline{B} = rot\overline{A}_m$.

Due to the simetry of electromagnets, the field problem can be solved for plane realms by calculating the magnetig potential $\overline{A}_m$ from within the equation:

$$-div\frac{1}{\mu}grad\,\overline{A}_m = J + \overline{k}\cdot rot\,\overline{M}, \tag{4}$$

which along the considered realm boundary accepts null Dirichlet requirement.

The relationship between magnetic potential, the electrical current and the air gap is characterized by a parabolic – hyperbolic evolutions.

For simplicity, the $\overline{A}_m = A\cdot 10^{-9}$ equation is used and it is measured in Wb/m where A is given in table 1; the proposed mathematical model is enunciated by the relationship:

$$A = \frac{kI^{\alpha}}{\delta^{\beta}} \tag{5}$$

where I is the electrical current intensity, δ is the air gap, and k, α and β are the factors of the regression dependency [4].

2.2 Auditing the likelihood of sample data

This requirement states that the concordancy of the statistical data presented in table 1 must be examined. In order to validate them, the Shapiro – Wilk test shall be used [4]-[6].

Table 2 presents the necesary calculation elements to determine the quantile of the test [5], [6] expressed by way of the following double inequality:

$$W^{\inf} < W_0 < W^{\sup} \tag{6}$$

where, $W^{\inf}, W^{\sup}$ are the inferior/superior quntiles of the test and W_0 is the calculation quantile:

$$W_0 = \frac{\sum_i f_i\left(A_i - \overline{A}\right)^2}{\left(\sum_i f_i A_i\right)^2}. \tag{7}$$

Table 1. Values obtained through numerical simulations

A										
I[A] / δ[mm]	0.1	0.2	0.3	0.4	0.5	0.6	0.7	0.8	0.9	1
0.0003	1	2,07	3,22	4,44	5,66	6,9	8	9,11	10	11,1
0.0004	0,83	1,68	2,6	3,52	4,5	5,46	6,42	7,37	8,28	9,16
0.0005	0,71	1,44	2,19	2,96	3,76	4,6	5,4	6,2	7	7,8
0.0006	0,62	1,25	1,9	2,55	3,23	3,92	4,63	5,32	6,02	6,7
0.0007	0,57	1,14	1,72	2,31	2,91	3,53	4,16	4,8	5,42	6
0.0008	0,51	1,08	1,55	2	2,63	3,18	3,73	4,3	4,87	5,43
0.0009	0,48	1,1	1,43	1,92	2,42	2,92	3,43	3,95	4,46	5
0.001	0,44	0,88	1,32	1,77	2,2	2,68	3,15	3,61	4,1	4,46
0.0011	0,41	0,82	1,23	1,65	2	2,49	2,92	3,35	3,79	4,22
0.0012	0,38	0,77	1,16	1,55	1,94	2,34	2,74	3,15	3,56	3,97
0.0013	0,36	0,72	1,03	1,44	1,81	2,2	2,55	2,92	3,3	3,68
0.0014	0,34	0,68	1	1,37	1,71	2,06	2,41	2,77	3,12	3,48
0.0015	0,32	0,65	0,98	1,3	1,63	1,96	2,3	2,63	2,97	3,31
0.0016	0,31	0,62	0,94	1,25	1,56	1,9	2,2	2,52	2,84	3,16

For this analysis, there shall be used nine entries $A_j\,(\mathrm{I}_j, \Delta_j)$ from table 1, according to some accepted $\delta I, \delta \Delta$ intervals, given in table 2.

Table 2. Values used to determine the test quantile

I[A] / δ[mm]	**0,1**	**0,5**	**0,9**
0,0003	1	5,66	10
0,0009	0,48	2,42	4,46
0,0015	0,32	1,63	2,97

There for $\delta I = 0,4\,A$ si $\delta \Delta = 6 \cdot 10^{-4}$ mm. Base on (7), the magnitude of the calculation quantile is $W_0 = 0,093$.

Acording to tabel 3, the restraint (6) regarding the validity of the nine entries sample is fullfiled:

$$W^{\inf}_{n^*=9;\,P=0,95} = 0,025 < W_0 =$$

$$= 0,93 < W^{\sup}_{n^*;\mathrm{P}=0,95} = 0,205.$$

Table 3. The quantiles of Shaphiro- Wilk test

i	n	P=0,95	
		$W^{\inf}$	$W^{\sup}$
1	7	0,025	0,260
2	8	0,025	0,230
3	9	0,025	0,205
4	10	0,025	0,184
5	11	0,025	0,166
6	12	0,025	0,153
7	13	0,025	0,140

In this table, P represents the likelihood threshold of the statistical data; it is a quantity complementary to α the risk factor:

$$P = 1 - \alpha. \tag{7}$$

2.3. Determining the regression coefficients

The least squares method shall be used [4], starting from (5), proposed for modelling the relation between the the three quantities: variabile (current and air gap) and the resulting quantity (the magnetic potential).
The calculation steps are as follows:
a) liniarization of the relationship (5),

$$\ln \Delta = \ln k + \alpha \ln I - \beta \ln \Delta \tag{8}$$

b) minimizing the sum of the square deviances between the A_i computed values and the calculated $\tilde{A}_i$ values obtained using the regression equation:

$$S = \sum_i [(\ln \mathrm{k} + \alpha \ln \mathrm{I} - \beta \ln \Delta_i) - \ln \mathrm{A}_i]^2 \tag{9}$$

The minimization process involves the consequent setup of restraints:

$$\frac{\partial S}{\partial k} = 0; \frac{\partial S}{\partial \alpha} = 0; \frac{\partial S}{\partial \beta} = 0\ . \tag{10}$$

c) the restraints lead to the subsequent linear equations system:

$$\begin{cases} n\ln k+\alpha\sum_i \ln I_i-\beta\sum_i \ln\Delta_i=\sum_i \ln\Delta_i \\ \ln k\sum_i \ln I_i+\alpha\sum_i \ln^2 I_i-\beta\sum_i \ln I\ln\Delta_i=\sum_i \ln\Delta_i\ln I_i \\ -\ln k\sum_i \ln\Delta_i-\alpha\sum_i \ln I\ln\Delta_i+\beta\sum_i \ln^2\Delta_i=-\sum_i \ln A_i\ln\Delta_i \end{cases} \quad (11)$$

The obtained equations system is:

$$\begin{cases} 9\ln k-9,30327\alpha+64,88142\beta=6,11866 \\ -9,30327\ln k+17,38035\alpha-67,06879\beta=1,64607 \\ 64,88142\ln k-67,06879\alpha+471,7911\beta=47,1213 \end{cases}$$

The regression coefficients are:

$k=0,0275;\ \alpha=1,027;\beta=0,74.$

Therefore , there regression equation associated to $A=f(\mathrm{I},\Delta)$ is:

$$A=\frac{0,0275\cdot I^{1,027}}{\Delta^{0,74}}. \quad (12)$$

2.4 The likelihood degree of the regression equation

To this end, two instruments shall be used: the Spearman correlation ratio and the Hamming distance.

The Spearman correlation ratio

The similarity of the (A_i) computed values and the ($\tilde{A}_i$) values obtained using the regression equation is confirmed by the Spermann correlation ratio [7]:

$$\eta=\sqrt{1-\frac{\sum_i(\mathrm{A}_i-\tilde{\mathrm{A}}_i)^2}{\sum_i(\mathrm{A}_i-\bar{\mathrm{A}})^2}}\ \square\ 0,996557. \quad (13)$$

Thus, the similarity of the magnitude values of the magnetic potential obtained through two different methods is very high, therefore confirming one more time the accuracy of the calculation data.

The Hamming distance

Another proposed method for correlating the the (A_i, $\tilde{A}_i$) set of values is the Hamming distance, a concept related to Fuzzy logic:

$$d_H=\frac{\sum_i\left|A_i^F-\tilde{A}_i^F\right|}{2}. \quad (14)$$

In the relation (14) A_i^F, $\tilde{A}_i^F$ are the A_i, respectively $\tilde{A}_i$ quantities expressed using fuzzy logic:

$$\begin{cases} A_i^F=\dfrac{A_i}{A_{\max}}\le 1 \\ \tilde{A}_i^F=\dfrac{\tilde{A}}{\tilde{A}_{\max}}\le 1 \end{cases}. \quad (15)$$

This operation is mandatory because the fuzzy logic operates with $M\le 1$ quantities. Table 4 shows the calculation of this index.

Therefore the Hamming distance is:

$$d_H=\frac{\sum_i\left|A_i^F\in M_{A^F}-\tilde{A}_i^F\in M_{\tilde{A}^F}\right|}{2}, \quad (16)$$

where $M_A, M_{\tilde{A}}$ are the groups that include the A_i^F respectively $\tilde{A}_i^F$ elements:

$$\begin{cases} M_{A^F}=\{\mathrm{A}_i^F\} \\ M_{\tilde{A}_F}=\{\tilde{\mathrm{A}}_i^F\} \end{cases}. \quad (17)$$

In order to confirm the likelihood level, we propose the subsequent restraint:

$$d_H<\max\left|A_i^F-\tilde{A}_i^F\right|. \quad (18)$$

Indeed, by replacing with values, the result is: $0,02145<\max\left|A_i^F-\tilde{A}_i^F\right|=0,0243$.

Table 4 The calculation elements neccesary to obtain the Hamming distance

i	**1**	**2**	**3**	**4**	**5**	**6**	**7**	**8**	**9**
$A_i\Rightarrow A_i^{\max}=10$	0,32	0,48	1	1,63	2,42	2,97	4,46	5,66	10
M_{A^F}	0,032	0,048	0,1	0,163	0,242	0,297	0,446	0,566	1
$\tilde{A}_i\Rightarrow\tilde{A}_i^{\max}=10,8$	0,32	0,46	1.04	1,66	2,42	3,03	4.44	5,46	10,08
$\tilde{M}_{A^F}$	0,0317	0,0456	0,1032	0,1647	0,2401	0,3006	0,4405	0,5417	1
$\left\|A_i-\tilde{A}_i^F\right\|$	0,0003	0,0024	0,0032	0,0017	0,0019	0,0036	0,0055	0,0243	0
$\sum_i\left\|A_i^F-\tilde{A}_i^F\right\|$	0,0429								

3. CONCLUSIONS

The proposed relation for evaluating the magnetic potential in regard to the feeding current and the air gap models the interdepency state of these three quantities at a very high likelihood level.

Using the Gregory – Newton interpolation method based on regressive or progressive finite differences becomes cumbersome, because the interpolation operation must be itteratively repeated for each and every entry of the current magnitude, but maintaining the same set of air gap value entries.

We conclude that the parabolic – hyperbolic nature of the analyzed phenomenon is confirmed also by the accuracy of statististical sample entries, a condition validated according to the Shapiro – Wilk criterion, appropriate for complex parabolic – hyperbolic relations.

4. REFERENCES

[1] COSTEA M.A., VĂRĂTICEANU B. D., BĂLAN C., "*Timpul de actionare al unui electromagnet excitat în tensiune continuă*" **(***The Actuating Time of an Electromagnet excited by DC Voltage)***.** Revista Electrotehnică Electronică Automatică, vol. 60, nr. 1, Bucuresti, 2012

[2] COSTEA M. A., VASILESCU M., ., "*Timpul de actionare al unui electromagnet cu armături feromagnetice neliniare*" **(***The Actuating Time of an Electromagnet with nonlinear ferrromagnetic armature)***.** Revista Electrotehnică Electronică Automatică, Vol. 59, nr. 3, pp 64, Bucuresti, 2011

[3] VASILESCU M., Mihai MARICARU M., VĂRĂTICEANU B. D., COSTEA M. A., *An Efficient Integral Method For Computation Of Bodies Motion In Electromagnetic,* Field, Rev. Roum. Sci. Techn. Ser. Électrotechn. et Énerg., vol. 56, no. 2, pp.134-143**,** Buchatest, 2012

[4] BARON T.(coordonator), ISAIC-MANIU Al., TÖVISSI L., NICULESCU D., BARON C., ANTONESCU V., ROMAN I.,"*Calitate si fiabilitate. Manual practic*" (Quality and reliability. Practice Manual). Editura Tehnică, Bucureşti,1998

[5] VODĂ V. Gh., "*Controlul durabilităţii produselor industriale*" (*The durability test of industrial products*). Editura Tehnică, Bucureşti,1981

[6] PANAITE V., MUNTEANU R, "*Control statistic si fiabilitate*" (*Statistical Control and Reliability*). Editura Didactică si Pedagogică, Bucureşti,1982

[7] YULE UDNY G., KENDALL G.M., "*Introducere în teoria statisticii*" (*Introduction in the theory of statistics*), traducere din limba engleză. Editura Tehnică, Bucureşti,1969.

SECTION IV
MATHEMATICAL SCIENCES AND PHYSICS

CHARACTERIZATION OF GUMOWSKI – MIRA TRANSFORM'S ATTRACTORS USING CORRELATION DIMENSION

DELEANU DUMITRU

Constanta Maritime University, Romania

ABSTRACT

In the paper we proposed an algorithm implemented under Matlab software package which computes the standard Grssberger – Procaccia correlation dimension of an attractor. This tool is briefly reviewed and applied to the very interesting two-dimensional Gumowski-Mira map. The relative merits and drawbacks of this indicator of order and chaos are pointed out.

Keywords: *Correlation dimension, Gumowski – Mira map, order and chaos, dynamical systems.*

1. INTRODUCTION

From a practical point of view, chaos can be seen as a bounded steady-state behavior that is not an equilibrium or a periodic or a quasi-periodic solution of some dynamical system. Strange attractors associated to a chaotic solution in state space are complicated geometrical objects, which not resemble a finite number of points, a closed curve or a torus, and that possess fractal dimensions. A fractal dimension is any dimension measurements that allows non-integer values. A fractal is a set with a non-integer fractal dimension. A strange attractor is a particular case of fractal.

Examples of fractal dimensions include the Hausdorff dimension (or box-counting dimension), information dimension, spectrum dimension and correlation dimension. Details regarding fractal dimensions are given in great details by Grassberger and Proccacia [1] and Falconer [2]. It is generally accepted that a non-integer fractal dimension is a good indicator of chaos [3 - 5].

We will focus in this paper on the correlation dimension, which is among the most widely used method for estimating fractal dimension of a scalar set of data points. This fractal dimension is sensitive to the process of coverage of the attractor, and tells us how frequently different parts of the attractor are visited by the trajectory. Additionally, the theory is easy to implement in a numerical algorithm. On the other side, there are a number of limitations and potential pitfalls with the correlation algorithm but one problem has always been that the computation can be very time consuming. To avoid this drawback, Theiler [6] had proposed an algorithm which can realize speedup factors of up to a thousand over the usual method.

The rest of the paper is organized as follows. In Section 2, the Gumowski-Mira map is presented. Section 3 describes the standard Grassberger – Procaccia correlation dimension and outlines the steps of the algorithm implemented in Matlab. Section 4 reports the results of applying this algorithm on the Gumowski-Mira map and points-out the merits and demerits of the correlation dimension in characterizing attractors and chaos. Finally, Section 5 discusses the conclusions and future work derived.

2. GUMOWSKI – MIRA MAP

In our work, we take up as basic units a 2 – dimensional nonlinear discrete dynamic system defined by the following recurrent equations

$$\begin{cases} x_{n+1} = y_n + a\left(1 - b y_n^2\right) y_n + f\left(x_n\right) \\ y_{n+1} = -x_n + f\left(x_{n+1}\right) \end{cases} \quad (1)$$

where

$$f(x) = \mu x + \frac{2(1-\mu)x^2}{1+x^2}, a, b, \mu \text{ constants} \quad (2)$$

This map is known as *Gumowski – Mira transform* (hereafter referred as GM map) and has been introduced for modeling and study accelerated particles trajectories at CERN in 1980 [7 - 11]. The final attractor of the GM map depends very sensitively on the value considered for parameter μ and it reminds us about "living marine creatures" like a jellyfish, a starfish or a plankton or about other interesting objects like a slice of tomato, a butterfly, a cut end of an orange and so on. Some phase space plots presented in Figure 1 illustrates this.

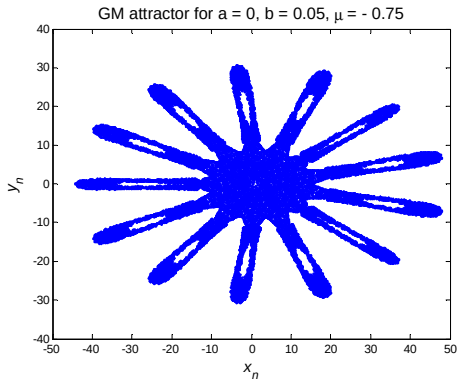

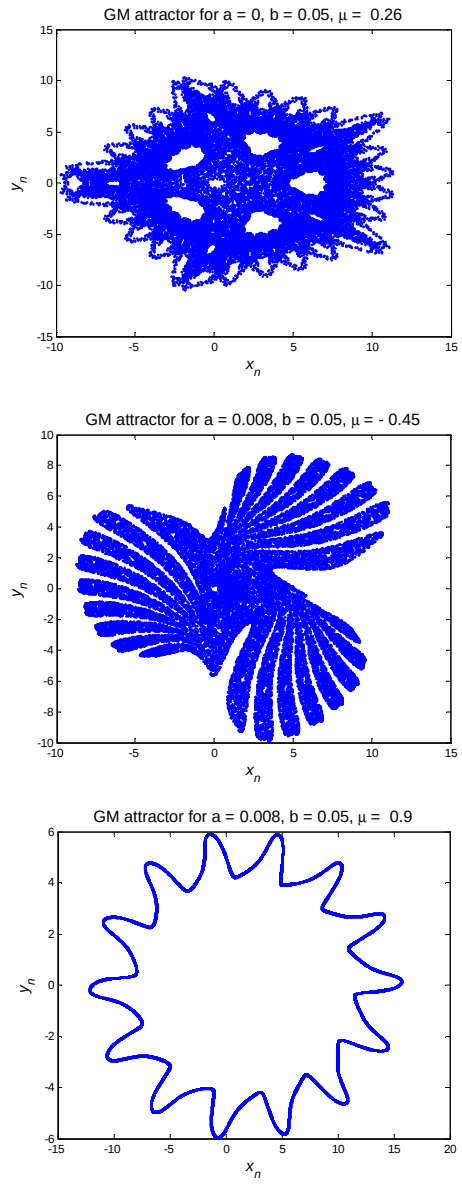

Figure 1 Some phase space diagrams of Gumowski – Mira map

The sensitive dependence of the attractors on μ is due to the recurring periodic and self similar substructures in the bifurcation scenario, each with its own intermittency, periodicity, quasi-periodic band and merging of bands leading to chaos [7-8].

3. CORRELATION DIMENSION OF AN ATTRACTOR. DEFINITION AND ALGORITHM

In this section we introduce the correlation dimension and its definition given by Grassberger and Proccacia in terms of the numerical problem that is to be solved.

Suppose we want to estimate the dimension of an attractor $\mathbb{A}$ from a finite sample of discrete points $\{\mathbf{x}_1, \mathbf{x}_2, ..., \mathbf{x}_N\}$ on the attractor. In our paper this sample of points represents a part of an orbit $\mathbf{O}$ of Gumowski – Mira map. The Grassberger – Proccacia algorithm measures the probability that two points randomly chosen on the orbit will be within a certain distance ε of each other. It needs the correlation integral

$$C(N,\varepsilon) = \frac{2}{N\cdot(N-1)} \cdot \sum_{\mathbf{i=1}}^{\mathbf{N}} \sum_{\mathbf{j=i+1}}^{\mathbf{N}} H\left(\varepsilon - \left\|\mathbf{x_i} - \mathbf{x_j}\right\|\right) \tag{3}$$

where

$$H(x) = \begin{cases} 0, x < 0 \\ 1, x \geq 0 \end{cases} \tag{4}$$

is the Heaviside function (unit-step function). It is obvious that summation counts the number of pairs $(\mathbf{x_i}, \mathbf{x_j})$ for which the distance $\left\|\mathbf{x_i} - \mathbf{x_j}\right\|$ is less than ε. With other words, $C(N,\varepsilon)$ measures the density of pairs of distinct points that are closer to ε. It decreases monotonically to 0 as $\varepsilon \to \infty$. The symbol $\|\cdot\|$ denotes the Euclidean norm. Other metrics have also been considered and it was found that the choose of metric did not affect the scaling of the correlation integral with ε.

The correlation dimension, D_C, is defined as

$$D_C = \lim_{\varepsilon \to 0} \lim_{N \to \infty} \frac{\log C(N,\varepsilon)}{\log \varepsilon} \tag{5}$$

The simplest way to estimate D_C is to plot $C(N,\varepsilon)$ against ε in a log – log plot and fit with least square method a straight line to the small ε tail of the curve. D_C is than the slope of this line.

As a remark, the numerical operations performed for determining the $N(N-1)/2$ distances dominate the computational workload in estimating D_C and make it very expensive for large N.

Moreover, the reliability of determining the above-mentioned slope is a possible source of error in D_C finding. The scheme used in the paper supposes a plot of $\log_2 C(N,\varepsilon)$ versus $\log_2 \varepsilon$ for a number of equally spaced values of $\log_2 \varepsilon$ between $\log_2 \varepsilon_{\min}$ and $\log_2 \varepsilon_{\max}$., where $\varepsilon_{\min}$ and $\varepsilon_{\max}$ are the maximum and minimum separation distances between two arbitrary points of chosen sample, respectively. To avoid the irregularities near $\varepsilon_{\min}$ and $\varepsilon_{\max}$ we neglect the first and the last few points of the plot.

In conclusion, the steps of the algorithm we will used for finding correlation dimension of an attractor are as follows:

Step 1: Start with any initial condition $\mathbf{x}_0$ in the basin of attraction and iterate until the orbit is on the attractor. Thus, the first points of the numerical orbit are not used in order to eliminate data that are not sufficiently close to the attractor;

Step 2: Generate the finite sample of discrete points $O = \{\mathbf{x}_1, \mathbf{x}_2, ..., \mathbf{x}_N\}$ from the next iterations of the map (after discarding the transition points);

Step 3: Compute the separation distance matrix between every two points of the set *O*;
Step 4: Find the minimum and maximum separation distances, $\varepsilon_{\min}$ and $\varepsilon_{\max}$, respectively, and divide the interval $[\log_2 \varepsilon_{\min}, \log_2 \varepsilon_{\max}]$ in equally spaced subintervals of length one;
Step 5: Construct correlation integral $C(N,\varepsilon)$ and plot $\log_2 C(N,\varepsilon)$ against $\log_2 \varepsilon$;
Step 6: Ignore a few points on either ends of the plot and fit a line, with least square method, to compute correlation dimension D_C.

4. NUMERICAL RESULTS

The algorithm described in the previous section was implemented under Matlab 7.6 (R 2008 a), a software package which is optimized for matrix operations. As model for numerical study on correlation dimension the Gumowski – Mira map presented in Section 2 is considered.

We set b = 0.05 and $a \in \{0.0, 0.008\}$. Changing the value of parameter μ, one obtains very diversified attractors in the x – y plane, which could be periodic, quasi-periodic or chaotic. Some of them are depicted in Figures 2 and 3.

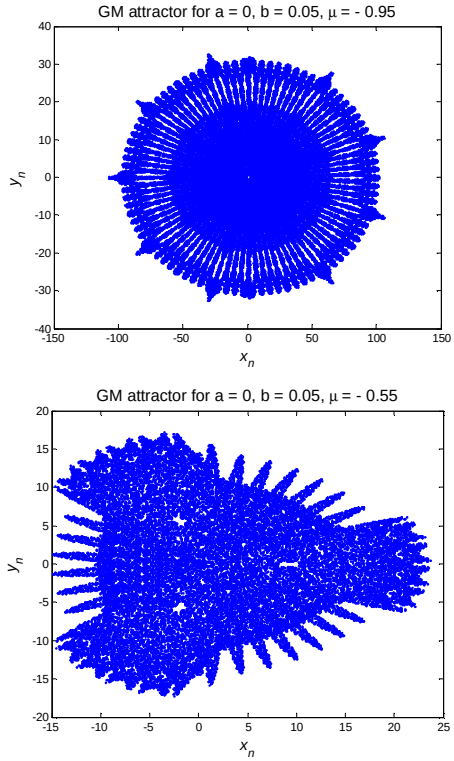

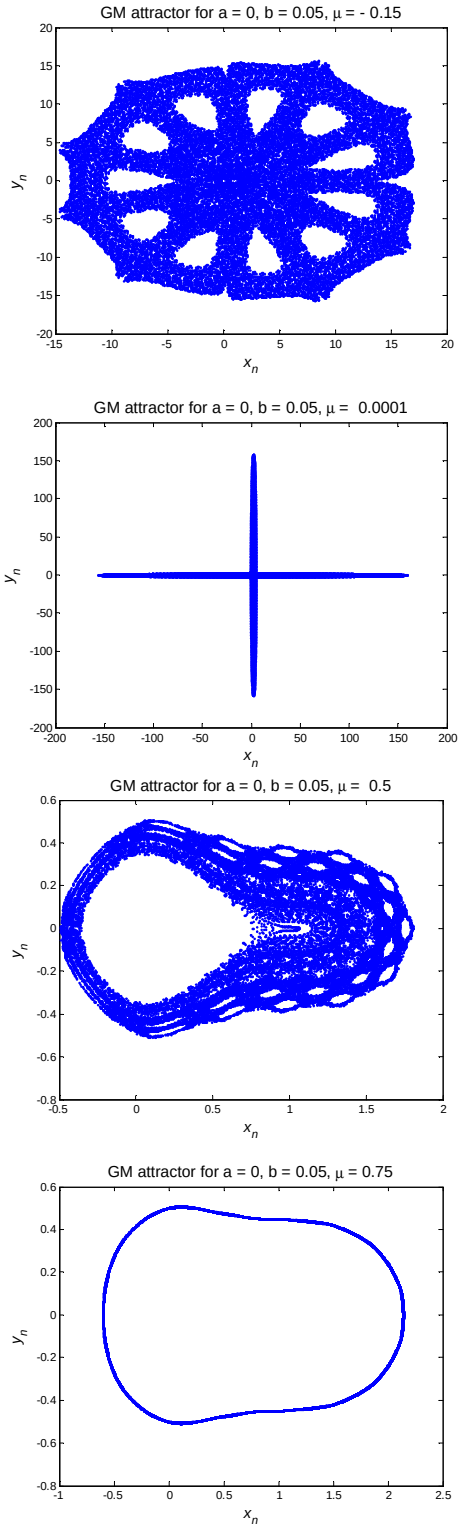

Figure 2 Examples of GM patterns with a = 0, b = 0.05

The same initial conditions, $x_0 = 0.0$, $y_0 = 0.5$, were considered for all orbits, the first 10,000 iterations were discarded and the next 50,000 iterations were used for representations.

To construct correlation integral, $C(N,\varepsilon)$, and find the correlation dimension, D_C, N = 5,000 points were used. The curves for $\log_2 C(N,\varepsilon)$ against $\log_2 \varepsilon$ are presented in Figure 4 just for the case a = 0.0.

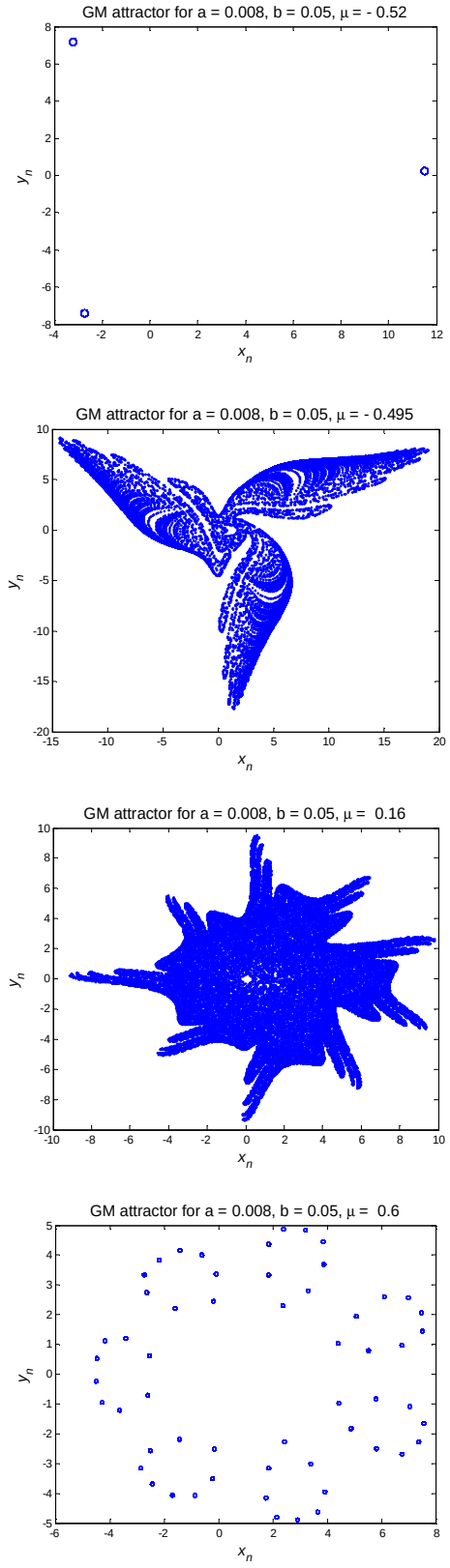

Figure 3 Some GM patterns with a = 0.008, b = 0.05

Four points on either ends of the plots were ignored in computing correlation dimension (see blue and magenta lines). The other points were used to fit the red line. The slope of this line represents the D_C number. The obtained values for D_C are given in Table 1.

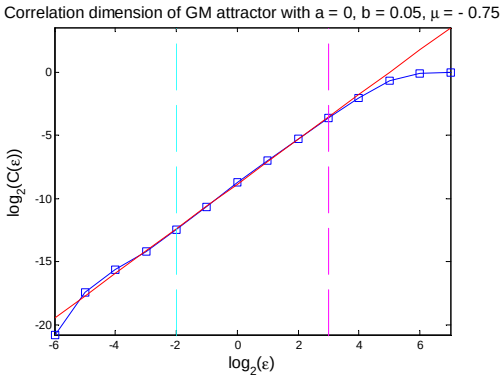

It is worth to notice that for a periodic orbit D_C approaches zero, for a quasi – periodic orbit it is close to one, while for a chaotic orbit of GM map D_C is somewhere between 1 and 2, depending on the phase plane filling property of the attractor.

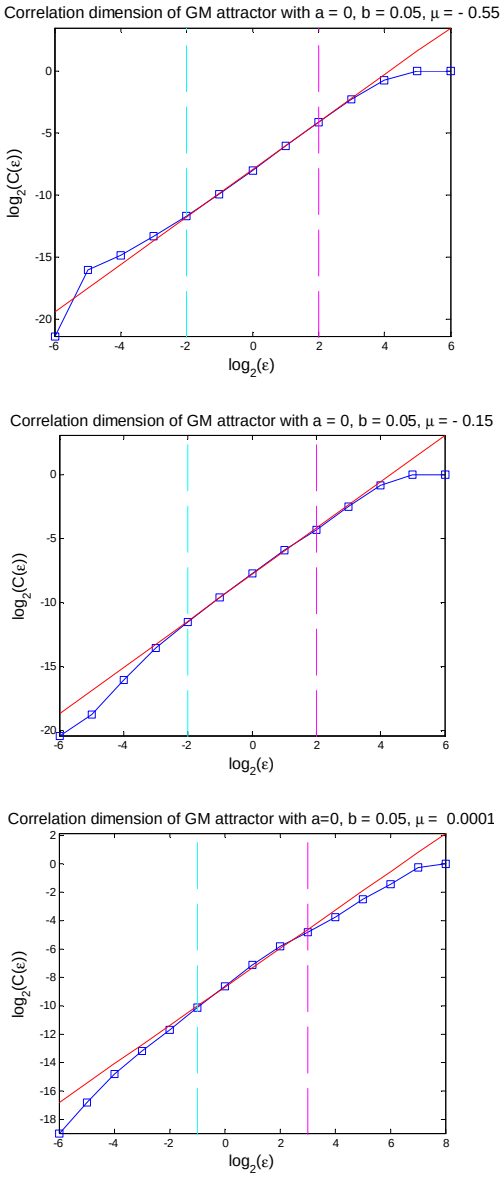

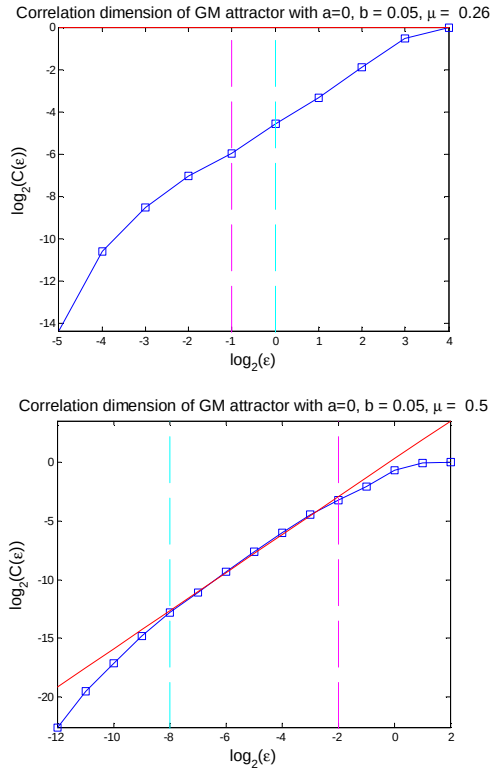

Figure 4 The curves for $\log_2 C(N,\varepsilon)$ against $\log_2 \varepsilon$ in the case of GM map with a = 0.0 and b = 0.05

Table 1. Correlation dimension for GM map with b = 0.05, $a \in \{0.0, 0.008\}$ and μ values considered in Figures 2 and 3

a	μ	D_C	**Type of orbit**
0.0	- 0.95	1.8464	Chaotic
	- 0.75	1.8093	Chaotic
	- 0.55	1.9053	Chaotic
	- 0.15	1.8186	Chaotic
	0.0001	1.3813	Chaotic
	0.26	1.8211	Chaotic
	0.50	1.6176	Chaotic
	0.75	1.0098	Quasi – periodic
0.008	- 0.52	0.00002	Periodic (T = 3)
	- 0.495	1.1932	Chaotic
	- 0.45	1.8380	Chaotic
	0.16	1.9050	Chaotic
	0.60	0.0885	Periodic (T = 56)
	0.90	1.0814	Quasi - periodic

Dependence of D_C on the number N of the data points

The D_C value for a given set of parameters (a,b,μ) depends smoothly on the number N of the data points used in the relation (3). On the other side, the computational time increases strongly with N (see Table 2). As is it observed in all the analyzed cases, the value N = 2,000 realizes a good compromises between computational time and an acceptable value or correlation dimension.

Table 2 Dependence on number of points N of the correlation dimension D_C and computational time T_C for a = 0.008, b = 0.005, μ = 0.16

N	T_C **(seconds)**	D_C
500	3.12	1.8034
1,000	11.66	1.9114
2,000	69.35	1.9019
3,000	202.23	1.9633
4,000	436.72	1.9234
5,000	823.82	1.9050
6,000	1,123.15	1.9115

More than three quarters of the computational time is used to compute the separation distance matrix between every two points of the set O (step 3). Thus, for μ = 0.16 and N = 5,000, computational time is equal with 823.82 sec. From this time, 0.01097 sec were used for generating the orbit O (step 2), 662.32 sec for computing the separation distance matrix and 161.49 sec for constructing correlation integral and computing the correlation dimension.

How many points to ignore on either ends of the plot of $\log_2 C(N,\varepsilon)$ against $\log_2 \varepsilon$?

A more serious source of errors in D_C finding is the number of points to ignore on either ends of the plot of $\log_2 C(N,\varepsilon)$ against $\log_2 \varepsilon$ before fitting a (red) line with least square method. If this number is chosen in an unsuitable way, then wrong conclusions on the type of orbit are to be expected.

As an example, let consider the case a = 0.008, b = 0.05, and μ = 0.6, corresponding to a 56 – periodic orbit. Table 3 shows the values of the correlation dimension for different numbers of ignored points on either ends of the above-mentioned graph. The right value, D_C = 0, is obtained by ignoring an important number of points (see also the Figure 5)

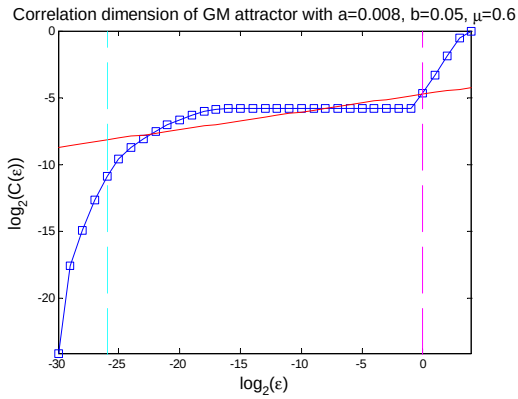

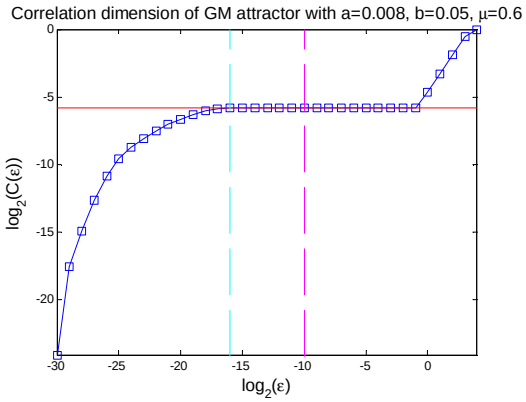

Figure 5 Influence of number of ignored points on either ends of the plot of $\log_2 C(N,\varepsilon)$ against $\log_2 \varepsilon$ on the value of correlation dimension D_C
Up: 4 points are ignored (D_C = 0.1319)
Down: 14 points are ignored (D_C = 0.00002)

Table 3 Dependence of D_C on the number of ignored points on either ends of the plot of $\log_2 C(N,\varepsilon)$ against $\log_2 \varepsilon$

Number of ignored points on either ends	D_C
4	0.1319
6	0.0885
8	0.0620
10	0.0361
12	0.0101
14	0.00002

5. CONCLUSIONS

In the paper, the well-known Gumowski – Mira map has been considered, and an algorithm implemented under MatLab software package has been proposed that can be used to obtain the standard Grassberger - Procaccia correlation dimension of an attractor. Our main conclusions are as follows:

- the algorithm computes accurate values of the correlation dimension for different types of attractors, when compared with the reported values in the literature;
- the influence of some parameters like the length of the finite sample of discrete points on the attractor used in the algorithm or the number of neglected points on graph of $\log_2 C(N,\varepsilon)$ against $\log_2 \varepsilon$ is investigated. While a large value of the first parameter makes the algorithm very expensive from computational time of view, the second parameter could change the decision regarding the character of the analyzed orbit, especially for periodic and quasi-periodic cases;
- to take into account large sets of data, other algorithms, more efficient, are required.

6. REFERENCES

[1] GRASSBERGER, P., PROCACCIA, I., *Characterization of strange attractors*, Physical Review Letters, 50, p. 346 – 349, 1983.
[2] FALCONER, K., *Fractal geometry – Mathematical foundations and applications*, John Wiley and Sons Ltd., 1999.
[3] FARMER, J.D., OTT, J., YORKE, J.A., *The dimension of chaotic attractors*, Physica D, 7, p. 153-170, 1983.
[4] AL – SHAMERI, W.F.H., *Correlation dimension of an attractor generated by an orbit of general two – dimensional iterated quadratic map*, Int. J. Contemp. Math. Sciences, 7, p. 413 - 424, 2012.
[5] SAHA, L.M., SAHNI, N., *Chaotic evaluations in a modified coupled logistic type predator-prey method*, Applied Mathematical Sciences, 6, p. 6297 - 6942, 2012.
[6] THEILER, J., *Efficient algorithm for estimating the correlation dimension from a set of discrete points*, Physical Review A, 36, p. 4450-4462, 1987.
[7] DELEANU, D., *Comparative numerical analysis of largest Lyapunov exponent calculation techniques*, Constanta Maritime University Annals, 21, p. 141-148, 2013.
[8] GUMOWSKI, I., MIRA, C., *Recurrence and discrete dynamical systems*, Springer, 1980.
[9] KOTARSKI, W., LISAWSKA, A., *On Gumowski – Mira aesthetic super - fractal forms, http://www. Maplesoft.com/applications/view.aspx*
[10] OTSUBO, K., WASHIDA, M, ITOH, T., KATSUURA, K., HAYASHI, M., *Computer simulation on the Gumowski – Mira Transformation*, Forma, 15, p. 121 – 126, 2000
[11] SAHA, L.M., DAS, M.K., BUDHRAJA, M., *Characterization of attractors in Gumowski – Mira map using Fast Lyapunov indicators*, Forma, 21, p. 151 – 158, 200

ON A GEOMERIC APPROACH OF SAFE BASIN'S FRACTAL EROSION. APPLICATION TO THE SYMMETRIC CAPSIZE EQUATION

DELEANU DUMITRU

Constanta Maritime University, Romania

ABSTRACT

The paper investigates the fractal erosion of basins of attraction, which provide valuable information about the loss of engineering integrity of a ship and is one of the tools extensively used in an attempt to understand the mechanisms behind ship capsizing. As a model for a vessel capsize in quartering regular waves, the symmetric capsize equation derived by Kan and Taguchi is considered, which contains a cubic term in the restoring moment, a linear damping and a single harmonic excitation forcing term. The paper also proposes a new geometric way to evaluate the process of fractal erosion of the safe basin and presents some weak points of the coarse grid-of-starts method.

Keywords: *Capsize of a ship, safe basin of attraction, fractal erosion, normalized integrity curves.*

1. INTRODUCTION

By *capsizing* or *keeling over* of a ship we understand that situation when the ship is turned on its side or it is upside down. In the language of nonlinear dynamics, capsizing is a transition from a stable equilibrium point near the upright position to a stable equilibrium point near the upside-down position. This phenomenon is a challenging task for naval engineers because it is responsible not only for a lot of material damages, but also for human lives. Theoretical studies and experiments showed that the common reasons for capsizing of ships are parametric roll resonance, broaching, water on deck, extreme and Fricke waves or loss of stability at a wave crest [1].

Development of nonlinear dynamics in the 1980s and significant enhancement of computational capabilities opened new possibilities to study this dangerous phenomenon. Tools like safe basins and integrity curves [2, 3], Lyapunov exponents [4], correlation dimension and system entropy are extremely used in an attempt to understand the mechanisms behind capsizing.

In the paper, we concentrate mainly on the exact and approximate determination of boundaries of safe motion in the space of control parameters. There have been published many important studies of vessel capsizing using this technique. They were done by Rainey et al [5], Kan and Taguchi [6], McMaster and Thompson [7], Bishop and de Souza [8, 9], Falzano et al [10] and others. Most of them are dealing with a ship in regular waves. Simple equations have been used to model the ship's motion. Generally, they describe the roll motion using Newton's second law and contain a polynomial (usually quadratic or cubic) term in the restoring moment. The damping is assumed to be linear whereas the regular waves are represented by a single frequency harmonic excitation.

In present study the following equation, derived by Kan and Taguchi, is taken as a model for a vessel capsize in quartering regular waves:

$$\ddot{x} + \beta \dot{x} + x - x^3 = F \sin \omega t \qquad (1)$$

where β, ω and F are constants representing the normalized damping coefficient, the non-dimensional frequency and amplitude of the exciting moment, respectively, x is the normalized angle of roll and t is the normalized time. A dot denotes differentiation with respect to normalized time. The details about equation (1) can be found in [6].

Despite of its simplicity, equation (1) shows a wide spectrum of qualitatively distinct types of behaviors, including steady-state solutions, jumps to resonance or period doubling cascades leading to chaos. In the next sections, we make a short description of safe basins and integrity curves concepts, then apply them to the case of the symmetric capsize equation (1) and investigate the merits and the weak points of the coarse grid-of-starts method proposed by Bishop and de Souza [8].

2. SAFE BASIN CONCEPT. APPLICATIONS

Safe basin concept has been introduced in 1990s for the study of nonlinear ship rolling and capsize. The safe basin is the set of initial conditions in the phase plane $(x, \dot{x})$ which define the separatrix between capsize and non-capsize areas and illustrate the high sensitivity of capsize to initial conditions. In fact, for a given configurations of parameters (β, F, ω), the safe basin of attraction is formed by all initial conditions $(x(0), \dot{x}(0))$ that do not lead to capsize (escape). As Bishop and de Souza have pointed out, the size, shape and locations of safe basins provide valuable information about the engineering integrity of the ship. Safe basins can be generated numerically by various techniques including cell-to-cell mapping and coarse grid-of-start method. The simulation show that an increasing of the amplitude of the excitation leads to a process of fractal erosion of the safe basin, finished with a sharp decrease of safe area, well before the final loss of stability obtained by conventional steady-state analysis [11, 12].

This behavior was founded in our numerical investigation too. To show this, we assume throughout the paper the fixed value $\beta = 0.1$ and change the values

for ω and F. The capsize equation (1) is solved numerically by Runge-Kutta-Gill method, implemented in MatLab package environment, up to ten cycles of the forcing (having period $T = 2\pi/\omega$). Our investigation was restricted at this time interval because experiments and numerical simulations have showed that if escape has not occurred within 8 – 10 cycles than it is unlikely to appear in the following cycles. The initial conditions $(x(0), \dot{x}(0))$ was selected from a vast set having 48,000= 240 x 240 elements, obtained by dividing the rectangle $[-1.2,1.2]\times[-1.0,1.0]$ in equally spaced segments. Each point is tested against the escape criterion, and classified as safe or not. If it is safe then a small black rectangle is drawn around it in the phase plane $(x, \dot{x})$, otherwise the rectangle is maintain white. In this way, the safe basin is given by the black area in the phase plane. The escape criterion is suggested by our numerical experience on equation (1). We considered the point $(x(0), \dot{x}(0))$ safe if the absolute value of the displacement *x(t)* not exceeds 1, that means the distance between local minimum and one of the local maxima of the potential function $(V(x) = x^4/4 - x^2/2$, associated to equation (1).

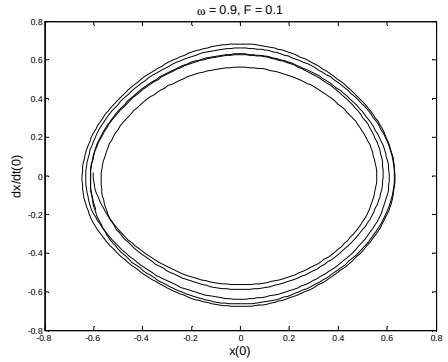

(a)

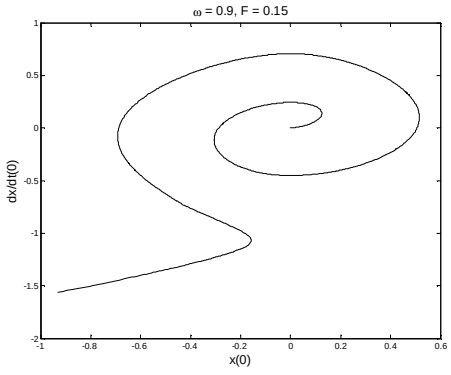

(b)

Figure 1The phase trajectory of: a) a non-capsizing oscillation; b) a capsizing oscillation

For a non-safe point, the associated trajectory goes out in the phase plane, like a spiral with expanding amplitude (see Figure 1).

The fractal erosion experienced by the safe basin could follow different routes, as indicated in Figures 2 to 4. Thus, Table 1 and Figure 2 present a slow and permanent reduction of safe basin owing to he increasing of the excitation amplitude *F*. The boundary is eroded by very thin fractal striations.

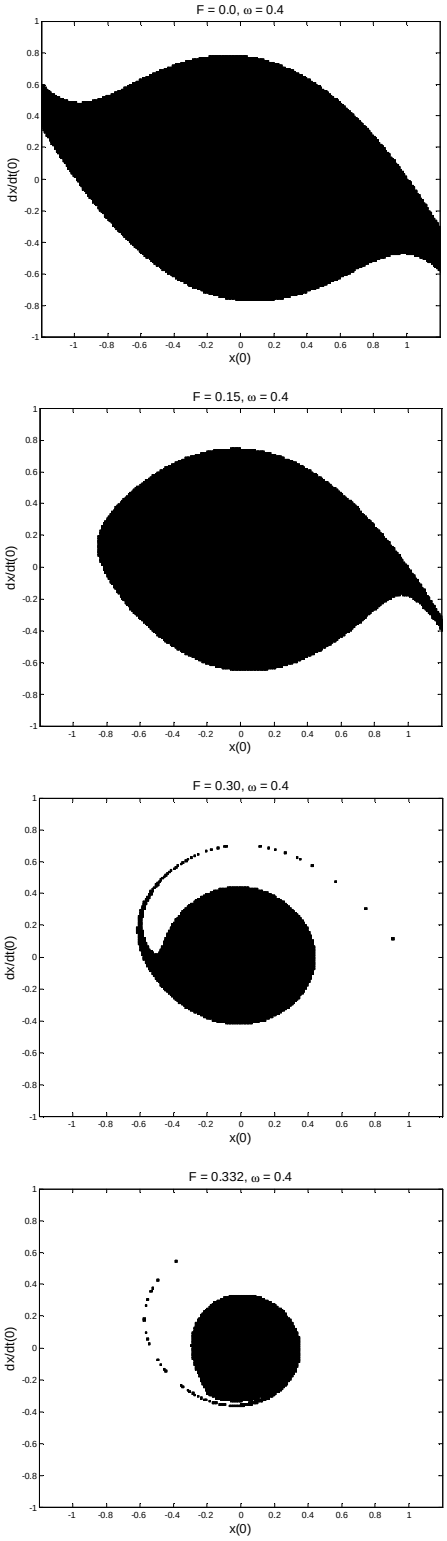

Figure 2 Slow erosion of the safe basin for equation (1) with $\omega = 0.4$

Table 1. Erosion of safe basin for eq. (1) with $\omega = 0.4$

F	**0.0**	**0.15**	**0.30**	**0.332**
Safe basin (number of black points)	24,573	18,415	6,465	3,537

Other type of fractal erosion is shown in Figure 3. Now, if the forcing amplitude *F* increases, the safe basin is eroded in a more complicated way. The start is given by a thin whiskers that begin to invade into the safe basin (see Figure 3 a). If *F* continues to grow, the whiskers increase in number and area and transform into thick fingers (see Figures 3b and 3c). The safe basin of attraction diminishes and, at $F \cong 0.3$, disappears completely (See Figure 3d). This scenario is reproduce also in Table 2.

Finally, Figure 4 displays an intermediate situation. First, as *F* increases, the safe basin is eroded outside, especially on $\dot{x}$ direction. The first whiskers begins to appear just at $F \cong 0.65$ but then grow very quickly and invade almost all basin (see also Table 3).

Table 2. Erosion of safe basin for eq. (1) with $\omega = 0.9$

F	**0.0**	**0.11**	**0.15**	**0.20**	**0.26**
Safe basin (number of black points)	24,573	22,490	12,764	5,383	2,484

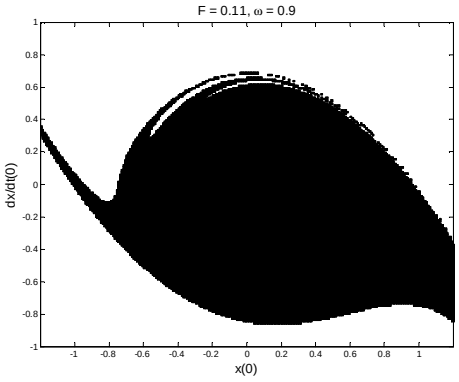

(a)

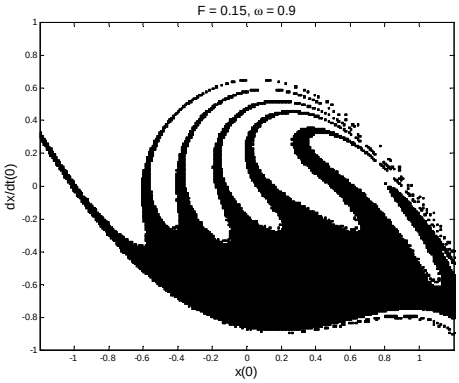

(b)

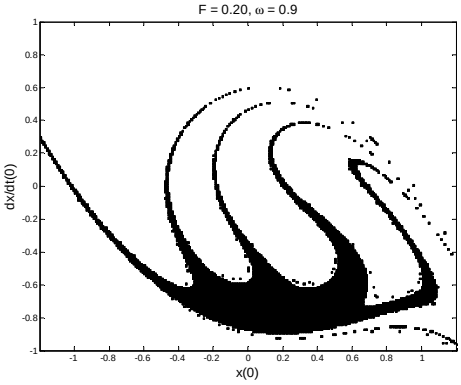

(c)

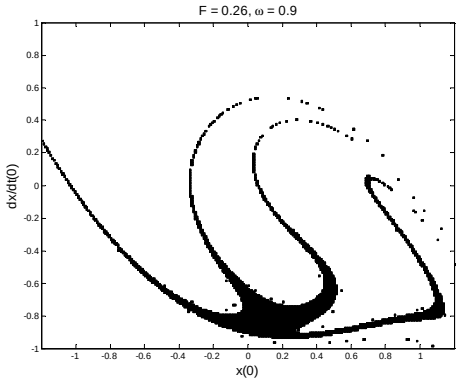

(d)

Figure 3 Erosion of the safe basin for equation (1) with $\omega = 0.9$

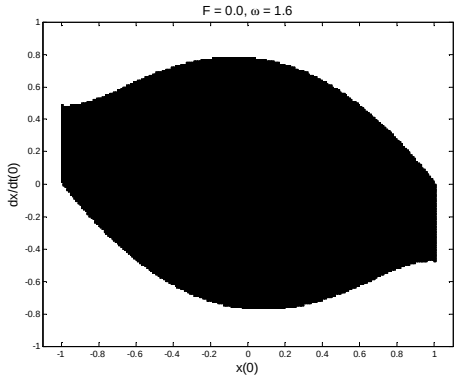

(a)

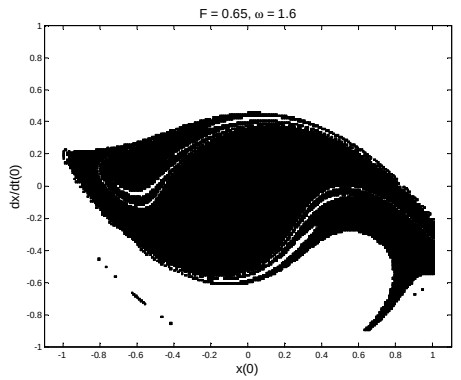

(b)

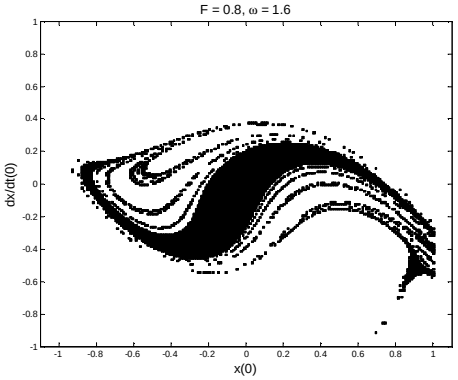

(c)

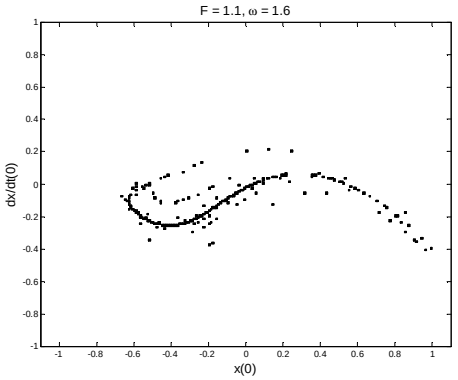

(d)

Figure 4 Erosion of the safe basin for equation (1) with $\omega = 1.6$

Table 3. Erosion of safe basin for eq. (1) with $\omega = 1.6$

F	**0.0**	**0.65**	**0.80**	**1.10**
Safe basin (number of black points)	24,573	13,050	4,469	200

3. INTEGRITY CURVE CONCEPT. APPLICATION TO EQUATION (1)

Every panel in Figures 2 to 4 requires apx. 80 min CPU time on our computer, so the computational cost for having a complete image of the fractal erosion of safe basin for a given (β, ω) pair is remarkably high.

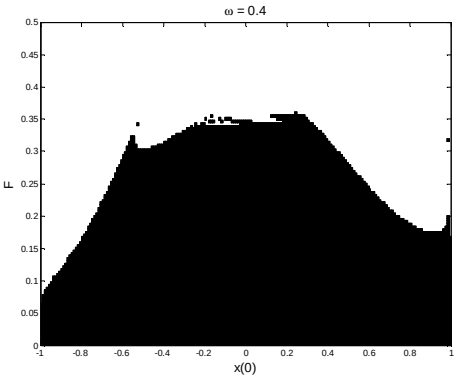

(a)

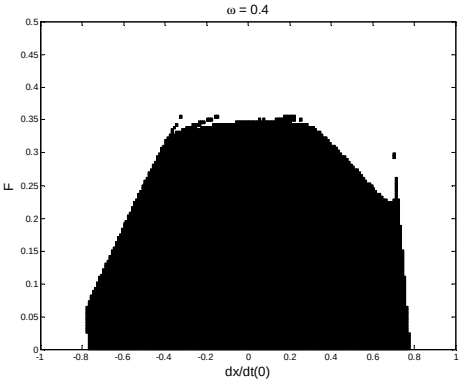

(b)

Figure 5 Intersection between safe basins and: a) x axis; b) $\dot{x}$ axis, for $\omega = 0.4$

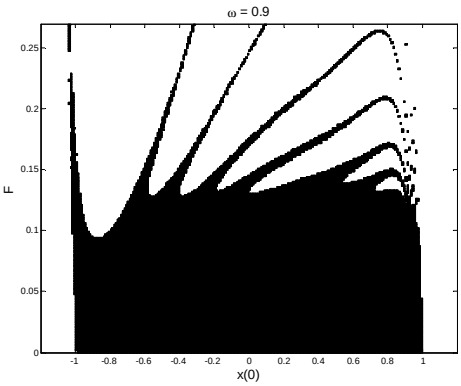

(a)

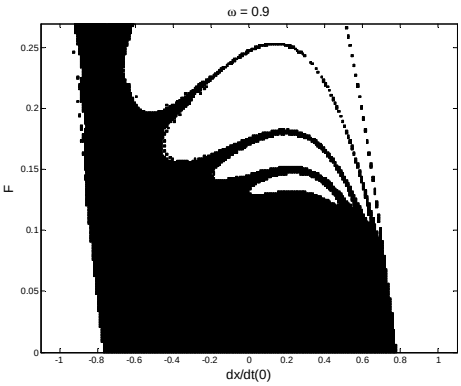

(b)

Figure 6 Intersection between safe basins and: a) x axis; b) $\dot{x}$ axis, for $\omega = 0.9$

To avoid this, we plot instead the intersection between safe basins and x, respectively $\dot{x}$ axis, for any value of excitation's amplitude F that leads to emptiness safe basins. The results are given in Figures 5 to 7. The panels have been constructed for 100 values of F chosen uniformly in the mentioned intervals.

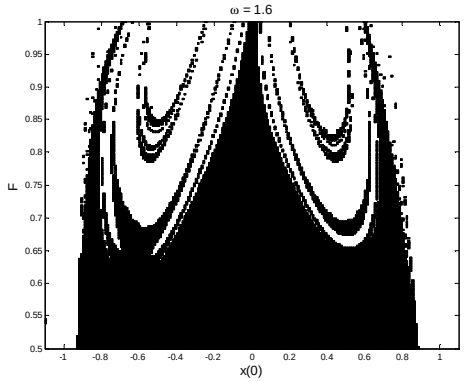

(a)

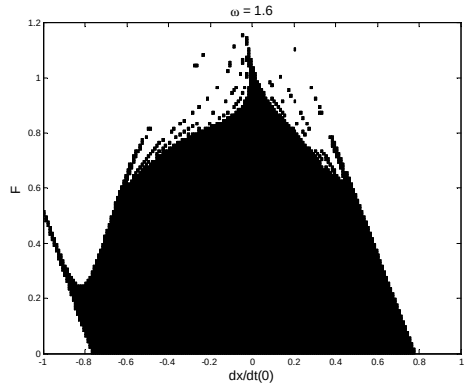

(b)

Figure 7 Intersection between safe basins and: a) x axis; b) $\dot{x}$ axis, for $\omega = 1.6$

Although less than an hour have been necessary for the whole computational process (for every panel), we have now a clear image of both exterior and interior erosion of safe basin. Moreover, these pictures will be helpful in the next section.

The integrity curves show the relative influence of wave excitation's amplitude F on capsize relative to vessel safety in the absence of incident waves. They could be generated by plotting the safe area, normalized to unity at $F = 0$, over the same ranges of F values used in Figures 5 to 7. The simulations results are displayed in Figures 8 to 10 (the asterisks). They must be considered together with Tables 1 to 3. The above-mentioned figures contain also the curves giving the dependence of safe segments (normalized to unity at $F = 0$) along x and

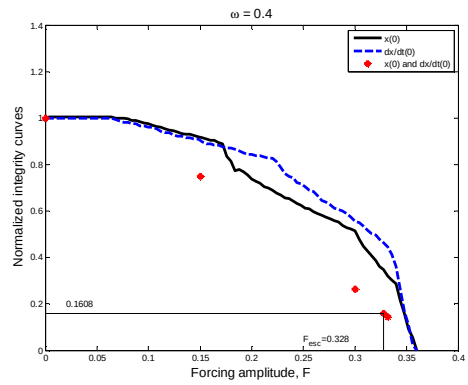

Figure 8 Normalized integrity curves for $\omega = 0.4$

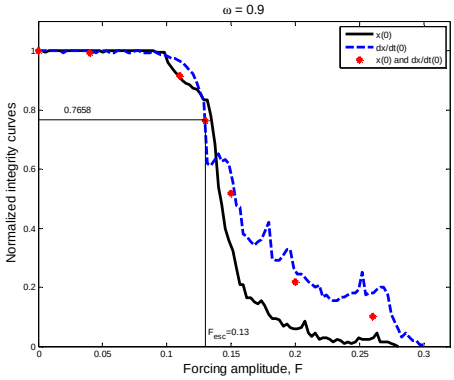

Figure 9 Normalized integrity curves for $\omega = 0.9$

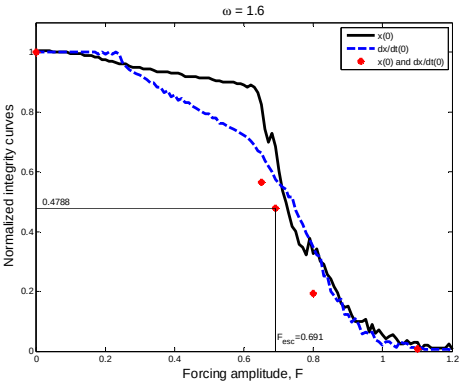

Figure 10 Normalized integrity curves for $\omega = 1.6$ $\dot{x}$ axis, respectively, on excitation's amplitude.

Although the computational cost for constructing these curves is small compared with that needed for a complete integrity curve, these additional curves provide practically the same behavior for the safe basin. Looking for a compromise between computational cost and accuracy of the results, the use of additional curves seems to be very promising.

4. COMMENTS ON COARSE GRID-OF-STARTS METHOD

In the 1990s, Bishop and de Souza proposed the coarse grid-of-starts method as a means of quickly estimating the boundaries of safe motion in the control parameter space of periodically forced nonlinear oscillators [9]. By performing numerical integrations of equations of motion from different starting points around the origin they were able to detect any significant change in the size and nature of the safe basin of attraction.

More precisely, they have considered a uniform one-dimensional grid, laid along the x axis, having a given number of starting points and length. The equation of motion is integrated for each point of the grid and for a given pair (β, ω), under transient conditions of up to 8 waves. The escape value, F_{esc}, is defined as the smallest value of excitation's amplitude F for which escape occurs for any starting point of the grid. The authors observed little sensitivity of the results to the number of points of the grid and the fact that longer grids predict the smallest escape value F_{esc}. For these

reasons, they adopted grids with just three starting points placed in origin and in symmetrically positions around it.

We implemented their algorithm in the case of capsize equation (1) and we think that some observations are worth to be mentioned.

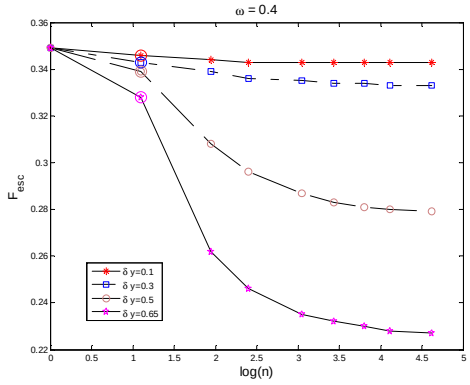

(a)

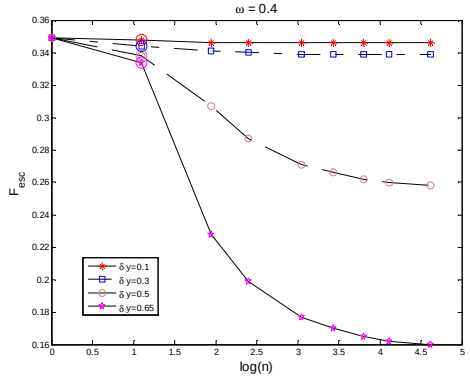

(b)

Figure 11 Effect of number n of starting points and of the grid's length on the escape force for $\omega = 0.4$:

a) grid laid along x axis; b) grid laid along $\dot{x}$ axis

First of all, we started our investigation with sensitivity tests involving grid size and length. Grids were considered both on x and $\dot{x}$ axis and the simulations have been restricted to transient motions of 10 cycles of the forcing. At least two situations are possible. For $\omega = 0.4$, the safe basin decreases almost linearly with F until $F \cong 0.3$ and then it is swiftly eroded till total disappearance around $F \cong 0.35$ (see Figures 5 and 8). In this case, the sudden loss of integrity could be detected from just one point, the origin, for lengths smaller than 0.6. For bigger lengths, the algorithm provides information about exterior erosion of safe basin, and there exist a strong dependence of the results on the number of points in the grid (see also Tables 4 and 5). This is obvious from Figure 11 where the effect of number of starting points and grid length on escape force is emphasized, both on x and $\dot{x}$ directions. The encircled points and the bolded numbers correspond to the coarse grid-of-starts method (n = 3).

Table 4. Effect of number n of starting points and of grid's length on the escape force for $\omega = 0.4$. Grid is laid along x axis

N	**1**	**3**	**11**	**31**	**101**
$\Delta x = 0.1$	0.349	0.346	0.343	0.343	0.343
$\Delta x = 0.3$	0.349	0.343	0.336	0.334	0.333
$\Delta x = 0.5$	0.349	0.339	0.296	0.283	0.279
$\Delta x = 0.65$	0.349	**0.328**	0.246	0.232	0.227

Table 5. Effect of number n of starting points and of grid's length on the escape force for $\omega = 0.4$. Grid is laid along $\dot{x}$ axis

n	**1**	**3**	**11**	**31**	**101**
$\Delta \dot{x} = 0.1$	0.349	0.348	0.346	0.346	0.346
$\Delta \dot{x} = 0.3$	0.349	0.344	0.341	0.339	0.339
$\Delta \dot{x} = 0.5$	0.349	0.344	0.287	0.266	0.258
$\Delta \dot{x} = 0.65$	0.349	**0.334**	0.199	0.170	0.160

For $\omega = 0.9$, the exterior erosion of safe basin for F smaller than 0.11 is of little importance. Starting with $F \cong 0.12$, the thin escape whiskers rapidly transform themselves into thick fingers that penetrate the bulk of the basin and produce a rapid erosion of the entire basin of attraction (see Figures 5, 6 and 9). Figure 12 shows the basic idea behind the course grid-of-starts method. Green lines represent the grid with three starting points for $\Delta x = 0.1$, while the red lines give the same grid for $\Delta x = 0.65$. Because the "fingers" penetrated the entire safe basin beginning with almost the same F value, the escape show little sensitivity to the number of starting points and size of the grid (see also Figure 13a and Table 6). When the grid is chosen on $\dot{x}$ axis, a grid with $\Delta \dot{x} = 0.65$ and $n \geq 10$ is able to detect the appearance of the whiskers into the safe basin (see Figures 3a, 6b, 13b and Table 7).

An intermediate situation was founded for $\omega = 1.6$. Here, the interior erosion is divided into two significant areas that does not contain $\dot{x}$ axis (see Figure 7).

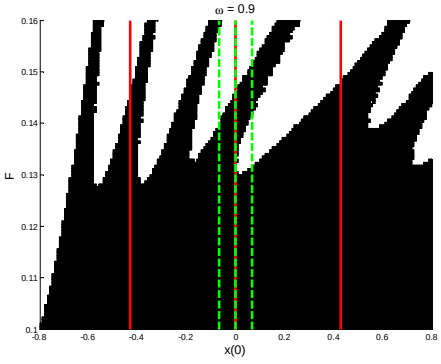

Figure 12 Basic idea of coarse grid-of-starts method

The grids with one single starting point give less conservative estimate for escape while long grids with three points are not capable to detect the exterior erosion of safe basin along $\dot{x}$ axis (see also Figure 14 and Tables 8 and 9).

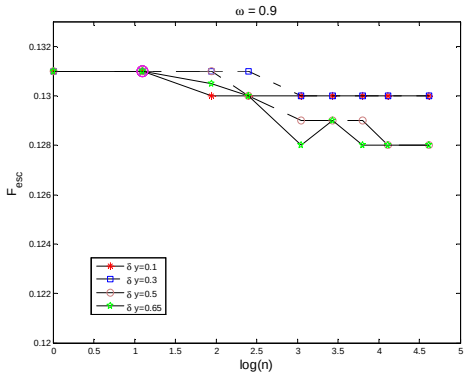

(a)

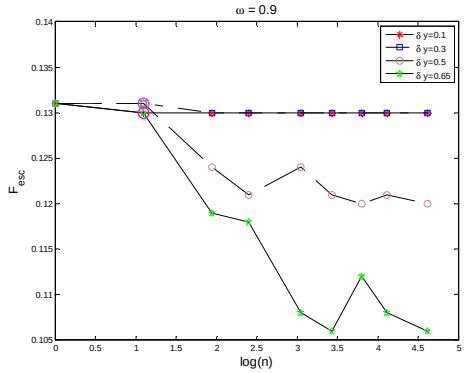

Figure 13 Effect of number n of starting points and of the grid's length on the escape force for $\omega = 0.9$:

a) grid laid along x axis; b) grid laid along $\dot{x}$ axis

Table 6. Effect of number n of starting points and of grid's length on the escape force for $\omega = 0.9$. Grid is laid along x axis

n	1	3	11	31	101
$\Delta x = 0.1$	0.131	0.131	0.130	0.130	0.130
$\Delta x = 0.3$	0.131	0.131	0.131	0.130	0.130
$\Delta x = 0.5$	0.131	0.131	0.130	0.129	0.128
$\Delta x = 0.65$	0.131	**0.131**	0.130	0.129	0.128

Table 7. Effect of number n of starting points and of grid's length on the escape force for $\omega = 0.9$. Grid is laid along $\dot{x}$ axis

n	1	3	11	31	101
$\Delta \dot{x} = 0.1$	0.131	0.130	0.130	0.130	0.130
$\Delta \dot{x} = 0.3$	0.131	0.131	0.130	0.130	0.130
$\Delta \dot{x} = 0.5$	0.131	0.131	0.121	0.121	0.120
$\Delta \dot{x} = 0.65$	0.131	**0.130**	0.118	0.106	0.106

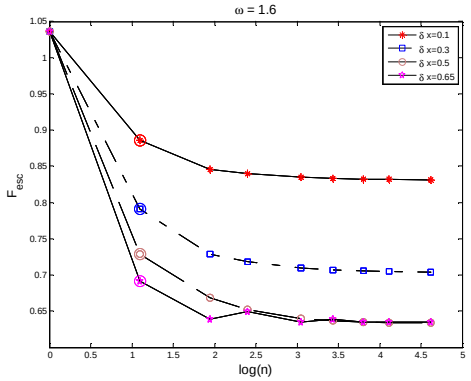

(a)

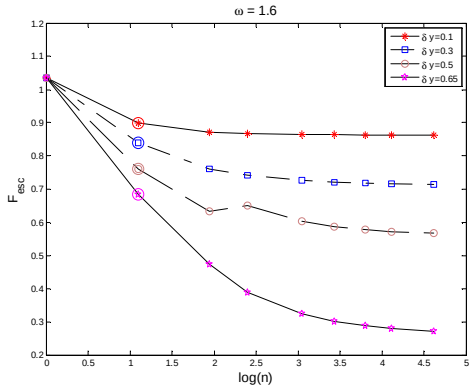

(b)

Figure 14 Effect of number n of starting points and of the grid's length on the escape force for $\omega = 1.6$:

a) grid laid along x axis; b) grid laid along $\dot{x}$ axis

Table 8. Effect of number n of starting points and of grid's length on the escape force for $\omega = 1.6$. Grid is laid along x axis

n	1	3	11	31	101
$\Delta x = 0.1$	1.036	0.886	0.840	0.833	0.831
$\Delta x = 0.3$	1.036	0.791	0.718	0.707	0.704
$\Delta x = 0.5$	1.036	0.729	0.652	0.637	0.634
$\Delta x = 0.65$	1.036	**0.691**	0.649	0.639	0.635

Table 9. Effect of number n of starting points and of grid's length on the escape force for $\omega = 1.6$. Grid is laid along $\dot{x}$ axis

n	1	3	11	31	101
$\Delta \dot{x} = 0.1$	1.036	0.899	0.868	0.864	0.863
$\Delta \dot{x} = 0.3$	1.036	0.840	0.741	0.721	0.714
$\Delta \dot{x} = 0.5$	1.036	0.760	0.651	0.587	0.566
$\Delta \dot{x} = 0.65$	1.036	**0.685**	0.389	0.302	0.271

5. CONCLUSIONS

In this study, a thorough numerical analysis of the safe basin's fractal erosion is performed, using as model the symmetric capsize equation derived by Kan and Taguchi. Different ways of erosion of safe basin were presented and normalized integrity curves were plotted. The paper proposed a new geometric way to estimate the process of fractal erosion of safe basin, by considering the intersection of safe basin with the axis defining the roll angle and roll velocity. This approach allowed us to discuss and to present some weak points of the coarse grid-of-starts method proposed by Bishop and Souza.

6. REFERENCES

[1] HINZ, T., *Mathematical models in description of capsizing scenarios*, Archives of Civil and Mechanical Engineering, 7 (3), p. 125 – 134, 2007.
[2] WU, X., TAO, L., LI, Y., *The safe basin erosion of a ship in waves with single-degree-of freedom*, 15th Australian Fluid Mechanics Conference, Sydney, Australia, 2004.
[3] HUANG, X., *The investigation of the safe basin erosion under the action of random waves*, 8th International Conference on the Stability of Ships and Ocean Vehicles (STAB' 2003) , Spain, 2003.
[4] DELEANU, D., *Comparative numerical analysis of largest Lyapunov exponent calculation techniques*, Constanta Maritime University Annals, 21, p. 141-148, 2013.
[5] RAYNEY, R.C.T., THOMPSON, J.M.T., *The transient Capsize Diagram, A new method of quantifying stability in waves*, Journal of Ship Research, 35(1), 1992.
[6] KAN, M., TAGUCHI, H., *Chaos and fractals in ship capsizing*, Towards the Harnessing of Chaos, ed. M. Yamaguti, p. 365 – 368, Elsevier Science, Amsterdam, 1994.
[7] THOMPSON, J.M.T., RAYNEY, R.C.T., SOLIMAN, M.S., *Mechanics of ship capsize under direct and parametric wave excitation*, Philosophical Transactions of the Royal Society A, 338, p. 471 – 490, 1992.
[8] BISHOP, S.R., SOUZA, J.R., *Transient and steady state operational limits for ship roll*, Applied Mechanics Revue, 46, no. 11, p. 47 – 52, 1993.
[9] SOUZA, J.R., BISHOP, S.R., *Boundaries of safe motion through a coarse grid-of-starts*, Journal of the Brazilian Society of Mechanical Sciences, 20(4), p. 564 – 575, 1998.
[10] FALZARO, J.M., *Predicting complicated dynamics leading to vessel capsizing*, Ph.D. Thesis, Department of Naval Architecture and Marine Engineering, University of Michigan, Ann Arbor, MI, 1990.
[11] THOMPSON, J.M.T., *Chaotic phenomena triggering the escape from a potential well*, Proceedings of the Royal Society London A, 421, p. 195 – 225, 1989.
[12] SOLIMAN, M.S., THOMPSON, J.M.T., *Transient and steady state analysis of capsize phenomenon*, Applied Ocean Research, 13, p. 82 – 92, 1991.
[13] TAYLAN, M., *Static and dynamic aspects of a capsize phenomenon*, Ocean Engineering, 30, p. 331 – 350, 2003.
[14] VIRGIN, L.M., *The nonlinear rolling response of a vessel including chaotic motions leading to capsize in regular seas*, Applied Ocean Research, 9(2), p. 89 – 95, 1987.
[15] McCUE, L.S., TROESCH, A.W., *Use of Lyapunov exponents to predict chaotic vessel motions*, 7th International Ship Stability Workshop, Shangai Jiao Tong University, China, 2004.
[16] FALZARO, J.M., SHAW, S.W., TROESCH, A.W., *Application of global methods for analyzing dynamical systems to ship rolling motion and capsizing*, International Journal of Bifurcation and Chaos, 2(1), p. 101 – 115, 1992.

AN IMPROVED GENETIC ALGORITHM FOR SOLVING CONSTRAINED NONLINEAR OPTIMIZATION PROBLEMS

DINU SIMONA

Constanta Maritime University, Romania

ABSTRACT

Constrained nonlinear optimization problems represent a class of mathematic programming problems commonly found in real-world applications. Evolutionary Algorithms have been intensively used to solve this kind of problems, especially for continuous optimization problems whose search space is restricted by a large set of constraints. The strategy used for constraint handling represents an important aspect of evolutionary constrained optimization. The proposed Genetic Algorithm is based on homomorphous mappings which transform the representations space in the feasible solutions space, according to the problem. The algorithm also integrates a preselection scheme in order to guide the search process toward the global optimum. The performance of the adopted approach is tested and analysed on two benchmark functions, with promising results.

Keywords: *Genetic Algorithm, constrained nonlinear optimization, homomorphous mappings.*

1. INTRODUCTION

Constrained optimization problems are often used in practical applications in economics, finance, statistics, medicine, etc. Most economic decisions are the result of optimization problems that pursue goals that are subject to one or more restrictions, such as:
- consumers seeking to maximize the utility, taking decisions on what to buy, constrained by the available budget;
- firms are taking decisions regarding production in order to maximize profits, constrained by limited production capacities;
- marketing managers, aiming to maximize sales, being constrained by a fixed budget allocated for advertising;
- production managers aiming to choose the optimal economic process with the maximum economic benefit, meeting in the same time the required quality level; the minimizing of the total production cost while the domestic or foreign market place requirements impose limitations on quantities produced; another objective may be to maximize output while keeping the consumption of resources (human, material, financial, equipment) within the available stocks;
- portfolio managers seeking optimal capital allocation for those investments that offer maximum profit under minimum risk conditions;
- in macroeconomics, one seeks tax (fiscal) policy formulation, for example determining the maximum amount for a tax on gasoline, while minimizing customer dissatisfaction, etc.

2. CONSTRAINED OPTIMIZATION PROBLEM

A constrained optimization problem, generally, may be written as:

$$\textbf{min } f(x) \qquad (1)$$

$$\text{with constraints: } \begin{cases} x \in A \\ x \in B \end{cases}$$

where:

**) f is the objective function (criterion function or goal function) and represents the mathematical expression of the optimization criterion/criteria

**) $x \in R^n$ is the decision variable vector

***) the restriction $x \in A$ is defined by the parametrical restrictions $x_i^{\min} \le x_i \le x_i^{\max}$ which define the n-dimensional search space S={ $x \in R^n \mid x_i^{\min} \le x_i \le x_i^{\max}$, i=1,...,n}

****) the restriction $x \in B$ is defined by restrictions such as $g_p(x) \le 0$, $p=1,...,\overline{p}$; $h_q(x)=0$, $q=1,...,\overline{q}$ which define the allowed domain (the feasible region) $F \subset S$, $F=\{x \in R^n \mid g_p(x) \le 0, p=1,...,\overline{p}\ ; h_q(x)=0, q=1,...,\overline{q}\}$

Observations:
1) Any problem regarding the determination of the maximal value of a function *f(x)* can be written as a problem of the determination of the minimum value of the function *-f(x)*, because $\max_{x \in F} f(x) = -\min_{x \in F} -f(x)$.

2) The objective function and the functions that define the restrictions can be linear or nonlinear.

3) Equality restrictions, $h_q(x)=0$, $q=1,...,\overline{q}$, can be transformed in inequality restrictions after performing a transformation such as:

$$|h_q(x)| - \varepsilon \le 0, \text{ where } \varepsilon \text{ is a very small tolerance} \qquad (2)$$

3. CONSTRAINT HANDLING TECHNIQUES

Constraint handling techniques for classical optimization algorithms are classified by K. Deb [4] as follows:

-generic methods (universal) - in which the linearity/ non-linearity of the restrictions is not taken into consideration, for instance the Lagrange multipliers method, penalty functions;

-specific methods - applicable only to certain types of restrictions (convex feasible domains or a small number of variables, linear restrictions, etc.), for instance the Simplex method, gradient-based methods, cutting-plane method.

Evolutionary Algorithms represent one of the most important methods for solving nonlinear constraint optimization problems. Due to the fact that the genetic operations that transform the genotype have a random character, the applications of those algorithms in the constraint optimization problems can lead to infeasible solutions.

This aspect can be solved in several ways [3]:

- through direct techniques, in which the search procedure takes into account only feasible solutions: "death penalty" - the rejection of infeasible individuals, "repairing" techniques of the infeasible individuals, decoding functions, homomorphous mappings;
- through indirect techniques - in which the search procedure considers both the feasible and the infeasible solutions: penalty functions - the most utilized functions, strategies favoring feasible solutions in relation to the infeasible ones, techniques based on Multi-Objective Evolutionary Algorithms;
- through hybrid approaches, for instance the GENOCOP III Algorithm [9]- a combination between the repairing algorithms and co-evolutionary concepts, the Segregated Genetic Algorithm [8] - a combination between penalty functions and populations which co-evolve, AIS-GA [2] - a combination between an artificial immune system and a genetic algorithm, etc.

3.1 Constraints handling by homomorphous mappings

The homomorphous mappings [7] transform the n-dimensional cube $[-1,1]^n$ (the representations space) in the feasible solutions space, F, according to the problem, through a mapping T.

$[-1,1]^n$ is the cartesian product of n sets [-1,1],where n is the length of the chromosome and implicitly the length of the decision variable vector.

For two elements (n=2), the representation space $[-1,1]^2$ represents a square.

First of all, an one to one mapping is defined Ψ: $[-1,1]^n \rightarrow S$, where S is the problem's search space, defined as the cartesian product of the ranges of values for the variables of the problem.

In order to define the mappingΨ, this study proposes a complex codification with a diploid genotype [12], a population (of a fixed size, PS) of diploid chromosomes, being given as:

$$\rho_i^{gen} = (\rho_{[1]i}^{gen} \ldots \rho_{[p]i}^{gen} \ldots \rho_{[n]i}^{gen}), \text{ gen}=0,\ldots,G_{MAX}, \qquad (3)$$

$$\theta_i^{gen} = (\theta_{[1]i}^{gen} \ldots \theta_{[p]i}^{gen} \ldots \theta_{[n]i}^{gen})$$

i=1,…,PS

where $\rho_{[p]i}^{gen}$ and $\theta_{[p]i}^{gen}$ represent the module respectively the angle of the complex representation for gene p of the individual i.

The initial population is randomly generated, based on the following equations:

$$\rho_{[p]i}^{0} = [rand]\frac{u(p)-l(p)}{2} \qquad (4)$$

$$\theta_{[p]i}^{0} = [rand]2\pi; \quad y_{[p]i}^{0} = \cos\theta_{[p]i}^{0} \qquad (5)$$

i=1,…,PS

The mapping Ψ is defined as follows:

$$\Psi(y_{[1]},\ldots,y_{[p]},\ldots,y_{[n]})=(x_{[1]},\ldots,x_{[p]},\ldots,x_{[n]})$$

where:

$$x_{[p]i}^{gen} = \rho_{[p]i}^{gen} y_{[p]i}^{gen} + \frac{u(p)+l(p)}{2} \qquad (6)$$

p=1,...,n; i=1,...,PS ; gen=0,...,G_{MAX}

l(p) and u(p) represent the lower limit respectively the upper limit of the decision variable x_p

One can notice that $u(p) \leq x_{[p]i}^{gen} \leq l(p)$, p=1,...,n; i=1,...,PS ; gen=0,...,G_{MAX} .

A reference point $r_0 \in F$ forms a line segment L with the point $s=\Psi(y/y_{max})$ located on the border of space S. The segment L is defined by:

$$L(r_0,s)= r_0+q\,(s- r_0) \text{ for } 0\leq q\leq 1 \qquad (7)$$

If F is convex, L intersects F's border in exactly one point, for a $q_0 \in [0,1]$:

$$x_{q0} = r_0+q_0(s- r_0) \text{ for } 0\leq q_0\leq 1 \qquad (8)$$

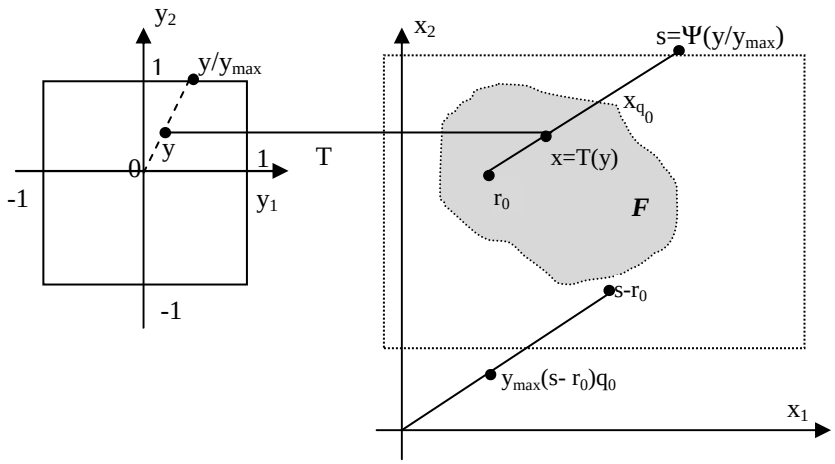

Figure 1 Mapping T between cube *[-1,1]*^{n} and space F in the bi-dimensional case [7]

Based on the intersection point, homomorphous mapping defines a mapping T between the decoded solution, y, and the feasible point x on segment L, which belongs to F.

The mapping T is defined as follows:

$$T(y)= r_0+y_{max}(s- r_0)q_0 \quad (9)$$

where $y_{max}=max_{p=1..,n}|y_p|$

Because $y_{max}\in[0,1]$, T(y) will always be a feasible solution, x.

Each restriction $g_i(x)\leq 0$, i=1, …, m of the problem can be represented as a function βi of the independent variable q (for a fixed reference point r_0 and a point s, which is located on the border of S):

$$\beta_i(q) = g_i(L(r_0,s)) = g_i(r_0+q(s- r_0)) \quad (10)$$

for $0\leq q\leq 1$and i=1,..,m

Once the intersection points q_0 between segment L and restrictions $g_i(x)\leq 0$, i=1,..,m have been determined, as solutions to the equations $\beta_i(q)=0$, the feasible solutions x=T(y) will be calculated, according to (9).

An extensive study for handling the problems where the region F is non-convex or consisting of disjoint sub-regions is presented in [7].

4. DESCRIPTION OF THE PROPOSED ALGORITHM

The proposed algorithm follows the steps corresponding to the general scheme of a Genetic Algorithm:

```
t←0; // initialize the iteration index
 Population P(t)←Create_Population(PS)
 //PS represents the population size
 while (¬Termination_condition)
          // number of iterations
    Evaluation P(t) ← Fitness_Assignment(P(t))
    Intermediate population P1(t) ←
    Population_Selection (P(t))
      Population P(t) ←Variation (P1(t))
    // applying crossover and mutation operators
      t←t+1;
  repeat
```

Initial population $P(0) = \{y_1^0, \ldots, y_{PS}^0\}$ is generated as follows:

Generate:

$$(\rho^0_{[1]1}\ldots\rho^0_{[p]1}\ldots\rho^0_{[n]1})\ldots\ldots\ldots(\rho^0_{[1]PS}\ldots\rho^0_{[p]PS}\ldots\rho^0_{[n]PS})$$

$$(\theta^0_{[1]1}\ldots\theta^0_{[p]1}\ldots\theta^0_{[n]1})\ldots\ldots\ldots\ldots(\theta^0_{[1]PS}\ldots\theta^0_{[p]PS}\ldots\theta^0_{[n]PS})$$

Where

$$\rho^0_{[p]i} = [rand]\frac{u(p)-l(p)}{2} \quad (11)$$

i=1,…,PS, p=1,…,n

$$\theta^0_{[p]i} = [rand]2\pi \quad (12)$$

where l(p) and u(p) represent the lower limit respectively the upper limit of the decision variable x_p

Then define:

$$(y^0_{[1]1}\ldots y^0_{[p]1}\ldots y^0_{[n]1})\ldots\ldots\ldots(y^0_{[1]PS}\ldots y^0_{[p]PS}\ldots y^0_{[n]PS})$$

↧ ↧

y_1^0 y_{PS}^0

i=1,…,PS, p=1,…,n

where:

$$y^0_{[p]i} = \cos\theta^0_{[p]i} \quad (13)$$

Step 1:

Generate randomly $r_0=(r_{[1]0}, \ldots, r_{[p]0},\ldots,r_{[n]0}) \in F$

Then, for each point $y_i^0=(y_{[1]i}^0...y_{[p]i}^0...y_{[n]i}^0)$ *i=1,…,PS*

Determine $\tau=\max_{p=1,n}|y_{[p]i}^0|$

Then, determine the point s=($s_{[1]}$, …, $s_{[p]}$, …,$s_{[n]}$), where:

$$s_{[p]}=\begin{cases}\rho_{[p]i}*(y_{[p]i}^0/\tau)+\dfrac{u(p)+l(p)}{2}, \text{if } (y_{[p]i}^0/\tau)\notin\{-1,1\}\\ l(p), \text{ if } (y_{[p]i}^0/\tau)=-1\\ u(p), \text{ if } (y_{[p]i}^0/\tau)=1\end{cases} \quad (14)$$

Solve equations $g_k(r_0+q(s-r_0))=0$, where $q\in[0,1]$

and k= 1,…,m.

Choose that solution $q_0\in[0,1]$ as the solution of

that equation $g_k(r_0+q(s-r_0))=0$ (namely $\beta_k(q)=0$) and which verifies that the point $x_{q0}=r_0+q_0(s-r_0)$ lies on the border of F, therefore the conditions $\beta_j(q_0)\leq 0$ are fulfilled, j=1,…,m, j≠k.

Generate the point $x_i=(x_{[1]i},\ldots,x_{[p]i},\ldots,x_{[n]i})\in F$,

$$x_i=r_0+\tau(s-r_0)q_0 \quad (15)$$

Note: Each point $y_i\in[-1,1]^n$ corresponds now to a point

$x_i\in F$, *i=1,…,PS.*

Step 2:
Set t=0.

Step 3:
The chromosomes of population P(t) = {y_1,…, y_{PS}} are evaluated as follows:

$$fitness(y_i)=\varphi(y_i)=\frac{f(x_i)}{\sum_{i=1}^{PS}f(x_i)} \quad (16)$$

The algorithm continues with the main processing steps involved in a Genetic Algorithm.

In order to improve the performances, the algorithm is hybridized with a preselection scheme in a non-generational algorithm (in the new population are introduced the most performing individuals in both the populations, the parents chromosomes and the offspring chromosomes, as well).

The preselection scheme consists of the following steps:

1. Select a pair of two parents chromosomes p_1 and p_2, randomly.
2. Apply crossover operator N_r times; N_r offsprings will be generated.
3. Apply mutation operator; the next N_r offsprings will be generated.
4. The best individual, c_1, in the first set of N_r offsprings shall be obtained.
5. The best individual, c_2, in the next set of N_r offsprings (that have mutations) shall be obtained.
6. If c_1 is a better individual than p_1, then p_1 will be replaced by $c_1$in the population; if c_2 is a better individual than p_2, then p_2 will be replaced by c_c in the population.

The scheme works for each generation, the chromosomes being paired randomly.

The crossover operation takes place both for the module and for the angle of the complex representation. Thus, for two chromosomes with modules:

$\rho_1=(\rho_{[1]1}...\rho_{[p]1}...\rho_{[n]1})$ and respectively

$\rho_2=(\rho_{[1]2}...\rho_{[p]2}...\rho_{[n]2})$

and angles:

$\theta_1=(\theta_{[1]1}...\theta_{[p]1}...\theta_{[n]1})$ and respectively

$\theta_2=(\theta_{[1]2}...\theta_{[p]2}...\theta_{[n]2})$

after crossover, the two offsprings will have:

$$\rho_{c_1}=(....,r\times\rho_{[p]1}+(1-r)\times\rho_{[p]2},....) \text{ and}$$
$$\theta_{c_1}=(....,r\times\theta_{[p]1}+(1-r)\times\theta_{[p]2},....) \quad (17)$$

and respectively

$$\rho_{c_2}=(....,(1-r)\times\rho_{[p]1}+r\times\rho_{[p]2},....) \text{ and}$$
$$\theta_{c2}=(....,(1-r)\times\theta_{[p]1}+r\times\theta_{[p]2},....) \quad (18)$$

where r is a random number between 0 and 1.

This study uses the non-uniform mutation [10] for an argument module.

Thus, if $\rho=(\rho_{[1]}...\rho_{[p]}...\rho_{[n]})$ is the module of an offspring obtained after crossover, and $\rho_{[p]}$ is the randomly selected gene for mutation, the result will be:

$\rho^{mut}=(\rho_{[1]}...\rho_{[p]}^{mut}...\rho_{[n]})$, where:

$$\rho_{[p]}^{mut}=\begin{cases}\rho_{[p]}+(x_{[p]}^{\max}-\rho_{[p]})f(gen), \text{ if } r_1<0.5\\ \rho_{[p]}+(\rho_{[p]}-x_{[p]}^{\min})f(gen), \text{ if } r_1>0.5\\ \rho_{[p]}, \text{ otherwise}\end{cases} \quad (19)$$

where:

$$f(gen)=(r_2(1-\frac{gen}{G_{\max}}))^{\tau} \quad (20)$$

r_1, r_2 are randomly generated numbers in the range (0,1);

gen is the current generation;

τ is a parameter that determines the dependence on the number of iterations. In this study we consider $\tau = 3$.

For the angle of an argument, we propose an operator defined by Dinu [5]. Thus, if: $\theta = (\theta_{[1]}...\theta_{[p]}...\theta_{[n]})$ is the module of an offspring obtained after crossover, and $\theta_{[p]}$ is the randomly selected gene for mutation, the result will be $\theta^{mut} = (\theta_{[1]}...\theta^{mut}_{[p]}...\theta_{[n]})$,where:

$$\theta^{mut}_{[a_k]} = \begin{cases} \max(\theta_{[p]} - f(gen)\cdot\pi,\ 0), \text{ if } r_1<0,5 \\ \min(\theta_{[p]} + f(gen)\cdot\pi,\ 2\pi), \text{ if } r_1>0,5 \\ \theta_{[p]}, \text{ otherwise} \end{cases} \quad (21)$$

where: $$f(gen)=1-r_2^{(1-\frac{gen}{G_{\max}})^{\tau}} \quad (22)$$

and the other parameters are as defined above.

As shown in the equations (20) and (22), the magnitude of the change decreases with the proximity to the maximum number of generations. Thus, these mutation operators perform a global search at the beginning of iterative searching process and a local search in the final generations. Moreover, both the ability of local search algorithm and algorithm efficiency are improved.

5. CASE STUDY AND RESULTS

The performance of the described algorithm is analyzed on the basis of two test functions in the literature:

1) Min $f_1(x) = 5.3578547\cdot x_3^2 + 0.8356891\cdot x_1x_5 + 37.293239x_1 - 40792.141$

with restrictions:

$g_1(x) = 85.334407 + 0.0056858\cdot x_2x_5 + 0.00026\cdot x_1x_4 - 0.0022053\cdot x_3x_5$

$g_2(x) = 80.51249 + 0.0071317\cdot x_2x_5 + 0.0029955\cdot x_1x_2 + 0.0021813\ x_3^2$

$g_3(x) = 9.300961 + 0.0047026\cdot x_3x_5 + 0.0012547\cdot x_1x_3 + 0.0019085\cdot x_3x_4$

$0 \le g_1(x) \le 92$
$90 \le g_2(x) \le 110$
$20 \le g_3(x) \le 25$
$78 \le x_1 \le 102$
$33 \le x_2 \le 45$
$27 \le x_3 \le 45$
$27 \le x_4 \le 45$
$27 \le x_5 \le 45$

The problem was originally proposed by Himmelblau [6] and subsequently used in the approaches based on penalty functions.

The problem has the optimal solution x^*=[78 , 33 , 27.070 , 45 , 44.969] with f^* = -31026.032, restrictions g_1 and g_3 being active at the optimum point.

2) Min $f_2(x) = x_1 + x_2 + x_3$

with restrictions:

$g_1(x) = 1-0.0025(x_4 + x_6)$
$g_2(x) = 1-0.0025(x_5 + x_7 - x_4)$
$g_3(x) = 1-0.01(x_8 - x_5)$
$g_4(x) = x_1x_6 - 833.33252x_4 - 100x_1 + 83333.333$
$g_5(x) = x_2x_7 - 1250x_5 - x_2x_4 + 1250x_4$
$g_6(x) = x_3x_8 - 1250000 - x_3x_5 + 2500x_5$
$0 \le g_1(x)$
$0 \le g_2(x)$
$0 \le g_3(x)$
$0 \le g_4(x)$
$0 \le g_5(x)$
$0 \le g_6(x)$
$100 \le x_1 \le 10000$
$1000 \le x_i \le 10000$ i=2,3
$10 \le x_i \le 1000$ i=4,..,8

The problem was proposed in [11] and has the optimal solution x* = (579.3167, 1359.943, 5110.071, 182.0174, 295.5985, 217.9799, 286.4162, 395.5979) cu f(x*) = 7049.33, all the 6 restrictions being active in the optimum point.

To summarize, each problem is characterized by various parameters analyzed, according to Table 1: number of decision variables (n), function type, the relative size of the feasible region in the search space (ρ), the number of restrictions in each category (linear inequalities IL, respective nonlinear inequality IN) and the number of active constraints at the optimum point (α).

Table 1. Parameters characterizing the analyzed problems

function	n	function type	ρ	*IL*	*IN*	α
$f_1(x)$	5	quadratic	46.87%	0	6	2
$f_2(x)$	8	linear	0.002%	3	3	6

The value for ρ was determined experimentally, generating randomly 1,000,000 points in the search space S and checking whether or not they are belonging to feasible region F. The lower value of ρ, the more difficult to solve the problem. Also, the difficulty of the problem is given by the specific objective function, but also by the feasible region topology.

Average normalized Euclidean distance is obtained by calculating the average of these distances for all individuals of the population.

Following the study presented in [1], Figure 2 and Figure 3 present the average normalized Euclidean

distance and the proportion between the known optimum and the best feasible determined value for the two test functions.

Population diversity prevents premature convergence. An indicator of diversity is the distance between members of the population, calculated as the normalized Euclidean distance:

$$d_{ij} = \sqrt{\frac{1}{n}\sum_{k=1}^{n}\left(\frac{x_k^i - x_k^j}{x_k^{\max} - x_k^{\min}}\right)^2} \quad \text{i,j =1,...,PS} \qquad (23)$$

30 runs of the algorithm were performed for each problem, with a population of 20 individuals and 200 generations. For each run, as a reference point r_0 was selected the first point of the randomly generated admissible points.

Average normalized Euclidean distance is obtained by calculating the average of these distances for all individuals of the population.

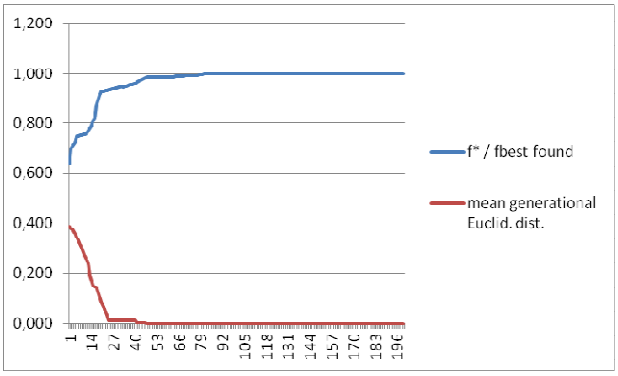

Figure 2 Results obtained for function $f_1(x)$

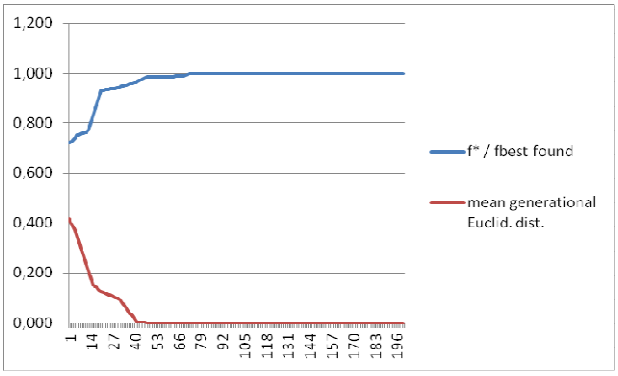

Figure 3 Results obtained for function $f_2(x)$

Figure 4 and respectively Figure 5 present the evolution of the objective functions $f_1(x)$ and $f_2(x)$.

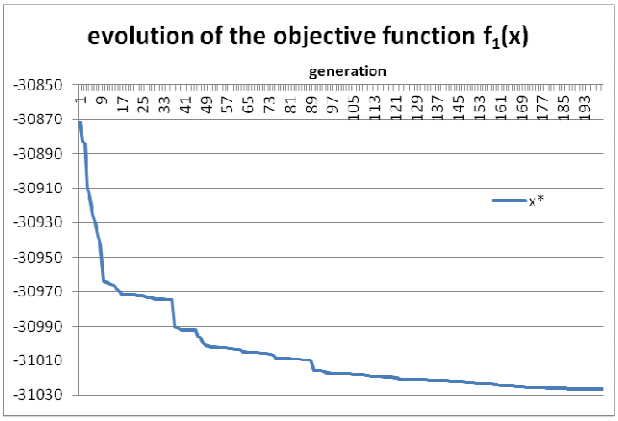

Figure 4: The evolution of the objective function $f_1(x)$

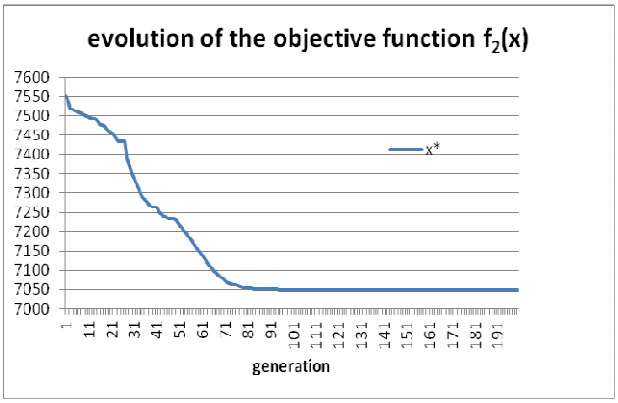

Figure 5 The evolution of the objective function $f_2(x)$

Table 2 present the results obtained by the proposed algorithm in 30 runs for the two functions.

SD is the standard deviation of the objective function values obtained in 30 runs:

$$SD = \sqrt{\sigma^2} = \sqrt{\frac{\sum(f(x) - \overline{f(x)})^2}{30}} \qquad (24)$$

AVEDEV function calculates the average of the absolute deviations of the objective function values from their arithmetic mean.

$$\frac{\sum|f(x) - \overline{f(x)}|}{30} \qquad (25)$$

Table 2. Results obtained by the proposed algorithm

Function	Average running time	$f(x)_{best}$	$f(x)_{worst}$	$\overline{f(x)}$	SD	AVEDEV
$f_1(x)$	28 s	-31026.032	-31025.882	31026.0264	0.0071	0.0053
$f_2(x)$	204 s	7049.332	7050.981	7050.201	0.0083	0.00061

6. CONCLUSIONS

Many real-world applications are expressed as constrained nonlinear optimization problems. These problems are very complex and difficult to solve.

In order to address these problems, this study proposes a non-generational Genetic Algorithm based on homomorphous mappings. The adopted approach incorporates a preselection scheme in order to guide the search process toward the global optimum.

The proposed algorithm does not depend on the characteristics of the objective function and functions

defining constraints, on the number and the type of decision variables and constraints or on structural characteristics of the search space. It doesn't require the use of a penalty function, whose main disadvantage is the fact that the penalty parameters are specific to each problem and need numerous attempts of tuning.

Experiments performed on two benchmark functions have shown that the proposed approach is efficient and is promising for wide adaptation in real life problems.

7. REFERENCES

[1] AL JADAAN, O., RAJAMANI, L. AND RAO, C.R., *Adaptive Penalty Function For Solving Constrained Evolutionary Optimization*, Journal of Theoretical and Applied Information Technology, Vol. 5, No. 3, 2009.

[2] BERNARDINO, H.S., BARBOSA, H.J., LEMONGE, A.C.C. and FONSECA, L.G., *On GA-AIS Hybrids for Constrained Optimization Problems in Engineering*, Constraint-Handling in Evolutionary Optimization, Studies in Computational Intelligence, Vol. 198, 2009

[3] COELLO, C.A. , MENZURA-MONTES, E., *A Survey of Constraint-Handling Techniques Based on Evolutionary Multiobjective Optimization*, PPSN workshop on Multiobjective Problem Solving from Nature, Reykjavik, Iceland, 2006

[4] DEB, K., *An efficient constraint handling method for genetic algorithms*, Computer Methods in Applied Mechanics and Engineering,186 (2–4), 2000

[5] DINU, S., BORDEA, GH., *A new genetic approach for transport network design and optimization*, Bulletin of the Polish Academy of Sciences: Technical Sciences, Vol. 59 (4) , 2011

[6] HIMMELBLAU, D., *Applied Nonlinear Programming, McGraw-Hill*, 1992

[7] KOZIEL, S., MICHALEWICZ, Z., *Evolutionary algorithms, homomorphous mappings, and constrained parameter optimization*, Evolutionary Computation, Vol. 7(1), 1999

[8] LE RICHE, R., KNOPF-LENIOR, C. and HAFTKA, R.T., *A segregated genetic algorithm for constrained structural optimization*, Proceedings of the 6th International Conference on Genetic Algorithms, 1995.

[9] MICHALEWICZ, Z., NAZHIYATH, G., *Genocop III: A co-evolutionary algorithms for Numerical Optimization Problems with Nonlinear Constraints*, IEEE Proc. of the Second International Conference of Evolutionary Computation, Perth, Australia, 1995

[10] MICHALEWICZ, Z., *Genetic Algorithms + Data Structures = Evolution Programs*, Berlin, Springer, 1994

[11] MICHALEWICZ, Z., DEB, K., SCHMIDT, M. and STIDSEN, T., *Test-case generator for nonlinear continuous parameter optimization techniques*, IEEE Trans. Evolutionary Computation 4(3), 2000

[12] WANG, Y., GAO, S., ZHANG, H. and TANG, Z., *An Improved Genetic Algorithm Based Complex-valued Encoding*, IJCSNS International Journal of Computer Science and Network Security, VOL.10 (6), 2010

SECTION V
TRANSPORT ECONOMICS

EUROPEAN UNION'S FUNDING INSTRUMENTS IN TRANSPORT IN THE PERIOD 2014-2020

BRANZA GRATIELA

Constanta Maritime University, Romania

ABSTRACT

For the period 2014-2020, European Union has settled vital objectives through its Europe 2020 Strategy. All these are not possible without the support of funding instruments. So, the Commission promotes an integrated investment, combining three financing instruments of the European Union: European Regional Development Fund, Cohesion Fund and European Social Fund. The present paper presents a history of cohesion policy and its role in order to meet the goals of Europe 2020 strategy. Having in view that in the core of the Strategy there are four priorities (innovation and research, digital agenda, support for SMEs and low-carbon economy), the paper aims to stress the importance of promoting sustainable transport and improving network infrastructures, especially through developing resource-efficient, secure and competitive transport system like high-speed lines.

Keywords: *European Union, Transport, Cohesion Policy, Europe 2020 Strategy, Funding, TEN-T, High-Speed Rail*

1. COHESION POLICY

Cohesion Policy is an important tool of investment, being concentrated on reducing the economic, social and territorial disparities, in order to meet the goals of Europe 2020 strategy, meaning: job creation, business competitiveness, economic growth, sustainable development, improving people's quality of life.[1]

Table 1. History of Cohesion Policy in the European Union

Year	Action
1957	The Treaty of Rome mention for the first time the regional differences issue.
1958	The creation of European Social Fund (ESF).
1975	Creation of the European Regional Development Fund (ERDF).
1986	The Single European Act established the legal framework for "Regional Policy".
1988	The integration of Structural Funds into "Cohesion Policy" in order to cope with the accession of Greece, Spain and Portugal.
1993	Maastricht Treaty introduces the Cohesion Fund (CF), the Committee of the Regions and the principle of subsidiarity.
1994-1999	Almost a third of the European Union budget is allocated to the Funds.
1995	The sparsely-populated regions of Finland and Sweden are supported.
2000	Growth, jobs and innovation become the European Union's priorities, mentioned in "Lisbon Strategy".
2000-2006	The accomplishments of Lisbon Strategy's objectives.
2004	The European Union's population has increased by 20% when ten new member states joined.
2007-2013	30% of the budget goes to environmental infrastructure and solutions to combat climate change and 25% for research and innovation.
2014-2020	The introduction of simplified rules and a better focus on outcomes in a new programming period.

Source:[5]

The European Union's strategy for the period 2014-2020 has a budget of 351,8 billion euro and concentrates on 11 thematic objectives:
- "strengthening research, innovation, technological development;
- enhancing access to and quality of, information and communication technologies;
- enhancing the competitiveness of SMEs;
- supporting the shift towards a low-carbon economy;
- promoting climate change adaptation, risk prevention and management;
- preserving and protecting the environment and promoting resource efficiency;
- promoting sustainable transport and improving network infrastructures;
- promoting sustainable and quality employment and supporting labour mobility;
- promoting social inclusion, combating poverty and any discrimination;
- investing in education, training and lifelong learning;
- improving the efficiency of public administration."[5]

This investment tool can be efficient, unless there is a well-defined strategy. In the field of transport it can be used in the frame of an existing national or regional transport strategy. In the core of Europe 2020 Strategy there are four priorities and to them must be allocated the ERDF investments: innovation and research, digital agenda, support for SMEs and low-carbon economy.[4]

In the period 2014-2020, the Commission's programmes concentrate more on delivering their objectives. So, the share of Cohesion Policy budget allocated for programmes is reconsidered. Having in view that two thirds of Europeans live in cities, around

50% of ERDF will be spent in cities, helping these to achieve sustainable and smart growth.

Overall, around 336 billion euro are allocated to national and regional programmes for growth and job's investments. The resources are: 187,5 billion euro to the ERDF (European Regional Development Fund), 63 billion euro to the Cohesion Fund, 85 billion euro to the ESF (European Social Fund). The biggest amount is allocated (124 billion euro) to research, development and innovation, small and medium enterprises (SMEs) and low-carbon economy.[4]

The second area of investment (98 billion euro) is represented by employment, social inclusion and education. On the third place are transport and energy network infrastructure with 59 billion euro allocated. The smallest amount (4,3 billion euro) will be invested in the capacity of public institutions and in the efficiency of public administrations and services.[4]

In 2014-2020 the Commission promotes an integrated investment, combining three financing instruments of the European Union: ERDF, CF and ESF. As an example, 88 programmes in 16 countries will be "multi-fund programmes". Cohesion Policy is the biggest funding instrument of the European Union, guiding the investment of a third of its budget in order to achieve the objectives of the Europe 2020 Strategy.

2. A RESOURCE-EFFICIENT TRANSPORT IN EUROPE

Focusing on resource efficiency in policy making is both a necessity and an opportunity for the European Union. This flagship initiative sets out a framework to help ensure that long-term strategies in areas such as energy, climate change, research and innovation, industry, transport, agriculture, fisheries and environment policy produce results on resource efficiency.

In 2011, there were adopted several initiatives to deliver on the resource-efficient Europe flagship, such as: "Low-carbon economy 2050 roadmap", "European Energy Efficiency Plan 2020", "White Paper on the future of transport", "Revision of the Energy Taxation Directive", "Roadmap for a resource-efficient Europe", "Cohesion Policy", "TEN-T revision", "Energy roadmap 2050", ""Smart grids", "Strategic Technology Plan in Transport" and others.[2]

The initiatives in the field of transport concentrate on a "low-carbon, resource-efficient, secure and competitive transport system by 2050 that removes all obstacles to the internal market for transport, promotes clean technologies and modernises transport networks."[2]

To enjoy the benefits of a resource-efficient and low-carbon economy, the European Commission need to fulfil three conditions. First, it has to take coordinated action in a wide range of policy areas and this action has to be supported by political environment. Secondly, the Commission must act urgently due to long investment lead-times. Last, there is a great need to empower consumers to move to resource-efficient consumption, to drive continuous innovation and ensure that efficiency gains are not lost.[3]

A resource-efficient Europe is one of the seven flagship initiatives as part of the Europe 2020 Strategy, aiming to deliver smart, sustainable and inclusive growth. This lead to investment for jobs and growth in economy.

2.1. Financing instruments for TEN-T

In the 2000-2006 period, the European Union' Structural and Cohesion Funds contributed approximately 26 billion euro to TEN projects. From 1995 to 2005, European Investment Bank (EIB) granted loans for TEN projects totalling about 65 billion euro.

For the period 2007-2013 the Council approved 8.01 billion euro in the area of transport and 0.16 billion euro in the area of energy. Because of the scarcity of resources, the Commission indicated that European Union financing resources have to be focused on the projects with the greatest added value for the entire network (for example, projects that have the goal to remove bottlenecks). In addition, the general cohesion policy operational programmes contributed to TEN-T with 43 billion euro. Starting from January 2014, the Connecting Europe Facility (CEF) is the new TEN infrastructure policy of the European Union with a budget of over 33.24 billion euro up to 2020. [9]

The general objectives in transport sector are:

-to remove bottlenecks and to improve cross-border sections;

-to ensure sustainable and efficient transport systems;

-to boost the decarbonisation of all modes of transport;

-to optimise the integration and interconnection of transport modes;

-to enhance the interoperability of transport services and to ensure the accessibility of transport infrastructure.

From the total fund of 33.24 billion euro for the implementation of the CEF for 2014-2020 period, for transport sector have been allocated over 26 billion euro in current prices, of which over 11 billion euro from the Cohesion Fund.[9]

According to the European Parliament's wishes, the priority in terms of funding will be given to more environmental–friendly modes of transport being allocated over 50% of financial fund to rail projects and 25% for road projects. The Commission has to coordinate the projects that are financed from Union's financing instruments (Union budget, the EIB, the Cohesion Fund, the European Regional Development Fund). [9]

The new European Union transport network is vital for the smart and efficient development of Europe. It will improve connections between different modes of transport and contribute to the European Union's climate change objectives. As European Commission Vice-President, responsible for transport, stated: "Transport is fundamental to an efficient European Union economy, but vital connections are currently missing. Europe's railways have to use seven different gauge sizes and only 20 of our major airports and 35 of our major ports are directly connected to the rail network. Without good connections Europe will not grow or prosper." [10]

The final purpose is that the new transport network will ensure safer and less congested travel; smoother and

quicker journeys and progressively, by 2050, the great majority of Europe's citizens and businesses will arrive in almost 30 minutes at any destination they want through this network.

The corridor approach is very important for the core network implementation and 10 corridors will be the basis for the network infrastructure. Each corridor must include three modes, three member states and two cross-border sections. The core network will connect: 83 main European ports with rail and road links, 37 key airports with rail connections into major cities, 15.000 km of railway line upgraded to high speed, 35 cross border projects to reduce bottlenecks. "This will be the economic lifeblood of the single market, permitting a real free flow of goods and people around the Union". [10]

3. HIGH-SPEED RAIL

High-speed lines (HSLs) offer European citizens a fast, secure and environmental-friendly mode of transport. HSLs revolutionised sustainable mobility, as high-speed trains develop speeds of 360 km/h. Europe wants to use the trans-European transport network "to link all HSLs on the continent into a proper integrated European high-speed network."[6] The first trans-European HSL between Paris, Brussels, Cologne, Amsterdam and London reduce significantly travel times between major German, French, Belgian, Dutch and British cities, the number of passengers increasing from 15.2 billion passenger-kilometres in 1990 to 92.33 billion in 2008.[6]

Over a half of the 30 TEN-T priority projects have been regarded high-speed lines. One good example of this type of project is ERTMS (European Rail Traffic Management System). ERTMS is an instrument co-financed by the European Union to accomplish "interoperability". It includes the wireless global system for mobile communications – railways (GSM-R) and the European train control system (ETCS). ERTMS makes HSLs interoperable and optimises rail traffic management along international corridors.

Nowadays high-speed trains are the most competitive mode of transport, because "access time is much shorter than by airplane and journey times are shorter than by car."[6] But TEN-T programme boost the cooperation between rail, air and road sector to optimise the integration of transport at European level and in order to improve transport energy use and to protect all the environmental benefits.

The competitive advantage of rail transport is even higher, due to its lowest impact on the environment. For example, a trip from Paris to Marseilles means 2,7 g/pkm (grams per passenger-kilometre) by HS train for CO_2 emissions, compared with 153 g/pkm by air and 115,7 g/pkm by car. As to energy efficiency, HS trains use 12,1 grams of petrol per passenger-kilometre, compared with 17,6 for conventional trains, 18,3 for a coach, 29,9 for a car and 51,5 for an aircraft.[6]

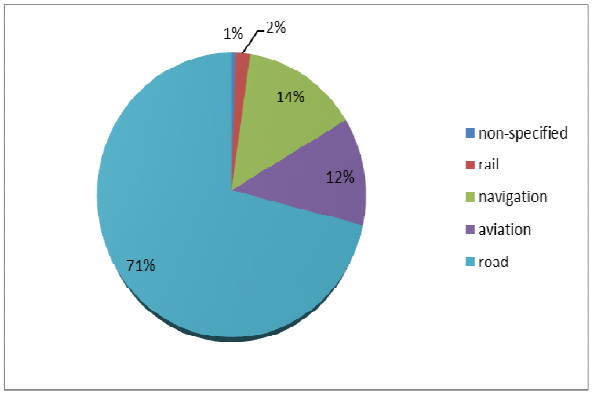

Figure 1 Transport sector CO_2 emissions by mode in 2009 in European Union
Source: [7]

High-speed trains are a truly technological success, the best result of research, development and innovation in European industry. The system parts (platforms, bridges, tunnels, track and power supply) and ERTMS work together perfectly. Due to this fact, ERTMS has become the "global industry standard".[6] Countries, like India, Mexico, South Korea, Taiwan have imported this system for its cost, its technological performance and its positive feedback.

To maintain the environmental-friendly characteristic as the most important advantage of the railway sector, the International Union of Railways and the Community of European Railways agreed on a new strategy towards 2030, focusing especially on CO_2 emissions and energy efficiency levels. The main objectives are:

-"reduce specific final energy consumption from train operation by 30% with respect to 1990 levels (pkm and gross tkm);

-reduce specific average CO_2 emissions from train operation by 50% with respect to 1990 levels (pkm and gross tkm)."[7]

4. CONCLUSIONS

Cohesion Policy is the biggest funding instrument of the European Union, guiding the investment of a third of its budget in order to achieve the objectives of the Europe 2020 Strategy.

A resource-efficient Europe is one of the seven flagship initiatives as part of the Europe 2020 Strategy, aiming to deliver smart, sustainable and inclusive growth. The new European Union transport network is vital for the smart and efficient development of Europe. The final purpose is that the new transport network will ensure safer and less congested travel; smoother and quicker journeys and progressively, by 2050, the great majority of Europe's citizens and businesses will arrive in almost 30 minutes at any destination they want through this network.

5. REFERENCES

[1] BRÂNZĂ, G., *Sustainable regional development of tourism in the European Union. Perspectives for Romanian tourism*, Masa rotundă "Dezvoltarea turistică regională în statele membre ale Uniunii Europene. O abordare cantitativă", Societatea Română de Statistică – Filiala Suceava, Universitatea "Stefan cel Mare" Suceava, 5-6 decembrie, 2014, în curs de aparitie

[2] EUROPEAN COMMISSION, *A resource-efficient Europe-Flagship initiative under the Europe 2020 strategy*, COM(2011)21, Brussels, 26.01.2011

[3] EUROPEAN COMMISSION, *Regional policy for smart growth in Europe 2020*, 2011, http://ec.europa.eu/regional_policy/index_en.htm

[4] EUROPEAN COMMISSION, *Investment for jobs and growth*, Sixth report on economic, social and territorial cohesion, Luxembourg: Publications Office of the European Union, july 2014, http://ec.europa.eu/regional_policy/cohesion_report

[5] EUROPEAN COMMISSION, *An introduction to European Union Cohesion Policy 2014-2020*, june 2014, http://ec.europa.eu/regional_policy

[6] EUROPEAN COMMISSION, *High-speed Europe, a sustainable link between citizens*, DG for Mobility and Transport, Luxembourg: Publications Office of the European Union, 2010

[7] IEA (International Energy Agency), UIC (International Union of Railways), *Railway handbook 2012*, *Energy consumption and* CO_2 *emissions*, OECD/IEA, 2012, www.iea.org

[8] IFEU (Institut fur Energie und Umweltforschung), *EcoPassenger. Environmental methodology and data, Final report*, Commissioned by UIC, Heidelberg, june 2008, http://www.ifeu.de

[9] http://www.europarl.europa.eu

[10] http://ue.mae.ro/en/

MACROECONOMIC MODELS IMPACT ASSESSMENT METHODS OF STRUCTURAL INSTRUMENTS

CIOBANU CARMEN-LILIANA

"Alexandru Ioan Cuza" University, Iasi, Romania

ABSTRACT

Macroeconomic models are instruments that can provide an integrated approach to the economy with the help of an mathematical model, calibrated on an mixture of techniques and taking into account changes made in all social and economic ensemble.

The Hermin model is a dynamic and multi-sector model that is used by most member states to assess the impact of structural funds on national economies and comparative trend analysis of financial transfers.

The Herom model offers the posibility of estimating the costs and benefits at a sectorial, at a global social and economic level, separately analysing multiple institutional and economic sectors and the economic policies results.

Keywords: *model, impact, instruments, macroeconomic.*

1. INTRODUCTION

Various macroeconomic models were studied assessing the impact of Structural Instruments on sustainable development such as Hermine, HEROM, QUEST and ECOMODE models. These models take into account historical data for long periods of time, by processing them with instruments, having the role of composing configurations adapted for restructural development models

Macroeconomic models take into account all the changes made in social and economic terms. The benefits of using macroeconomic modelelor is to enable estimation of costs and benefits at the sectoral level, social and global economic, can be analyzed separately several institutional and economic sectors and the effects of economic policies.

2. THE HERMIN MODEL

Various macroeconomic models were studied assessing the impact of Structural Instruments on sustainable development such as Hermine, HEROM, QUEST and ECOMODE models. These models take into account historical data for long periods of time, by processing them with instruments, having the role of composing configurations adapted for restructural development models

Hermin, is an annual model which makes an overview of the current situation and time horizon based on information retained, a prediction in two versions: with money and without money.

The Hermin model includes four sectors: manufacturing, services, agriculture and governmental services, being structured on three main elements: offer for each sector, absorption and distribution of income.

The Hermin model facilitates the study of the following facts:

The influence of commerce upon the studied economy, the potential of that economy to react to endogenous and exogenous stimulation;

features of different economic spheres, technological processes, configuration changes;

Instruments for adjusting and applying on the labour market Public and private sector contribution.

The basic ideas of this model, derive from the following elements: Community financial aid has, over the states, the efect consisting of two interrelated variables: long-term supply and short term demand.

The Cohesion Policy influence has been studied, using the HERMIN model, for two time horizons: 2000-2006 and 2007-2013.

Between 2000–2006, it was taken into consideration the aspect of payment and allocation of unexecuted expenses; Between 2007–2013, the study was based on sources provided by the General Directorate for Regional Policy, or it was based on the quantification of the average annual expenditure of the six beneficiary countries.

The Hermin model fulfills its role through a series of interconnected relationships between all its parts. The model is divided into three main components: supply, absorption and distribution of income. The model presents two scenarios:

a. With funds scenario;
b. Without funds scenario .

This model allows a general overview of the current situation and a simulation for the following interval, based on the information collected. The Hermin model began by studying the applicability on less developed regions such as Portugal, Greece, Spain, Ireland towords the impact of structural funds absorption. From this perspective, the public use of goods and services is interdependent with income and purchasing power. In the manufacturing sector, the GDP, is based on a supply – demand equality, under the incidence of global and national demand.

For a successful implementation of the Hermin model, there are certain useful schematization in the programs financed by the European Social Found:

- The relation between the number of students and number of people trained to be 15/1

- The cost of machinery, equipment, buildings should not exceed 50% of the total cost of wages;
- Students must receive an average annual income of about 50% of the average salary in the industry sector;
- The training staff should have a fee similar to the services sector;

According to the Hermin Model, the influence produces by the infrastructure development can be viewed from two angles :

- The direct impact of infrastructure development - - infrastructure stock increases from baseline - help improve the industrial output;
- Global productivity of the production factors - - will increase in the services and industrial sectors, which could have a negative effect rising unemployment, as advanced technology leads to less intensive use of labor.

Placing equity in human resources with the help of the European Social Fund - are supported by public funds.

The intensity of externalities system is determined by the level of development of human infrastructure on attracting EU funding and is calculated as:

$$Efectulexternalitatilor = KTRNR^{\eta}$$

Were:

KTRNR - Human capital stock resulting from Community financing;

 - elasticity coefficient of externalities.

Total expenditure in terms of industry and services for the industry sector, and for the services sector have a positive impact on economic progress by implementing programs.

European funding contributes to GDP growth in the short term, it reduces the interruption of financial support. The Hermin model's downside is that it does not take into account differences between realised investments and ex-ante allocation of EU funds.

3. THE HEROM MODEL

The Herom model (Romania's version of the Hermin model) has been designed for less developed economies, analysing the impact of structural founds over the economies, the variables transformation at macroeconomic level, over the pre-accession phenomena, with the purpose of uniforming national economic policies with those of the European Union.

The Hermin model was implemented in Romania between 1997–1999, by the Romanian Center of Economic Modelling (CERME), then improved through a project supported by the World Bank. This model directly addresses Romania and it's current situation, allowing also making long-term forecasts (2007-2020).

The Herom model is used to analyze and estimate forecast by the Ministry of Finance for long time horizons

The privileges of using the Herom model for estimating the impact of structural founds in the Romanian economy are:

- It represents a sectorial model, helping the evaluation of economic policies effects and highlighting developments across all sectors;
- It was done according to the overall configuration of the market economy;
- It estimates relations based on Romanian statistics, highlighting the specific parameters of the Romanian economy;
- It is approved by the European Commission, as a model for other states in the pre-accession and post-accession process.

The Herom model has the same time intervals, 2007 – 2013 and 2014 – 2020, as the Hermin model. When this model was designed, it was taken into account the future trend, not the study of past or present stage.

The model is based on micro-economic elements: the nature of the offer includes the aggregation of important instruments through which the Structural and Cohesion Funds induce productive potential effects (direct externalities on the output). There are also indirect externalities production factors embedded. (capital and human factors).

In order to estimate structural and cohesion founds impact, ex ante evaluation model included direct externalities (over the output) and indirect instruments (over the production factor). In order to evaluate the impact of structural founds, it's required that this instruments be incorporated in economical nature categories. The values allocated to various programs are centralized in three categories of expenditure:

a) investment in technical infrastructure;
b) improving human capital investment;
c) financial support for investment in the industrial sector, market services and agriculture;

The Herom model enables decision-makers, based on projections to make the appropriate decisions, offering the posibility to test various financial and fiscal policies, scenarios on the allocation of financial and material resources.

There are two scenarios for impact assessment analyzes on the structural funds in the period 2007-2013 and 2014-2020, both periods including analyzes related effects on the economy.

- "No funds" scenario – implies that structural founds are not taken into account, the financial financing between 2007 – 2013 lacks altogether, the financial aid level is based only on pre-accession founds at the end of 2006.
- "With funds" scenario – in which the structural founds taken into account are set by the National Development Plan, in terms of absorption rate of 100%. It is assumed that after 2013, funds are reduced to zero, which will generate an economic imbalance.

By confronting the two scenarios, "with" and "without" structural funds, it is clear that what differentiates them is the effect of attracting structural funds at a macroeconomic level. Range considered extends to the end of 2020 as the impact of structural funds on a wider horizon is more relevant.

Financial support from the Structural and Cohesion Funds will result in increased investment in 2020, they are expected to register a growth rate about 20% higher, due to the impact of structural funds.

4. THE QUEST MODEL

Quest is a neoclassic model - Keynesian, global macroeconomic, being able to study the impact of cohesion policy on the European Union. This model is based on the same principles as HERMIN model: financial management and appropriate investment plans. This model takes into account the assumption that public investments are as productive as private investment. There are several interpretations of economists, each version representing a completion of economic evaluations.

The Quest II model in Roeger and Veld's opinion, is configured on the following three levels:

- Household consumption is directly proportional to actual income and savings provided at a time;

$$C_i = \frac{(\theta + p)[V_i + I_i]P_i}{PC_i}$$

- In the business department, organizations lead to the obtaining of GDP because of capital, labor and energy used;

$$PIB_i = \left(\left[aK_i^{-p} + (1-a)E_i^{-p} \right]^{-1/p} U_{Ki} \right)^{(1-a)} (M_i U_{Ni})^a$$

- In the government department. Government expenditures are financed by income taxes, social contributions, taxes on industry, energy, VAT

$$CcG_{ii} = i_i G_i + ABS_i + i_i M_i + TNG_i + S_i + ATR_i -$$
$$-(TV_i + CAS_i + TI_i + TE_i + VAT_i + R_i)$$

Quest III model was designed in 2007-2013, specifically to evaluate the impact of Structural and Cohesion Funds to the new Member States. This model is divided into the following components: households, business department, research department, the monetary authority and the tax authority. In the business department, final goods producers, uses national and imported goods, weak, medium and strong qualified labor. Public investment in infrastructure accumulated public capital stock is given by the following formula:

$$K_i^G = (1 - \delta_G) K_{1-i}^G + I_i^G$$

5. THE ECOMODE MODEL

ECOMODE is a computerized model for general equilibrium, being a multi-sectoral model. Using this model led to the conclusion that Member States accessing EU funding higher socio-economic benefits from significant positive effects. Observable effect of European funding will be extended further due to favorable circumstances supporting infrastructure development, improving the quality of human factor productivity growth and capital.

The development is supported by public and private sector investment, which is the most crucial element of consumer investment being maintained as a result of the decrease in unemployment and increase revenues.

ECOMODE model is divided into the following three groups:

- Investment in infrastructure services sector *INVISS*
  Investment in infrastructure in the service sector in national currency in real terms

$$INVISSR = INVISS \cdot \frac{RS}{IP}$$

- Investments in workforce *INVFM* Investments in workforce expressed in national currency in real terms

$$INVFMR = INVFM \cdot \frac{RS}{IP}$$

- Investments in product development *INVDP* Investment in production development in national currency in real terms

$$INVDPR = INVDP \cdot \frac{RS}{IP}$$

6. CONCLUSIONS

Multisectoral macroeconomic evaluation models are tools able to provide a holistic approach over the computer-assisted mathematical based economy models.

Their use involves the application of econometric techniques based on statistical data on wide horizons of time and the transition to equations models, assessment of financial flows surprising directions in which changes occur in economic structure, labor or income and expenditure.

The Hermin model establishes consequences that impact the performance of application programs funding infrasturcture consequences tender with diminished effects of changes in relative prices. It is necessary that the model equations to be recalibrated annually by extrapolation of time series with a record of each variable input-output tables. The area must be detailed impact of structural funds on the factors of production, to take indirect effects of structural funds injection.

Hermin model explores the effect of a general time horizon of the Cohesion Policy, is based on the theory of growth, and was designed to study the impact of Cohesion Policy in the Member States, based on the basic idea that technical progress is determined by external factors excluding the control of economic policy, therefore, are difficult to study long-term effects in the context of accepting the possibility of increasing the productivity of factors of production.

Hermin model is a dynamic macroeconomic model, which in addition to the above virtues, manifest limitations in use among them should be emphasized in particular that this model requires a large amount of information to be applied.

Macroeconomic models have the capacity to capture reactions occurring in the economy and allow the estimation of costs and benefits across society. Unlike purely econometric models that can not be large because of lack of data on long horizons, hybrid general equilibrium models - statistical calibration has the advantage of multiple separate institutional sector analysis, and economic impact study economic policies in separate sections.

Major deficiencies are arising from the fact that most of the parameters depend on the amount of resources used. The quality of the model is closely related to the quality coefficients and applied elements which are difficult to validate.

The limits of this model should be viewed whith caution, especially in the Romanian economy, where statistical data are insuficient of inadequate fo econometrical evaluations, given the specified transition period and reduced range of time series for key variables such as those related to capital and investment types (infrastructure, machinery and equipment, etc.).

7. REFERENCES

[1] CIUPAGEA C.&MANDA A., *The Romanian HERMIN Model – ACE Project* P96-6242-R Paper, Presented in Seminar Brussels, Belgium, 1999;

[2] AMFIRESCU IULIA, *Costuri şi beneficii ale aderării la Uniunea Europeană pentru Ţările candidate din Europa Centrală si de Est*, Institutul European din România, Bucuresti, 2001;

[3] DOBRE ANA-ARIA, RAMONA COMAN (coord.), *România şi integrarea europeană*, Institutul European, Iaşi, 2005;

[4] VICTOR BOŞTINEANU - Ultimii paşi – *Absorbţia Fondurilor Structurale şi de Coeziune 2007-2013* – martie 2013;

[5] BARRY F., BRADLEY J., HANNAN A., MCCARTAN J. and Sosvilla-Rivero S., Single Market Review 1996: *Aggregate and regional impact: the cases of Greece, Spain, Ireland and Portugal*, Office for Official Publications of the European Comunities in association with Kogan page, London, 1997.

AN APPROACH FOR FORMING THE BRAND COMMUNICATION STRATEGY

DIMITRAKIEVA SVETLANA

"Nikola Vaptsarov" Naval Academy, Varna, Bulgaria

ABSTRACT

In contemporary conditions many companies are striving to develop strong brands. This gives them opportunity to win the consumers trust, to differentiate themselves from competitors and to provide additional profit. Prerequisite for brand influence of the organization on market success are its basic functions, which are implemented in the process of the brand interaction with the consumers. Its communication strategy has an important role in this process. This article is dedicated to the analysis of this topic. In the paper is clarified the brand essence and its place in the market strategy of the business organization. It is pointed out that the brand contents are based on two components: on the process of formation of the symbol of the brand and on the system of consumer relations with the brand. In this connection the communication strategy is determined as brand leading component. The main principles, to which the strategy has to meet, are pointed out and its basic elements are examined.

Keywords: *brand, branding, brand loyalty, brand communication strategy.*

1. INTRODUCTION

The mechanisms for increasing competitiveness of the entrepreneurial structures are constantly improving and developing. One of them is the brand. The theoretical and practical problems, which are connected with it, are gaining more and more significance.

On the present markets the competition between trademarks is intensifying, the contest between their advertising images for place in consumer's consciousness is deepening. Often in the consumer's attitude the emotions predominate over the rationalism. Often as a result of all of this the success of goods and services on the market is based not on objectively defined competitive advantages, but subjectively perceived by consumers. These advantages are contained in the trademarks uniqueness and in the consumers' ability to identify them. They provide the appearance of effective brands, which are designing in the branding process.

Recently the branding is an independent trend in the scientific studies. Its different aspects are researched in the studies of the specialists as Aaker. D., Kapferer J.N., Chernatony L., Maslow A., Schultz D., Trout J., Keller K., Al and Laura Ries, Jacoby J. etc.

The scientists pay attention on the human nature of the brand. It connects the identification of the trademark with the consumers' loyalty, which is expressed in preference for the respective product. [Keller, K., 2008]

The branding is examined as one of the trends of the market strategy of business structures at all, which is playing an important rolefor providing its competitiveness [De Chernatony, L., 2010].

Unfortunately the experience in brand building is not enough generalized and formalized, which impedes its wide distribution. In this problem the practice is ahead of the theory. In recent years the scientists' interest in branding is increased, but the theoretical and methodical researches are not enough. There is a lack of unified conceptual approach to the branding process. The scientists do not have a unified opinion even in relation to the terminology.

On the other hand the development of the economic relations in contemporary terms stimulates companies to develop their brands. This gives them opportunity to win the consumers' trust, to differentiate themselves from the competitors and to gain good profits [Kapferer, J.-N, 2004].

Each brand has its own characteristic, i.e. totality of specific distinguishing marks and advantages. The brand ensures interaction between itself and the consumers via practical proof for mark position and value and persuasion the consumers in its advantages. Its communication strategy has an important role for this.

2. BRAND AND ITS PLACE IN THE STRATEGY OF THE BUSINESS ORGANIZATION

On the different stages of marketing development the scientists have been proposed different definitions for the very complicated and multifaceted term "brand". The brand was received a wide distribution at the end of XIX – in the beginning of XX century.

Many famous brands were designed simultaneously with the appearance of the modern concepts about branding at the end of XIX century with the building of companies like Procter&Gamble (1882 – the first national brand), Coca-Cola, American Express, Kodak film, Heinz (1896 – the firs umbrella brand) etc.

The development of the economic relations moves brand on higher level. The brand is determined as mechanism for achievement of competitive advantage for firms via differentiation of their products.

There are many points of view for the term "brand". The closest to the author is the suggested by the company "Interbrand":

"Brand – this is a sum of all seeing and hidden characteristics, which are making the proposal unique".

Analyzing the brand definitions, which are given by different dictionaries and experts in the field of branding, we can presume that the basic argument from which they

are guided is the role of the brand, which is expressed in the design of unique impression.

For this reason not every mark can be called brand, but only this, which:

- Are capable to create something important and valuable for its consumers;
- Are capable to express this in attributes and communications;
- Are capable to gain the desired recognition and long-term consumer preference, i.e. loyalty.

Specialists from the BBDO company are defined the brand as sustainable promise, given by the company. This is the face of the company, its representative side.

The brand can be determined as mechanism for achievement of competitive advantage for firms via differentiation of their produced products.

As we said, between definitions "brand" and "trademark" shell not be placed equal sign. Brand – this is the degree of knowledge of the trademark and goods and services, which are standing behind it.

The brand is certain idea, philosophy, which defines all business trends. Here can be defined brand elements such as:

- Brand Essence;
- Brand Attributes;
- Brand Name;
- Brand Image;
- Brand Power;
- Brand Identity;
- Brand Value;
- Brand Development Index;
- Brand Loyalty.

We suggest including the Brand Society Value in the set of constituting elements too. This term means the reflection of the social responsibility of the business in the brand.

Depending on addressee the brand is performing different functions.

For brand consumers the brand is performing the following functions:

- Communicative function;
- Function for minimizing the risk of purchase;
- Function for self-identification.

For producers the brand is performing the following functions:

- Opportunity to sell the goods at higher price (price premium);
- Stimulation of consumers loyalty;
- Minimizing the risks of purchase;
- Increasing the brand equity;
- Decreasing the brand expenses.

The contents of the term "brand" are based on two components:

- On the process of formation of the symbol of the brand
- On the system of consumer relations with the brand. They are forming on basis of the marketing communications and the information about the product or the trademark.

Depending on contents of symbols in the trademark and the brand image are formed tree types of relations with consumers:

- *Emotional* – they are formed on basis of feelings arising from the emotional brand perception (positive or negative) in the consumer;
- *Behavioral*–they are arose when consumers carrying out actions motivated by brand to practical result, i.e. acquisition of goods;
- *Rational* – they are formed on the basis of buyer's evaluation, conviction and awareness for the commodity. [Keller, K, 2008].

Practically all these relations are closely interacting. From their harmonic interaction, which provides an effective and full-value brand image, depends how correct the symbols of the brand communications are formed.

Main signs of the brand are:

- *Functionality* – reflection of the commodity qualitative features and purpose in the brand contents. This sign allows consumer to identify his own consumer interests with the use of the brand reflecting the commodity features;
- *Sociality* – reflection on the form of the trademark of the commodity features and interests, which are identified with the contents of the trademark;
- *Sociability* – ability of the trademark to form relations with consumers.

The brand effectiveness and viability depend on the interaction of the mentioned signs and on how full they are shown in the trademark [Kapferer, J.-N, 2004].

In the brand building is necessary to be guided by following requirements:

- The brand signs have to be included in the trademark considering the interests and needs of consumers;
- The external form of the brand has to contribute to the creation of the communication provision in order to form relations between the brand and consumers;
- The brand image has to be objective and convincing, but not rude and intrusive arising negative emotions in the buyer;

The effectiveness of the brand functionality depends on formation of relations with the consumers. The creation of an effective communication strategy has an important role in this process.

3. APPROACH FOR FORMATION OF BRAND COMMUNICATION STRATEGY

The task for creation of an effective communication strategy in branding is not examined in the scientific literature. All opinions are undefined and contradictory in respect to the practical implementation of this task. On the other hand the communication strategy is one of the most effective elements of the branding strategy. It establishes the brand image in consumers mind.

In our opinion the branding communication strategy has to meet the following principles:

- *Adequacy*. The created brand has to correspond to this, which already exists. The degree of discrepancy must be clear defined;
- *Originality*. Brand has to be easily recognizable and easy to remember;

- *Direction*. Brand has to have an exact address, i.e. to attract certain market segments and consumer groups;
- *Plausibility*. If the brand causes mistrust, it is not carried out its functions;
- *Concrete definition*. The reflected qualities of the object in the brand must be well considered and distinguishable.

To create successful brand we have to admit maximum factors, including: development history of the product; development history of the product producer; examples for its use etc.

It is necessary to influence the consumers by means of all known marketing communication resources.

In accordance with the study of D. Aaker because of the many barriers during the trademarks development, only 20% of them are transformed into brands [Aaker D. A., 2009].

By means of interviews carried out are identified the typical barriers in the brand positioning and methods for their elimination are suggested (table 1).

Table 1. Typical barriers in the brand positioning and features of their elimination

Name of the barrier	**Barrier characteristic**	**Methods for eliminating**
Knowledge	Low level of advertising provision	Estimation of optimal advertising budget and its performance
Interest	Weakness of the emotional/rational elements	Deepen study of consumers
Experience in using	Weak call to purchasing and inaccessibility to the commodity	Personnel stimulation, trainings, use of an effective distribution channels
Brand loyalty	Price actions, which destroy the brand loyalty	Optimal price strategy based on research of the demand and price policy of the competitors

The examination by elements of the brand configuration allows to be carried out following conclusions:

1. When the consumer chooses brand, he is influenced by the following product characteristics:
   - high quality and reliability;
   - good functional characteristics;
   - level of knowledge(popularity);
   - experience in using;
   - convenience in delivery;
   - "price-quality" ratio;
   - good service;
   - efficient advertising.
2. The effective brand gives answers to following questions:
   - related with consumers – who, where, how, why the product is using;
   - related with the producer – where, from who and how is produced.

When the earmarked audience is determined we have to agree with the D. Aaker's opinion, who determines five levels of attitude of brand consumers:

- lack of brand loyalty;
- the consumer has no reason to change his attachment to the brand;
- the consumer suffers a loss when changing the brand;
- the consumer values the brand;
- the consumer is loyal to the brand [Aaker, D., 2009].

Determining of the earmarked audience allows us to choose the optimal method for influence on consumers mind.

First we have to distinguish and to aware the consumer for the "unique feature of the product", which this and only this product can provide him. This unique feature must not create artificially. If we do this we will lose the consumers.

When examining the different methods for influence on consumers' feelings, on first place in our opinion, should create trust to the brand. This could be achieved via informing for the high qualitative raw materials used and ecological methods for producing.

An effective way for implementation of the brand idea in the consumers' mind is the logo.

The basic requirements for good logo are:

- Easy to remember and originality – starting from the position of the trademarks as an instrument for identification and recognition of the product;
- Associativity – a graphic decision, how an unusual it can be, it has to cause certain image, which is directly connected with the company activity or product features;
- Universality in measure change – this is the one of general criteria for qualitative logo. The reason is that in the process of the advertising campaign usually it has to be used for variety of advertising materials – from business card to banners for external advertising;
- Color universality.

Strong influence on the consumer has the most important, in our opinion, brand component - the name.

The name plays an important role in the brand building process. It is the most memorable element of the brand individuality. All other elements can be reexamined and modified in time, but commonly the name is inviolable. It is changed very rare, i.e. the name is a sustainable element in the brand building process. It defines the connection between brand and consumers [Aaker, D., 1991].

It is important that the chosen name has to express the nature of the brand, to leave a good impression and to be correct in structure sense. The name determines the

brand position in the consumers mind and it is an insurmountable barrier for competitors.

When is organized the work for forming the name it is necessary for us to be guided by following principles:

- The name has to include general element of emotional and rational profits;
- The name has to be legally protected and do not allow forgery of goods;
- The name has to be easy to read and pronounce;
- The name has to make good impression on consumer.

The objective reflection of the product features in the name makes the company proposal unique, and this turns it on the most effective marketing instrument. The name has to point out these product profits or value that occur positive emotions in the consumer.

The good name has to:

- occur positive associations;
- make sense, which is connected with the general product characteristics;
- be easy for remembering;
- sound good and to be easily pronounced in different languages.

Other verbal problem of the brand is the slogan.

Among specialists there is no unified opinion for that if the slogan is differed from advertising title. Some of them determine these two elements separately. The opponents of this opinion consider that both the slogan and advertising title are built by the same rules and carried out same function.

In our opinion the title is more particular instrument, which is adaptive to conditions changing and less durable than the slogan. If there is a qualitative slogan, which contains attractive and unique commercial proposal, the title is non-compulsory. The slogan unlike the title can be used independent for advertising purposes.

Examining the communication strategy as general, we can say that the "slogan" is more complete and conceptual characteristic of brand than advertising title. Besides the slogan is an effective instrument for distinguishing from the competitors. Exactly the slogan is used for creation of brand image and unifies a series of advertising messages, which are connected with the general theme of the campaign.

The slogan ensures a connection between the company mission and the brand (fig.1).

Figure 1 Connection between the mission of the firm and the brand

The slogan has to abet to action. In this connection it has to contain only this information that will be interesting for consumers. It is established that the people, who notice the slogan are 4-5 times more than people, who read the whole advertisement.

In principle the consumers are reading a print advertising "diagonally", watching a TV advertisement with "half-opened eyes" and listening to a radio-advertisement "with one ear". Only if they notice something important for them they are carefully familiarizing with the whole contents of the advertisement [Belch, G., Belch M, 2004].

The effective slogan influences on the conscious and subconscious of the consumer and occurs in him the necessary for the advertiser emotional reaction.

The advertising title is an important component of other element of the marketing communication – the advertising message. The title has to contain not less than 25% of the important advertising information to remain the main idea of the advertisement in the consumer's mind. The creation of advertising title is based on the principle: "People love to talk with them and about them". The main accent has to be the profits for the consumer.

The emotions of the consumer, which arose in result of the influence or the advertising title, are instantaneous and reflect the quality of the relations between the brand and the consumer, and also the efficiency of the information for the product and brand image.

4. CONCLUSIONS

At the end of this paper the following conclusions can be done:

4.1. In practice and theory of marketing there is no unified opinion about the terminology in branding.

4.2. The contents of the term "brand" are based on two components: on the process of formation of the symbol of the brand and on the system of relations of consumer to brand on basis of the marketing communications and other information about the product or trademark.

4.3. When the elements of the brand are examined we suggest including one more - the Brand Society Value.

4.4. The communication strategy is determined as leading component of the branding.

4.5. Here are pointed out the general principles, which the communication strategy has to meet.

4.6. The most common barriers for brand positioning are identified and methods for their elimination are suggested.

4.7. The name plays an important role in the process of brand building. It is the most memorable element of the brand individuality. Its efficiency depends on how correct the name reflects the features and value of the product.

4.8. The connection between the mission, the brand and the slogan has shown. In this connection the effective slogan influences on the conscious and subconscious of the consumer and abets the desired emotional reaction for brand owner in him.

5. REFERENCES

[1] AAKER D. A. *Building Strong Brands*, New York, The Free Press, 1996
[2] AAKER D. A. *Strategic Market Management*, Edition 9, New York, The Free Press, 2009
[3] AAKER D. A. *Managing Brand Equity: Capitalizing on the Value of a Brand Name*, New York, The Free Press, 1991
[4] AAKER D. A. *Dimensions of Brand Personality*, Journal of Marketing Research, 1997
[5] AMBLER T. *Marketing and the Bottom Line*, London: Prentice Hall, 2003
[6] AZOULAY, A., KAPFERER, J.-N., *Do Brand Personality Scales Really Measure Brand Personality*, Journal of Brand Management, Vol.11, №2,2003
[7] BELCH, G., BELCH M., *Advertising and Promotion: An Integrated Marketing Communications Perspective*, Boston, McGraw-Hill Irwin, 2004
[8] De CHERNATONY, L., *From Brand Vision to Brand Evolution*, Butterworth-Heinemann, 2010
[9] DOYLE, P., *Value-Based Marketing. Marketing Strategies for Corporate Growth and Shareholder Value*, John Wiley & Sons, Chichester, 2000
[10] HILL, C., JONES G., *Strategic Management Theory, An Integrated Approach*, Houghton Mifflin, Boston, 2001
[11] HILL, C., ETTENSON, R., TYSON, D., *Achieving the Ideal Brand Portfolio*, MIT Sloan Management Review, Vol.46, №2, 2005
[12] KAPFERER, J.-N., *The New Strategic Brand Management*, Kogan Page, London, 2004
[13] KELLER, K., *Strategic Brand Management*, Upper Saddle River, Prentice-Hall, New Jersey, 2008
[14] KOTLER, Ph., PFOERTSCH W., *B2B Brand Management*, Springer, Berlin, 2006
[15] KOTLER, Ph., ARMSTRONG, G., Principles of *Marketing*, Pearson Global Edition, 2010

INTERMODAL TRANSPORT- A WAY OF ACHIVING SUSTAINABLE DEVELOPMENT

STINGA (CRISTEA) VIORELA-GEORGIANA

Constanta Maritime University, Romania

ABSTRACT

Through this paper we tried to establish the important role of intermodal transport, but also the role of co-modal transport, concept that was introduces in 2006 by the European Commission, regarding the sustainable development. Both concepts refer to the efficient use of at least two modes of transport, with the difference that the second one takes also in consideration the optimal and sustainable utilization of resources. We showed that in order to obtain sustainable development it is important to realize a diverse, multimodal transportation system. Within our study we tried to present the benefits obtained by using the intermodal transport due to the transfer of freight to modes that generate less external effects.

Keywords: *Efficiency, sustainability, co-modal transport, external costs.*

1. INTRODUCTION

In 2001, the European Commission submitted a white paper on the future transport policy "European Transport Policy for 2010: Time to Decide" (European Commission, 2001). Through this white paper the European Union promotes an increased usage of intermodal transports, which is identified as a way of using the existing infrastructure more efficiently in order to achieve sustainable transport.

According to the UN/ECE, 2001, the standard definition of intermodal transport, define it as a transport that refers to the movement of goods in a single loading unit or vehicle that successively uses at least two modes of transport without handling the goods themselves in changing modes, trying to utilize the bests benefits from every type of transport mode in one integrated transport chain (Flodén, 2007). This transport is made in order to improve the economic performance of freight transport (Mathisen and Hanssen, 2014; Rodrigue et al., 2009), performance that it is obtain due to the fact that the most suitable transport mode is used on each part of a trip (OECD, 2001).

The evolution of "door-to-door" transport requires the development of intermodal transport because it allows the combination in a more advantageous manner of the benefits related to each mode of transport (on a particular route). Intermodal transport allows the convenient use of vehicles in order to achieve a much faster transport of goods at the lowest possible cost.

In intermodal transport results should be viewed in terms of intermodal transport company, in terms of users of the national economy (exporters / importers), but also in terms of benefits related to the environment. Thus for an intermodal transport system to be effective it is necessary to ensure the highest level of users satisfaction, users that benefit from the intermodal transport service.

So bet on the process of intermodal transport, the results obtained are complex:

- Direct results: here we can refer to the effects that relate to the movement of goods;
- Indirect results: here we can refer to the role that intermodal transport has in terms of:
  - creating new jobs in the country in which they run their activities;
  - supplying the national economy with imported goods;
  - reducing the harmful effects of pollution due to the use of means of transport that are less polluting;
  - the most important one refers to the introduction of modern technologies using containerization.

There are many advantages in using the intermodal transport but the most important one, related to our study, refers to its comparatively low external costs (Hanssen and Mathisen, 2011). When referring to congestion or energy consumption (Woodburn et al., 2007) it is clear that intermodal freight transport has an important contribution in achieving a sustainable European transport sector (European Commission, 2009), that is why it has been promoted by policymakers on all levels (Macharis et al., 2011). Sustainable development is one of the themes not only of the European Union but also of the world today, due to the fact that it is very important especially considering growing urban traffic problems and urban environmental problems (Xing, YY.; Liang, HY.; Xu, DB., 2013). We can easily say that intermodal transport offers an advanced platform for more efficient, flexible, reliable and sustainable freight transportation. In order to create sustainable urban environments it is very important to realize a diverse, multimodal transportation system (B. J. Wickizer and A. Snow, 2011).

When we talk about environmentally sustainable transport it is important to define three factors that contribute in promoting it (Elvik, R.; Ramjerdi, F., 2014):

- Modifying road user behaviour so that the external effects of transport may be reduce (some external effects include congestion, accidents, traffic noise and emissions to air);
- Transferring the freight transport to modes that

- generate less external effects;
- Reducing the volume of motorized travel.

2. THE CONCEPT OF CO-MODALITY

After some years of promoting intermodal transport solution the European Commission extended the meaning of inter-modality to full interoperability of transport modes. For economic and environmental reasons, the European Commission introduced in 2006 a new notion called co-modality that refers to "the efficient use of different modes on their own and in combination that will result in an optimal and sustainable utilization of resources". This concept entails the development of infrastructures and actions that will ensure optimum combination of individual transport modes allowing them to be combined effectively in terms of environmental, economic, service and financial efficiency, etc. (Jeribi, K. et al., 2011).

There are many freight transport policies in the European Union that aim to increase co-modality and promote the sustainability of the European Freight Transport System. So, in 2007 in European Commission introduced the concept of "e-Freight" that tries to support the transport users, the transport infrastructure providers, the transport service providers and the transport regulators. In autumn 2007 was presented the Freight Transport Logistics Action Plan[1] that focuses among others on "Green" transport corridors for freight or sustainable quality and efficiency and relies on co-modality and on advanced technology in order to provide a competitive European surface freight transport system whilst promoting environmental sustainability.

Studies have revealed that, taking into consideration the infrastructural framework, co-modality is a process capable of reducing congestion and externalities, but also enhancing effectiveness and efficiency of transport (Enrico Musso, Alberto Cappato, 2010). There may be many differences between inter-modality and co-modality but the most important one is that the new concept focuses not on the freight transfer (from one way of transport to another, i.e. from road to maritime, river or rail transport) but on the total efficiency of the transport sector.

When we refer to co-modality we have to think about the principle that "public transport operates more successfully when it is planned as a unified network to support seamless multi-destination travel rather than as individual lines catering to single trips" (Dodson, Mees, Stone, & Burke, 2011), principle that is based on the concept of public transport network planning. i.e. "serving the maximum number of possible journeys with the minimum of operational resources" (Mees, Stone, Imran, & Nielson, 2010).

There were many studies showing that co-modal transport cuts transport cost, leading directly to the maximization of the efficiency of the transport chain, co-modal practices being profitable and sustainable. So did the study of Gomes and others (2010) that showed the advantages of a co-modal transport system, taking in consideration both internal and external (accidents and pollution) cost, a system that reduce the social externalities.

So co-modal transport covers three important aspects (see figure 1) like the use of more than one mode of transport and their optimization (i.e. truck full), but also the use of the Intermodal Transport Unit. It tries to reduce the environmental impact of freight transport, but on the same time it requires a specific legal and interoperability framework (Silvia Rossi, 2012).

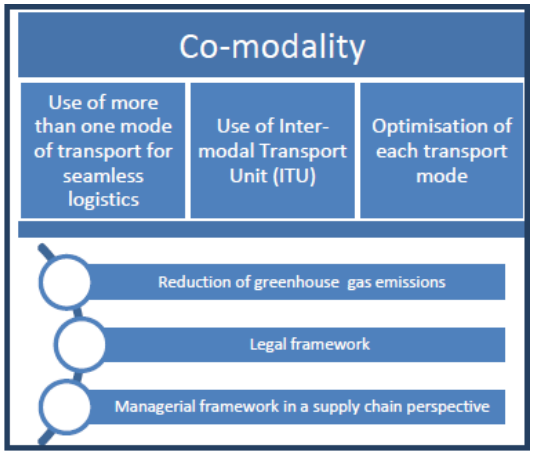

Figure 1 Dimensions of co-modality
Source: Silvia Rossi, CO³ Project, 2012

3. CASE STUDY

To show the importance of intermodal transport (taking into account the role of sustainability) we analysed the carriage of 4,000 tons between two different points A (a city) and B (a port). Within this study we have taken into account different types of transports, both unimodal and intermodal obtaining different costs, but we analyse only two of them: a unimodal transport[2] (road transport) and an intermodal one (rail-river transport). We analysed the total cost obtained for each solution considering both internal and external costs. It is important to say that when using different modes of transport the distance between A and B is not the same (referring to the final two solutions, due to the accessibility of road transport and also considering the rail infrastructure and river trail).

The results showed that intermodal transport cuts transport costs, the rail-river transport being with approximately 30% cheaper (see Figure 2).

Referring to the external costs it is clear that when using rail-river transport the social externalities are reduced, so we can easily say that using an intermodal transport will certain lead to an environmentally sustainable transport due to the transfer of freight to modes that generate less external effects.

[1] Communication from the Commission COM 2007 / The EU's freight transport agenda: Boosting the efficiency, integration and sustainability of freight transport in Europe COM(2007) 606 final

[2] A transport that uses only one mode of transport and where each carrier issues his own transport document

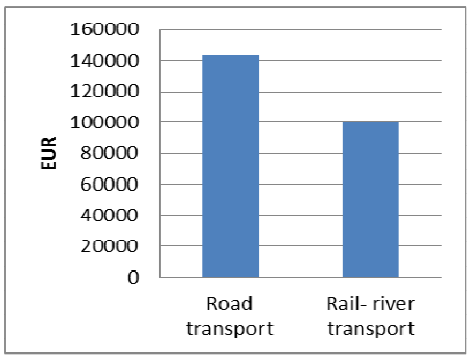

Figure 2 Transport costs chart

As highlighted by the study of CE Delft (2011), we can see that external costs in EU-27[3] for road transport are much higher than for rail or inland waterways transport (see Table 1), when referring to accidents, air pollution, noise and some others categories of external costs.

Table 1. Total external costs for EU-27 by cost category and transport mode

Cost category	Road		Rail (freight transport)	Inland waterways
	LDV	HDV		
	Mio €/a	Mio €/a	Mio €/a	Mio €/a
Accidents	18,677	19,604	71	0
Air pollution	5,933	12,995	426	782
Noise	2,094	3,537	476	0
Biodiversity losses	208	893	1	69
Nature and landscape	284	284	21	64
Soil and water pollution	601	1,629	164	0
Urban effects	1,035	965	59	0

Source: CE Delft, Infras, Fraunhofer ISI, External Costs of Transport in Europe, 2011

The study showed that the use of an intermodal transport allows obtaining benefits far superior to unimodal transport especially if there is a large amount of goods (we need to say that for this distance we have needed 84 trucks with a capacity of 24 tons in order to deliver 4,000 tons). Using an intermodal transport allows a considerable discount of transport costs but also of the external costs. It is important to note that the benefits obtained may undergo small changes because the transport system is a more complex one, especially when referring to variables that have an impact on sustainability.

4. CONCLUSIONS

There were many studies showing that co-modal transport cuts transport cost, leading directly to the maximization of the efficiency of the transport chain. As we saw intermodal transport is a key system in the international transport, mainly because through it, transport modes compete with each other, benefiting the entire transport of goods. We should also notice that intermodal transport takes in consideration customers' demands (trying to satisfy them), but also the environment, sustainability being an important element of European Union policies, due to the fact that co-modal transport implies non-road freight transport on the long-haul.

We should also take in consideration the impact of external costs, that's why was introduced the concept of co-modal transport, that tries to obtain sustainable development. It is important to say that the main idea of intermodal transport is to utilize the strengths of different transport modes in one integrated transport chain (Flodén, 2007), so that in the end the economic performance obtained is the highest. So, it is clear, that intermodal transport leads to a significant contribution for sustainable development.

[3] Data include the EU-27 with the exemption of Malta and Cyprus, but including Norway and Switzerland

5. REFERENCES

[1] BENJAMIN J. WICKIZER, ANDREW SNOW, *Rediscovering the Transportation Frontier: Improving Sustainability in the United States through Passenger Rail*, Sustainable Development Law & Policy: Vol. 11: Iss. 1, Article 8, 2011

[2] CE Delft, Infras, Fraunhofer ISI, External Costs of Transport in Europe, Update Study for 2008, Delft, CE Delft, 2011

[3] CLAUDIA DE STASIO, DAVIDE FIORELLO, SILVIA MAFFII, *Public transport accessibility through co-modality: Are interconnectivity indicators good enough?*, Research in Transportation Business & Management, pp.48-56, Milano, Italy, 2011

[4] DODSON, J., MEES, P., STONE, J., & BURKE, M., *The principles of public transport network planning: A review of the emerging literature with select examples*, Griffith University. Urban Research Program, Issues Paper 15. Brisbane, 2011

[5] ELVIK, R.; RAMJERDI, F., *A comparative analysis of the effects of economic policy instruments in promoting environmentally sustainable transport*, Transport policy, Volume: 33, pp. 89-95, DOI: 10.1016/j.tranpol.2014.02.025, 2014

[6] ENRICO MUSSO, ALBERTO CAPPATO, *Co-modality as a solution to enhance modal shift in freight transport: ICT applications can help*, Round Table on Information and Communications Technologies for Innovative Global Freight Transport Systems, , Genoa Round Table, 2010

[7] ERICK LEAL, *Logistics platforms as a pivotal element in competitiveness and sustainability*, Issue No. 302, the FAL Bulletin- Facilitation of transport and trade in Latin America and the Caribbean, 2011

[8] ERNEST CZERMAŃSKI, *Intermodality turns into co-modality*, Baltic Transport Journal, 2009

[9] European Commission, *A sustainable future for transport: Towards an integrated, technology-led and user friendly system*, Luxembourg, 2009

[10] FLODÉN, J., *Modelling Intermodal Freight Transport - The Potential of Combined Transport in*

Sweden, Department of Business Administration. Gøteborg University, 2007
[11] GOMES, P., LOPES, M., MARTINS, H. AND CARVALHO, J., *Internal and external costs of transport in Portugal*, CITTA 3rd Annual Conference on Planning Research Bringing City Form Back Into Planning, 2010
[12] HANSSEN, T. E. S. & MATHISEN, T. A., *Factors facilitating intermodal transport of perishable goods - transport purchasers viewpoint*. European Transport - Trasporti Europei, pp. 75-89, 2011
[13] JERIBI, K.; ZGAYA, H.; ZOGHLAMI, N.; HAMMADI, S., *Distributed Architecture for a Co-modal Transport System*, IEEE International Conference on Systems Man and Cybernetics Conference Proceedings, pp. 2797-2802, Anchorage, AK, 2011
[14] MACHARIS, C., CARIS, A., JOURQUIN, B., PEKIN, E., *A decision support framework for intermodal transport policy*, European Transport Research Review, 3, 167-178, 2011
[15] MATHISEN TERJE ANDREAS, Hanssen Thor-Erik Sandberg, *The academic literature on intermodal freight transport*, 17th Meeting of the EURO Working Group on Transportation, Transportation Research Procedia 3, pp.611 – 620, Sevilla, Spain, 2014
[16] MEES, P., STONE, J., IMRAN,M., & NIELSON, G., *Public transport network planning: a guide to best practice in NZ cities*, New Zealand Transport Agency research report 396, Wellington, 2010
[17] OECD, *Intermodal freight transport: institutional aspects*, Paris, Organisation for Economic Co-operation and Development (OECD), 2001
[18] RODRIGUE, J.-P., COMTOIS, C. & SLACK, B., *The geography of transport systems*, London, Routledge, 2009
[19] SILVIA ROSSI, *CO³ position paper: challenges of co-modality in a collaborative environment*, Cranfield University, CO³ Project, Deliverable D2.3, 2012
[20] STEADIESEIFI, M.; DELLAERT, N. P.; NUIJTEN, W.; VAN WOENSEL, T.; RAOUFI, R., *Multimodal freight transportation planning: A literature review*, European journal of operational research, Volume: 233, Issue: 1, pp. 1-15, DOI: 10.1016/j.ejor.2013.06.055, 2014
[21] WOODBURN, A., BROWNE, M., PIOTROWSKA, M. & ALLEN, J., *Litterature Review WM7: Scope for modal shift through fiscal, regulatory and organisational change*, University of Westminster and University of Leeds, 2007
[22] XING, YY.; LIANG, HY.; XU, DB., *Sustainable development evaluation of urban traffic system*, Intelligent and integrated sustainable multimodal transportation systems proceedings from the 13th COTA International Conference of Transportation Professionals (CICTP), Book Series: Procedia Social and Behavioral Sciences, Volume: 96, pp. 496-504 DOI: 10.1016/j.sbspro.2013.08.058, China, 2013
[23] ZOGRAFOS, KONSTANTINOS G.; SEDLACEK, NORBERT; BOZUWA, J., *A comparative assessment of freight transport and logistics policies in Europe*, Conference on Transport Research Arena, Book Series: Procedia Social and Behavioral Sciences, Volume: 48, pp. 2523-2532, DOI: 10.1016/j.sbspro.2012.06.1223, Athens, GREECE, 2012

HIGHER EDUCATION'S IMPORTANCE. CASE STUDY ON UNEMPLOYMENT RATE

[1]STINGA (CRISTEA)VIORELA- GEORGIANA, [2]OLTEANU ANA-CORNELIA

[1,2]Constanta Maritime University, Romania

ABSTRACT

Through our paper we tried to highlight the importance of diversity in higher education system, but also the important role of higher education for the economy in general. The skills and advantages of higher education graduates play an important role in reducing the unemployment rate, due to the fact that in order to obtain a good job one need to be prepared, when referring to both transversal core skills and subject or sector-specific skills. Within our case study we showed that higher education graduates have been comparatively protected from unemployment than lower qualified groups, this being confirmed through the low rate of unemployment.

Keywords: *Institutional diversity, unemployment rate, higher education graduates, labour market.*

1. INTRODUCTION

As stated by the European Commission[1], higher education plays an important role in Europe's collective well-being, due to the fact that it creates new knowledge that in the end is transmitted to students. Even if in Europe there is a large institutional diversity, this is in the same time one of the major key strengths of higher education in Europe. It is well known that almost four thousand higher education institutions (that operate within the legal and administrative frameworks of their national or regional higher education systems) are the ones that made the higher education landscape of Europe. We have to highlight that studies have shown that this diversity is the one that has a positive impact on performance (van Vught, F.A.et al.; 2010). Even if we speak about small specialized teaching colleges or about large research-intensive universities, they all play an important role in Europe's higher education system. Considerable diversity remains in European higher education, between systems, which retain their own characteristics, between institutions, which vary in size, mission and profile and even, within institutions (Reichert, S.; 2009).

Why do we need diversity in higher education system? According to the European Commission there are many reasons that support it like: diversity is the one that sustains institutional specialization (every institution try to became the best in what they do), it allows access to higher education to students with different educational backgrounds, it responds better to labour market needs (due to the increased variety of specializations) and it offers greater possibilities for exploring new approaches. But beside these reasons it is important to say that in the end higher education institutions contribute to socio-economic development, improving individual's knowledge and skills and contributing to innovation in the wider economy.

2. THE SKILLS AND ADVANTAGES OF HIGHER EDUCATION

When referring to higher education graduates, we need to highlight the importance of both transversal core skills and subject or sector-specific skills for all individuals. Studies have revealed that the most important transversal core skills are considered to be: team-working, communication skills, computer skills and adaptability. So higher education programmes should focus not only on sector-specific knowledge and skills, but also on core transversal competences notably in terms of critical thinking and learning, communication, entrepreneurship and creativity. Table 1 shows the ten most important capabilities that an employee, as a higher education graduate, should have, together with their importance ranking. We can see that the degree classification, relevance and reputation of qualifications achieved by graduates are very important. Figure 1 shows the employers' main complaints concerning the higher education graduates as presented by many studies.

Table 1. Top 10 capabilities employers are most satisfied with and their importance ranking

Capabilities	Satisfaction rank
IT skills	1
A postgraduate qualification	2
Good degree classification	3
Qualification from an institution with a good reputation	4
Intellectual ability	5
Character/personality	6
Team-working skills	7
Relevant course of study	8
Integrity	9
Cultural fit with your company	10

Source: Will Archer, Jess Davison, 2008

[1] The Commission's Communication on Supporting growth and jobs – an agenda for the modernization of Europe's higher education systems, 2011

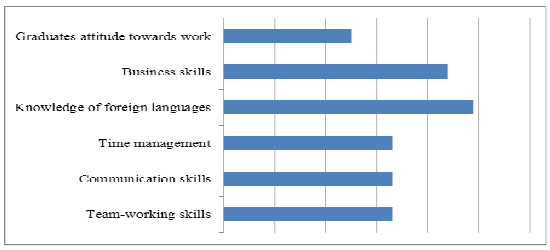

Figure 1 The employers' main complaints

At present, in Romania, the rate of leaving in education is quite high about 19% (while at European level this rate is 15%) which will adversely affect the European level of competence. It is important to highlight that many studies conducted by the Romanian Ministry of Education showed that almost 75-80% of high school graduates go to college and 17% of Romanians of all ages have higher education.

The advantages that higher education graduates have are:

- The unemployment rate for college graduates is lower;
- The revenues are much higher, the taxes on income for college graduates are higher than those with low qualifications, this leading automatically to higher state revenues and to higher pensions;
- Lower stress and higher levels of health;
- Greater opportunities in changing the workplace and to promote;
- Higher level of satisfaction at work;
- Parents that are higher education graduates are more interested in their children's education and they are willing to spend more money for their school training;
- High school graduates are three times more likely to live in poverty and eight times more likely to seek social assistance programs that higher education graduates.

Why should high school graduates go to university? First of all there are the legal policies that stipulate a higher remuneration for those who hold a university degree, second of all there are the skills acquired during their studies (from their lectures or during their practice) and the last one refers to the professional network that ones can build upon their work relations.

Figure 2 and 3 present the results that were obtained during a sociological study that was made among high school students in 2009, trying to find out which are their opinions regarding their future plans. The study investigates high school students' opinion concerning their prospects for future employment.

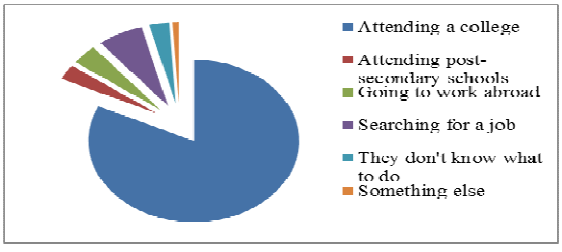

Figure 2 Which are the future plans of a high school graduate?

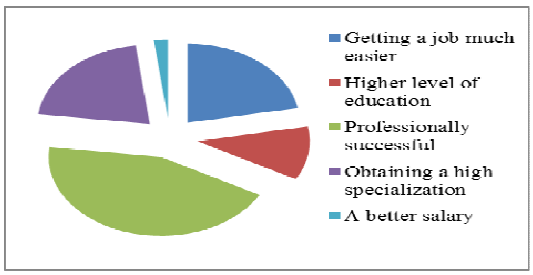

Figure 3 Which is the main advantage gained through a college graduation?

3. CASE STUDY: THE UNEMPLOYMENT RATE AMONG GRADUATES

It is clear that higher education has a positive impact on employment outcomes, at both individual and societal level, due to the fact that European higher education graduates have significantly higher rates of employment than those with less advanced levels of qualification. Compared to forecast future labour market needs and taking into consideration the European Union's target, the number of Romania's students is insufficient.

Studies have shown that by 2020 in Europe, over 35% of jobs will require higher qualifications (it will increase from 29% in 2010), around 50% of jobs will require medium-level qualifications and the share of jobs employing those with low qualifications will decrease from 20% to less than 15% (CEDEFOP, 2010a), due to the global economy, which requires specialized people in all sectors. The European Commission stated that by 2020, the demand for highly-qualified people is projected to rise by almost 16 million; this is why it becomes urgent to support and encourage high school students to attend university cycles.

It is important to say that an unemployed person is defined by Eurostat, according to the guidelines of the International Labour Organization, *as someone aged 15 to 74 without work during the reference week who is available to start work within the next two weeks and who has actively sought employment at some time during the last four weeks.*

According to the National Institute of Statistics in December 2014, the Romania unemployment rate (the number of people unemployed as a percentage of the labour force) was at 6.40%, compared to 7.00% last year. This is lower than the long term average of 6.76%. The employment rate for the population aged 20-64 years was 67.2%, at a distance of 2.8 percentage points of the national target of 70% established in the context of the Strategy Europe 2020. Figure 4 presents the number of persons unemployed from 2004 till 2014 in Romania.

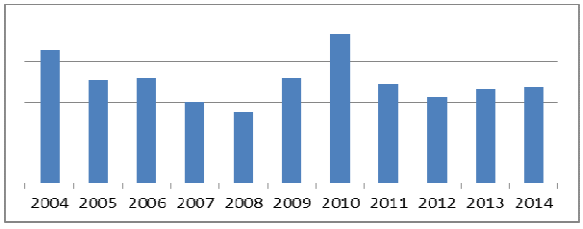

Figure 4 The number of persons unemployed
Source: www.anofm.ro

In Romania, as in most European countries, unemployment among young people remains a major social problem. In November 2014 a percentage of 22.5 young people (15-24 years old) were not employed, as for people over 25, the unemployment rate was of 5.2%. This problem is due transition from school to work, a transition that refers to the period between graduation and employment on a stable full time job (Boajă, D. M.; 2011).

Studies have shown that over the last years, higher education graduates have been comparatively protected from unemployment than lower qualified groups in most Member States even if in some countries there have been moments when the graduate unemployment rates have bucked the general trend.

According to the data revealed by AMIGO, the structure of unemployment by level of educational attainment in 2014 is presented in the figure below. It is important to notice that the "employment advantage" of tertiary graduates over those with only upper secondary qualifications is highest in almost all European Member States. As we can see in Romania, in 2014, the number of unemployed persons with high school is of 19.24% from the total number of unemployed persons, while the ones that are higher education graduates totals a percentage of 6.05%.

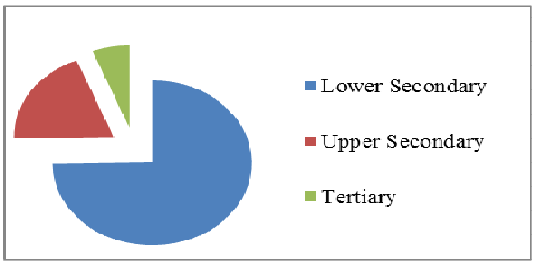

Figure 5. The structure of unemployment by level of educational attainment

Source: National Institute of Statistics

4. CONCLUSIONS

Studies have shown that young people are recognized as one of the most vulnerable categories in society and nowadays more young people have been affected by unemployment, but we need to highlight that even on the sever economic crisis on employment, the tertiary education graduates were less affected than those with lower levels of qualification.

As shown in our paper there are many advantages that came along with education especially when referring to higher education. In the end higher education is a very good investment in terms of annual earnings compared to those of high school graduates, but also when referring to knowledge or to work habits, people with a higher level of education being more satisfied in their jobs (Hardy Marcelina, 2014). We should also say that higher education definitely has a positive impact on employment outcomes, an on the economy in general when referring to unemployment rate.

5. REFERENCES

[1] BOAJĂ DAN MARIN, *Youth unemployment rate in European Union. Regional approach – Romania*, Annals of the University of Craiova Economic Sciences, No. 39, 2011

[2] CEDEFOP, *Skills supply and demand in Europe: Medium-term forecast up to 2020*, http://www.cedefop.europa.eu/en/Files/3052_en.pdf, 2010a

[3] EGGINS, H and P West, *The global impact of the financial crisis: Main trends in developed and developing countries*, Higher Education Management and Policy, Volume 22 Issue 3/ Journal of the Programme on Institutional Management in Higher Education, 2011

[4] EUROPEAN COMMISSION, Commission staff working document on recent developments in European higher education systems, Accompanying the document "*Communication from the commission to the European parliament, the council, the European economic and social committee and the committee of the regions-Supporting growth and jobs – an agenda for the modernization of Europe's higher education systems*", Brussels, SEC(2011) 1063 final, 2011

[5] FDP CampusNews, *Avantajele absolvirii unei facultati: salariu mai mare, risc redus de somaj*, 2010

[6] HARDY MARCELINA, *6 Benefits Of Earning A College Degree- Check out these interesting benefits linked to higher education*, 2014

[7] National Institute of Statistics, *Employment and unemployment in Q III 2014- Household Labour Force Survey (AMIGO), Romania*, Press release No. 311 of December 19, 2014

[8] OECD Social employment and migration working papers, 2010

[9] RARIȚA M., DINICĂ R., RUSU D., *Studiu sociologic: Opțiunile profesionale ale elevilor din clasele a XII-a*, Universitatea „Dunărea de jos" Galați, 2009

[10] RICHARD VEDDER, *Why College Isn't for Everyone*, 2012

[11] REICHERT, S., *Institutional diversity in European higher education: Tensions and challenges for policy makers and institutional leaders*, EUA, 2009

[12] VAN VUGHT, F.A. et al., *U-Map: The European Classification of Higher Education Institutions*, Center for Higher Education Policy Studies (CHEPS), University of Twente. Project funded by the EU's Lifelong Learning Programme www.u-map.eu, 2010

[13] WILL ARCHER, JESS DAVISON, *Graduate Employability: What do employers think and want?*, the Council for Industry and Higher Education, 2008

*** http://www.anofm.ro

ISSN 1582 – 3601

„Nautica” Publishing House,
Constanta Maritime University

Editura
NAUTICA